Advanced Bioconjugation Technologies for Site-selective Protein Modification

Antibody Drug Conjugates

Grier, Katja Egeskov

Publication date:
2022

Document Version
Publisher's PDF, also known as Version of record

Advanced Bioconjugation Technologies for Site-selective Protein Modification:

Antibody Drug Conjugates

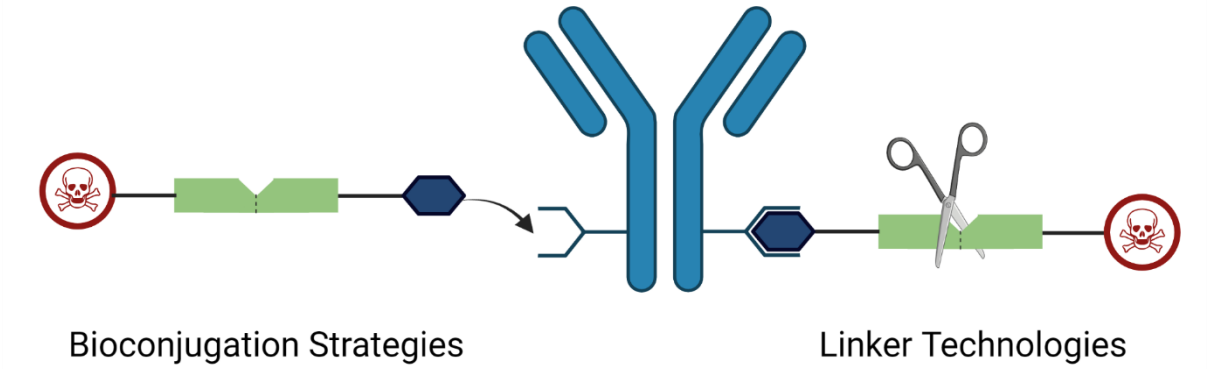

Katja Egeskov Grier

PhD thesis

April 2022

DTU

Advanced Bioconjugation Technologies for Site-selective Protein Modification: Antibody Drug Conjugates

PhD Thesis

Katja Egeskov Grier

April 2022s

Department of Chemistry

Technical University of Denmark

Kemitorvet, building 206

2800 Kgs. Lyngby

Denmark

PhD Supervision

Associate professor Katrine Qvortrup

Co-supervisor Professor Mads H. Clausen

Preface

The work presented in this thesis, is the result of my PhD studies conducted at the Department of Chemistry at the Technical University of Denmark, under the supervision of Associate professor Katrine Qvortrup and co-supervisor Mads H. Clausen from February 2019 to May 2022. I was fortunate to complete a three month external stay at Cambridge University in the group of professor David Spring.

During the studies, I have completed ~30 ECTS point of relevant course work and have taught courses both practical and theoretical.

A number of people have contributed to the work presented in Chapter 3, including MSc student Freja Grauslund, research assistant Christina Sofie Haxvig and postdocs Anders Højgaard Hansen and Charlotte Uldahl Jansen. The linkers were designed by myself and most optimizations were performed by me. It has been noted throughout Chapter 3, the work that has been performed by others and contributors have been credited by name.

Figures 1.1, 2.1, 3.1, 3.3, 3.12 and the front page figure have been designed using Biorender.com.

Carlsberg Fondet provided funding for this project.

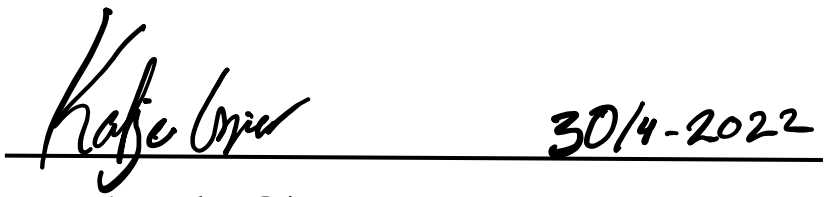

Katja Egeskov Grier Date

Abstract

Antibody drug conjugates (ADCs) present a targeted cancer chemotherapy, that combine the specificity of an antibody with the toxicity of a small molecule drug. The enormous potential of ADCs, drives the need for the development of novel technologies, allowing for tuning of the properties of ADCs.

Chapter 2 Part I covers the development of a novel site-selective serine conjugation method, inspired by the catalytic triad found in the active site of hydrolytic enzymes. The N-heterocyclic carbene (NHC) organocatalyst IMes was used to introduce O-selectivity and through screening, it was found that short vinyl esters displayed O-selectivity. The subsequent screening of peptides containing a serine, activated by adjacent amino acids, demonstrated the feasibility of this sequence specific serine conjugation strategy. Part II describes the synthesis of a tetra anchor containing four disulfide rebridging head groups able to tether the 4 interchain disulfide bonds of antibodies together. This novel cysteine conjugation strategy, enables access to odd numbered DARs, as well as reforming the covalent bonds responsible for the stability of the antibody.

In Chapter 3, the development of sulfatase cleavable linkers is described. In part I, a novel sulfatase cleavable linker was designed and synthesized for the release of alcohol functionalized drugs. The linker was attached to MMAE and the payload was conjugated to trastuzumab via maleimide-cysteine chemistry. Subsequent *in vitro* testing of the ADC towards HER2 positive breast cancer cells displayed an antigen dependent dose-response curve. To increase the potency of the ADC, a nitro group was introduced in the *ortho* position to the aryl sulfate of the linker. However, unforeseen acid sensitivity of the *o*-nitro aryl sulfate moiety was observed during linker synthesis and *in vitro* assays of the ADC containing the *o*-nitro aryl sulfate-auristatin E payload are pending. Part II investigates how substitution of the aryl sulfate moiety affects sulfatase mediated hydrolysis rates. Four probes were synthesized and it was observed that introduction of electron withdrawing groups (EWG) enhanced the cleavage rates significantly, highlighting the opportunity to tune the specificity and efficiency of sulfatase cleavable linkers. Part III describes the synthesis of three novel sulfatase cleavable payloads decorated with different EWG. The payloads were conjugated to trastuzumab and in *in vitro* assays against HER2 positive breast cancer cells, ADC potency varied significantly for the differently substituted aryl sulfates.

In conclusion, the work presented in this thesis may provide useful contributions towards the development of safer and more efficacious ADCs to battle cancer.

Resume

Antistof lægemiddel konjugater (ADCer) tilbyder patienter en målrettet kræft kemoterapi som kombinerer specificiteten af et antistof med toxiciteten af et lægemiddel. ADCers enorme potentiale skaber et behov for nye teknologier, der kan bruges til at tune nye ADCers egenskaber for højere patientsikkerhed.

I Kapitel 1 del I drages inspiration fra den katalytiske triade, ofte fundet i det aktive site af hydrolytiske enzymer, til udviklingen af en ny sekvens specifik serin konjugationsstrategi. Den organokatalytiske N-heterocykliske carbene (NHC) IMes blev anvendt for at øge O-selektiviteten. I de initiale forsøg blev det observeret, at korte vinylestere udviste O-selektivitet. Efterfølgende peptidforsøg demonstrerede potentialet af denne sekvens specifikke serine konjugations strategi. I Del II beskrives syntesen af et tetra-anker, der indeholder 4 disulfid gendannende grupper med formålet at tøjre de 4 interkæde disulfid broer, fundet i antistoffer, sammen til fremstillingen af homogene ADCer.

I Kapitel 3 beskrives udviklingen af sulfatase kløvbare linkere. Del I beskriver design, syntese og *in vitro* test af en ny sulfatase kløvbar linker, som er i stand til at frigive alkohol funktionaliserede lægemidler. Efter syntese blev MMAE påsat og det færdige payload blev konjugeret til trastuzumb via maleimide-cystein kemi. Ved *in vitro* eksperimenter kunne en dosis-respons kurve observeres mod HER2 positive bryst kræft celler. For at øge potensen af ADCet, blev der også syntetiseret en analog indeholdende en nitro funktionalitet i ortho positionen til aryl sulfate enheden. Dog blev uforudset syre ustabilitet observeret. *In vitro* resultater for *o*-nitro analogen afventes. I Del II undersøges sulfatase hydrolyse raten på aryl sulfate enheder substitueret med forskellige elektron tiltrækkende grupper (EWG). Fire prober blev syntetiseret og ved introduktion af EWG kunne en signifikant stigning i kløvningshastigheden observeres. Disse resultater fremhæver muligheden for at tune specificiteten og effektivitet af sulfatase kløvbare linkere. Del III beskriver syntesen af tre nye sulfatase kløvbare payloads indeholdende forskellige EWG på aryl sulfat enheden. Disse payloads blev konjugeret til trastuzumab og *in vitro* assays af de resulterende ADCer viste, at der var en signifikant forskel i IC_{50} værdier af de forskelligt substituerede aryl sulfater.

Resultaterne præsenteret i denne afhandling kunne muligvis bidrage til udviklingen af nye ADCer med bedre sikkerhed og højere effektivitet i kampen mod kræft.

Acknowledgements

Of the many of people who deserve my gratitude, above all, I would like to thank my supervisor Katrine Qvortrup. Thank you for your tireless, open door enthusiasm that motivates and encourages even the bleakest of students. Your passion for research is infectious. Thank you for offering me this amazing opportunity, it has truly been a journey, challenging me every day and developing, not only my skills in chemistry and research, but my patience, my focus and my team working skills. I could not imagine doing this under the supervision of anyone else.

To my fellow PhDs through thick and thin, Amalie Nørskov and Charlotte Uldahl Jansen, thank you for the companionship, the laughs, the frustrations, the dances, the shenanigans and everything in between. Thank you for sharing in my misery as well as in my joy. My sanity has endured these three years, in large part due to the two of you.

To members of the Qvortrup group, past and present, thank you for contributing to an engaging learning environment and delightful lunch discussions, the topics of which can be unpredictable and ever changing. Special thanks to Anders H. Hansen, Christina S. Haxvig, Jesper Uhd, the Utzons and Stavroula Louka.

To the many students I have supervised, who have endured me fumbling through the role of a teacher and mentor, thank you for the challenges and experiences. I hope you learned through our collaborations. Melissa E. I. McGrail, Sofie L. H. Pedersen, Andreas Hemmingsen, Lise B. Bastue, Joakim M. Svensson, Katia E. Thomsen, Laura Rosenkrands, E. Nathalie T. Wissing, Alexander T. Brandt, Freja Grauslund, Nicholai Ebert and Christoffer Wrist-Jensen, thank you for your work.

I want to thank the technical staff at DTU Chemistry, who make the world go round. Well maybe just the Depart of Chemistry, but that is no small feat. To Philip Charlie Johansen, thank you for always accommodating my need for help with the preparative HPLC and showing me the wonders of bouldering. The NMR department for maintaining the NMR machinery. To the building operations for providing support, especially Andreas G. Pedersen for fixing UV-lamps and oil pumps at a moment's notice. Lisbeth Riber for support through cleaning of glassware. To Charlotte Dansholm for starting with me on my climbing journey. Thank you.

My gratitude extends to Professor David Spring for allowing me to join his bustling and ambitious group. I learned lots during my stay. Thank you to Tom King and Fredereike Danheim for guidance in the lab. To the entire Spring group, thank you for welcoming me with open arms and making my stay truly enjoyable. A special thanks to Bethany Cooper for inviting me to sit in the rain for a couple of hours.

To my friends (Hügge and Klatrevennerne) and family who have patiently listened and supported me throughout my studies. Thank you for daring to ask about my research, nodding politely and feigning interest, it always helps to have an ear. To my mom, Lotte, and my grandparents, Lis and Frits, for feeding me and opening your homes to me during the writing period. It helped more than you realize. To my dad, Chris, for proofreading the thesis, without your commas my thesis would not be the same. To my boyfriend Michael for supporting my studies unblinkingly and wholeheartedly.

Thank you, I am truly fortunate to have you all in my life.

List of Abbreviations

AA	Amino Acid
Ac	Acetyl
ACN	Acetonitrile
ADC	Antibody Drug Conjugate
AMC	7-Amino-4-methylcoumarin
aq	Aqueous
Boc	*Tert*-butyloxycarbonyl
Bu	Butyl
DAR	Drug-antibody ratio
DBTDL	Dibutyltin dilaurate
DBU	1,8-Diazabicyclo[5.4.0]undec-7-ene
DCM	Dichloromethane
DIBO	4-Dibenzocyclooctynol
DIPEA	N,N-Diisopropylethylamine
DMAP	4-Dimethylaminopyridine
DMF	Dimethylformamide
DMP	Dess Martin periodinane
DMSO	Dimethylsulfoxide
EDC	1-Ethyl-3-(3-dimethylaminopropyl)carbodiimide
EEDQ	N-Ethoxycarbonyl-2-ethoxy-1,2-dihydroquinoline
et al.	et alia
equiv.	Equivalents
EWG	Electron withdrawing groups
FCC	Flash Column Chromatography
FDA	US Food and Drug Administration
Fmoc	Fluorenylmethoxycarbonyl
GlcNac	N-Acetylglucosamine
h	Hour(s)
HATU	1-[Bis(dimethylamino)methylene]-1H-1,2,3-triazolo[4,5-b]pyridinium 3-oxid hexafluorophosphate
HBTU	N,N,N',N'-Tetramethyl-O-(1H-benzotriazol-1-yl)uronium hexafluorophosphate
HOBt	1-Hydroxybenzotriazole
HPLC	High Performance Liquid Chromatography
IC_{50}	Inhibitory concentration 50
IgG	Immunoglobulin G
IMes	1,3-Bis(2,4,6-trimethylphenyl)-1,3-dihydro-2*H*-imidazol-2-ylidene
mc	Maleimidocaproyl
Me	Methyl
min	Minute(s)
MMAE	Monomethyl auristatin E

Ms	Methanesulfonyl
MTD	Maximum Tolerated Dose
MTS	3-(4,5-Dimethylthiazol-2-yl)-5-(3-carboxymethoxyphenyl)-2-(4-sulfophenyl)-2H-tetrazolium
MW	Microwave
NaHMDS	Sodium bis(trimethylsilyl)amide
NC	Non-cleavable
NHC	N-Heterocyclic Carbene
NHS	N-hydroxy-succinic
np	Neopentyl
pabc	*p*-Aminobenzyloxycarbonyl
PBD	Pyrrolobenzodiazepine
PBS	Phosphate buffered saline
PEG	Polyethylene glycol
Pnp	*p*-Nitrophenol
pyr	Pyridine
quant	Quantitative
RNA	Ribonucleic acid
rt	Room temperature
SAR	Structure-activity relationship
sat	Saturated
smcc	Succinimidyl-4-(N-maleimidomethyl)cyclohexane-1-carboxylate
SPPS	Solid phase peptide synthesis
TBAF	Tetrabutylammonium fluoride
TBAI	Tetrabutylammonium iodide
TBDMS	*tert*-Butyldimethylsilyl
TCE	Trichloroethanol
TCEP	Tris(2-carboxyethyl)phosphine
TEA	Triethylamine
Tf	Triflate
TFA	Trifluoroactetic acid
THF	Tetrahydrofuran
TMS	Trimethylsilyl
tol	Toluene
UNAA	Unnatural amino acid
UPLC-MS	Ultra performance liquid chromatography mass spectrometry
UV	Ultra violet

Contents

Introduction

Antibody drug conjugates (ADCs) aim to offer patients safer and more effective cancer chemotherapies. An ADC consists of an antibody, targeting antigens overexpressed on the surface of cancer cells, and a payload consisting of a chemical linker and a drug. Combining the specificity of an antibody with the potency of a small molecule cytotoxin, has been seen as a "magic bullet". Unfortunately, the reality is, there are yet many points at which the ADC can falter and after more than 20 years since the first FDA approval of an ADC, there is still room for improvement. Even though the technology of ADCs is still in its adolescence, the commercial market for is rapidly expanding, evidenced by the FDA approval of 7 ADCs in the last three years[1,2]. This attests to the enormous potential of next generation ADCs in the treatment of cancer. However, a striking trend emerges, when comparing the diversity of targets and cytotoxins employed in ADCs, with the limited selection of linkers and bioconjugation techniques used in commercial ADCs.

In an effort to amend this gap and expand the toolbox to towards safer and more effective ADCs, the following thesis has made the first steps in the development of a site-selective antibody bioconjugation strategy and has researched novel linkers for the incorporation into ADCs and

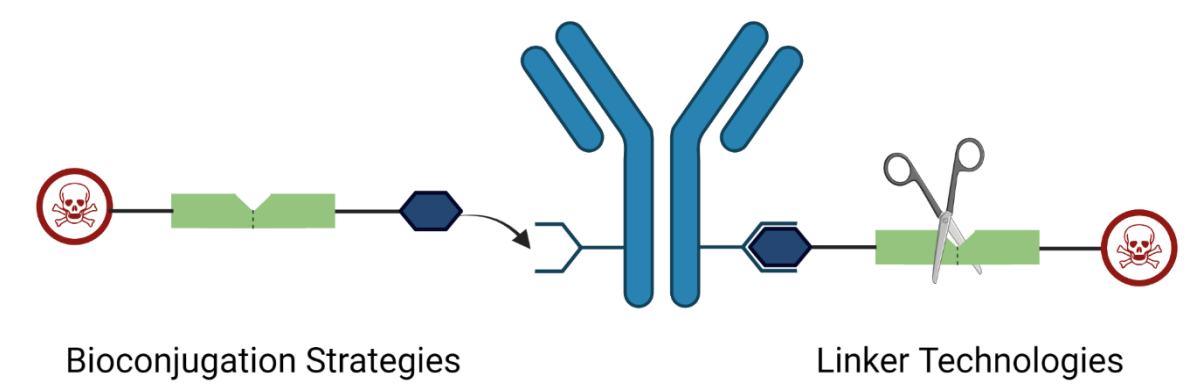

Chapter 1 briefly introduces antibody drug conjugates.

Chapter 2 covers the development of two novel bioconjugation techniques for antibodies.

Chapter 3 describes the synthesis and investigation of novel arylsulfatase cleavable linkers for the incorporation into ADCs.

Chapter 1 Antibody Drug Conjugates

Antibody-drug conjugates (ADCs) for the chemotherapeutic treatment of cancer, combine the specificity of an antibody with the toxicity of a small molecule to selectively kill cancer cells[1–7].

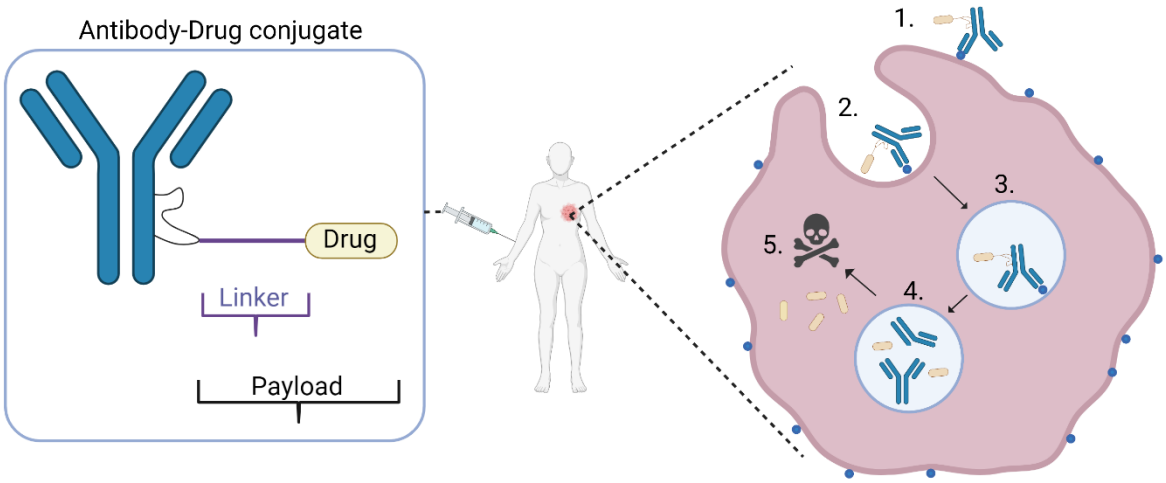

Figure 1.1. Structure and general mechanism of action of an ADC.

As seen in Figure 1.1, the antibody recognizes an antigen overexpressed on the surface of the cancer cell (1) and antigen binding triggers the internalization of the ADC (2) into an endosome (3). Upon fusion to a lysosome (4), the drug is released, as mediated by the linker, before the drug can enter the cytosol to perform its cell killing mechanism (5). In this dissertation, payload refers to the linker-drug moiety as it is attached to the antibody. ADCs offers many points at which the drug can be optimized and has thus captured the attention of scientists from many different fields. There are four key parts to consider in an ADC, (1) Choice of the antigen, (2) Choice of conjugation method, (3) Choice of linker and (4) Choice of drug[8]. ADC conjugation and linker properties will be covered in Chapters 2 and 3, respectively.

1.1 Choice of Antigen

Identification of novel targets for ADCs is of great importance, as this expands the types of cancers that ADCs can target[9]. Antigen expression and rate of internalization constitute important factors contributing to the efficacy and toxicity of the ADC[10]. Classically, the antigen should be internalizing, however, it has been hypothesized, that extracellular release in the cancer microenvironment could increase ADC potency towards solid tumors[11,12]. ADCs suffer from poor solid tumor penetration, due to their large size, which hampers diffusion into the tumor[13]. Furthermore, cancers display heterogeneous antigen expression leading to ADC resistance of antigen negative cells[14,15]. One drawback of extracellular release is the potential unselective diffusion of the released drug into healthy tissue.

1.2 Choice of Drug

The requirements of a drug used in an ADC are different to the chemotherapeutic drugs administered in their native form. Due to the antigen dependent internalization, intracellular concentrations of the drug remain relatively low, resulting in the need for highly potent drugs. Another factor to consider, is the so-called bystander effect, stemming from the release of cytotoxic drugs to the microenvironment upon apoptosis of the cell[16]. If the released drug is uncharged, it can unselectively diffuse across the cell membrane of the surrounding cell causing further cells deaths independent of antigen expression. It is not yet clear whether this phenomenon contributes enough to ADC potency to outweigh the potential off-target toxicity, however, many drugs incorporated into ADCs today, are able to diffuse across the cell membrane once released (e.g. MMAE).

1.2.1 Auristatins: A brief case study

Extensive SAR studies of Dolastatin 10 analogues have been conducted, due to the anti-cancerous nature of these exotic penta-peptide tubulin inhibitor[17–20]. Despite the scientific interest, it was not until the discovery of an amine handle for ADC linker attachment, by removal of a methyl group of the N-terminal dolavaline, that the true potential of these moieties was realised[21](Figure 1.2).

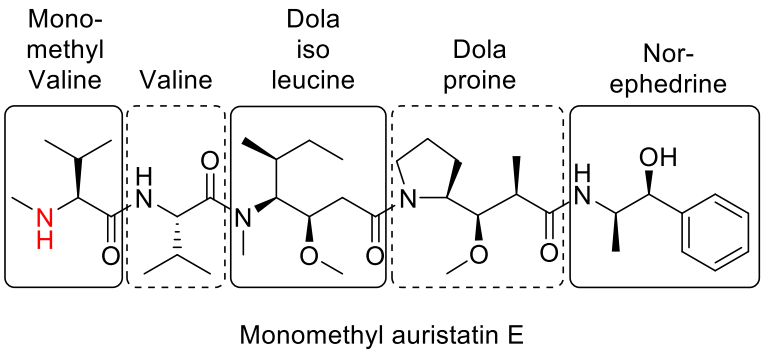

Figure 1.2. Structure of monomethyl auristatin E.

Despite the lowering of potency compared to the tertiary analogues (around a factor of 10), the mono-methyl auristatins have received unprecedented attention and MMAE is commonly used as the reference drug to compare and assess the potential of new drugs for ADCs [22–24].

1.3 The commercial market for ADC

An overview of all ADCs currently on the market can be seen below in Table 1.1 [25–28].

	Mylotarg	Adcetris	Besponsa	Lumoxiti	Polivy	Blenrep	Kadcyla	Enhertu	Trodelvy	Padcev	Akalux	Zynlonta	Tidvak	**Mode of action**
Target														*Cancer*
CD33[29–32]														AML
CD30[33–35]														Lymphoma
CD22[36–38]														Leukaemia
CD79b[39,40]														Lymphoma
BCMA[41,42]														Myeloma
HER2[43–45]														Breast
Trop2[46–49]														Breast
Nectin-4[50–55]														Urothelial
EGFR[56–60]														Head/neck
CD19[61,62]														Lymphoma
TF[63]														Cervical
Cytotoxin														*Target*
Cali[64,65]														DNA
MMAE[22]														Tubulin
MMAF[20]														Tubulin
Mertansine[66]														Tubulin
PE38[67]														eEF-2
DXd[68]														Topo I
SN-38[69]														Topo I
IR700[70]														ROS
SG3199[71]														DNA
Linker														*Cleavage*
Acid labile														pH ↓
Peptide														Peptidases
Disulfide														Reductive
NC														ADC deg.
Conjugation method														

Maleimide[72]														
Lysine[73]														
Recom[74]														

Table 1.1. Overview of all ADCs currently on the market for the treatment of cancer.

Of the 12 FDA approved ADCs, 7 have been launched since 2019, highlighting the rapid expansion and great potential within this field[75,76]. One interesting observation to be made from the impressive effort applied in the development of novel ADCs, is that the diversity of the used linkers and conjugation methods is limited in comparison to the extensive work applied for the identification of novel antigen targets and the variety of cytotoxins that are incorporated into ADCs. This gap in technological advances may decelerate the otherwise fast development of ADCs, as both conjugation and linker technologies significantly influence the safety and efficacy of ADCs[5,7,25,77–80].

1.4 Literature

1. Fu, Z., Li, S., Han, S., Shi, C. & Zhang, Y. Antibody drug conjugate: the "biological missile" for targeted cancer therapy. *Signal Transduct. Target. Ther.* **7**, (2022).

2. Jin, S. *et al.* Emerging new therapeutic antibody derivatives for cancer treatment. *Signal Transduct. Target. Ther.* **7**, (2022).

3. Mckertish, C. M. & Kayser, V. Advances and limitations of antibody drug conjugates for cancer. *Biomedicines* **9**, (2021).

4. De Cecco, M., Galbraith, D. N. & McDermott, L. L. What makes a good antibody–drug conjugate? *Expert Opin. Biol. Ther.* **21**, 841–847 (2021).

5. Dal Corso, A., Pignataro, L., Belvisi, L. & Gennari, C. Innovative Linker Strategies for Tumor-Targeted Drug Conjugates. *Chemistry - A European Journal* **25**, 14740–14757 (2019).

6. Alley, S. C., Okeley, N. M. & Senter, P. D. Antibody-drug conjugates: Targeted drug delivery for cancer. *Current Opinion in Chemical Biology* **14**, 529–537 (2010).

7. Drago, J. Z., Modi, S. & Chandarlapaty, S. Unlocking the potential of antibody–drug conjugates for cancer therapy. *Nat. Rev. Clin. Oncol.* **18**, 327–344 (2021).

8. Tang, H. *et al.* The analysis of key factors related to ADCs structural design. *Front. Pharmacol.* **10**, 1–11 (2019).

9. Criscitiello, C., Morganti, S. & Curigliano, G. Antibody–drug conjugates in solid tumors: a look into novel targets. *J. Hematol. Oncol.* **14**, 1–18 (2021).

10. Mathur, R. & Weiner, G. J. Picking the Optimal Target for Antibody-Drug Conjugates. *Am. Soc. Clin. Oncol. Educ. B.* 103–107 (2013). doi:10.14694/edbook_am.2013.33.e103

11. Dal Corso, A., Gébleux, R., Murer, P., Soltermann, A. & Neri, D. A non-internalizing antibody-drug conjugate based on an anthracycline payload displays potent therapeutic activity in vivo. *J. Control. Release* **264**, 211–218 (2017).

12. Staudacher, A. H. & Brown, M. P. Antibody drug conjugates and bystander killing: is antigen-dependent internalisation required. *Br. J. Cancer* **117**, 1736–1742 (2017).

13. Vasalou, C., Helmlinger, G. & Gomes, B. A Mechanistic Tumor Penetration Model to Guide Antibody Drug Conjugate Design. *PLoS One* **10**, 1–20 (2015).

14. Fisher, R., Pusztai, L. & Swanton, C. Cancer heterogeneity: Implications for targeted therapeutics. *Br. J. Cancer* **108**, 479–485 (2013).

15. Dagogo-Jack, I. & Shaw, A. T. Tumour heterogeneity and resistance to cancer therapies. *Nat. Rev. Clin. Oncol.* **15**, 81–94 (2018).

16. Li, F. *et al.* Intracellular released payload influences potency and bystander-killing effects of antibody-drug conjugates in preclinical models. *Cancer Res.* **76**, 2710–2719 (2016).

17. Maderna, A. & Leverett, C. A. Recent advances in the development of new auristatins: Structural modifications and application in antibody drug conjugates. *Mol. Pharm.* **12**, 1798–1812 (2015).

18. Dugal-Tessier, J., Barnscher, S. D., Kanai, A. & Mendelsohn, B. A. Synthesis and Evaluation of Dolastatin 10 Analogues Containing Heteroatoms on the Amino Acid Side Chains. *J. Nat. Prod.* **80**, 2484–2491 (2017).

19. Gao, G., Wang, Y., Hua, H., Li, D. & Tang, C. Marine antitumor peptide dolastatin 10: Biological activity, structural modification and synthetic chemistry. *Mar. Drugs* **19**, (2021).

20. Waight, A. B. *et al.* Structural basis of microtubule destabilization by potent auristatin anti-mitotics. *PLoS One* **11**, 1–14 (2016).

21. Akaiwa, M., Dugal-Tessier, J. & Mendelsohn, B. A. Antibody – Drug Conjugate Payloads ; Study of Auristatin Derivatives. *Chem. Pharm. Bull. (Tokyo).* **68**, 201–211 (2020).

22. Li, C. *et al.* Clinical pharmacology of vc-MMAE antibody–drug conjugates in cancer patients: learning from eight first-in-human Phase 1 studies. *mAbs* **12**, (2020).

23. LI, L. *et al.* Conjugating MMAE to a novel anti-HER2 antibody for selective targeted delivery. *Eur. Rev. Med. Pharmacol. Sci.* **25**, 12929–12937 (2021).

24. Lofgren, K. A., Sreekumar, S., Jenkins, E. C., Ernzen, K. J. & Kenny, P. A. Anti-tumor efficacy of an MMAE-conjugated antibody targeting cell surface TACE/ADAM17-cleaved Amphiregulin in breast cancer. *Antib. Ther.* **4**, 252–261 (2021).

25. Sheyi, R., de la Torre, B. G. & Albericio, F. Linkers: An Assurance for Controlled Delivery of Antibody-Drug Conjugate. *Pharmaceutics* **14**, (2022).

26. Lin, A. Y. & Dinner, S. N. Moxetumomab pasudotox for hairy cell leukemia: Preclinical development to FDA approval. *Blood Adv.* **3**, 2905–2910 (2019).

27. Shitara, K. *et al.* Discovery and development of trastuzumab deruxtecan and safety management for patients with HER2-positive gastric cancer. *Gastric Cancer* **24**, 780–789 (2021).

28. Kitamura, N. *et al.* Current trends and future prospects of molecular targeted therapy in head and neck squamous cell carcinoma. *Int. J. Mol. Sci.* **22**, 1–13 (2021).

29. Molica, M. *et al.* Cd33 expression and gentuzumab ozogamicin in acute myeloid leukemia: Two sides of the same coin. *Cancers (Basel).* **13**, 1–20 (2021).

30. Walter, R. B., Raden, B. W., Kamikura, D. M., Cooper, J. A. & Bernstein, I. D. Influence of CD33 expression levels and ITIM-dependent internalization on gemtuzumab ozogamicin-induced cytotoxicity. *Blood* **105**, 1295–1302 (2005).

31. Walter, R. B. The role of CD33 as therapeutic target in acute myeloid leukemia. *Expert Opin. Ther. Targets* **18**, 715–718 (2014).

32. Liu, J., Tong, J. & Yang, H. Targeting CD33 for acute myeloid leukemia therapy. *BMC Cancer* **22**, 1–7 (2022).

33. Shen, Y. *et al.* Conjugation of DM1 to anti-CD30 antibody has potential antitumor activity in CD30-positive hematological malignancies with lower systemic toxicity. *MAbs* **11**, 1149–1161 (2019).

34. Hansen, H. P., Paes Leme, A. F. & Hallek, M. Role of ADAM10 as a CD30 Sheddase in Classical Hodgkin Lymphoma. *Front. Immunol.* **11**, 1–5 (2020).

35. van der Weyden, C. A., Pileri, S. A., Feldman, A. L., Whisstock, J. & Prince, H. M. Understanding CD30 biology and therapeutic targeting: a historical perspective providing insight into future directions. *Blood Cancer J.* **7**, e603 (2017).

36. Clark, E. A. & Giltiay, N. V. CD22: A Regulator of Innate and Adaptive B Cell Responses and Autoimmunity. *Front. Immunol.* **9**, (2018).

37. Yu, S. F. *et al.* A novel anti-CD22 anthracycline-based antibody-drug conjugate (ADC) that overcomes resistance to auristatin-based ADCs. *Clin. Cancer Res.* **21**, 3298–3306 (2015).

38. Ereño-Orbea, J. *et al.* Molecular basis of human CD22 function and therapeutic targeting. *Nat. Commun.* **8**, 1–11 (2017).

39. Havranek, O. *et al.* B-cell receptor signaling in diffuse large B-cell lymphoma. *Blood* **130**, 995–1006 (2017).

40. Pfeifer, M. *et al.* Anti-CD22 and anti-CD79B antibody drug conjugates are active in different molecular diffuse large B-cell lymphoma subtypes. *Leukemia* **29**, 1578–1586 (2015).

41. Cho, S. F., Anderson, K. C. & Tai, Y. T. Targeting B cell maturation antigen (BCMA) in multiple myeloma: Potential uses of BCMA-based immunotherapy. *Front. Immunol.* **9**, (2018).

42. Yu, B., Jiang, T. & Liu, D. BCMA-targeted immunotherapy for multiple myeloma. *J. Hematol. Oncol.* **13**, 1–24 (2020).

43. Zanto, T. P., Hennigan, K., Östberg, M., Clapp, W. C. & Gazzaley, A. The oncogene HER2. *Oncogene* **45**, 6469–6487 (2007).

44. Martínez-Sáez, O. & Prat, A. Current and Future Management of HER2-Positive Metastatic Breast Cancer. *JCO Oncol. Pract.* **17**, 594–604 (2021).

45. Mitri, Z., Constantine, T. & O'Regan, R. The HER2 Receptor in Breast Cancer: Pathophysiology, Clinical Use, and New Advances in Therapy. *Chemother. Res. Pract.* **2012**, 1–7 (2012).

46. Lenárt, S. *et al.* Trop2: Jack of all trades, master of none. *Cancers (Basel).* **12**, 1–28 (2020).

47. Adc, T., Food, U. S., Sankyo, D. & Sankyo, D. Dendritic cell revival. *Nat. Biotechnol.* **39**, 124 (2021).

48. Zaman, S., Jadid, H., Denson, A. C. & Gray, J. E. Targeting trop-2 in solid tumors: Future prospects. *Onco. Targets. Ther.* **12**, 1781–1790 (2019).

49. Shvartsur, A. & Bonavida, B. Trop2 and its overexpression in cancers: Regulation and clinical/therapeutic implications. *Genes and Cancer* **6**, 84–105 (2015).

50. Chatterjee, S., Sinha, S. & Kundu, C. N. Nectin cell adhesion molecule-4 (NECTIN-4): A potential target for cancer therapy. *Eur. J. Pharmacol.* **911**, 174516 (2021).

51. Heath, E. I. & Rosenberg, J. E. The biology and rationale of targeting nectin-4 in urothelial carcinoma. *Nat. Rev. Urol.* **18**, 93–103 (2021).

52. Wong, J. L. & Rosenberg, J. E. Targeting nectin-4 by antibody-drug conjugates for the treatment of urothelial carcinoma. *Expert Opinion on Biological Therapy* **21**, 863–873 (2021).

53. Liu, Y. *et al.* Role of Nectin-4 protein in cancer (Review). *Int. J. Oncol.* **59**, 1–14 (2021).

54. Deng, H., Shi, H., Chen, L., Zhou, Y. & Jiang, J. Over-expression of Nectin-4 promotes progression of esophageal cancer and correlates with poor prognosis of the patients. *Cancer Cell Int.* **19**, 1–13 (2019).

55. Zeindler, J. *et al.* Nectin-4 Expression Is an Independent Prognostic Biomarker and Associated With Better Survival in Triple-Negative Breast Cancer. *Front. Med.* **6**, 1–7 (2019).

56. Si, Y. *et al.* Anti-EGFR antibody-drug conjugate for triple-negative breast cancer therapy. *Eng. Life Sci.* **21**, 37–44 (2021).

57. Sabbah, D. A., Hajjo, R. & Sweidan, K. Review on Epidermal Growth Factor Receptor (EGFR) Structure, Signaling Pathways, Interactions, and Recent Updates of EGFR Inhibitors. *Curr. Top. Med. Chem.* **20**, 815–834 (2020).

58. Cai, W. Q. *et al.* The Latest Battles Between EGFR Monoclonal Antibodies and Resistant Tumor Cells. *Front. Oncol.* **10**, (2020).

59. Thomas, R. & Weihua, Z. Rethink of EGFR in cancer with its kinase independent function on board. *Front. Oncol.* **9**, 1–16 (2019).

60. Santos, E. da S. *et al.* EGFR targeting for cancer therapy: Pharmacology and immunoconjugates with drugs and nanoparticles. *Int. J. Pharm.* **592**, (2021).

61. Stevens, M. *et al.* The British Childhood Cancer Survivor Study: Objectives, methods, population structure, response rates and initial descriptive information. *Pediatr. Blood Cancer* **50**, 1018–1025 (2008).

62. Wang, K., Wei, G. & Liu, D. CD19: a biomarker for B cell development, lymphoma diagnosis and therapy. *Exp. Hematol. Oncol.* **1**, 1–7 (2012).

63. Unruh, D. & Horbinski, C. Beyond thrombosis: The impact of tissue factor signaling in cancer. *J. Hematol. Oncol.* **13**, 1–14 (2020).

64. Ricart, A. D. Antibody-drug conjugates of calicheamicin derivative: Gemtuzumab

ozogamicin and inotuzumab ozogamicin. *Clin. Cancer Res.* **17**, 6417–6427 (2011).

65. Vollmar, B. S. *et al.* Calicheamicin Antibody – Drug Conjugates with Improved Properties. **33**, 18–20

66. Choi, W. G. *et al.* Mertansine inhibits mRNA expression and enzyme activities of cytochrome P450s and uridine 5'-diphospho-glucuronosyltransferases in human hepatocytes and liver microsomes. *Pharmaceutics* **12**, (2020).

67. Safari, E. *et al.* Cytotoxic effect of immunotoxin containing the truncated form of pseudomonas exotoxin A and anti-VEGFR2 on HUVEC and MCF-7 cell lines. *Cell J.* **16**, 203–210 (2014).

68. Okamoto, H. *et al.* Pharmacokinetics of trastuzumab deruxtecan (T-DXd), a novel anti-HER2 antibody-drug conjugate, in HER2-positive tumour-bearing mice. *Xenobiotica* **50**, 1242–1250 (2020).

69. Mullangi, R., Ahlawat, P. & Srinivas, N. R. Irinotecan and its active metabolite, SN-38: Review of bioanalytical methods and recent update from clinical pharmacology perspectives. *Biomedical Chromatography* **24**, 104–123 (2010).

70. Mączyńska, J. *et al.* Immunomodulatory activity of IR700-labelled affibody targeting HER2. *Cell Death Dis.* **11**, (2020).

71. Tiberghien, A. C. *et al.* Design and Synthesis of Tesirine, a Clinical Antibody-Drug Conjugate Pyrrolobenzodiazepine Dimer Payload. *ACS Med. Chem. Lett.* **7**, 983–987 (2016).

72. Ravasco, J. M. J. M., Faustino, H., Trindade, A. & Gois, P. M. P. Bioconjugation with Maleimides: A Useful Tool for Chemical Biology. *Chem. - A Eur. J.* **25**, 43–59 (2019).

73. Gautier, V., Boumeester, A. J., Lössl, P. & Heck, A. J. R. Lysine conjugation properties in human IgGs studied by integrating high-resolution native mass spectrometry and bottom-up proteomics. *Proteomics* **15**, 2756–2765 (2015).

74. Agrawalla, B. K. *et al.* Chemoselective Dual Labeling of Native and Recombinant Proteins. *Bioconjug. Chem.* **29**, 29–34 (2018).

75. Tong, J. T. W., Harris, P. W. R., Brimble, M. A. & Kavianinia, I. An insight into fda approved antibody-drug conjugates for cancer therapy. *Molecules* **26**, (2021).

76. Food and Drug Administration. FDA grants accelerated approval to tisotumab vedotin-tftv for recurrent or metastatic cervical cancer. *U.S Food and Drug administration* (2021). Available at: https://www.fda.gov/drugs/resources-information-approved-drugs/fda-grants-accelerated-approval-tisotumab-vedotin-tftv-recurrent-or-metastatic-cervical-cancer.

77. Bargh, J. D., Isidro-Llobet, A., Parker, J. S. & Spring, D. R. Cleavable linkers in antibody-drug conjugates. *Chem. Soc. Rev.* **48**, 4361–4374 (2019).

78. Su, D. & Zhang, D. Linker Design Impacts Antibody-Drug Conjugate Pharmacokinetics and Efficacy via Modulating the Stability and Payload Release Efficiency. *Front. Pharmacol.*

12, (2021).

79. Kostova, V., Désos, P., Starck, J. B. & Kotschy, A. *The chemistry behind adcs*. *Pharmaceuticals* **14**, (2021).

80. Su, Z. *et al.* Antibody–drug conjugates: Recent advances in linker chemistry. *Acta Pharm. Sin. B* **11**, 3889–3907 (2021).

Chapter 2 Bioconjugation

The chemical modification of proteins by the attachment of small molecules, offers scientists a powerful tool to explore biological pathways and develop novel therapeutics. However, the diverse and polymeric nature of proteins presents a unique challenge, due to the difficulty of differentiation of one site or residue over the other, that has sparked the development of diverse site-selective bioconjugation technologies[3–26]. Despite the expanding toolset, few procedures are utilized practically, due to either convention or convenience.

The main categories of strategies used for bioconjugation and the advantages and limitations as well as some well-known examples are briefly summarized below (Table 2.1)[11].

Method	Advantages/Limitations	Examples
	Direct modifications of native proteins	
N/C terminal [7,9]	Advantages: No protein engineering, termini are often solvent accessible, selective, homogeneous conjugates. Limitations: Termini availability (i.e. not required for activity or PTM), can be dependent on terminal AA, only 1 conjugation site per monomer.	Chemical ligation[7] Amine conjugation[27]
Side chain [16,18]	Advantages: No protein engineering, attachment of several moieties per chain. Limitations: Heterogeneous conjugation, can rely on distinct micro-environmental features.	Maleimide[28] Lysine[17] Tyrosine[20] Cysteine[24] Cysteine rebridging[29–35] Photo-redox[21]
PTM [4]	Advantages: Orthogonality, homogeneous conjugates. Limitations: Disruption of signaling, expression system PTM variability[36].	Glyclick[37–39]
	Protein modification via genetic manipulation	
Unnatural amino acids (unAA)[40–47]	Advantages: Homogenous conjugates, control of number and placement of conjugation sites. Limitations: Cumbersome development of expression systems using unAA, low expression levels, expensive amino acids used as starting material.	Azido containing AAs Ketone containing AAs
Insertion of recognition motif using	Advantages: Easier expression when using nAA, homogeneous conjugates.	Sequence recognition by enzyme[48–51]

natural amino acids (nAA)	Limitations: Protein engineering required, sustained protein function limits the number of motifs that can be introduced, short motifs required.	SpyCatcher/ SpyTag[52]

Table 2.1. Overview of bioconjugation methods, advantages and limitations with examples in each category.

As described above, there are many factors to consider when choosing a suitable bioconjugation method highlighting the need for developing novel bioconjugation strategies. The development of a sequence specific conjugation of serine method will be covered in part I, inspired by the catalytic triad of hydrolytic enzymes. Cysteine conjugation will be covered in more detail in part ii, in relation to the development of a method for the preparation of highly homogeneous antibody conjugates.

2.1 Part I

2.1.1 Aim

The aim of this project is to develop a novel site-selective serine conjugation method driven by the microenvironment introduced by a specific sequence of natural amino acids, inspired by the catalytic triad of hydrolytic enzymes with, O-selectivity promoted by use of an N-heterocyclic carbene (NHC) (Figure 2.1). It is envisaged, that the sequence can be introduced using recombinant methods to select the optimal position for attachment. The novel strategy could expand the toolset for site-selective protein conjugation, as well as investigating utility of NHCs in bioconjugation.

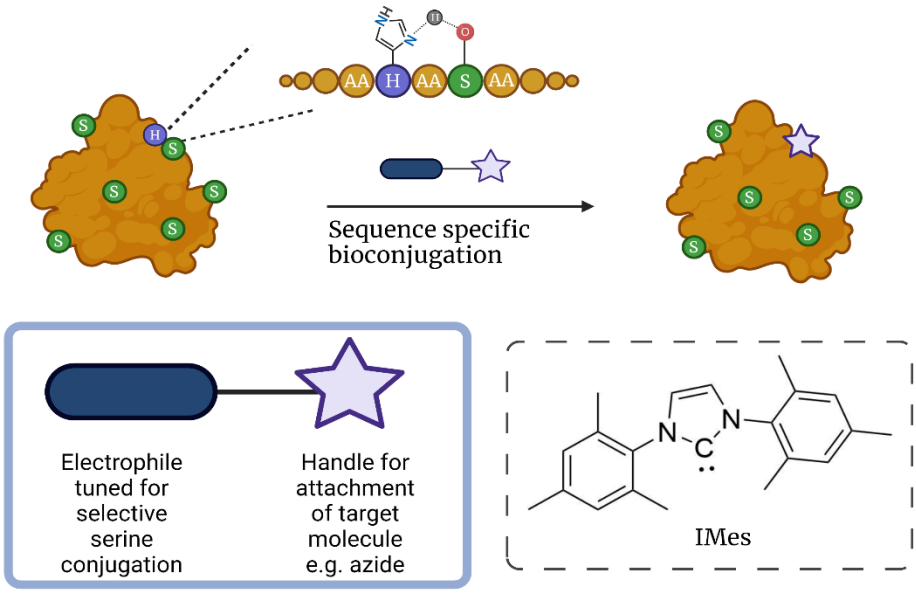

Figure 2.1. The concept of a novel sequence specific serine bioconjugation.

2.1.2 Introduction

Serine bioconjugation

Serine/threonine residues are often found in the catalytic site of hydrolytic enzymes acting as a nucleophile[1]. The nucleophilicity of the serine is enhanced by hydrogen bonding to surrounding residues[2]. Despite the potential utility of serine selective bioconjugation[3], little progress has been made towards developing serine/threonine selective bioconjugation stemming from the nucleophilic competition of lysine and cysteine residues, as well the aqueous solvent. To date, one serine selective conjugation method has been published, by Vantourout et al., that harnesses the inherent oxophilic nature of phosphorous to access selective serine conjugation (Scheme 2.1)[4].

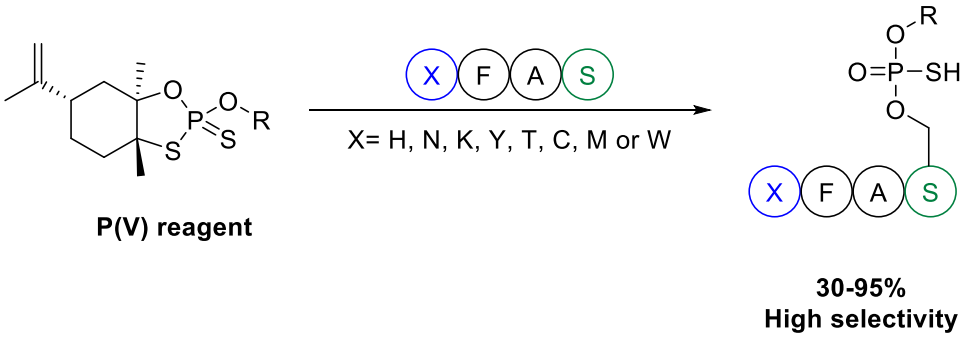

Scheme 2.1. First published serine conjugation takes advantage of P(V) reagents to attach small molecules via a phosphorothioate linkage.

The authors were able to selectively modify longer peptides, as well as the proteins ubiquitin and 434 repressor in modest yields (20-40%). This ground breaking technique might, however, prove to have limited applications in a practical sense. Firstly, conjugation is carried out in 4:1 DMF:water, conditions that are not generally applicable when working with large biomolecules, due to possible denaturation. Secondly, an excess of strong base (DBU, 50 equiv.) is used, which may be incompatible with many proteins. Lastly, compared to established procedures, low conjugation yields were achieved (up to 40%) on larger proteins. Thus, developing new serine conjugation tools could prove valuable for the bioconjugation field.

Sequence activated serine

First described by Miller et al. during biotinylation of peptides with NHS-esters and Pnp-esters, hydroxy-functionalized residues displayed surprising reactivity when in close proximity to a histidine residue[5]. It was proposed that the histidine hydrogen bonds the proton of the adjacent alcohol, thereby increasing the nucleophilicity of the alcohol (Figure 2.2).

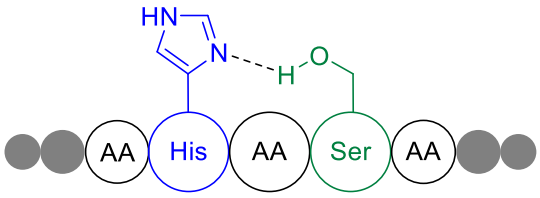

Figure 2.2. Proposed mechanism of histidine activation by Miller et al.

In 2008 Mädler et al. systematically elucidated the pH and residue microenvironment effects on homo-bifunctional NHS-ester cross-linking reactivity[6]. Significant reaction was observed on tyrosine and serine residues adjacent to histidine and a new mechanism was proposed (Figure 2.3), whereby the histidine is temporarily acetylated by the secondary NHS-ester of the cross-linking species, thereby increasing the local concentration of the reagent to promote esterification.

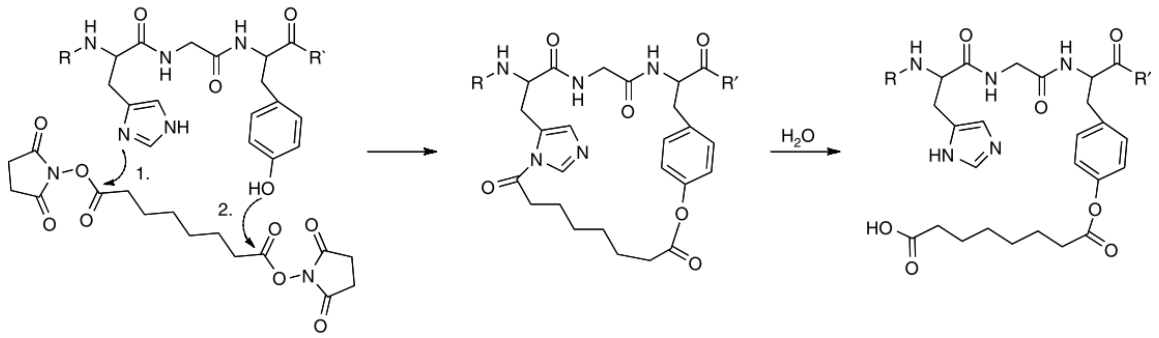

Figure 2.3. Proposed mechanism for the enhanced tyrosine reactivity by Mädler et al. Figure is inserted from ref[6]

Katrine Qvortrup further investigated histidine activation of serine in unpublished work, envisioning that this enhanced reactivity could be harnessed to develop novel site-selective bioconjugation reactions.

Several peptides were synthesized and tested with various mono-acetylating reagents and it was discovered that efficient conjugation (100%, 2h) could be accomplished when 1 alanine was inserted between the His and Ser residues (see Table 2.2). Furthermore, 0% conjugation was observed for the peptide not containing His, supporting the mechanism proposed by Miller.

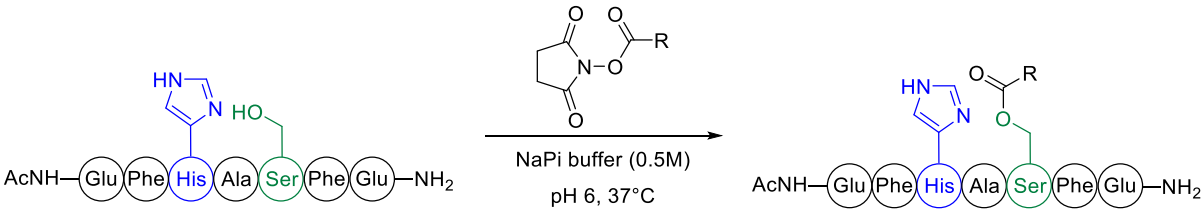

Nr of Alanine	Conversion 2h %
No Hisitidine	0
0	18
1	100
2	41
3	59
4	29
5	72

Table 2.2. Study of the effect of the distance between serine and histidine on serine reactivity.

Unfortunately, it was not possible to outcompete lysine reactivity towards the NHS-ester, thus, a secondary component was required to enhance the O- versus N-selectivity and potentially, organocatalysis could provide the solution.

N-heterocyclic carbenes

Carbenes are neutral species containing a carbon atom with six valence electrons, which are normally too reactive to be observed, due to the rapid insertion into σ C-H bonds[7]. However, the discovery of the stabilization of carbenes by the introduction of adjacent heteroatoms, the so-called persistent carbenes, has inspired the use of this exotic species as ligands in transition metal catalysts and in organocatalysis[8–17]. Particularly, N-heterocyclic carbenes (NHCs) containing proximal bulky substituents have been investigated and the simple synthesis has enabled the tuning of the electronic effects for a wide range of applications. The surprising stability arises from the σ-withdrawing nature of the nitrogen, while the lone pair donates electron density into the unfilled p-orbital (Figure 2.4)[16]. There are four key structural features defining an NHC: heteroatoms, ring size, backbone structure and substitution[18]. Insertion of proximally positioned bulky groups prevents dimerization and backbone unsaturation provides enhanced stability via the aromaticity of the heterocycle. Finally, ring size can modulate the ground state preference of the carbene and heteroatoms modulate stability.

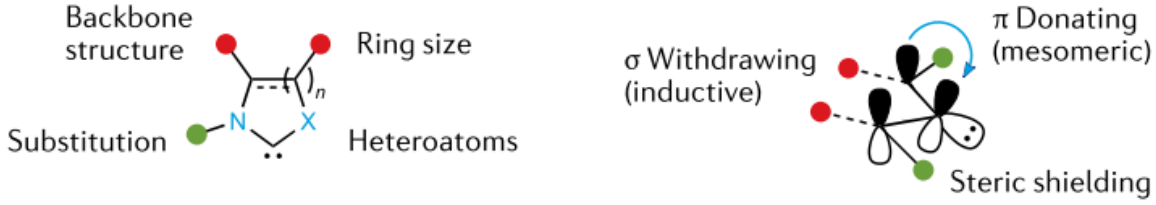

Figure 2.4. Key features of NHCs and the stabilization effects of amines on carbenes. Figure is inserted from reference [18].

These modular properties introduce the potential to explore novel reactivity that can be tuned towards the desired outcome[19,20].

Many O-selective acylation reactions have been developed[21–24], however, most require harsh conditions not applicable for bioconjugation, such as strong base and high temperatures. An interesting method for selective O-acylation catalyzed by the NHC 1,3-bis(2,4,6-trimethylphenyl)-1,3-dihydro-2H-imidazol-2-ylidene (IMes) in the presence of amines, was developed by Samanta et al.[25]. Advantages of this method include, mild reaction conditions, high selectivity, high yields and a large substrate scope, leaving room for fine tuning. The paradigm of the requirement of inert glovebox conditions for the use of NHCs as organocatalysts, has recently been shifted, as syntheses in aqueous media are being reported[26–29]. Thus, it was envisaged, that addition of IMes could enhance O-selectivity for the development of a serine selective bioconjugation method.

2.1.3 Initial screening

The following section will report and discuss the results and progress achieved towards the development of a sequence specific serine conjugation method.

Initially, 2,2,2-trifluoro ethyl benzoate **2.3** was synthesized, as this moiety displayed high selectivity in the article by Samanta[25]. NHS-esters **2.1** and **2.2** were also synthesized to determine whether IMes activation of the alcohol could outcompete the inherent amine reactivity of these moieties. Lastly, the 2,2,2-trifluoro propyl benzoate **2.4** was prepared to probe the leaving group properties required of the electrophile. The conditions and yields of the synthesis of compounds **2.1-2.4** are reported in Table 2.3. The low yield reported for compound **2.3** was due to the low boiling point of the product, resulting in loss during purification.

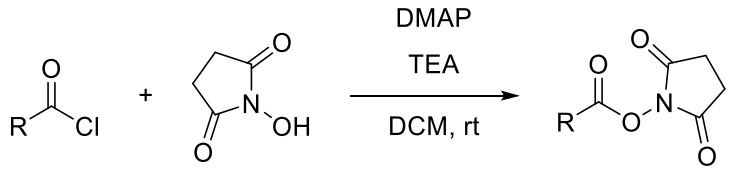

	Structure	Yield		Structure	Yield
2.1	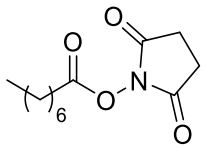	63%	**2.2**	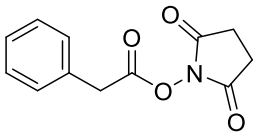	63%

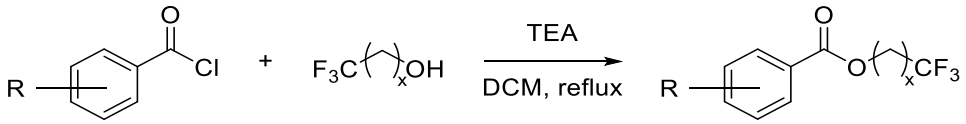

	Yield		Yield
2.3	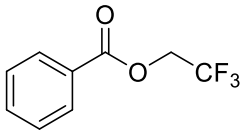 26%	**2.4**	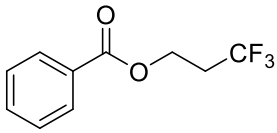 66%

*Table 2.3. Synthetic conditions and yields of compounds **2.1-2.4**.*

Screen 1

Initially, a reactivity screen was designed to verify the method for selectivity and analysis. Furthermore, the screen was designed to determine the relationship between IMes concentration and selectivity. Benzyl alcohol and benzyl amine were used as model compounds, while also providing UV-activity to the product for ease of analysis by UPLC-MS. The screens were carried out in LCMS vials under stirring. The reactions were carried out at rt and were analyzed by UPLC-MS after 3h. Results from the first screen are reported in Figure 2.5.

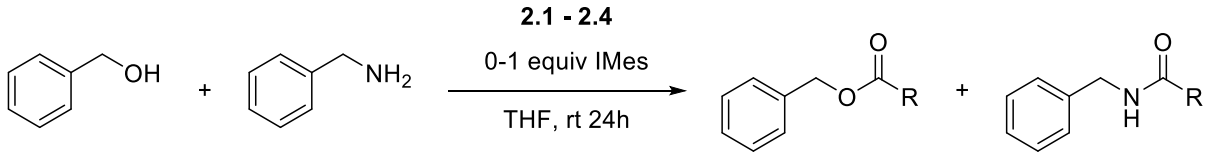

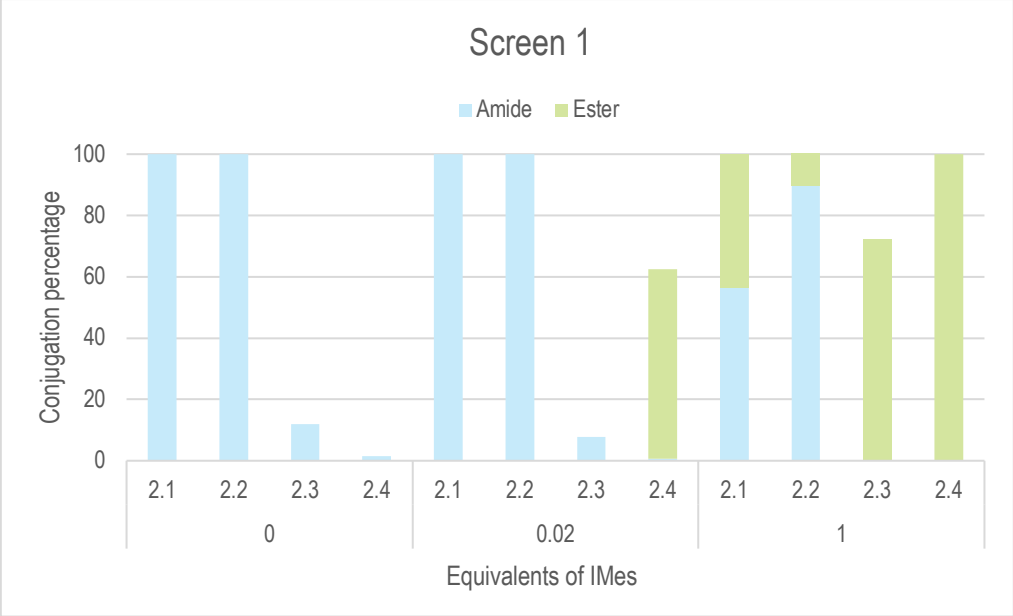

Figure 2.5. Results of screen 1 as analyzed by UPLC-MS. Yields were determined by integration of the UV-trace of the products compared to the remaining starting electrophile after 3h reaction time.

As expected, the NHS-esters (**2.1** and **2.2**) efficiently reacted with amines without the presence of IMes and at low IMes loading, complete amidation was observed. In the presence of 1 equivalent of IMes, alcohol reactivity was sufficiently high to enable some ester formation (57-90%), however, NHS-ester amine reactivity might be too high to achieve complete selectivity. Thus, the NHS-esters were not investigated further. The trifluoro esters, **2.3** and **2.4**, displayed little reactivity towards benzylamine and addition of IMes encouraged 100% selectivity and high reactivity (72-100%). Generally, it was observed that IMes significantly impacted the esterification and that higher concentrations of IMes yielded higher O-selectivity. The encouraging results from **2.3** and **2.4** inspired a new series of electrophiles. It was especially interesting to investigate the effect of decorating the benzene ring reactivity and selectivity.

Synthesis of trifluoro ester analogues

Various benzoyl chlorides were commercially available and were reacted with 2,2,2-trifluro ethanol, propanol or butanol (Table 2.4).

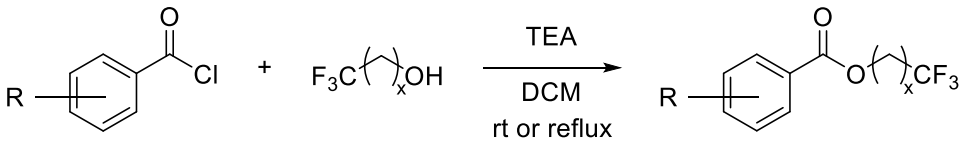

	Structure	Yield		Structure	Yield
2.5	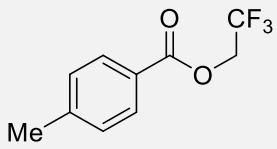	78%	**2.6**	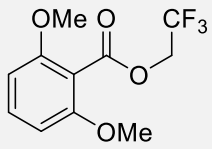	62%

2.7	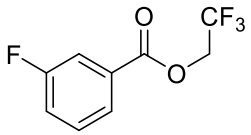	77%	
2.8	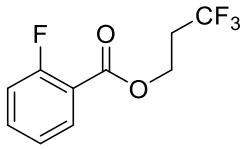	91%	
2.9	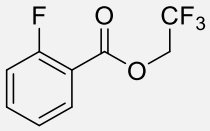	55%	
2.10	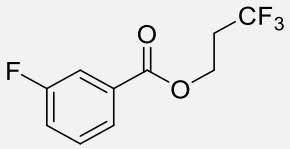	90%	
2.11	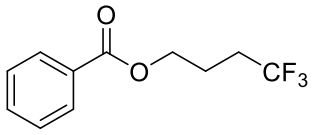	86%	

*Table 2.4. Conditions and yields of the syntheses of compounds **2.5-2.11**.*

The synthesis of this series of electrophiles proceeded with satisfactory yields (55-91%).

Screen 2

The screen was carried out at rt in LCMS vials in THF under stirring. The reactions were analyzed by UPLC-MS after 3h and 24h reaction times. The results reported in Figure 2.6 are after a 24h reaction time.

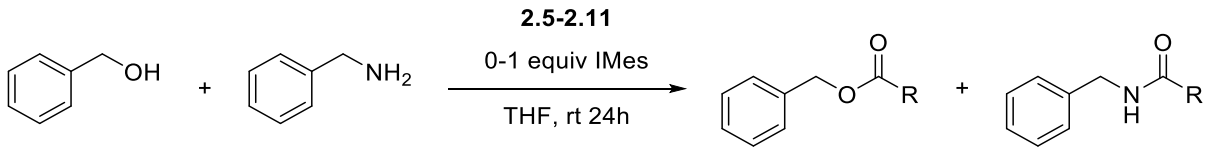

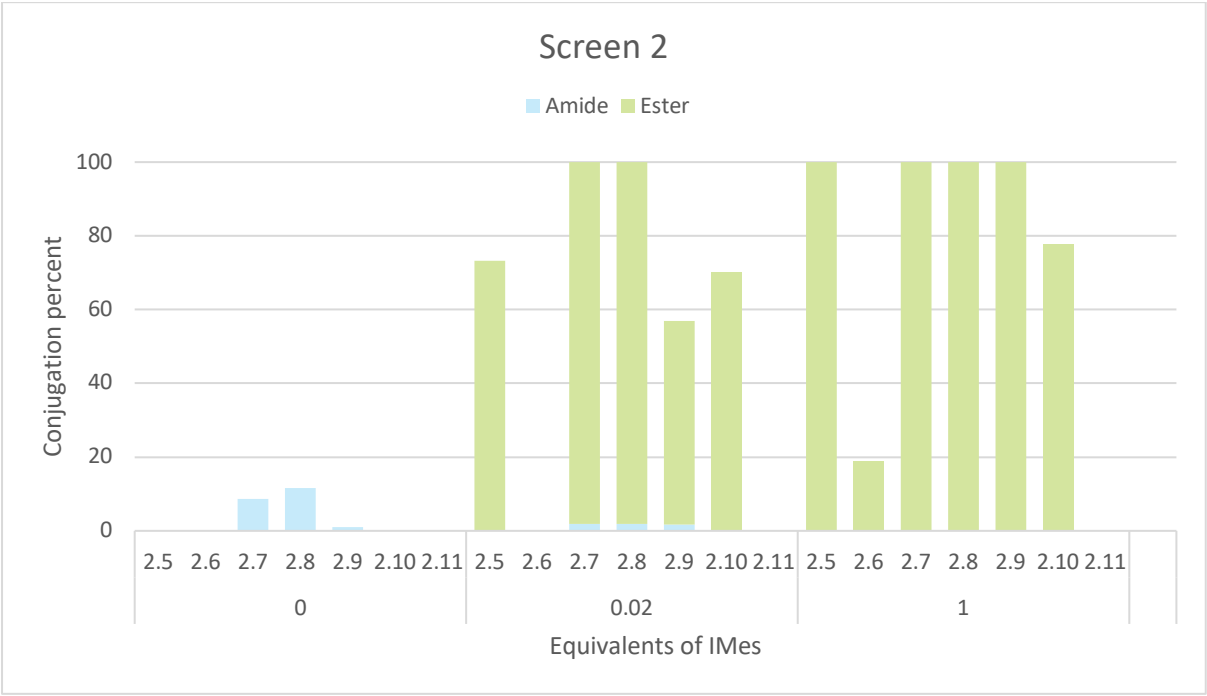

Figure 2.6. Results for screen 2 as analyzed by UPLC-MS. Yields were determined by integration of the UV-trace of the products and compared to remaining electrophile after 24h reaction time.

As observed in the initial screen, the trifluoro esters were generally unreactive towards benzylamine (max 12% amidation). In the presence of 0.02 equiv. of IMes, a significant rise in esterification, as well as suppression amide formation, was observed. In the presence of 1 equivalent of IMes, no amidation and generally higher ester-conversion (up to 100%) was observed. For compound **2.6**, only 19% esterification was observed in the presence of 1 equivalent of IMes, the low reactivity likely stemming from the steric bulk from the substituents. For compound **2.11**, the inductive effect of the CF_3 group was too far removed to promote esterification or amidation. Specifically, **2.7** and **2.9** were of interest, as complete reaction with high selectivity was observed after 3h reaction time when using 0.02 equivalents of IMes(results not shown).

With these results in hand, solvent tolerance was investigated, with an emphasis on aqueous media.

Screen 3

Both fluorine analogues (**2.7** and **2.9**) showed great selectivity and rapid reaction in the presence 0.02 equivalents of IMes and were, therefore, carried forward to investigate the solvent tolerability of the reaction by changing to the solvents DMSO and ACN, which are more compatible with bioconjugation. DMSO is commonly used during bioconjugation to dissolve the organic components[30]. Water concentration was also varied (0-50%) to investigate how the presence of aqueous media affected reaction efficiency and selectivity, as bioconjugations are commonly carried out in aqueous media for the stability of the biomolecule. Results are presented in Figure 2.7.

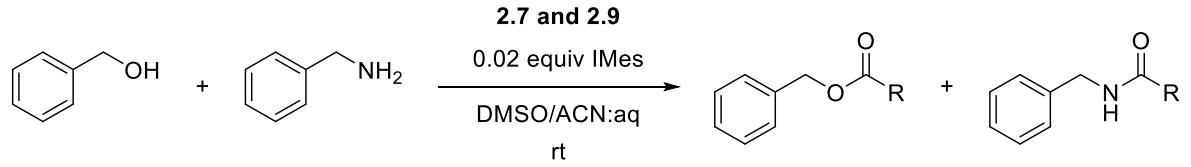

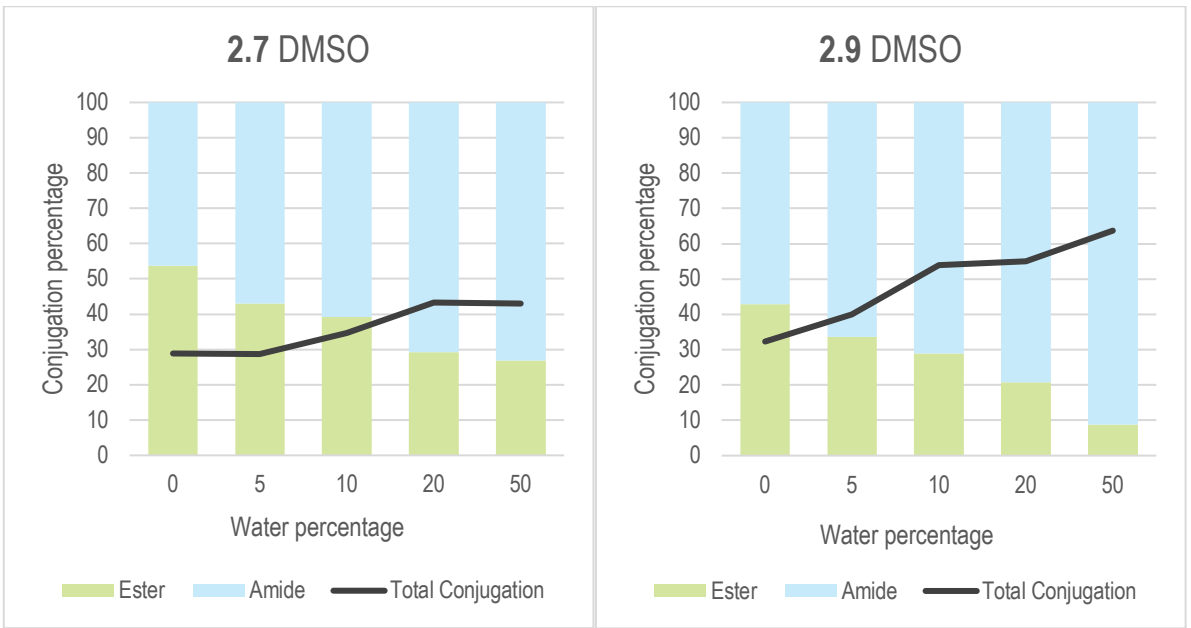

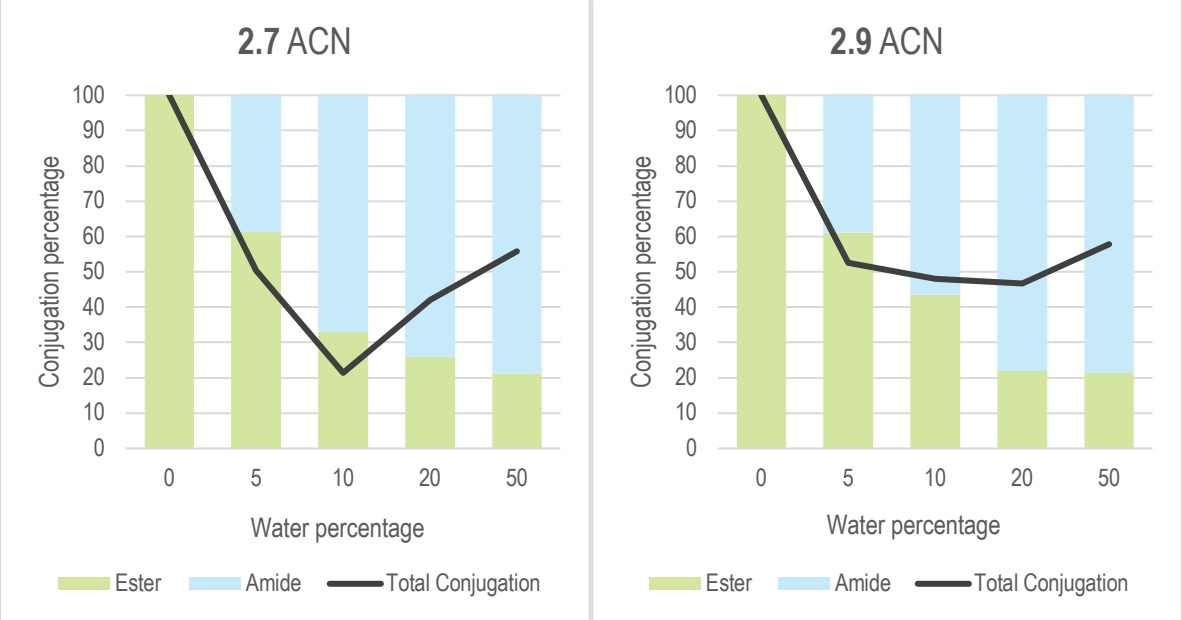

*Figure 2.7. Results from screen 3 as analyzed by UPLC-MS of compound **2.7** and **2.9** in DMSO and ACN in various concentrations of water after 24h. Selectivity was determined by integration of the UV-trace and comparison of ester vs amide formation, the relative ratio is reported. Total conjugation was determined by the combined integrals of ester and amide formation compared to the remaining electrophile represented by the black line.*

Reactivity and selectivity in DMSO were significantly reduced compared to the initial screens in THF, even without the addition of water. This was surprising, as DMSO is commonly used as solvent during NHC-metal reactions[31], although one paper reports a significant lowering of reaction yields in the presence of DMSO, when the NHC was employed as an organocatalyst.[8]. Furthermore, in DMSO, O-selectivity decreased with increasing water concentration.

The reactions in pure acetonitrile displayed the same characteristics as observed in THF, however, any addition of water decreased ester selectivity and overall reactivity. To understand this observed phenomenon, the mechanism of O-selectivity as suggested by Samanta et al. was reviewed. The theoretical study indicated that increased O-selectivity arose from activation by strong hydrogen bonding between IMes and the alcohol, leading to the increased nucleophilicity of the alcohol. Thus, it was hypothesized, that the lowered selectivity and reactivity resulted from the competitive hydrogen binding of water.

Vinyl ester activation mechanism

The poor reactivity and selectivity in the presence of water of the trifluoro esters, resulted in the investigation of a different type of electrophile, the vinyl esters. Esterification via vinyl ester can happen via two mechanisms, activation of the alcohol nucleophile, or activation of the electrophile via NHC covalently binding the electrophile, while coordinating the incoming alkoxide to increase the proximity of the reacting species according to paper by Samanta et al. (Scheme 2.2)[25].

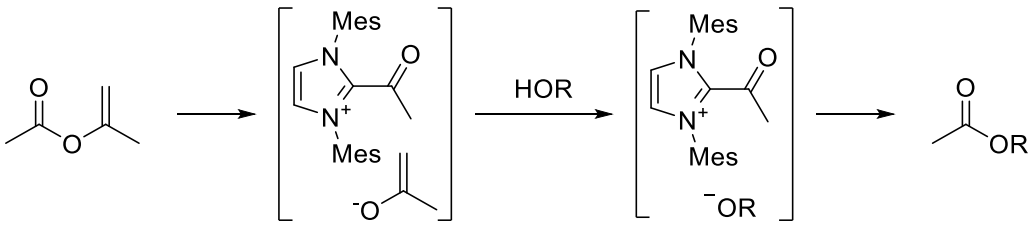

Scheme 2.2. Secondary mechanism of selective esterification catalyzed by IMes, proposed by Samanta et al.

This mechanism was suggested for the reaction of vinyl esters. It was hypothesized that pre-mixing of a vinyl ester with IMes in an organic solvent, could form the activated electrophile before the addition of the nucleophile in aqueous solution. With the IMes bound to the electrophile before the addition of water, it was thought that O-selectivity could be retained by avoiding IMes-water hydrogen bonding.

Synthesis of vinyl ester electrophiles

Samanta et al. studied the O-selectivity using isopropenyl acetate, however, synthesizing analogues of this would require working with propyne gas. It was envisaged that the longer hept-1-en-2-yl ester would react in a similar manner. Thus, the scaffolds displayed in Table 2.5 were synthesized. The synthetic procedure was based on literature[32].

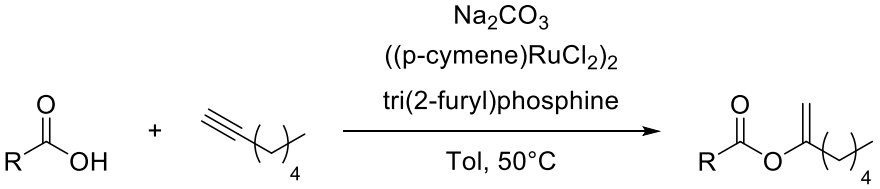

	Structure	Yield		Structure	Yield
2.12	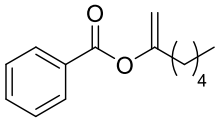	80%	**2.13**	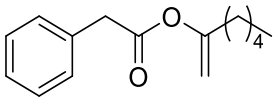	78%
2.14	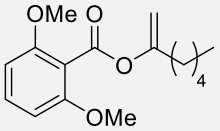	4%	**2.15**	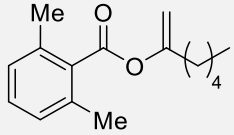	82%
2.16	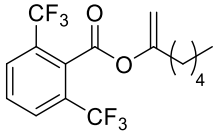	52%	**2.17**	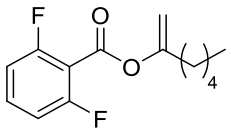	70%
2.18	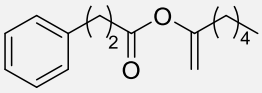	55%	**2.19**	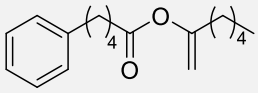	80%

*Table 2.5. Synthetic conditions and yields of compounds **2.12-2.19**.*

Synthesis and purification of **2.12-2.19** went smoothly with the exception of **2.14**. The reaction was slow and only afforded 4% conversion, however, only small amounts of material were needed for the screen and it was decided to proceed despite the low yield. Both aliphatic and benzylic

esters were synthesized. For the benzylic vinyl esters, various aromatic substituents were synthesized to determine the effect of substituents on selectivity and reactivity.

Screen 4

With the vinyl ester analogues in hand, the next screen was carried out in a similar manner to screen **1** and **2**. The commercially available isopropenyl acetate **2.20** was also included in the screen. Results are reported in Figure 2.8.

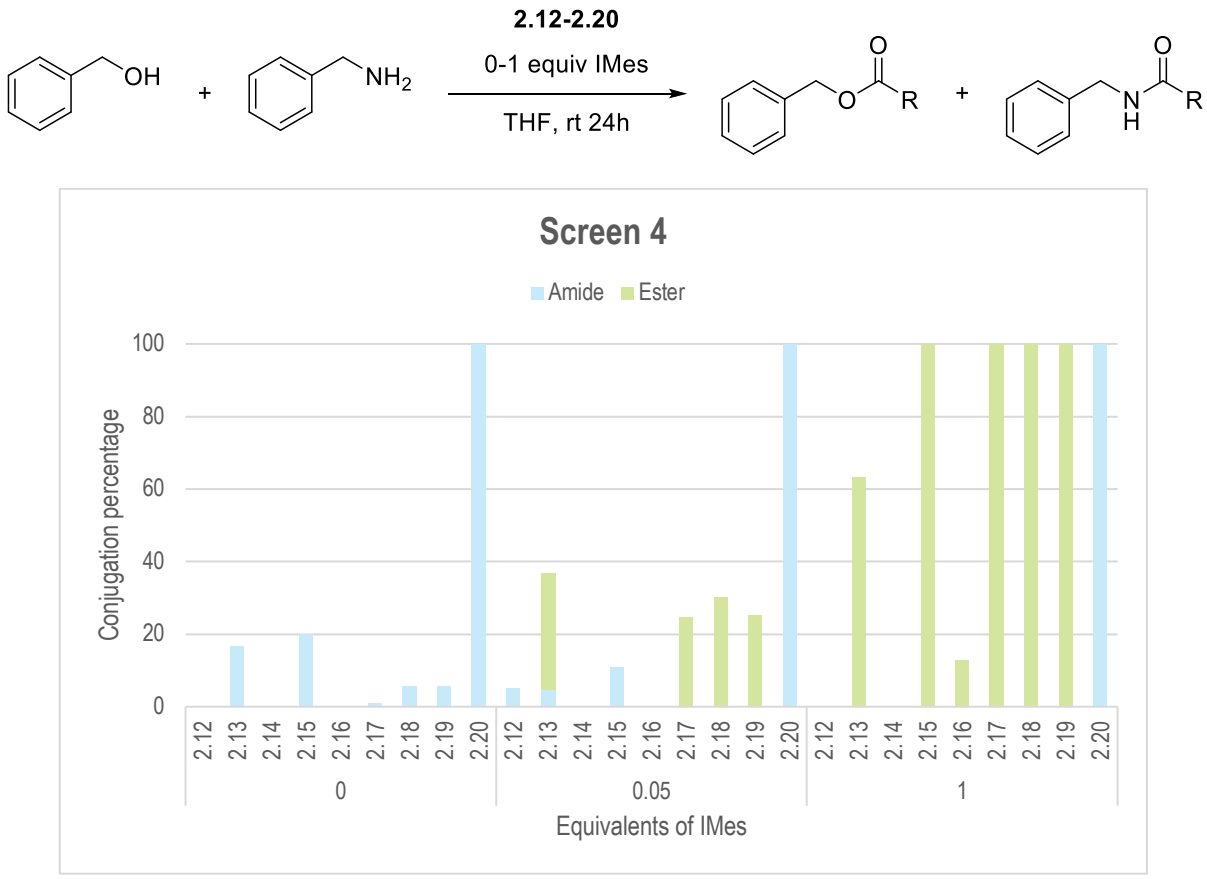

Figure 2.8.Results from screen 4 as analyzed by UPLC-MS. Yields were determined by integration of the UV-trace of the products and compared to remaining electrophile. The results reported, were recorded after 48h reaction time.

Isopropenyl acetate reacted only with benzylamine, regardless of IMes concentration. This was surprising, as Samanta et.al. reported selective esterification of this electrophile. In general, selective esterification was observed in the presence of 1 equivalent of IMes. Interestingly, the aliphatic vinyl esters displayed high O- over N-selectivity in the presence of high IMes concentration, as well as the difluoro and dimethyl analogues. Despite the encouraging results, all of the hept-1-en-2-yl esters reacted sluggishly and the results reported in Figure 2.8 were after 48h reaction time. Compared to the trifluoro esters, where complete reaction was observed after 3h, this left some room for improvement. It was hypothesized, that the longer aliphatic chain slowed down the reaction rate by steric hindrance, thus the shorter isopropenyl ester should be tested.

Discussion of the mechanism

In general, the aliphatic electrophiles displayed high reactivity. An explanation of this phenomenon was found a paper published in 2021 by Biswas et al. who suggested the azolium enolate as the key intermediate for both esterification of α,β unsaturated aldehydes and O-selective transesterification[33]. It was proposed that the azolium enolate reacts in a concerted manner to form the ester, instead of the acyl azylium cation reaction with a deprotonated alcohol, as previously proposed by Samanta et al. (Figure 2.9). The suggested mechanism was backed up experimentally by the reaction of the deuterated acetyl azolium triflate in DBU and benzyl alcohol, showing the incorporation of a proton from the alcohol.

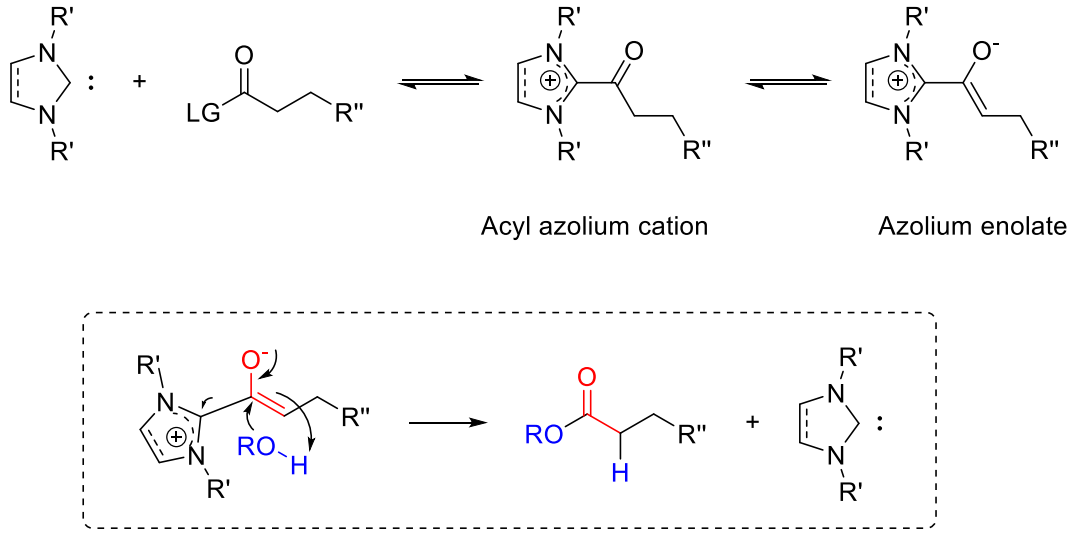

Figure 2.9. Formation of the key azolium enolate suggested by Biswas et al. to be the active species for esterification. Below is shown the suggested concerted reaction mechanism of the azolium enolate with the alcohol.

The aliphatic isopropenyl **2.21** was envisaged as a good target for water-tolerant NHC catalysis. To access the shorter isopronenyl esters without working with gaseous reagents, propenyl dissolved in THF was purchased. Furthermore, the reaction was carried out in a capped microwave (MW) vial to prevent propyne evaporation (Scheme 2.3).

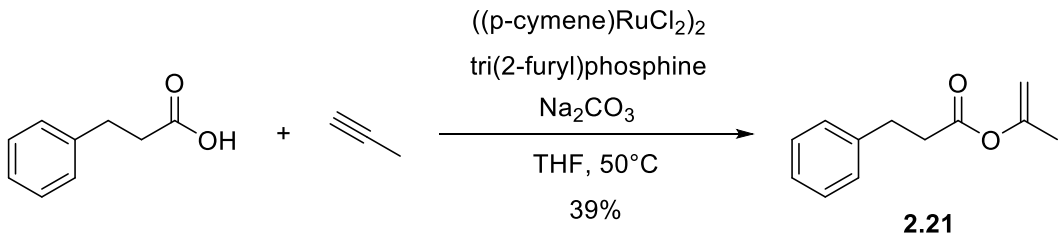

Scheme 2.3. Reaction conditions for isopropenyl ester synthesis.

The lower yield was expected due to the solvent change from toluene to THF.

Screen 5

With compound **2.21** in hand, investigation of water tolerance in THF and ACN was commenced. Aqueous content was varied from 0-50% in the presence of 0.5 or 0.05 equivalents of IMes. Results are reported in the figure below (Figure 2.10).

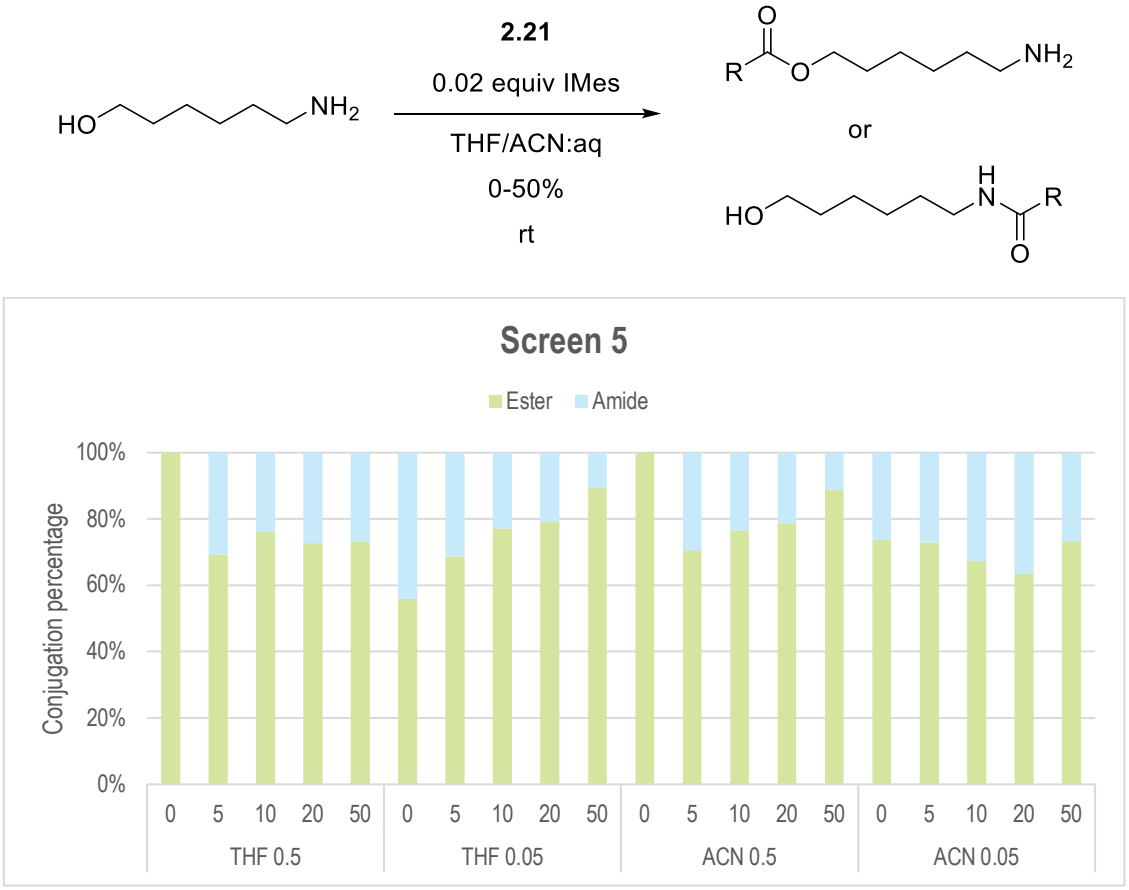

Figure 2.10. Results from screen 5 as analyzed by UPLC-MS. Yields were determine by the integration of mass intensities of ester and amide product. Complete reaction was observed for all reactions after 3h.

Complete consumption of the electrophile was observed after 3h, confirming the expected increased reactivity of the shorter aliphatic chain. Complete selectivity was observed in the presence of 0.5 equivalents of IMes in non-aqueous conditions, however, at 0.05 equivalents selectivity was compromised (56-73% ester formation in THF and ACN respectively). The addition of water seemed to lower the selectivity slightly, however, the selectivity did not decrease with increasing water concentration, either in THF or ACN.

With these results in hand, it was believed that the isopropenyl ester **2.21** would be good candidates for selective O-acylation in aqueous solution. Furthermore, the increased nucleophilicity of the serine in the activated peptide could enhance the O-selectivity to sufficiently suppress lysine conjugation.

2.1.4 Peptide screening

After identifying water tolerable conjugation conditions, the peptides shown in Figure 2.11 were synthesized using standard Fmoc SPPS and Rink amide-linkers. The peptides were acetylated and cleaved in TFA before purification by preparative HPLC (for more detail see experimental section). Phenylalanine was incorporated to enhance UV-activity to facilitate analysis by UPLC-MS. Glutamic acid was introduced to increase solubility of the peptides. Furthermore, in catalytic triads, an acidic residue is often present to increase the nucleophilicity of the histidine. N-terminals were capped to avoid nucleophilic competition. The peptides are denoted after the central residues, which are important for reactivity, as highlighted below the structures in Figure 2.11.

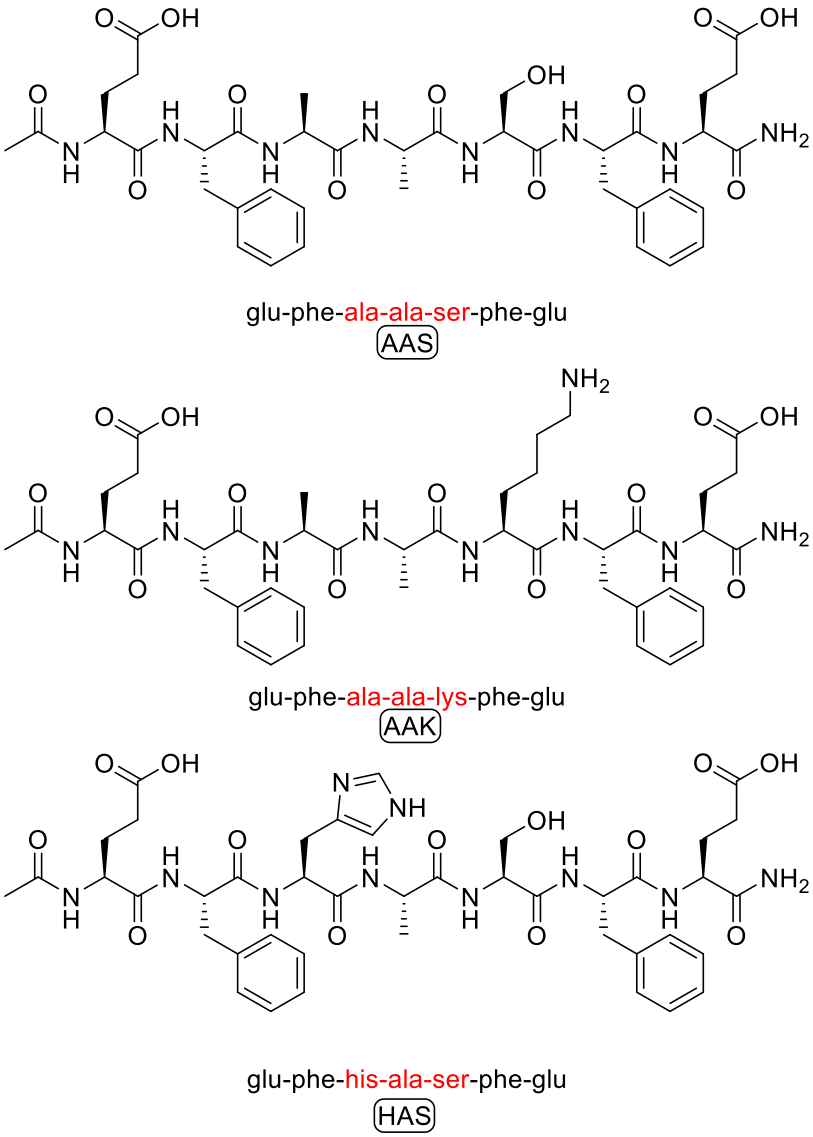

Figure 2.11. Structure of the peptides for the initial peptide screen.

Peptide screen 1

Reactions were carried out in Eppendorf tubes containing a triangular stir bar. The peptides were dissolved in PBS buffer with the addition of appropriate amounts of DMF to solvate the peptides.

20 equivalents of electrophile were used and the equivalents of IMes were varied from 0-20 equivalents. Control experiments were performed containing peptides and electrophiles, without the presence of IMes. The results are reported below in Figure 2.12.

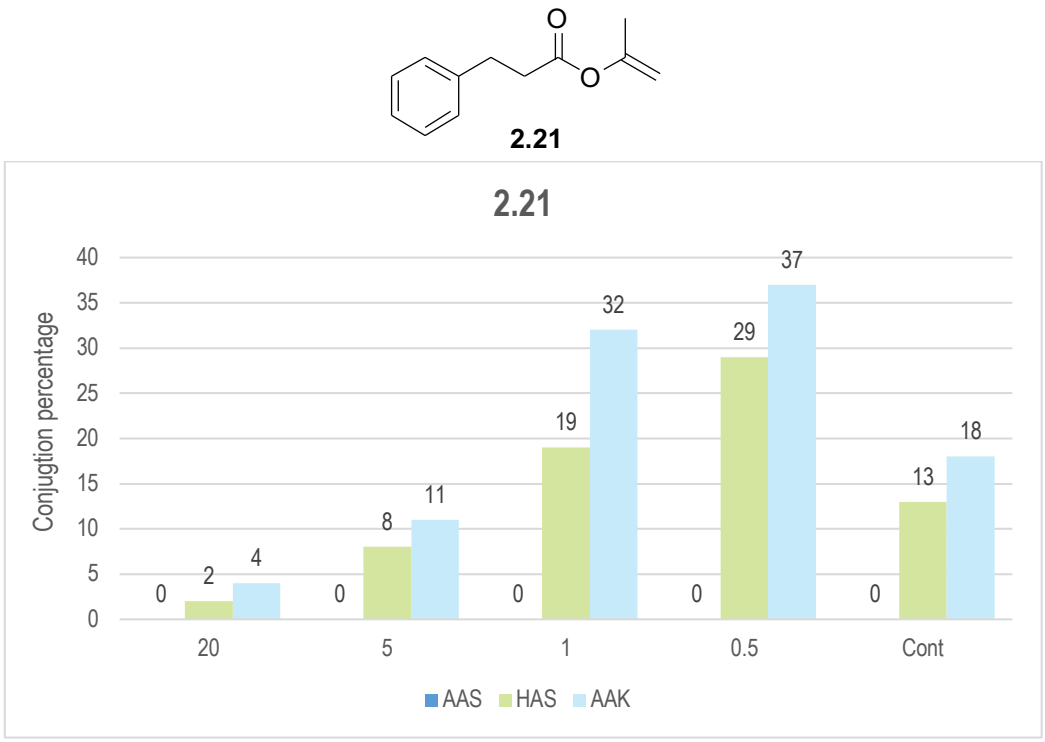

Figure 2.12. Results from Peptide screen 1 as analyzed by UPLC-MS. Conversion was determined by integration of the mass trace of the products and compared to remaining unmodified peptide. The results reported were recorded after 48h reaction time.

Gratifyingly, no reaction on the un-activated AAS peptide was observed, suggesting the activation by histidine on the synthesized peptide, as previously reported. Though reaction had been observed on benzyl alcohol, the peptide screen was run in lower concentrations, possibly explaining the lowered reactivity. Surprisingly, the inverse effect of IMes equivalents was observed compared to the initial screens, meaning that higher IMes concentration led to less reaction. The control experiments showed that the presence of IMes was important for conjugation when comparing reaction with no IMes (13% esterification), to low IMes loading (0.5 equivalents, 29% esterification). As opposed to the initial screen, where benzyl alcohol and benzyl amine were mixed before adding the electrophile, the peptides were kept separate for ease of analysis. Furthermore, the initial screen utilized an excess of nucleophile, whereas in the peptide screen, an excess of the electrophile was used, possibly increasing amidation. Encouraged by the initial results, the pH effects were studied.

Peptide screen 2

It was envisaged that lowering the pH could lower lysine reactivity by protonation of the free amine. Furthermore, the optimal equivalents of electrophile was determined by the addition of 5, 20 or 100 equivalents. Results are reported in Figure 2.13.

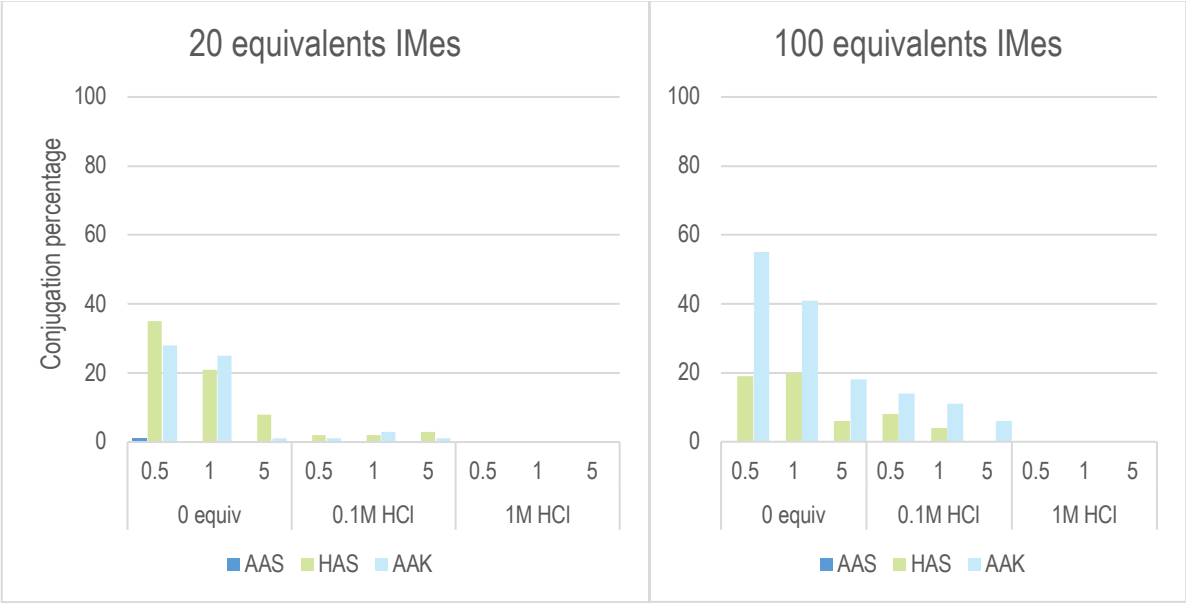

Figure 2.13. Results from screen 7 as analyzed by UPLC-MS. Yields were determined by integration of the corresponding mass trace of the product and compared to remaining un-modified peptide. The results were recorded after 24h.

It was immediately evident, that 100 equivalents of electrophiles mostly promoted higher amidation, resulting in up to 55% of the amide product, while not achieving higher esterification (up to 19%). Furthermore, the addition of acid to the reactions did reduce amine reactivity, however, it also reduced serine reactivity. As previously observed, higher IMes concentrations hampered overall reactivity. When using 5 or 20 equivalents of the electrophile **2.21**, O vs. N selectivity was significantly higher, however, total conjugation yield remained low (25-35%) and lysine conjugation was still significant. It was hypothesized that perhaps a more reactive serine residue could enable higher conjugation yields by inserting basic arginine residues. Furthermore, creating a local basic microenvironment could enable the use of more acidic buffers, thereby mitigating lysine conjugation.

2.1.5 The optimized peptide sequence

The encouraging observation, that one correctly spaced histidine residue could activate the serine to the extent observed in the previous screens, led to investigation of the addition of the more basic arginine residue. A paper published by Mädler et al. investigating the effect of arginine on serine, threonine and tyrosine reactivity, showed that arginine enhanced O-reactivity towards NHS-esters during crosslinking[33].

Therefore, the following sequence was synthesized using SPPS as described previously (Figure 2.14).

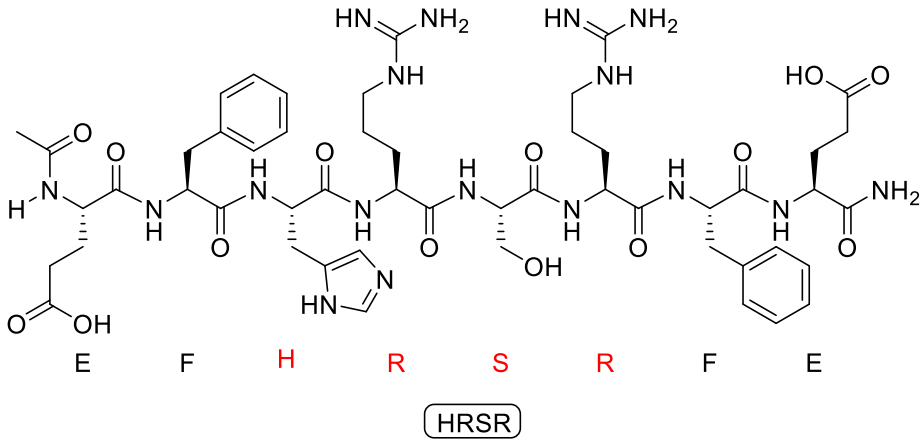

Figure 2.14. The structure of the optimized peptides sequence.

Peptide screen 3

In this screen, 20 and 5 equivalents of electrophile were tested at both 37°C and rt, to determine if increased temperatures could give higher reactivity of the serine. Based on the previous reactions, 1 equivalent of IMes was added. Reactions were carried out in Eppendorf tubes that were heated and stirred by a thermomixer. Results are summarized in the Figure 2.15.

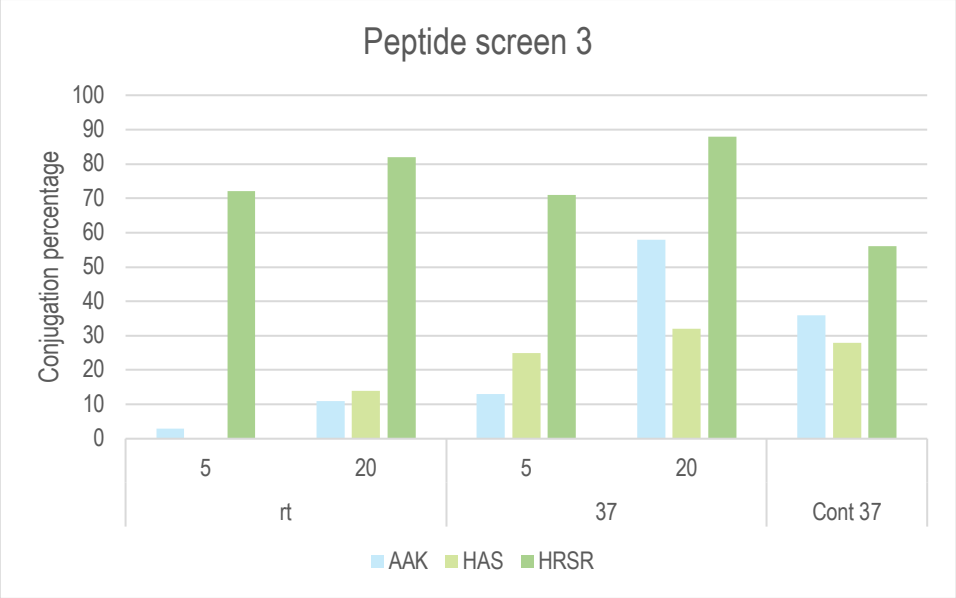

Figure 2.15. Results for peptide screen 3 as analyzed by UPLC-MS. Yields were determined by the integration of the mass intensities of the mass spectrum of the respective products and compared to remaining un-modified peptide. The results displayed were recorded after 24h reaction time.

A significant increase in reactivity was observed for the HRSR peptide, as compared to AAK and HAS in all experiments. Increasing the temperature to 37°C led to higher amidation (13 and 58%, 5 and 20 equivalents, respectively) compared to the conjugations carried out at rt (3 and 11%, 5 and 20 equivalents respectively). However, the increased temperature had little impact on the reactivity of HRSR that consistently displayed high conversion (71-88%). HAS conjugation was also increased with increased temperature (14-32%). The control experiments carried out at 37°C with 20 equivalents of electrophile suggested that the presence of 1 equivalent of IMes increased HRSR reactivity (56% vs 88%). I would like to highlight the most promising reaction conditions where 72% O-conjugation was achieved with only 3% amidation(5 equivalents of electrophile, rt). This result suggests that O-selectivity could be achieved by activation of the surrounding microenvironment, as well as using IMes organocatalysis to enhance O-selectivity.

2.1.6 Perspectives

During this project, two different electrophile groups were investigated for the development of a novel sequence-specific serine conjugation, where O-selectivity was enhanced by the addition of the N-heterocyclic carbene IMes. In dry conditions, the trifluoro ester scaffold showed promising properties, as they reacted selectively and efficiently with benzyl alcohol to form the corresponding ester in the presence of benzyl amine. However, the introduction of water compromised selectivity, likely due to competitive hydrogen bonding from the solvent interfering with the activation mechanism. Thus, the vinyl esters were investigated due to a different mechanism of activation. It was discovered that the aliphatic isopropenyl esters **2.21** displayed sustained O-selectivity in aqueous media and peptides studies were commenced.

It was observed, that an adjacent histidine residue did increase the nucleophilicity of the serine in the HAS sequence and that the addition of IMes increased the conjugation yields, promoting O-

selectivity. However, it was not possible to outcompete the inherent nucleophilicity of lysine of the AAK peptide. By the introduction two arginine residues, a new activated sequence was designed; the HRSR-peptide. This peptide was conjugated with **2.21** and it was possible to achieve a 72% conjugation efficiency compared to 3% lysine conjugation of the AAK peptide under the same conditions. In all experiments, the HRSR peptide displayed a superior reaction profile, suggesting the power of activation through the surrounding microenvironment and that it was possible to promote O- over N-selectivity using N-heterocyclic carbenes as organocatalysts to develop new serine conjugation methods.

Future work would include the systematic preparation of various peptides containing histidine and arginine at different distances from the serine to determine the optimal sequence for serine activation while avoiding nucleophilic competition. Furthermore, it could prove fruitful to try other NHCs with better properties for bioconjugation such as including aqueous solubility and higher stability. Lastly, the sequence should be recombinantly incorporated into a protein and conjugation should be carried out to demonstrate the applicability of the novel conjugation method.

2.2 Part II

2.2.1 Aim

The aim of this project was to demonstrate the utility of a novel tetra anchor designed to tether together the 4 disulfide interchain bonds of a reduced antibody, for the installation of a handle allowing for selective attachment of a relevant payload. This should not only provide a strategy for site-selective conjugation, but should also provide a highly stable antibody conjugate due to the reconstitution of covalent bonds. Two rebridging head groups were investigated, the bis-sulfone and the dibromo McSaf Inside (Figure 2.16). This project was undertaken during my external stay at Cambridge University in the group of Prof. David Spring, who has previously designed and synthesized the tetra anchor.

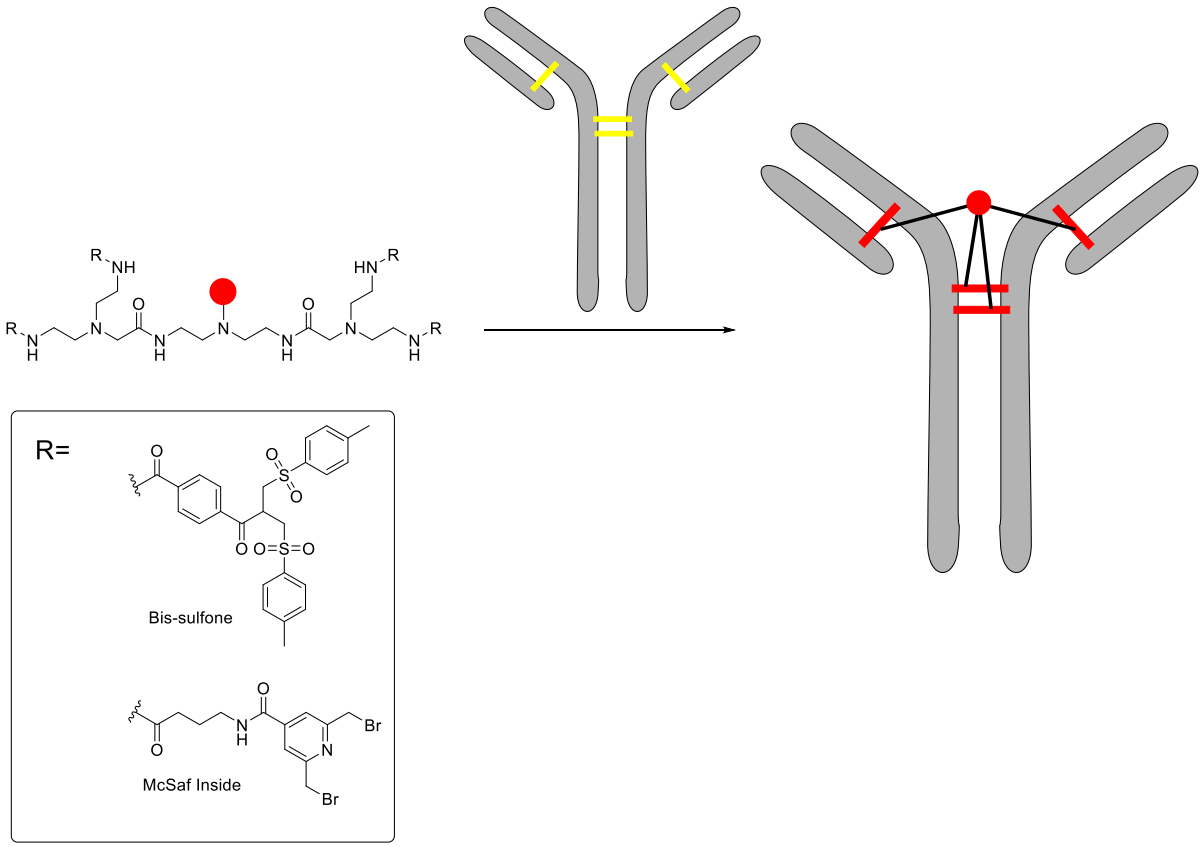

Figure 2.16. General structure of the tetra anchor and the head groups and the concept of tethering together the four rebridging head groups.

2.2.2 Introduction

Cysteine thiol conjugation is one of the most widely applied bioconjugation strategies, as it offers an easy and generally applicable method for protein modification and has been especially successfully employed in the preparation of ADCs[34]. Thiols offer a unique soft nucleophile that reacts rapidly with Michael acceptors. The Michael acceptor maleimide, has proved an immensely powerful tool for scientists[35–37]. As previously shown, 8 out of 15 ADCs currently on the market utilize cysteine chemistry for the attachment of payloads. Cysteine residues are most commonly bound in disulfides providing covalent stabilization to the protein, however, the interchain bonds

of an IgG can be selectively reduced to open up to 8 conjugation sites[38]. However, it is seldom advantageous to attach eight payloads onto the antibody, as this can influence the properties of the final conjugate. Attachment of less than eight moieties introduces another challenge, as it results in a heterogeneous conjugation distribution. Furthermore, reduction of disulfide bonds removes the covalent structural stabilization and can result in protein denaturation. Cysteine rebridging offers the benefit of homogeneously conjugated antibodies(DAR 4), as well as the re-formation of the covalent structural stabilization after disulfide bridge reduction[39–43], by reforming the covalent bond between the reduced sulfides(Figure 2.17). This strategy offers a unique possibility to tune antibody drug conjugates, however, rebridging can lead to scrambling of the disulfide bonds[44,45]. This scrambling results in half antibodies and can lead to aggregation and faster clearance, due to the smaller size[46].

The novel concept of anchoring together four rebridging head groups via a hydrophilic moiety that allows for the attachment of chemical payloads was envisaged (Figure 2.17). In addition to keeping the structural integrity of the antibody, this novel approach would enable access to homogenous antibody conjugates at DARs that have previously been challenging to access due to antibody symmetry (eg. 1 or 3).

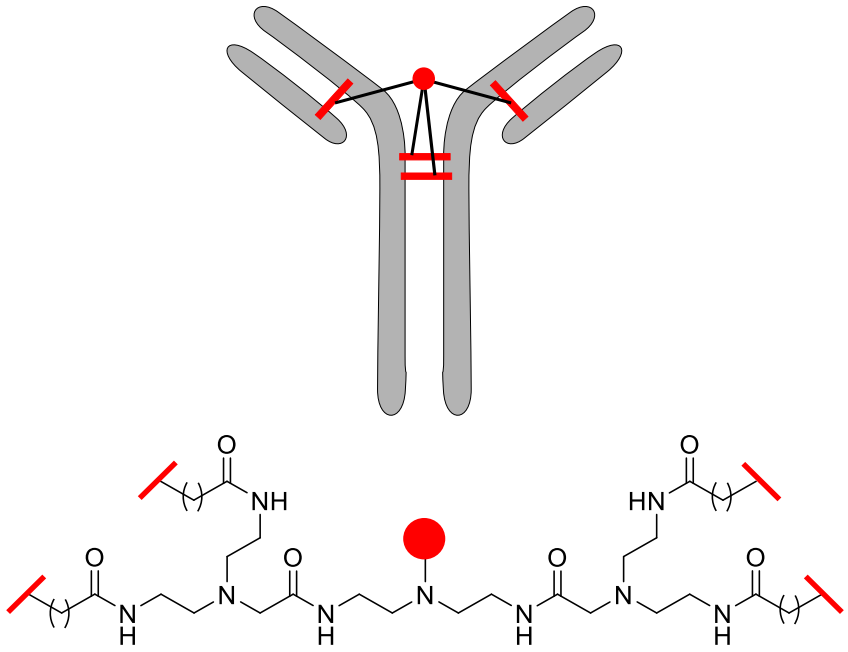

Figure 2.17. Structure of the tetra-anchor, tethering the four rebridging head groups together.

2.2.3 Synthesis of the central scaffold

The conditions and yields of the synthesis of the tetra-anchor, previously developed by Anders Hansen and Fredereike Danheim, is shown in Scheme 2.4. Terminal amine Boc protection of diethylene triamine with BocON proceeded smoothly in a satisfying yield of 78%, followed by α-substitution of methyl-bromoacetate yielding 81% of **2.23**. Diethylene triamine and **2.23** were heated together in a sealed MW vial, but due to slow reaction, compound **2.24** was isolated in a modest yield (35%), with the recovery of 60% starting material. Next, the alkyne handle **2.25** was

prepared from 2-bromo acetyl bromide and progargylamine with a 46% yield. This reaction needed to be cooled sufficiently to prevent alpha alkylation instead of amide formation. Lastly, the alkyne **2.25** and amine **2.24** were reacted to yield the final scaffold **2.26**. Boc deprotections were performed directly before attachment of the conjugation handles, due to the hygroscopic nature of the hepta-amine product.

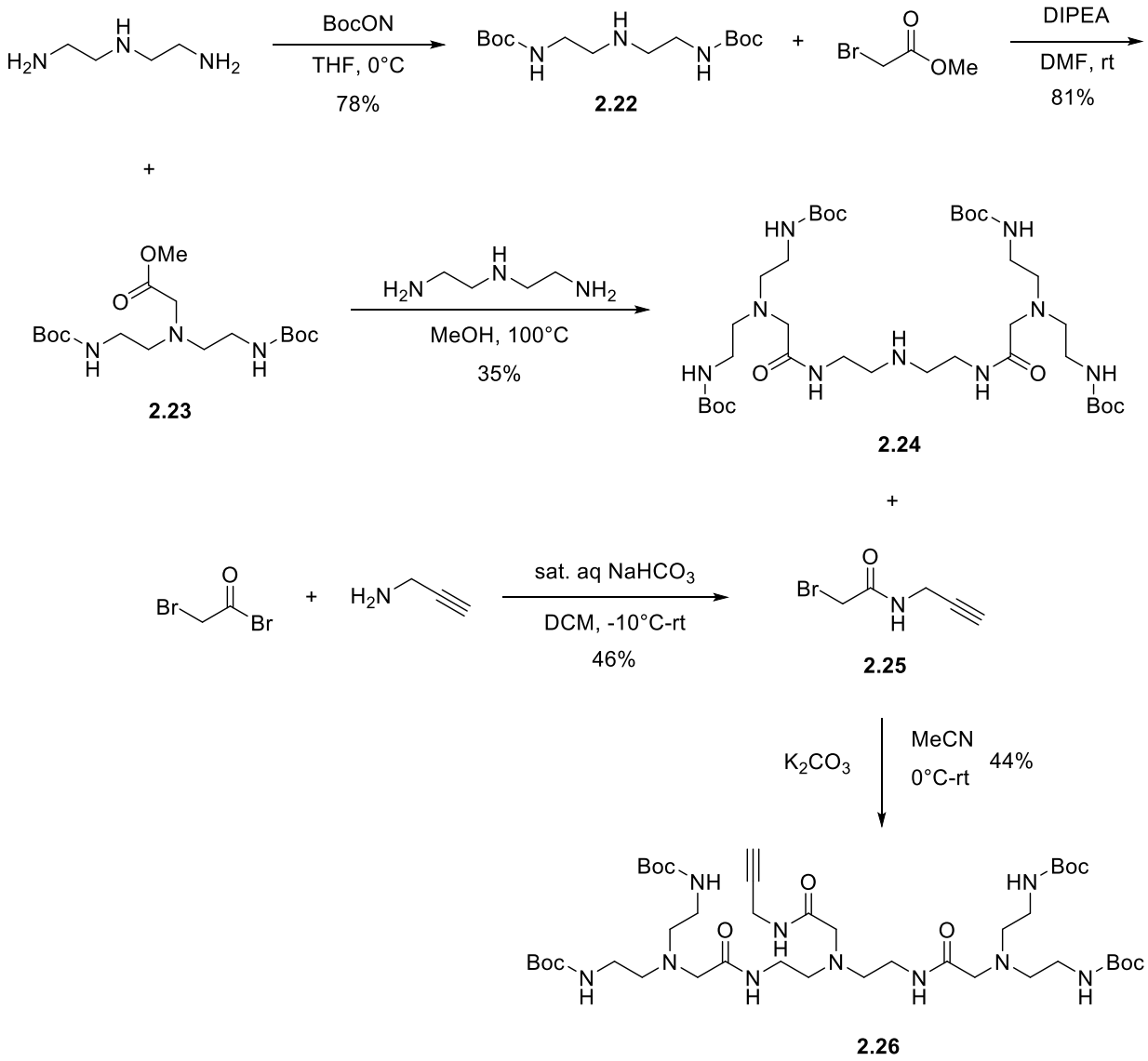

*Scheme 2.4. Conditions and yields for the synthesis of compound **2.26** as developed by Anders Hansen and Fredereike Danheim.*

The four-step synthesis yielded 10% of compound **2.26**, with recovery of starting material in the low yielding third step.

The original scaffold was attached to antibodies using the divinylpyrimidines developed in the David Spring group[40]. They were able to obtain homogeneously conjugated antibodies with a DAR of 1 and they were able to attach payloads to produce novel ADCs (unpublished work).

To expand the utility of the central scaffold, different rebridging head groups, reported in the literature, were attached.

2.2.4 Bis-sulfone head group

The bis-sulfones have been used numerous times to yield stable and well-defined conjugates including ADCs[43,47–53]. The mechanism of disulfide rebridging goes through base catalyzed step-wise elimination and Michael addition. Initially, mild basic conditions promote elimination of the sulfone forming an α, β unsaturated ketone, which can react with a free thiol (Figure 2.18). Upon Michael addition, an elimination reaction occurs, followed by a second Michael addition to reform a three carbon bridge.

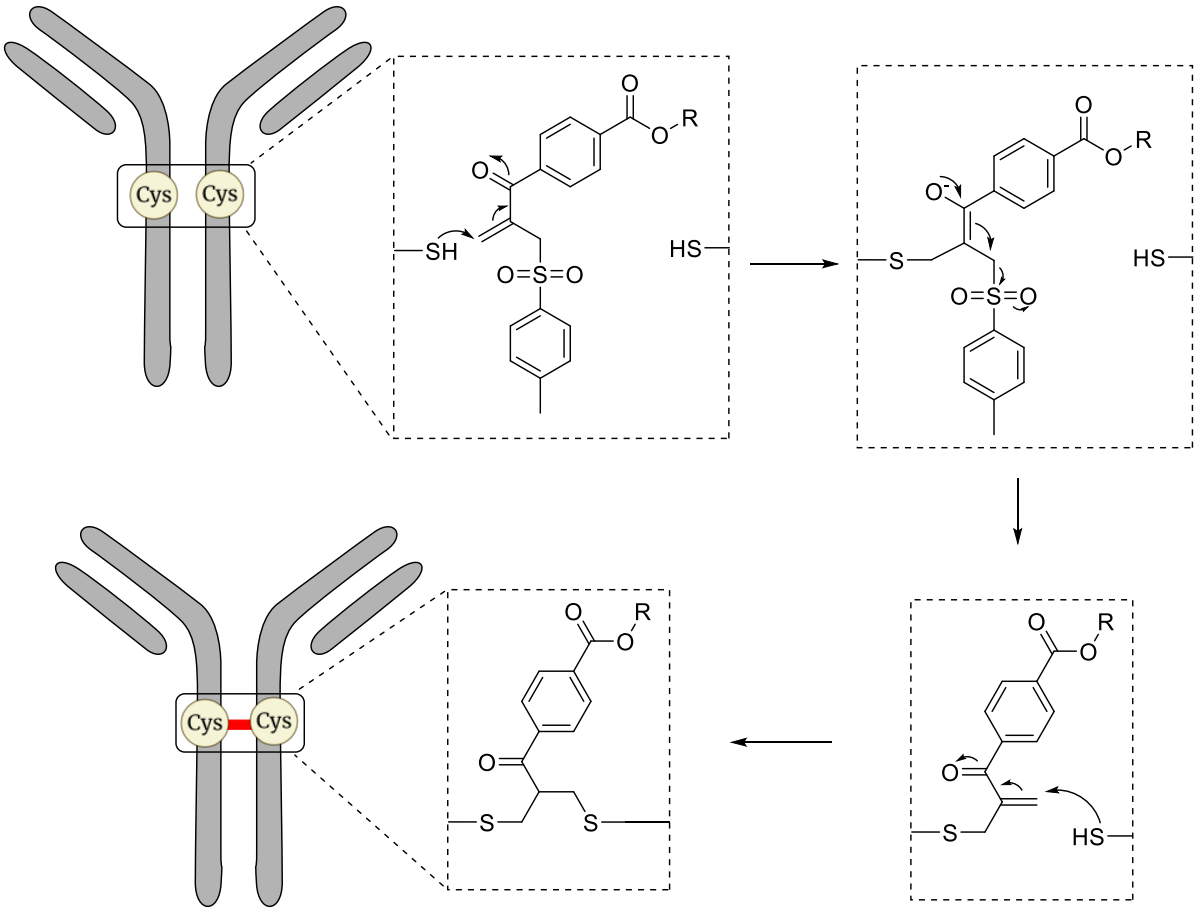

Figure 2.18. Mechanism of rebridging of the bis-sulfone group.

The synthetic conditions for the formation of the sulfone head group are reported in Scheme 2.5, as inspired from literature. The first step was a Mannich reaction by imine formation between piperidine and formaldehyde, followed by attack from the enol to form the Mannich salt **2.27**. The next step used the Mannich salt **2.27** in two step wise Mannich reactions to yield the disulfide **2.28**[54]. In the final step, compound **2.28** was oxidized using oxone yielding 94% of the bis-sulfone **2.29**.

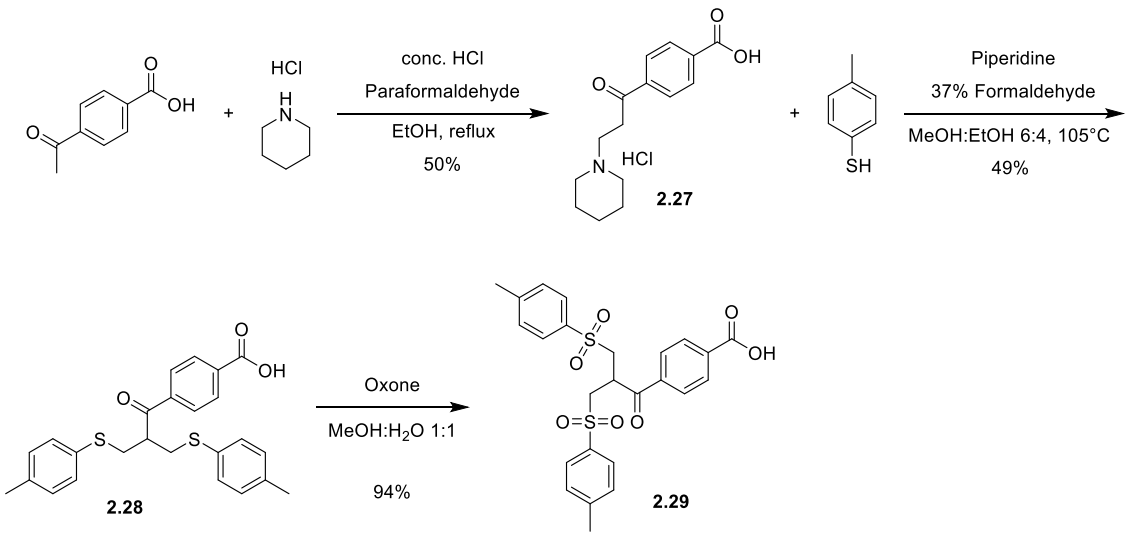

Scheme 2.5. Conditions and yields for the synthesis of the bis-sulfone head group.

This simple three-step synthesis afforded compound **2.29** in an overall yield of 23%, ready for attachment to the tetra anchor.

2.2.5 McSaf Inside head group

The second head group of this project, was the dibromo pyridine McSaf Inside disulfide rebridging head group , developed by the company McSAf for the production of homogeneous ADCs[55,56]. Conjugation occurs through nucleophilic substitution of the benzylic bromides yielding a five-atom bridge. The McSaf Inside conjugation protocol has recently been used to yield two highly homogeneous ADCs, that display good serum stability and high toxicity towards cancer cells[57,58].

Due to the availability of the starting material, it was decided to follow the synthetic strategy of the patent, as seen in Scheme 2.6[55]. Methyl isonicotinate was reacted with ammonium persulfate and methanol, through a radical reaction to attach two benzyl alcohols (compound **2.30**, 21% yield) that were converted to the corresponding bromides using PBr_3, affording **2.31** in a satisfying yield of 71%. It was expected that deprotection of the methyl ester, would result in hydrolysis of one of the bromides as reported in the patent, however, upon saponification of the ester, no hydrolysis was observed by UPLC-MS and the carboxylic acid **2.32** was isolated in a quantitative yield. Due to the immediately available chemicals, ethyl 4-aminobutanoate was used for the amide coupling that rather unsatisfactorily, yielded 25% of **2.33**. The low yield was hypothesized to arise from HOBt hydrolysis of the bromides. It was decided to move forward despite the low yield, however, saponification of **2.33** resulted in complete degradation of the starting material when using the conditions described in the literature.

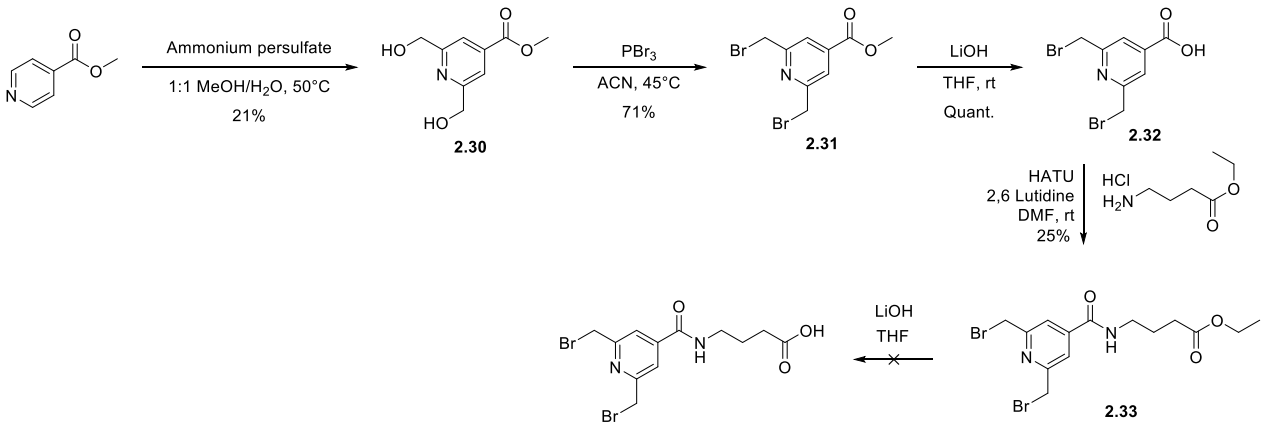

Scheme 2.6. Conditions and yields of the synthesis of the dibromo McSaf Inside head group.

It was hypothesized that the shorter chain contributed to the degradation, however, due to time restrictions during external stay, it was not possible to obtain the longer methyl 5-aminopentanoate used in the literature. Instead, it was decided to move ahead and attempt direct coupling of the aromatic acid onto the tetra anchor, being fully aware that the peptide coupling could be encumbered by direct attachment to the benzoate.

2.2.6 Head group attachment

The attachment of the head groups was expected to be the most difficult step in the synthesis, due to the sensitivity of the reactive head groups, as well as the large size of the product, further complicated by the necessity to complete of 4 amide couplings. Another complicating factor for the bis-sulfone reaction, was that the base catalyzed elimination of the sulfinic acid was expected to happen under the basic coupling conditions, yielding the possibility of several different products with a combination of mono, di or tri- elimination products. Inherently, the elimination in itself would still yield a useful conjugation handle, however, analysis and purification of the reaction could prove difficult.

Thus, great care was taken to consider which conditions should be applied. Before the final step was attempted, the Boc protection groups were removed by addition of 4M HCl/in dioxane. The reaction could not be followed by TLC or UPLC-MS, as the product was too polar and the number of ionizable groups results in m/z masses that are too low for detection. However, formation of a white precipitate could be observed indicating reaction.

Several difficulties were experienced during the attachment of both the bis-sulfone and the Mc Saf Inside head groups. In Table 2.6, an overview of the different conditions applied is provided.

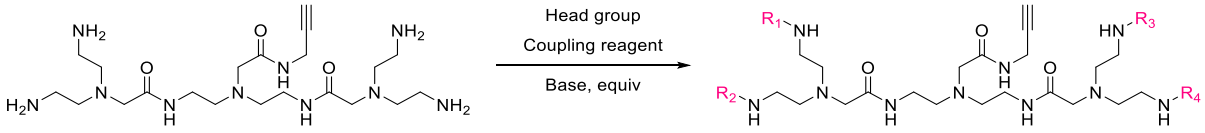

ENTRY	HEAD GROUP	COUPLING REAGENT	AMINE	BASE EQUIV.	COMMENTS

(1)	**2.29**	HBTU	**2.26**	TEA, 20 + 100 after 1 day	No reaction observed , only side reaction
(2)	**2.29**	HBTU	ethyl 4-amino butanoate	TEA, 1	No reaction observed
(3)	**2.29**	HBTU	2-phenyl ethan-1-amine	TEA, 1.2	No reaction observed
(4)	**2.29**	Oxalyl chloride	**2.26**	DIPEA, 20	Some product formation, sluggish
(5)	**2.29**	HATU	**2.26**	DIPEA, 15	Product + elimi-nated products
(6)	**2.28**	HBTU	**2.26**	TEA, 20	No product
(7)	**2.28**	Oxalyl chloride	**2.26**	DIPEA, 8	No product
(8)	**2.33**	EEDQ	**2.26**	DIPEA, 16	No product
(9)	**2.33**	EEDQ	**2.26**	DIPEA, 11	No product
(10)	**2.33**	EDC·HCl	**2.26**	DIPEA, 12	Product observed by UPLC-MS

Table 2.6. Overview of the various conditions for the synthesis of tetra anchor bioconjugation handles.

In entries (1-3) and (6) in Table 2.6, the conditions, previously used in the Spring group to attach the divinyl pyrimidine head groups onto the tetra scaffold, were applied. However, no product formation was observed, even when using simpler amines (entries 2-3), suggesting ineffective HBTU activation of the carboxylic acid of bis-sulfone **2.29**. In all reactions using bis-sulfone, the elimination reaction was observed. In entry (1), it was hypothesized that this elimination was consuming the base and the addition of more could yield the tetra-coupled product in the eliminated form. However, addition of more base resulted in the unwanted reaction of the free amines onto the formed Michael acceptor. Next, acid chloride formation was attempted (entries 4 and 7) using oxalyl chloride, which is considered milder than thionyl chloride[59]. Acid chloride formation was observed, but the subsequent reaction onto the tetra anchor was slow and resulted in the significant formation of by product.

In literature, amide couplings can be performed before oxidation of the thioether **2.28**[53]. For the reaction of the bis-sulfide **2.28** (entry 7), it was evident that eight equivalents of base was not sufficient and no product was observed. The best results were achieved by using HATU as coupling reagent (entry 5), in conjunction with sequential addition of base to limit the amount of elimination product. Taking a careful look at the reaction, it was hypothesized that the addition of exactly 15 equivalents of base would be sufficient for amide coupling, avoiding the addition of excess base to that promotes elimination. The 15 equivalents were utilized thus: 4 equivalents for the activation of **2.29** with HATU, 7 equivalents to remove the HCl from the 7 amines of the tetra

anhor and finally, 4 equivalents for the 4 amide couplings. This reaction yielded fully coupled product, as well as partially eliminated products (0-3 eliminated sulfinic acids). Purification by Combi Flash yielded 32% of a mixture of the products (0-3 eliminated sulfinic acids).

Also, reactions on the McSaf Inside head group were attempted. As HOBt was suspected to hydrolyze the starting material, EEDQ[60–63] was first attempted. However, it was not possible to observe any product formation. EDC·HCl was also used and product could be detected on UPLC-MS, suggesting that this approach could be promising.

2.2.7 Perspectives

During my external stay at Cambridge University, the tetra anchor group was synthesized in satisfying yields as previously designed by Hansen and Danheim. Furthermore, synthesis of two disulfide rebridging groups was attempted, obtaining the bis-sulfone **2.29** in an overall yield of 23% and the shortened dibromo **2.33** with a 15% overall yield. Synthesis of the dibromo McSaf Inside head group proved more difficult than expected and the shorter aromatic acid was carried forward for the attachment onto the tetra anchor. Despite the base labile nature of the bis-sulfone head group, careful addition of base afforded the final product in modest yield in conjunction with the mono, di and tri eliminated products.

The next step of the project consists of attachment of the purified bis-sulfone-tetra anchor scaffold, to evaluate the coupling properties and determine the compatibility between these two technologies. Further investigation is needed to replicate the synthesis of the McSaf Inside group, however, coupling of the aromatic acid was shown to be feasible. Ongoing research is looking into modification of the alkyne, to provide a longer PEG chain, as well as branching to allow for tuning of higher DAR.

2.3 Literature

1. Ribeiro, A. J. M., Tyzack, J. D., Borkakoti, N., Holliday, G. L. & Thornton, J. M. A global analysis of function and conservation of catalytic residues in enzymes. *J. Biol. Chem.* **295**, 314–324 (2020).

2. Buller, A. R. & Townsend, C. A. Intrinsic evolutionary constraints on protease structure, enzyme acylation, and the identity of the catalytic triad. *Proc. Natl. Acad. Sci.* **110**, 653–661 (2013).

3. DeGruyter, J. N., Malins, L. R. & Baran, P. S. Residue-Specific Peptide Modification: A Chemist's Guide. *Biochemistry* **56**, 3863–3873 (2017).

4. Vantourout, J. C. *et al.* Serine-Selective Bioconjugation. *J. Am. Chem. Soc.* **142**, 17236–17242 (2020).

5. Miller, B. T., Collins, T. J., Rogers, M. E. & Kurosky, A. Peptide biotinylation with amine-reactive esters: Differential side chain reactivity. *Peptides* **18**, 1585–1595 (1997).

6. Mädler, S., Bich, C., Touboul, D. & Zenobi, R. Chemical cross-linking with NHS esters: asystematic study on amino acid reactivities. *J. Mass. Spectrom* **44**, 694–706 (2009).

7. Doyle, M. P., Duffy, R., Ratnikov, M. & Zhou, L. Catalytic carbene insertion into C-H bonds. *Chem. Rev.* **110**, 704–724 (2010).

8. Su, L., Sun, H., Liu, J. & Wang, C. Construction of Quaternary Carbon Center via NHC Catalysis Initiated by an Intermolecular Heck-Type Alkyl Radical Addition. *Org. Lett.* **23**, 4662–4666 (2021).

9. Que, Y. & He, H. Advances in N-Heterocyclic Carbene Catalysis for Natural Product Synthesis. *European J. Org. Chem.* **2020**, 5917–5925 (2020).

10. Zhao, C., Blaszczyk, S. A. & Wang, J. Asymmetric reactions of N-heterocyclic carbene (NHC)-based chiral acyl azoliums and azolium enolates. *Green Synth. Catal.* **2**, 198–215 (2021).

11. Jalal, M., Hammouti, B., Touzani, R., Aouniti, A. & Ozdemir, I. Metal-NHC heterocycle complexes in catalysis and biological applications: Systematic review. in *Materials Today: Proceedings* **31**, 122–129 (2020).

12. Peris, E. Smart N-Heterocyclic Carbene Ligands in Catalysis. *Chem. Rev.* **118**, 9988–10031 (2018).

13. Liang, Q. & Song, D. Iron N-heterocyclic carbene complexes in homogeneous catalysis. *Chem. Soc. Rev.* **49**, 1209–1232 (2020).

14. Nagao, K. & Ohmiya, H. N-Heterocyclic Carbene (NHC)/Metal Cooperative Catalysis. *Top. Curr. Chem.* **377**, 1–15 (2019).

15. Wang, Z., Tzouras, N. V., Nolan, S. P. & Bi, X. Silver N-heterocyclic carbenes: emerging powerful catalysts. *Trends Chem.* **3**, 674–685 (2021).

16. Dröge, T. & Glorius, F. The measure of all rings - N-Heterocyclic carbenes. *Angew. Chemie - Int. Ed.* **49**, 6940–6952 (2010).

17. Liu, J., Xing, X. N., Huang, J. H., Lu, L. Q. & Xiao, W. J. Light opens a new window for

N-heterocyclic carbene catalysis. *Chem. Sci.* **11**, 10605–10613 (2020).

18. Bellotti, P., Koy, M., Hopkinson, M. N. & Glorius, F. Recent advances in the chemistry and applications of N-heterocyclic carbenes. *Nat. Rev. Chem.* **5**, 711–725 (2021).

19. Huynh, H. V. Electronic Properties of N-Heterocyclic Carbenes and Their Experimental Determination. *Chem. Rev.* **118**, 9457–9492 (2018).

20. Benhamou, L., Chardon, E., Lavigne, G., Bellemin-Laponnaz, S. & César, V. Synthetic routes to N-heterocyclic carbene precursors. *Chem. Rev.* **111**, 2705–2733 (2011).

21. Zhang, C., Zhang, G., Luo, S., Wang, C. & Li, H. Base-catalyzed selective esterification of alcohols with unactivated esters. *Org. Biomol. Chem.* **16**, 8467–8471 (2018).

22. Kristensen, T. E. Chemoselective O-acylation of hydroxyamino acids and amino alcohols under acidic reaction conditions: History, scope and applications. *Beilstein J. Org. Chem.* **11**, 446–468 (2015).

23. Mashima, K., Hayashi, Y., Agura, K. & Ohshima, T. Transition-metal clusters as catalysts for chemoselective transesterification of alcohols in the presence of amines. *Pure Appl. Chem.* **86**, 335–343 (2014).

24. Nelson, H. *et al.* Practical Chemoselective Acylation: Organocatalytic Chemodivergent Esterification and Amidation of Amino Alcohols with N-Carbonylimidazoles. *Angew. Chemie - Int. Ed.* **60**, 22818–22825 (2021).

25. Samanta, R. C., De Sarkar, S., Roland, F., Grimme, S. & Studer, A. N-Heterocyclic carbene (NHC) catalyzed chemoselective acylation of alcohols in the presence of amines with various acylating reagents. *Chem. Sci.* **4**, 2177–2184 (2013).

26. Suresh, P., Thamotharan, S. & Selva Ganesan, S. NHC Organocatalysis in D2O for the Highly Diastereoselective Synthesis of Deuterated Spiropyran Analogues. *ChemistrySelect* **6**, 2036–2040 (2021).

27. Leong, W. W. Y., Chen, X. & Chi, Y. R. NHC-catalyzed reactions of enals with water as a solvent. *Green Chem.* **15**, 1505–1508 (2013).

28. Suresh, P., Thamotharan, S. & Ganesan, S. S. Driving NHC organocatalysis on water through hydrophobic hydration for the synthesis of diverse heterocycles and carbocycles. *Catal. Commun.* **111**, 47–51 (2018).

29. Levin, E., Ivry, E., Diesendruck, C. E. & Lemcoff, N. G. Water in N-Heterocyclic Carbene-Assisted Catalysis. *Chem. Rev.* **115**, 4607–4692 (2015).

30. Awan, M. *et al.* Dimethyl sulfoxide: A central player since the dawn of cryobiology, is efficacy balanced by toxicity? *Regen. Med.* **15**, 1463–1491 (2020).

31. Schaper, L. A., Hock, S. J., Herrmann, W. A. & Kühn, F. E. Synthesis and application of water-soluble NHC transition-metal complexes. *Angew. Chemie - Int. Ed.* **52**, 270–289 (2013).

32. Goossen, L. J., Paetzold, J. & Koley, D. Regiocontrolled Ru-catalyzed addition of carboxylic acids to alkynes : practical protocols for the synthesis of vinyl esters. *Chem. Commun.* 706–707 (2003).

33. Biswas, A., Neudörfl, J. M., Schlörer, N. E. & Berkessel, A. Acyl Donor Intermediates in N-Heterocyclic Carbene Catalysis: Acyl Azolium or Azolium Enolate? *Angew. Chemie - Int. Ed.* **60**, 4507–4511 (2021).

34. Ochtrop, P. & Hackenberger, C. P. R. Recent advances of thiol-selective bioconjugation reactions. *Curr. Opin. Chem. Biol.* **58**, 28–36 (2020).

35. Shen, B. Q. *et al.* Conjugation site modulates the in vivo stability and therapeutic activity of antibody-drug conjugates. *Nat. Biotechnol.* **30**, 184–189 (2012).

36. Ravasco, J. M. J. M., Faustino, H., Trindade, A. & Gois, P. M. P. Bioconjugation with Maleimides: A Useful Tool for Chemical Biology. *Chem. - A Eur. J.* **25**, 43–59 (2019).

37. Ponte, J. F. *et al.* Understanding How the Stability of the Thiol-Maleimide Linkage Impacts the Pharmacokinetics of Lysine-Linked Antibody-Maytansinoid Conjugates. *Bioconjug. Chem.* **27**, 1588–1598 (2016).

38. Liu, H., Chumsae, C., Gaza-Bulseco, G., Hurkmans, K. & Radziejewski, C. H. Ranking the susceptibility of disulfide bonds in human IgG1 antibodies by reduction, differential alkylation, and LC-MS analysis. *Anal. Chem.* **82**, 5219–5226 (2010).

39. Wei, D. *et al.* Site-specific construction of triptolide-based antibody-drug conjugates. *Bioorganic Med. Chem.* **51**, 116497 (2021).

40. Walsh, S. J. *et al.* A general approach for the site-selective modification of native proteins, enabling the generation of stable and functional antibody-drug conjugates. *Chem. Sci.* **10**, 694–700 (2019).

41. Forte, N., Chudasama, V. & Baker, J. R. Homogeneous antibody-drug conjugates via site-selective disulfide bridging. *Drug Discov. Today Technol.* **30**, 11–20 (2018).

42. Forsythe, N. L. & Maynard, H. D. Synthesis of disulfide-bridging trehalose polymers for antibody and Fab conjugation using a bis-sulfone ATRP initiator. *Polym. Chem.* **12**, 1217–1223 (2021).

43. Badescu, G. *et al.* Bridging disulfides for stable and defined antibody drug conjugates. *Bioconjug. Chem.* **25**, 1124–1136 (2014).

44. Liu-Shin, L. P. Y., Fung, A., Malhotra, A. & Ratnaswamy, G. Evidence of disulfide bond scrambling during production of an antibody-drug conjugate. *MAbs* **10**, 1190–1199 (2018).

45. Kuan, S. L., Wang, T. & Weil, T. Site-Selective Disulfide Modification of Proteins: Expanding Diversity beyond the Proteome. *Chem. - A Eur. J.* **22**, 17112–17129 (2016).

46. Yang, M., Dutta, C. & Tiwari, A. Disulfide-bond scrambling promotes amorphous aggregates in lysozyme and bovine serum albumin. *J. Phys. Chem. B* **119**, 3960–3981 (2015).

47. Shaunak, S. *et al.* Site-specific PEGylation of native disulfide bonds in therapeutic proteins. *Nat. Chem. Biol.* **2**, 312–313 (2006).

48. Brocchini, S. *et al.* PEGylation of native disulfide bonds in proteins. *Nat. Protoc.* **1**, 2241–2252 (2006).

49. Brocchini, S. *et al.* Disulfide bridge based PEGylation of proteins. *Adv. Drug Deliv. Rev.* **60**, 3–12 (2008).

50. Balan, S. *et al.* Site-specific PEGylation of protein bisulfide bonds using a three-carbon bridge. *Bioconjug. Chem.* **18**, 61–76 (2007).

51. Bryant, P. *et al.* In vitro and in vivo evaluation of cysteine rebridged trastuzumab-MMAE antibody drug conjugates with defined drug-to-antibody ratios. *Mol. Pharm.* **12**, 1872–1879 (2015).

52. Wang, T. *et al.* Bis-sulfide bioconjugates for glutathione triggered tumor responsive drug release. *Chem. Commun.* **50**, 1116–1118 (2014).

53. Wang, T. *et al.* A disulfide intercalator toolbox for the site-directed modification of polypeptides. *Chem. - A Eur. J.* **21**, 228–238 (2015).

54. Thompson, B. B. The Mannich Reaction Mechanistic and Technological Considerations. *J. Pharm. Sci.* **57**, 715–733 (1968).

55. Joubert, N., Viaud-Massuard, M. C. & Respaud, T. R. Novel Antibody-Drug Conjugates and the Use of Same in Therapy. *United States Patent Application* (2016).

56. Juen, L. *et al.* Innovative Bioconjugation Technology for Antibody-Drug Conjugates: Proof of Concept in a CD30-Positive Lymphoma Mouse Model. *Bioconjug. Chem.* **32**, 595–606 (2021).

57. Juen, L. *et al.* Therapeutic Potential of MF-TTZ-MMAE, a Site-Specifically Conjugated Antibody-Drug Conjugate, for the Treatment of HER2-Overexpressing Breast Cancer. *Bioconjug. Chem.* **33**, 418–426 (2022).

58. Esnault, C. *et al.* Adcitmer®, a new CD56-targeting monomethyl auristatin E-conjugated antibody, is a potential therapeutic approach in Merkel cell carcinoma*. *Br. J. Dermatol.* **186**, 295–306 (2022).

59. Adams, R. & Ulich, L. H. The use of oxalyl chloride and bromide for producing acid chlorides, acid bromides or acid anhydrides. III. *J. Am. Chem. Soc.* **42**, 599–611 (1920).

60. Zacharie, B., Connolly, T. P. & Penney, C. L. A Simple One-Step Conversion of Carboxylic Acids to Esters Using EEDQ. *J. Org. Chem.* **60**, 7072–7074 (1995).

61. Hyun, M. H., Kang, M. H. & Han, S. C. Use of 2-ethoxy-1-(ethoxycarbonyl)-1,2-dihydroquinoline as a convenient reagent for the selective protection or derivatization of 2-hydroxycarboxylic acids. *Tetrahedron Lett.* **40**, 3435–3438 (1999).

62. Thomas, J. B., Fall, M. J., Cooper, J. B., Burgess, J. P. & Carroll, F. I. Rapid in-plate generation of benzimidazole libraries and amide formation using EEDQ. *Tetrahedron Lett.* **38**, 5099–5102 (1997).

63. Belleau, B. & Malek, G. A New Convenient Reagent for Peptide Syntheses. *J. Am. Chem. Soc.* **90**, 1651–1652 (1968).

2.4 Experimentals

General Procedures

Starting materials, reagents and solvents were purchased from commercial suppliers (Sigma Aldrich, Combiblocks, FluoroChem) and were not analyzed or purified before use. All solvents were of HPLC quality. Anhydrous THF, DCM, ACN, DMSO and DMF were obtained from a PureSolvTM MD-7 Solvent Purification System, Innovative Technology stationary phase being Al_2O_3. Other dry solvents were purchased under septum and under inert atmosphere.
Thin-layer Chromatography (TLC) analysis was performed using Merck aluminium sheets covered with silica gel C-60 F254 and developed by UV-light or stains ($KMnO_4$: 3.00g in 300mL water and ninhydrin: 0.10g in 0.5mL AcOH and 100mL acetone).
Flash column chromatography was performed using glass columns packed with Merck Geduran 60 Angstrom silica gel (40-64 μm particles) as stationary phase. Solvent evaporation was done on a Heidolph laborota 4000 rotary evaporator, efficient under reduced pressure (*in vacuo*) at temperatures ranging from 20 to 90 °C. Solvent traces were removed *in vacuo* at 0.27 mbar by a membrane pump, operating via a schlenk line. Inert atmosphere refers to the establishing of an N_2 atmosphere, dried using $CaCl_2$ drying tubes using a schlenk line.
Analytic UPLC-MS analyses were done on a Waters AQUITY UPLC system, equipped with PDA and SQD electrospray MS detectors. Column: Kinetex 1.7 μm XB-C18, 2.1 x 50mm. Column temperature: 50 °C. Flowrate: 0.6 mL/min. Solvent A: 0.1% HCOOH in H_2O, Solvent B: 0.1% HCOOH in ACN. Gradient: 5% B to 100% B in 2.4min or 4.8min, hold 0.1 min, total run time 2.6min or 5.0min. Alternatively, solvent C: 15mM NH_4OAc in H_2O, Solvent D: 15mM NH_4OAc in ACN:H_2O 90:10. Gradient: 5% D to 100% D in 2.4min or 4.8min, hold 0.1 min, total run time 2.6min or 5.0min.
Preparative HPLC was performed on a Waters 3767 Sample Manager equipped with a Waters 2545 Binary Gradient Module, a Waters UV Fraction Manager and C18 column for separation (flow: 20mL/min). Solvent A: 0.1% HCOOH in H_2O, Solvent B: 0.1% HCOOH in ACN. Alternatively, solvent C: 15mM NH_4OAc in H_2O, Solvent D: 15mM NH_4OAc in ACN:H_2O 90:10. Run time and gradient were determined for each specific purification.
NMR spectra were recorded on a Bruker Ascend spectrometer with a Prodigy cryoprobe operating at 400MHz for 1H-NMR and 101MHz for ^{13}C-NMR. Chemical shifts (δ) are reported in ppm downfield from TMS (δ = 0) using solvent resonance as the internal standard (chloroform-*d*, ^{1}H: 7.26ppm, ^{13}C: 77.16ppm; dimethylsulfoxide-*d5*, ^{1}H: 2.50ppm and 3.30ppm (water), ^{13}C: 39.52ppm, CD_3OD, ^{1}H: 3.31ppm and 4.87ppm (water), ^{13}C 49.00).
Coupling constants (J) are reported in Hz. Multiplicities are reported as singlet (s), broad singlet (br. s), doublet (d), doublet of doublets (dd), doublet of triplets (dt), doublet of doublet of doublets (ddd), doublet of doublet of triplets (ddt), triplet (t), triplet of doublets (td), quartet (q), pentet (p), septet (sep) and multiplets (m).

General procedure for SPPS

Standard Fmoc peptide synthesis was performed on a Biotage® Initiator+ Alstra™ using 500mg of Chematrix resin with a loading of 0.40mmol/g. Rink Amide linker was used. Each coupling was performed with 5 equivalents of Fmoc protected amino acid, with side chains functionalities protected where relevant, using oxyma and DIC as coupling reagents. 20% piperidine in DMF was used for Fmoc deprotection. The final amino acid was Fmoc deprotected and the liberated N-terminal was acetylated by hand, before global deprotection and resin cleavage by the addition of TFA:TIPS 95:5. The peptides were precipitated by the addition of cold Et_2O followed by sequential centrifugation, decantation and washing with cold Et_2O 6 times. Crude peptides were purified by preparative HPLC and the peptides were analyzed by UPLC-MS.

Ac-EFAASFE-NH_2:
UPLC MS (ESI) calculated for $C_{39}H_{53}N_8O_{13}^+$ m/z 841.4, found m/z 842.0 $[M+H]^+$
UPLC MS (ESI) calculated for $C_{42}H_{53}N_{10}O_{13}^-$ m/z 839.4, found m/z 839.9 $[M-H]^-$
Ac-EFAAKFE-NH_2:
UPLC MS (ESI) calculated for $C_{42}H_{60}N_9O_{12}^+$ m/z 882.4, found m/z 882.2 $[M+H]^+$
UPLC MS (ESI) calculated for $C_{42}H_{53}N_{10}O_{13}^-$ m/z 880.4, found m/z 880.2 $[M-H]^-$
Ac-EFHASFE-NH_2:
UPLC MS (ESI) calculated for $C_{42}H_{55}N_{10}O_{13}^+$ m/z 907.4, found m/z 907.1 $[M+H]^+$
UPLC MS (ESI) calculated for $C_{42}H_{53}N_{10}O_{13}^-$ m/z 905.4, found m/z 905.1 $[M-H]^-$
Ac-EFHRSRFE-NH_2:
UPLC MS (ESI) calculated for $C_{51}H_{74}N_{17}O_{14}^+$ m/z 1148.6, found m/z 1148.8 $[M+H]^+$
UPLC MS (ESI) calculated for $C_{51}H_{72}N_{17}O_{14}^-$ m/z 1146.5, found m/z 1146.8 $[M-H]^-$

General Procedure 1

Benzoyl chloride (1.5 equiv.) and 2,2,2-trifluoromethanol (1 equiv.) were dissolved in 1.5mL/mmol dry DCM and trimethylamine (1.2 equiv.) was slowly added. The reaction was brought to a reflux overnight. Upon completion, the reaction mixture was concentrated *in vacuo* and the crude was partitioned between EtOAc and sat. $NaHCO_3$. The organic phase was washed with sat. aq. $NaHCO_3$ and brine. The organic phase was dried over $MgSO_4$ and the solvent was removed *in vacuo*. The crude was purified by FCC.

General procedure 2

The relevant carboxylic acid (1 equiv.) and Na_2CO_3 (1 equiv.) were suspended in dry toluene (3.2mL/mmol) under inert atmosphere. A solution of $((p\text{-cymene})RuCl_2)_2$ (0.04 equiv.) and tri(2-furyl)phosphine (0.01 equiv.) in dry toluene (0.8mL/mmol) was added together with 1-heptyne (1.3 equiv.). The reaction was heated to 50°C and was stirred overnight. Upon completion, the solvent was removed and the crude was purified by FCC.

2,5-Dioxopyrrolidin-1-yl octanoate 2.1

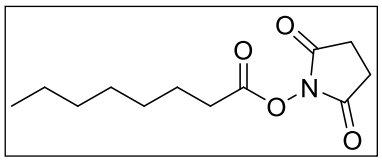

1-hydroxypyrrolidine-2,5-dione (707mg, 6.15mmol, 1.00 equiv.), TEA (0.90mL, 6.46mmol, 1.05 equiv.) and DMAP (75mg, 0.61mmol, 0.10 equiv. was dissolved in 20mL dry DCM under inert atmosphere. The solution was cooled to 0°C and octanoyl chloride (1.00g, 6.15mmol, 1 equiv.) was added. The reaction was allowed to reach rt. and was stirred overnight. The reaction was washed with 2M aqueous HCl and 2x brine. The organic phase was dried over $MgSO_4$ and solvent was removed. The crude was recrystallized from heptane/ diethyl ether yielding 63% of **2.1** as a white solid.

^{1}H NMR (400 MHz, DMSO-d_6) δ 2.81 (s, 4H), 2.65 (t, J = 7.2 Hz, 2H), 1.62 (p, J = 7.2 Hz, 2H), 1.42 – 1.16 (m, 8H), 0.86 (t, J = 7.1 Hz, 3H).
CNMR^{13}C NMR (101 MHz, DMSO-d_6) δ 170.24, 168.97, 31.05, 30.19, 28.16, 27.95, 25.44, 24.29, 21.98, 13.92.

2,5-Dioxopyrrolidin-1-yl 2-phenylacetate 2.2

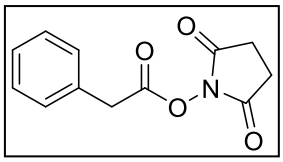

1-hydroxypyrrolidine-2,5-dione (744mg, 6.47mmol, 1.00 equiv.), TEA (0.99mL, 7.12mmol, 1.10 equiv.) and DMAP (79mg, 0.65mmol, 0.10 equiv.) were dissolved in 20mL dry DCM under inert atmosphere. The solution was cooled to 0°C and 2-phenyl acetyl chloride (1.00g, 6.47mmol, 1 equiv.) was added. The reaction was allowed to reach rt. and was stirred overnight. The reaction was with 2M aqueous HCl and 2x brine. The organic phase was dried over $MgSO_4$ and solvent was removed. The crude was recrystallized from heptane/ diethyl ether yielding 63% of **2.2** as a white solid.

HNMR ^{1}H NMR (400 MHz, DMSO-d_6) δ 7.40 – 7.27 (m, 5H), 4.11 (s, 2H), 2.81 (s, 4H).
CNMR ^{13}C NMR (101 MHz, DMSO-d_6) δ 170.61, 167.86, 132.82, 129.82, 129.06, 127.88, 37.09, 25.92.

2,2,2-Trifluoroethyl benzoate 2.3

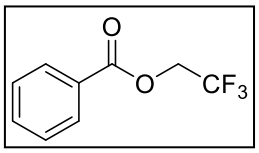

2.3 was prepared according to *General procedure 1* as a colorless oil. Yield = 26%.

HNMR ^{1}H NMR (400 MHz, Chloroform-d) δ 8.12 – 8.06 (m, 2H), 7.64 – 7.59 (m, 1H), 7.51 – 7.44 (m, 2H), 4.71 (q, J = 8.4 Hz, 2H).
^{13}C NMR (101 MHz, Chloroform-d) δ 164.92, 133.84, 129.99, 128.59, 128.41, 123.14 (d, J = 277.2 Hz), 60.58 (q, J = 36.4 Hz)

3,3,3-Trifluoropropyl benzoate 2.4

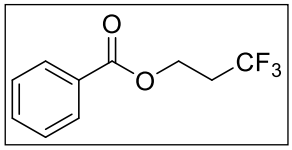

3,3,3-trifluoropropanol(0.88mL, 10mmol, 1 equiv.) and TEA (1.67mL, 12mmol, 1.2 equiv.) was dissolved in 15mL dry DCM and benzoyl chloride (1.74mL, 15.0mmol, 1.5 equiv.) was added carefully. The reaction was stirred for 1.5h at rt. The solvent was removed and the reaction was partitioned between EtOAc and sat $NaHCO_3$. The phases were separated and the organic phase was washed with $NaHCO_3$ and brine. The organic phase was dried over $MgSO_4$ and the solvent was removed. The crude was purified by FCC yielding **2.4** as a colorless oil. Yield = 66%.

^{1}H NMR (400 MHz, Chloroform-*d*) δ 7.93 – 7.82 (m, 2H), 7.44 – 7.36 (m, 1H), 7.28 (dd, *J* = 8.4, 7.1 Hz, 2H), 4.38 (t, *J* = 6.3 Hz, 2H), 2.53 – 2.32 (m, 2H).
^{13}C NMR (101 MHz, Chloroform-*d*) δ 166.17, 133.36, 129.74, 129.66, 128.53, 57.73, 124.62 (q, *J* = 276.9 Hz), 33.38 (q, *J* = 29.4 Hz).

2,2,2-Trifluoroethyl 4-methylbenzoate 2.5

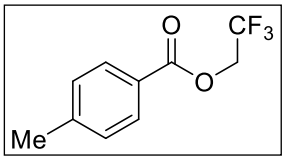

2.5 was prepared according to *General procedure 1*. Yield=78%.

Rf: 0.19 in 20 EtOAc in Hep

HNMR: ^{1}H NMR (400 MHz, Chloroform-*d*) δ 8.04 – 7.95 (m, 2H), 7.32 – 7.26 (m, 2H), 4.71 (q, *J* = 8.5 Hz, 2H), 2.45 (s, 3H).
CNMR: ^{13}C NMR (101 MHz, Chloroform-*d*) δ 164.97, 144.77, 130.03, 129.30, 125.65, 123.19 (q, *J* = 277.2 Hz), 60.64 (q, *J* = 36.6 Hz), 21.68.

2,2,2-Trifluoroethyl 2,6-dimethoxybenzoate 2.6

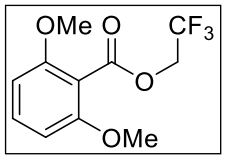

2.6 was prepared according to *General procedure 1*. Yield=1.63g (62%).

^{1}H NMR (400 MHz, Chloroform-*d*) δ 7.33 (t, *J* = 8.4 Hz, 1H), 6.57 (d, *J* = 8.4 Hz, 2H), 4.68 (q, *J* = 8.5 Hz, 2H), 3.82 (s, 12H).

^{13}C NMR (101 MHz, Chloroform-*d*) δ 164.92, 157.79, 131.97, 123.03 (q, *J* = 277.4 Hz), 111.18, 103.96, 60.71 (q, *J* = 36.6 Hz), 56.05.

2,2,2-Trifluoroethyl 3-fluorobenzoate 2.7

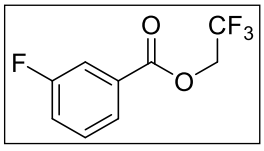

2.7 was prepared according to *General procedure 1*. Yield =1.70g (77%).

^{1}H NMR (400 MHz, Chloroform-*d*) δ 7.90 (dt, *J* = 7.7, 1.3 Hz, 1H), 7.77 (dt, *J* = 9.1, 2.7 Hz, 1H), 7.48 (td, *J* = 8.1, 5.5 Hz, 1H), 7.34 (td, *J* = 8.3, 2.7 Hz, 1H), 4.73 (q, *J* = 8.4 Hz, 2H).

^{13}C NMR (101 MHz, Chloroform-*d*) δ 163.82 (d, *J* = 3.3 Hz), 162.54 (d, *J* = 247.9 Hz), 130.45 (d, *J* = 7.6 Hz), 130.31 (d, *J* = 7.8 Hz), 125.75 (d, *J* = 3.2 Hz), 122.96 (q, *J* = 277.1 Hz) 121.00 (d, *J* = 21.3 Hz), 116.86 (d, *J* = 23.4 Hz), 61.00 (q, *J* = 36.8 Hz).

3,3,3-Trifluoropropyl 3-fluorobenzoate 2.8

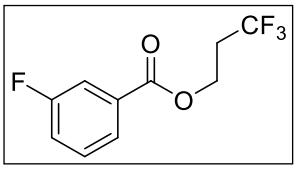

3-Fluorobenzoyl chloride (1.59g, 10.00mmol, 1 equiv.) was added dropwise to a solution of 3,3,3 trifluoro propanol (1.14g, 10.00mmol, 1equiv.) and TEA (1.81mL, 13.00mmol, 1.3 equiv.) 15mL dry DCM. The reaction was stirred at rt overnight and the solvent was removed *in vacuo*. The crude was taken up in EtOAC and the organic phase was washed with 3x sat. aq. $NaHCO_3$ and brine. The organic phase was dried over $MgSO_4$ and the solvent was removed *in vacuo*. The crude was purified by FCC affording compound **2.8** in a yield of 91%.

^{1}H NMR (400 MHz, Chloroform-*d*) δ 7.83 (dt, *J* = 7.7, 1.3 Hz, 1H), 7.70 (ddd, *J* = 9.2, 2.7, 1.6 Hz, 1H), 7.42 (td, *J* = 8.0, 5.5 Hz, 1H), 7.27 (ddt, *J* = 8.3, 6.1, 1.8 Hz, 1H), 4.55 (t, *J* = 6.2 Hz, 2H), 2.60 (qt, *J* = 10.4, 6.2 Hz, 2H).
^{13}C NMR (101 MHz, Chloroform-*d*) δ 164.95 (d, *J* = 3.0 Hz), 162.53 (d, *J* = 247.3 Hz), 131.65 (d, *J* = 7.6 Hz), 130.12 (d, *J* = 7.8 Hz), 125.79 (q, *J* = 276.7 Hz), 125.40 (d, *J* = 3.1 Hz), 120.37 (d, *J* = 21.3 Hz), 116.53 (d, *J* = 23.2 Hz), 57.94, 33.38 (q, *J* = 29.3 Hz).

2,2,2-Trifluoroethyl 2-fluorobenzoate 2.9

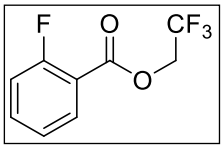

2.9 was prepared according to *General procedure 1*. Yield = 55%

HNMR ^{1}H NMR (400 MHz, Chloroform-*d*) δ 8.00 (td, *J* = 7.5, 1.9 Hz, 1H), 7.65 – 7.55 (m, 1H), 7.29 – 7.26 (m, 1H), 7.26 – 7.17 (m, 1H), 4.73 (q, *J* = 8.4 Hz, 2H).

^{13}C NMR (101 MHz, Chloroform-*d*) δ 162.49 (d, *J* = 3.9 Hz), 162.29 (d, *J* = 262.2 Hz), 135.55 (d, *J* = 9.2 Hz), 132.26, 124.16 (d, *J* = 4.0 Hz), 122.97 (q, *J* = 277.2 Hz), 117.22 (d, *J* = 22.0 Hz), 116.92 (d, *J* = 9.2 Hz), 60.82 (q, *J* = 36.8 Hz).

3,3,3-Trifluoropropyl 2-fluorobenzoate 2.10

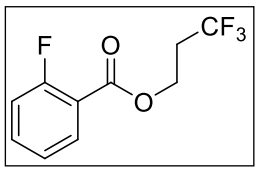

2-Fluorobenzoyl chloride (1.59g, 10.00mmol, 1 equiv.) was added dropwise to a solution of 3,3,3 trifluoro propanol (1.14g, 10.00mmol, 1equiv.) and TEA (1.81mL, 13.00mmol, 1.3 equiv.) in 15mL of dry DCM. The reaction was stirred at rt overnight and the solvent was removed *in vacuo*. The crude was taken up in EtOAC and the organic phase was washed with 3x sat. aq. $NaHCO_3$ and brine. The organic phase was dried over $MgSO_4$ and the solvent was removed *in vacuo*. The crude was purified by FCC affording compound **2.8** in a yield of 90%.

Rf= 0.38 in 20% EtOAc in Hep

^{1}H NMR (400 MHz, Chloroform-*d*) δ 7.93 (td, *J* = 7.6, 1.9 Hz, 1H), 7.56 – 7.50 (m, 1H), 7.20 (t, *J* = 7.6 Hz, 1H), 7.13 (dd, *J* = 10.8, 8.3 Hz, 1H), 4.55 (t, *J* = 6.3 Hz, 2H), 2.61 (qt, *J* = 10.4, 6.3 Hz, 2H).
^{13}C NMR (101 MHz, Chloroform-*d*) δ 163.77 (d, *J* = 3.7 Hz), 162.10 (d, *J* = 260.9 Hz)134.88 (d, *J* = 9.1 Hz), 132.07, 125.78 (q, *J* = 276.6 Hz), 124.01 (d, *J* = 4.0 Hz), 118.02 (d, *J* = 9.4 Hz), 117.04 (d, *J* = 22.2 Hz), 57.86 (q, *J* = 3.7 Hz), 33.38 (q, *J* = 29.3 Hz).

4,4,4-Trifluorobutyl benzoate 2.11

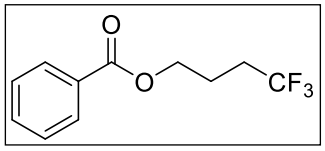

Benzoyl chloride (2.11g, 15.00mmol, 1.5 equiv.) was slowly added to a solution of 4,4,4-trifluorobutane-1-ol (1.05mL, 10.00mmol, 1 equiv.) and TEA (1.67mL, 12.00mmol, 1.2 equiv.) in 15mL dry DCM. The reaction was stirred at rt. for 3h before the solvent was removed and the crude taken up in EtOAc. The organic phase was washed with 2x sat. $NaHCO_3$ and brine, dried over $MgSO_4$ and the solvent was removed *in vacuo*. The crude washed purified by FCC affording **2.11** as a colorless oil. Yield= 86%. Rf= 0.21 in 5% EtOAc in Hep.

HNMR ^{1}H NMR (400 MHz, Chloroform-*d*) δ 8.09 – 7.97 (m, 2H), 7.62 – 7.55 (m, 1H), 7.53 – 7.39 (m, 2H), 4.39 (t, *J* = 6.3 Hz, 2H), 2.40 – 2.19 (m, 2H), 2.15 – 1.95 (m, 2H).
CNMR^{13}C NMR (101 MHz, Chloroform-*d*) δ 166.35, 133.15, 129.89, 129.56, 128.44, 126.91 (q, *J* = 276.3, Hz), 63.13, 31.26, 30.97, 30.67, 30.38, 21.69.

Hept-1-en-2-yl benzoate 2.12

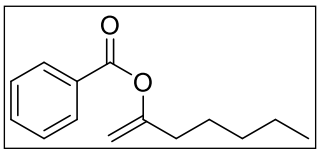

2.12 was prepared according to *General procedure 2*. Yield=80%.

HNMR^{1}H NMR (400 MHz, Chloroform-*d*) δ 8.13 – 8.09 (m, 2H), 7.64 – 7.58 (m, 1H), 7.53 – 7.43 (m, 2H), 4.90 – 4.84 (m, 2H), 2.36 (t, *J* = 7.7 Hz, 1H), 1.63 – 1.51 (m, 2H), 1.43 – 1.31 (m, 4H), 0.96 – 0.86 (m, 3H).

Hept-1-en-2-yl 2-phenylacetate 2.13

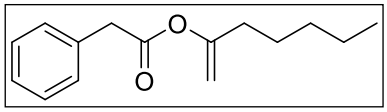

2.13 was prepared according to *General procedure 2*. Yield=78%

HNMR ^{1}H NMR (400 MHz, Chloroform-*d*) δ 7.39 – 7.28 (m, 5H), 4.74 (t, *J* = 6.5 Hz, 2H), 3.71 (s, 2H), 2.19 (t, *J* = 7.6 Hz, 2H), 1.40 (p, *J* = 7.4, 7.0 Hz, 2H), 1.35 – 1.20 (m, 4H), 0.90 (d, *J* = 6.8 Hz, 2H).

^{13}C NMR (101 MHz, Chloroform-*d*) δ 169.63, 156.65, 133.74, 129.26, 128.64, 127.22, 101.10, 41.53, 31.11, 26.02, 22.41, 13.98.

Hept-1-en-2-yl 2,6-dimethoxybenzoate 2.14

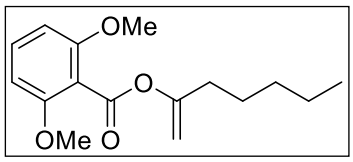

2.14 was prepared according to *General procedure 2*. Yield= 4%

HNMR ^{1}H NMR (400 MHz, Chloroform-*d*) δ 7.29 (t, *J* = 8.4 Hz, 1H), 6.60 – 6.52 (m, 2H), 4.88 (d, *J* = 1.3 Hz, 1H), 4.80 (d, *J* = 1.3 Hz, 1H), 3.83 (s, 6H), 2.35 (t, *J* = 7.7 Hz, 2H), 1.57 (p, *J* = 7.4 Hz, 2H), 1.34 (p, *J* = 3.8 Hz, 4H), 0.93 – 0.87 (m, 3H).
CNMR ^{13}C NMR (101 MHz, Chloroform-*d*) δ 164.61, 157.40, 156.96, 131.23, 112.84, 103.90, 101.47, 55.97, 33.37, 31.26, 25.97, 22.51, 14.02.

Hept-1-en-2-yl 2,6-difluorobenzoate 2.15

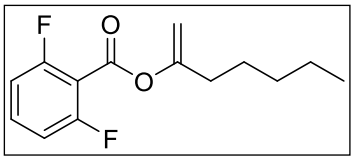

2.15 was prepared according to *General procedure 2*. Yield = 82%

HNMR ^{1}H NMR (400 MHz, Chloroform-*d*) δ 7.53 – 7.40 (m, 1H), 7.05 – 6.92 (m, 2H), 4.94 (d, *J* = 1.8 Hz, 1H), 4.86 (q, *J* = 1.3 Hz, 1H), 2.36 (t, *J* = 7.8 Hz, 2H), 1.63 – 1.49 (m, 2H), 1.36 (pd, *J* = 6.3, 4.1 Hz, 4H), 0.95 – 0.86 (m, 3H).
CNMR ^{13}C NMR (101 MHz, Chloroform-*d*) δ 160.71 (dd, *J* = 256.9, 6.0 Hz), 159.51, 156.50, 132.99 (t, *J* = 10.4 Hz), 112.04 (d, *J* = 25.5 Hz), 110.91 (t, *J* = 18.0 Hz), 101.83, 33.21, 31.09, 25.92, 22.37, 13.91.

Hept-1-en-2-yl 2,6-bis(trifluoromethyl)benzoate 2.16

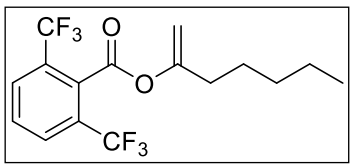

2.16 was prepared according to *General procedure 2*. Yield=73%.

^{1}H NMR (400 MHz, Chloroform-*d*) δ 7.96 – 7.91 (m, 3H), 7.71 (t, *J* = 7.9 Hz, 1H), 4.96 (d, *J* = 2.0 Hz, 1H), 4.88 (dt, *J* = 2.2, 1.2 Hz, 1H), 2.37 – 2.24 (m, 2H), 1.64 – 1.48 (m, 2H), 1.38 – 1.21 (m, 7H), 0.96 – 0.86 (m, 4H).

Hept-1-en-2-yl 2,6-dimethylbenzoate 2.17

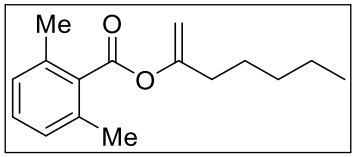

2.17 was prepared according to *General procedure 2*. Yield= 70%

^{1}H NMR (400 MHz, Chloroform-*d*) δ 7.26 – 7.20 (m, 1H), 7.08 (d, *J* = 7.6 Hz, 2H), 4.91 (d, *J* = 1.7 Hz, 1H), 4.89 (t, *J* = 1.4 Hz, 1H), 2.42 (s, 6H), 2.38 (t, *J* = 7.8, 7.2 Hz, 2H), 1.65 – 1.53 (m, 2H), 1.45 – 1.34 (m, 4H), 0.98 – 0.88 (m, 3H).
^{13}C NMR (101 MHz, Chloroform-*d*) δ 168.16, 156.76, 134.86, 129.50, 127.98, 127.64, 101.34, 33.56, 31.21, 26.21, 22.44, 19.72, 13.99.

Hept-1-en-2-yl 3-phenylpropanoate 2.18

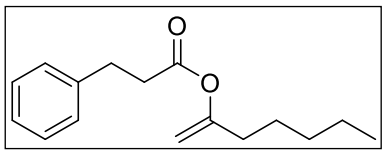

2.18 was prepared according to *General procedure 2*. Yield= (55%).

^{1}H NMR (400 MHz, Chloroform-*d*) δ 7.31 (t, *J* = 7.7 Hz, 2H), 7.26 – 7.21 (m, 3H), 4.71 (d, *J* = 1.5 Hz, 1H), 4.67 (d, *J* = 1.4 Hz, 1H), 3.01 (t, *J* = 7.7 Hz, 2H), 2.73 (t, *J* = 7.7 Hz, 2H), 2.21 – 2.12 (m, 2H), 1.42 (p, *J* = 7.0 Hz, 2H), 1.37 – 1.22 (m, 4H), 0.90 (t, *J* = 6.8 Hz, 3H).
^{13}C NMR (101 MHz, Chloroform-*d*) δ 171.06, 156.61, 140.23, 128.53, 128.34, 126.36, 101.02, 35.97, 33.29, 31.17, 30.98, 26.10, 22.42, 14.00.

Hept-1-en-2-yl 5-phenylpentanoate 2.19

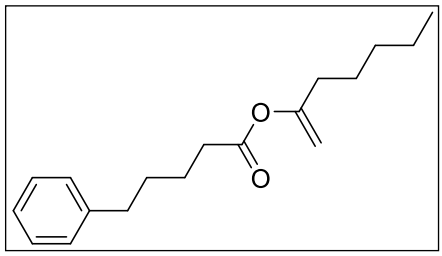

2.19 was prepared according to *General procedure 2*. Yield = (80%)

^{1}H NMR (400 MHz, Chloroform-*d*) δ 7.33 – 7.26 (m, 2H), 7.23 – 7.17 (m, 3H), 4.73 (s, 1H), 4.71 (s, 1H), 2.67 (t, *J* = 6.9 Hz, 2H), 2.43 (t, *J* = 6.8 Hz, 2H), 2.21 (t, *J* = 7.6 Hz, 2H), 1.79 – 1.66 (m, *J* = 3.9 Hz, 4H), 1.47 (p, *J* = 7.5 Hz, 2H), 1.38 – 1.28 (m, 4H), 0.95 – 0.85 (m, 3H).
^{13}C NMR (101 MHz, Chloroform-*d*) δ 171.74, 156.63, 142.05, 128.39, 128.35, 125.82, 100.96, 35.59, 34.25, 33.34, 31.18, 30.87, 26.16, 24.60, 22.44, 14.00.

Prop-1-en-2-yl 3-phenylpropanoate 2.21

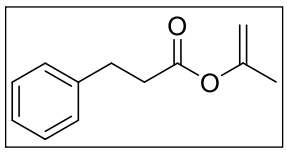

3-phenylpropanoic acid (2.00g, 13.33mmol, 1 equiv.), Na_2CO_3 (28mg, 0.27mmol, 0.02equiv.), $((p\text{-cymene})RuCl_2)_2$ (40mg, 0.53mmol, 0.04 equiv.) and tri(2-furyl)phosphine (40mg, 0.13mmol, 0.01 equiv.) were added to a MW under inert atmosphere. Propenyl (20mL, 1M in THF, 20mmol, 1.5 equivalents) was added and the vial was capped. The reaction was stirred at 80°C overnight. The solvent was removed and the crude was purified by FCC affording compound **2.21** in a yield of 39%.

^{1}H NMR (400 MHz, Chloroform-*d*) δ 7.33 (t, *J* = 7.5 Hz, 3H), 7.26 (d, *J* = 7.4 Hz, 4H), 4.72 (d, *J* = 1.6 Hz, 1H), 4.67 (s, 1H), 3.03 (t, *J* = 7.7 Hz, 3H), 2.75 (t, *J* = 7.7 Hz, 3H), 1.91 (s, 3H).
^{13}C NMR (101 MHz, Chloroform-*d*) δ 171.09, 153.08, 140.30, 128.64, 128.45, 126.47, 102.15, 36.05, 31.04, 19.63.

Di-tert-butyl (azanediylbis(ethane-2,1-diyl))dicarbamate 2.22

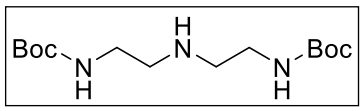

Diethylene triamine(2.16mL, 20mmol, 1equiv.) was dissolved in 40 mL dry THF and cooled to 0°C under inert atmosphere. In an addition funnel, Boc-ON was dissolved in 20 mL dry THF and was added dropwise to the cooled solution. After addition, the reaction was allowed to reach rt and was stirred for 1h and solvent was removed *in vacuo*. The residue was dissolved in DCM and the organic phase was washed with 10w/w% NaOH, water and brine. The organic phase was dried

over $MgSO_4$ and solvent was removed *in vacuo*. Crude was purified by FCC 100%DCM to 10% MeOH in DCM affording **2.22** a yellow oil. Yield= 78%. Rf =0,16 in 10% MeOH in DCM.

^{1}H NMR (400 MHz, $CDCl_3$) 4.93 (br s, 2H), 3.24-3.19 (m, 4H), 2.73 (t, 4H, J = 5.7 Hz), 1.44 (s, 18H)
^{13}C NMR (101 MHz, $CDCl_3$) 156.3, 79.4, 49.0, 40.4, 28.6

Methyl bis(2-((tert-butoxycarbonyl)amino)ethyl)glycinate 2.23

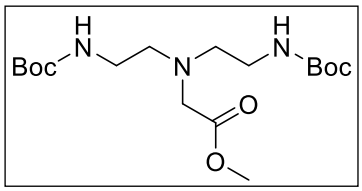

Di-tert-butyl(azanediylbis(ethane-2,1-diyl)) dicarbamate (4.5g, 14.8mmol, 1 equiv.) was dissolved in 50mL DMF and DIPEA(3.29mL, 22.3mmol, 1.5equiv.) and methyl bromoacetate (2.13mL, 17.8mmol, 1.2 equiv.) were added. The reaction was stirred overnight at rt. Solvent was removed under a stream of nitrogen and crude was purified by FCC (20% EtOAc in PE to 50% EtOAc in PE) afforded **2.23** a white solid in 81% yield. Yield=. Rf=0.29 in 50/50 EtOAc/PE.

^{1}H NMR (400 MHz, $CDCl_3$) 5.13 (br s, 2H, NH), 3.70 (s, 3H), 3.37 (s, 2H), 3.15 (q, 4H, J = 5.6 Hz), 2.72 (t, 4H, J = 5.9 Hz), 1.44 (s, 18H)
^{13}C NMR (101 MHz, $CDCl_3$) 172.3, 156.3, 79.3, 55.1, 54.3, 51.8, 38.7, 28.6

Compound 2.24

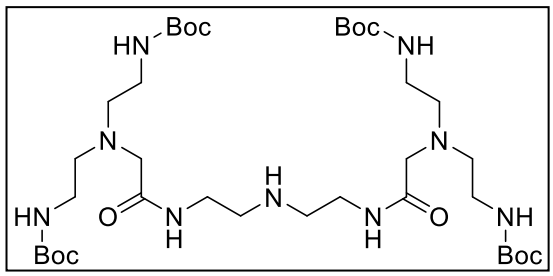

Methyl bis(2-((tert-butoxycarbonyl)amino) ethyl) glycinate (2.00g 5.33mmol, 5 equiv.) was dissolved in 3mL dry MeOH in a MW vial. Diethylene triamine (116µL, 1.07mmol, 1 equiv.) was added under inert atmosphere and the vial was capped. The reaction was heated to 100°C overnight. Solvent was removed and crude was purified by Fcc 0-20% MeOH in DCM yielding **2.24** in 35% as a colorless oil. Rf=0,22 in 10% MeOH in DCM.

^{1}H NMR (400 MHz, Chloroform-*d*) δ 5.80 (s, 2H), 3.49 (s, 8H), 3.45 (s, 4H), 3.25 – 3.16 (m, 8H), 3.13 (s, 4H), 2.86 (s, 4H), 2.62 (s, 8H), 1.45 (s, 36H).
^{13}C NMR (101 MHz, CD_3OD) 175.6, 158.6, 80.2, 59.9, 56.4, 49.5, 39.7, 38.4, 28.9

2-bromo-N-(prop-2-yn-1-yl)acetamide 2.25

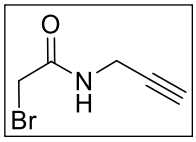

Propargylamine (1.67g, 18,2mmol, 1 equiv.) was dissolved in 33mL DCM and 33mL sat. $NaHCO_3$. The solution was cooled to -10°C and was added dropwise 2-bromo acetylbromide (2.42mL, 27.2mmol, 1.5 equiv.). The reaction was allowed to reach rt and was stirred for 1h. The two phases were separated and the aqueous phase was acidified and extracted with DCM. The combined organic phase was washed with sat $NaHCO_3$ and 1M HCl and dried over $MgSO_4$ and solvent removed *in vacuo*. Product was attained in a 46% yield affording **2.25** a white solid. Rf =0.65 in 50/50 EtOAc/PE.

^{1}H NMR (400MHz, $CDCl_3$) 6.70 (s, 1H), 4.08 (dd, J=2.5Hz 2H), 3.89 (s, 2H), 2.28 (t, J=2.6Hz, 1H)
^{13}C NMR (101 MHz, $CDCl_3$) 165.1, 78.5, 72.3, 30.0, 28.7

Compound 2.26

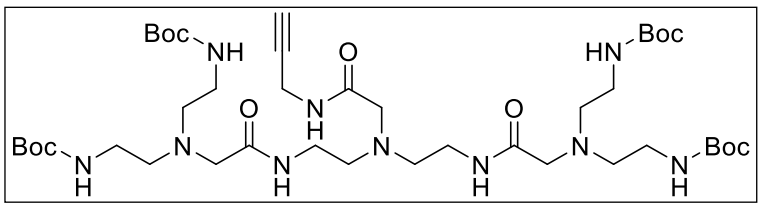

2.24 (300mg, 0.38mmol, 1 equiv.) was dissolved in dry 1mL MeCN under inert atmosphere, K_2CO_3 (104mg, 0.76mmol, 2 equiv.) was added and cooled to 0°C. 2-bromo-N-(prop-2-yn-1-yl)acetamide (83mg, 0.47mmol, 1.25 equiv.) was added in one portion. The reaction was allowed to reach rt and was stirred overnight. Solvent was removed and the reaction was purified by Fcc 0-10% MeOH in DCM. Yielding **2.26** in a 44% yield as a white solid. Rf = 0.72 in 10%MeOH in DCM.

^{1}H NMR (400 MHz, Chloroform-*d*) δ 7.79 (s, 2H), 5.68 (s, 4H), 4.05 (dd, *J* = 5.5, 2.5 Hz, 2H), 3.35 (m, 4H), 3.24 (s, 2H), 3.18 (m, 12H), 2.73 (t, *J* = 5.8 Hz, 4H), 2.58 (t, *J* = 5.5 Hz, 8H), 2.24 (d, *J* = 2.8 Hz, 1H), 1.89 (s, 2H), 1.43 (s, 36H).
^{13}C NMR (101 MHz, $CDCl_3$) 172.2, 171.5, 156.7, 80.0, 79.4, 71.5, 59.5 (two peaks), 55.8 (two peaks), 38.8, 37.9, 29.0, 28.6

4-(3-(Piperidin-1-yl)propanoyl)benzoic acid hydrochloride 2.27

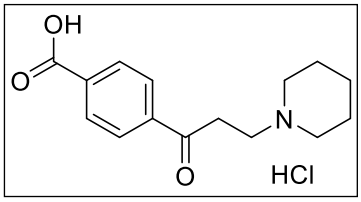

4-Acetyl benzoic acid (1.00g, 6.09mmol, 1 equiv.), piperidine HCl(0.74g, 6.09mmol, 1 equiv.) and paraformaldehyde (0.55g, 18.3mmol, 3 equiv.) were dispersed in 4mL EtOH and 60µL 37% HCl was slowly added. The reaction was heated to reflux for 3h before adding a second portion of paraformaldehyde (0.55, 18.3mmol, 3 equiv.) and the reaction was refluxed overnight. The reaction mixture was cooled before adding acetone to precipitate the product. The reaction was stirred for 5 min. to dissolve any impurities and was filtered. The white precipitate was washed extensively with acetone and EtOAc, before drying under vacuum yielding 50%of **2.27** as a white solid.

^{1}H NMR (400 MHz, Methanol-d_4) δ 8.20 – 8.13 (m, 4H), 3.72 – 3.50 (m, 4H), 3.14 – 2.96 (m, 2H), 2.05 – 1.75 (m, 6H).

^{13}C NMR (101 MHz, Methanol-d_4) δ 196.74, 168.62, 131.04, 130.82, 130.63, 129.28, 54.75, 34.44, 24.25, 23.97, 22.52.

4-(3-(p-tolylthio)-2-((p-tolylthio)methyl)propanoyl)benzoic acid 2.28

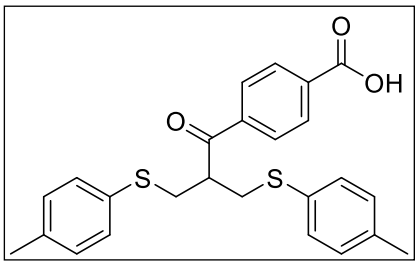

4-(3-(piperidin-1-yl)propanoyl)benzoic acid hydro-chloride **2.27**(0.50g, 1.68mmol, 1 equiv.) in a MW vial was dispersed in 1.2mL EtOH and 0.8mL MeOH. Then 4-mehtylbenzenethiol (0.42g, 3.36mmol, 2 equiv.), piperidine (72μL, 0.729mmol, 0.03 equiv.) and formaldehyde (50mg, 1.68mmol, 1 equiv.) were added and the MW vial was capped. The reaction was heated to 105°C and was stirred overnight. The solvent was removed and the crude was purified by FCC (50/50 PE/EtOAc to 20% MeOH in EtOAc) yielding 49% of **2.28** as a yellow solid in. Rf= 0.2 in EtOAc.

^{1}H NMR (400 MHz, Chloroform-*d*) δ 8.07 (d, *J* = 8.1 Hz, 2H), 7.64 (d, *J* = 8.1 Hz, 2H), 7.17 (d, *J* = 7.8 Hz, 5H), 7.09 (d, *J* = 7.9 Hz, 4H), 3.84 (p, *J* = 6.8 Hz, 1H), 3.28 (dd, *J* = 13.3, 7.6 Hz, 2H), 3.19 (dd, *J* = 13.6, 6.1 Hz, 2H), 2.38 (s, 6H).
^{13}C NMR (101 MHz, Chloroform-*d*) δ 200.47, 170.56, 140.47, 137.26, 133.06, 131.55, 131.07, 130.27, 129.86, 128.32, 45.88, 36.40, 21.11.

4-(3-Tosyl-2-(tosylmethyl)propanoyl)benzoic acid 2.29

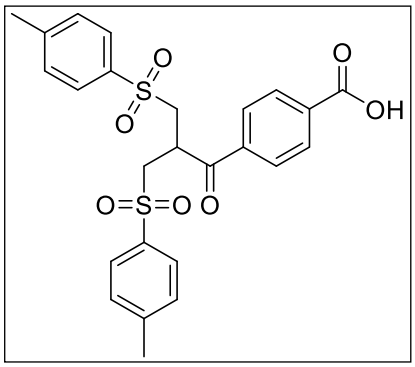

4-(3-(p-tolylthio)-2-((p-tolylthio) methyl) propanoyl) benzoic acid **2.28** (200mg, 0.46mmol, 1 equiv.) was dissolved in 40mL of MeOH:water 1:1 and to the solution oxone (1.68g, 11.09mmol, 6 equiv.) was added. The reaction was stirred at rt overnight, after which the solvent was removed *in vacuo*. The crude was purified by FCC affording compound **2.29** in a yield of 94%.

^{1}H NMR (400 MHz, Chloroform-*d*) δ 8.07 (d, *J* = 8.1 Hz, 2H), 7.70 (dd, *J* = 8.4, 3.2 Hz, 6H), 7.36 (d, *J* = 8.0 Hz, 4H), 4.39 (t, *J* = 6.3 Hz, 1H), 3.64 (dd, *J* = 14.3, 6.6 Hz, 2H), 3.54 – 3.46 (m, 2H), 2.48 (s, 5H).
^{13}C NMR (101 MHz, Chloroform-*d*) δ 195.50, 155.43, 153.80, 145.74, 138.19, 135.40, 130.66, 130.34, 128.66, 128.46, 55.76, 35.87, 21.87.

Methyl 2,6-bis(hydroxymethyl)isonicotinate 2.30

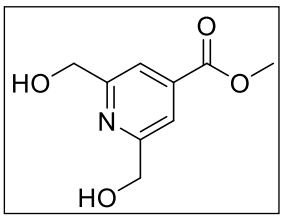

Methyl isonicotinate (1.72mL, 14.6mmol, 1 equiv.) was dissolved in 40mL MeOH and conc. H_2SO_4 (390μL, 7.3mmol, 0.5 equiv.) was added. The reaction was heated to 50°C and ammonium persulfate (33.30g, 146mmol, 10 equiv.) in 40mL H_2O was added, firstly 3mL and then rapidly dropwise. The reaction was heated overnight and MeOH was removed. Residue was

taken up in EtOAc and the aqueous phase was neutralized. The aqueous phase was extracted 2x with EtOAc and the combined organic phase was washed with brine and dried over $MgSO_4$. The product was purified by FCC 0-10%MeOH in DCM, yielding 21% of **2.30** as a beige solid. Rf= 0.56 in 10% MeOH in DCM.

^{1}H NMR (400 MHz, Chloroform-*d*) δ 7.75 (s, 2H), 4.81 (s, 5H), 3.95 (s, 4H).
^{13}C NMR (101 MHz, Chloroform-*d*) δ 165.45, 160.01, 138.87, 118.59, 64.43, 52.81.

Methyl 2,6-bis(bromomethyl)isonicotinate 2.31

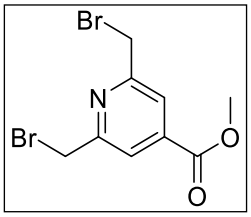

Methyl 2,6-bis(hydroxymethyl)isonicotinate **2.30** was suspended in dry ACN and PBr_3 was added dropwise. The reaction was heated to 45°C and was stirred for 2.5h. The reaction was carefully quenched with water and the aqueous phase was extracted with EtOAc 3x. The combined organic phase was washed with brine, dried over $MgSO_4$ and the solvent was removed. The crude was purified by FCC (PE to 50/50 EtOAc/PE) yielding 71%of **2.31** as white crystals. Rf= 0.18 in PE.

^{1}H NMR (400 MHz, Chloroform-*d*) δ 7.94 (s, 2H), 4.60 (s, 4H), 4.00 (s, 3H).
^{13}C NMR (101 MHz, Chloroform-*d*) δ 164.74, 157.95, 139.76, 122.23, 52.94, 32.81.

2,6-Bis(bromomethyl)isonicotinic acid 2.32

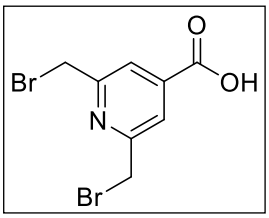

Methyl 2,6-bis(bromomethyl)isonicotinate (350mg, 1.08mmol, 1 equiv.) was dissolved in THF and LiOH (78mg, 3.25, 3equiv.) and the reaction was stirred at rt overnight. EtOAc and 1M HCl was added. The reaction was extracted 2 times with EtOAc. The combined organic phase was dried over $MgSO_4$ and the solvent was removed *in vacuo*, yielding 2,6-bis(bromomethyl)isonicotinic acid **2.32** quantitatively as a white powder.

^{1}H NMR (400 MHz, Methanol-d_4) δ 7.95 (s, 2H), 4.65 (s, 4H).
^{13}C NMR (101 MHz, Methanol-d_4) δ 165.54, 158.25, 141.03, 122.23, 33.60, 31.77.

Ethyl 4-(2,6-bis(bromomethyl)isonicotinamido)butanoate 2.33

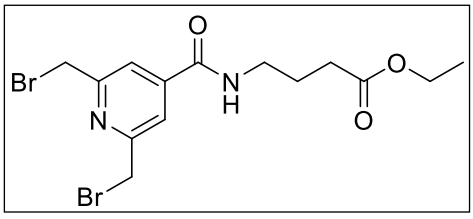

2,6-bis(bromomethyl)isonicotinic acid (300mg, 0.97mmol, 1 equiv.) was dissolved in 15mL dry DMF under inert atmosphere. Lutidine (489mg, 4.56mmol, 4.7 equiv.) and HATU (554mg, 1.46mmol, 1.5 equiv.) were added and the reaction was stirred for 15min. Then ethyl 4-aminobutanoate hydrochloride was added and the reaction was at rt overnight. Upon completion, the reaction was partitioned between water and EtOAc. The organic phase was dried over $MgSO_4$ and the solvent was removed *in vacuo*. The crude was purified by FCC yielding ethyl 4-(2,6-bis(bromomethyl)isonicotinamido)butanoate **2.33** as a white solid in a yield of 25%.

^{1}H NMR (400 MHz, Chloroform-*d*) δ 7.80 (s, 2H), 4.72 (s, 4H), 4.18 (q, *J* = 7.1 Hz, 2H), 3.55 (q, *J* = 6.2 Hz, 2H), 2.50 (t, *J* = 6.6 Hz, 2H), 2.00 (p, *J* = 6.6 Hz, 2H), 1.75 (s, 2H), 1.28 (t, *J* = 7.1 Hz, 3H).
^{13}C NMR (101 MHz, Chloroform-*d*) δ 174.26, 164.76, 157.46, 144.10, 119.52, 60.97, 50.84, 46.12, 40.28, 32.24, 23.78, 14.19.

Screen procedures

Screen setup 1 (Screen **1**, **2** and **4**)

The following stock solutions were prepared: 1M and 20mM IMes in THF, 1M benzyl alcohol and benzyl amine in THF and electrophiles in THF (0.43M).

200μL IMEs stock and 100 μL electrophile stock were mixed in an LCMS vial and stirred for 15 min before addition of 200μL nucleophile at rt. Samples were taken at different time intervals and were analyzed by UPLC-MS.

Screen setup 2 (Screen **3** and **5**)

The following stock solutions were prepared: 40mM IMes in DMSO/ACN, 2M benzyl alcohol and benzyl amine or 6-amino-hexanol in DMSO/ACN and 0.86M electrophiles in DMSO/ACN.

100μL IMEs stock and 50 μL electrophile stock were mixed and stirred for 15 min before addition of 250μL DMSO/ACN:Aq mixture and the of 100μL nucleophile stock. Samples were taken at different time intervals (4h and 48h) and were analyzed by UPLC-MS.

Peptide screen setup

Peptide stock solution of the relevant peptide in 6.67mM in PBS buffer were prepared. Electrophile was dissolved in the relevant concentrations in DMF. 90μL of the peptide stock, 20μL of the IMes stock, 5μL electrophile stock and 5μL for screen tuning (HCl or PBS buffer), resulting in a total reaction volume of 120μL and a 5mM peptide concentration. The reactions were carried out in 500μL Eppendorf tubes and were mixed at 1200rpm in a thermomixer. Unless otherwise stated, the screens were carried out at rt.

Chapter 3 Linkers in antibody drug conjugates

Linkers in antibody drug conjugates must leverage high stability during circulation with efficient and selective release upon delivery to the target cell, thereby providing both safety and efficacy to the ADC[1–7]. Additionally, the linker must contain appropriate handles for both the attachment of the drug and for the conjugation onto the antibody Figure 3.1.

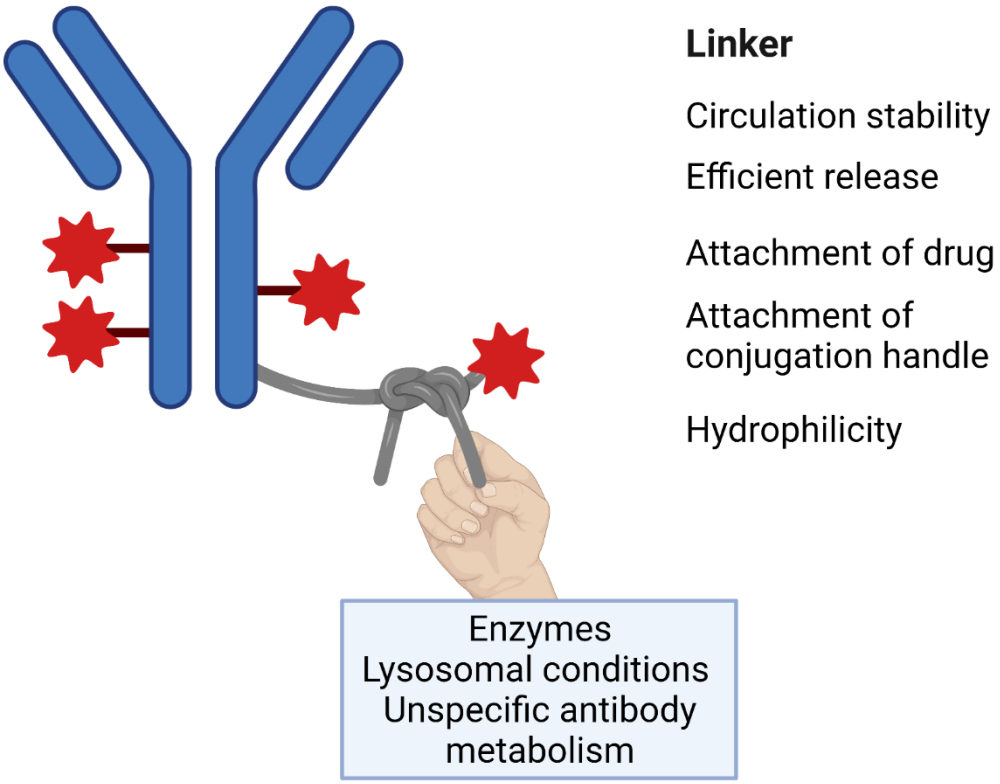

Figure 3.1. General concept of linkers in ADCs.

Apart from the main task of stability and release, next generation linkers are being designed to incorporate cancer specific triggers for added safety. In addition, integration of hydrophilic groups provide access to ADCs with high DAR by preventing the ADC aggregation induced by the hydrophobicity of the cytotoxin[8–10]. Designing ADCs with higher DARs could be advantageous, due to the higher intracellular drug concentration delivered per antibody internalised. Killing cells more efficiently could mitigate the development of resistance[11].

Generally, cleavable linkers are preferred, due to the release of the native drug, however, the stability of the non-cleavable linkers can outweigh the disadvantage of the release of modified drug moieties[1,4–7]. Non-cleavable linkers do not contain a particular weak bond that can be specifically cleaved and are instead, metabolised non-specifically in the lysosome releasing the drug with an amino acid appendage. If this modification does not interfere with the central pharmacophore, cytotoxicity may not be attenuated, as observed in the case of mc-MMAE linkers and the ADC Blenrep[12,13]. Another consideration for the non-cleavable linkers is that the charge of the amino acid appendage prevents the released drug in participating in bystander killing, limiting the potency.

Despite these drawbacks, there are currently two FDA approved ADCs incorporating non-cleavable linkers, Blenrep, using the mc-linker[14] and Kadcyla, using the SMCC-linker[15–17].

Cleavable linkers take advantage of the change of the environment upon delivery to the target, to trigger the release of the native drug. This trigger can cause the linker to be less stable (eg. hydrazone and carbonate acid cleavable linkers), however, stability can be modulated through choice of conjugation method, as the steric bulk provided by the antibody can enhance stability. Below in Table 3.1, is an overview of cleavable linkers published for the incorporation into ADCs.

Linker type	Cleavage	Advantages//Disadvantages	Examples
		Chemically cleaved	
Hydrazone	Lysosomal pH	Simple linker design// Low plasma stability	Mylotarg[18–21] Besponsa[22–24]
Carbonate	Lysosomal pH	Release of alcohol functionalised drugs // Low circulation half-life Extracellular release	Trodelvy [25–28]
Dissulfide	Lysosomal reduction	Stable in circulation// Drug must be thiol functionalized	Lumoxiti[29–31]
		Enzyme cleavable	
Peptide	Peptidase	Stable Efficient release Peptidases are upregulated in certain cancers// Non-specific cleavage by other peptidases Some scaffolds are hydrophobic Limited functionality release	Val-cit[32] Adcetris[33–36] Polivy[37,38] Padcev[39] Tidvak[39] Dipeptides[40–42] Val-ala Zynlonta[39] Gly-gly-phe-gly Enhertu[39]
Sugar moieties	Glucosidase, galactosidase	Highly hydrophilic trigger Exclusive lysosomal enzyme High plasma stability// Low MTD* when compared to val-cit linker (glucuronide linker)	Glucoronide[43–47] Galactoside[48]
Phosphate	Phosphatase	Hydrophilic trigger Release of alcohol functionalized drugs// Release affected by steric bulk limiting substrate scope	Pyro-phosphate[49]
Sulfate	Sulfatase	Highly hydrophilic trigger Amine release	Arylsulfatase [50]

Dienzymatic	Improved safety Highly hydrophilic triggers// Dual dependency may slow down drug release	Sulfated sugar moiety[51]

*Table 3.1. Overview of the cleavable linkers developed for the incorporation into ADCs. Advantages and disadvantages have been listed as well as examples of linkers or ADCs incorporating these linker types. *MTD=maximum tolerated dose.*

Sulfatase

Sulfatases are a class of hydrolytic enzymes that cleave the S-O bond of sulfates esters [52] via post translationally derived formylglycine from either serine or cysteine[53]. Substrates include sulfated sugars and steroids, suggesting an active site able to accommodate bulky substrates. Despite the nomenclature (e.g. arylsulfatase A-K), the natural substrates of sulfatases are sulfated sugar moieties, with the exception being steroid sulfatase (arylsulfatase C), which hydrolyses sulfated steroids. However, most sulfatases display aryl sulfate ester hydrolysis activity.

Sulfatases present an interesting target for linker design, as they are primarily located in the lysosome (Table 3.2) and altered expression has been linked to several cancers[54–58].

GENE NAME	CELLULAR LOCATION	SUBSTRATE
ARSA[59,60]	Lysosomal	Cerebrosid-3-sulfate
ARSB[60–62]	Lysosomal	Chondroitin, Dermatan sulfate
ARSC (STS) [63]	ER	Sulfated steroids
ARSD[60,64,65]	ER	Unknown
ARSE [66]	Golgi apparatus	Unknown
ARSF[66]	ER	Unknown
ARSG[60,66]	Lysosomal	Heparan sulfate
ARSH[67]	Unknown	Unknown
ARSI[67]	Unknown	Unknown
ARSJ[67]	Unknown	Unknown
ARSK[60,68,69]	Lysosomal	Heparan sulfate Chondroitin sulfate
GALNS[60,62]	Lysosomal	Chondroitin sulfate Keratan sulfate
GNS[60]	Lysosomal	Heparan sulfate Keratan sulfate
IDS[60]	Lysosomal	Dermatin sulfate Chondroitin sulfate
SULF1[70]	Cell surface	Heparan sulfate
SULF2[70]	Cell surface	Heparan sulfate
SGSH[60]	Lysosomal	Heparan sulfate

Table 3.2. Overview of Human sulfatases, their cellular location and known substrates.

Interestingly, sulfatase triggered release in prodrug and linker design remains mostly unexploited with most sulfatase probes being based on unadorned aryl-sulfate scaffolds[71–76]. Currently, only 17 human sulfatases have been identified, making this hydrolytic enzyme family more exclusive than many other hydrolytic enzymes[67].

Self-immolative spacers in ADCs

The development of spacers for the traceless delivery of cargo, has been sought after in many fields, including polymer chemistry, nanoparticles and targeted drug delivery[77–81]. Self-immolative spacers are covalently attached to the cargo and upon encountering the correct stimuli, they are able to release the cargo in its native form. One of the most popular strategies for selective release, is the incorporation of self-immolative spacers relying on an electronic cascade. An external trigger initiates the cascade by revealing a nucleophilic functionality, whereupon the spontaneous and irreversible release happens, driven by the formation of CO_2 to release hydroxyl-, amino- or sulfur functional groups (Scheme 3.1).

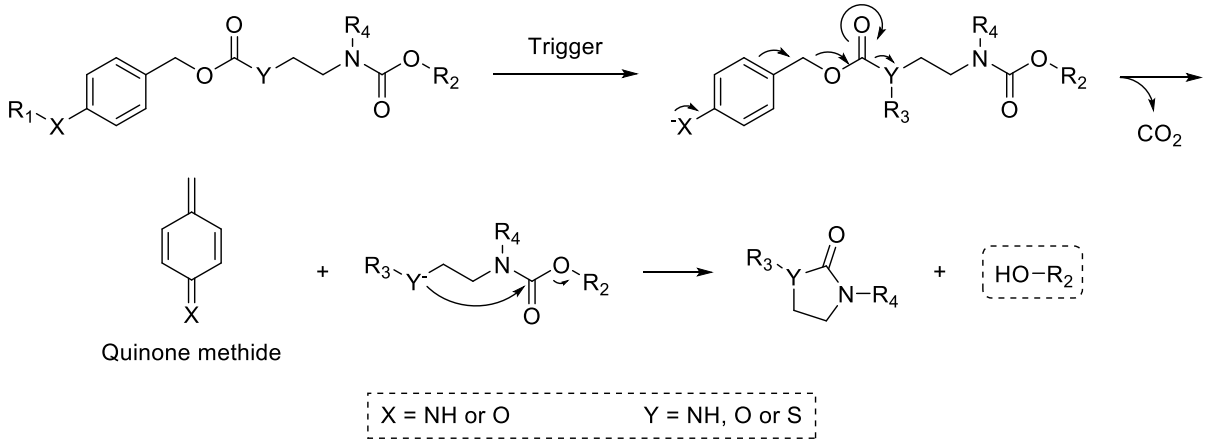

Scheme 3.1. The general overview of the 1,6-elimination that is coupled to a 1,5-cyclisation moiety for the release of alcohol functionalities.

Substitution of the benzene ring influences the rate of release, with EWG decreasing release rates[82]. A disadvantage to these cascade reactions, is the release of a highly reactive quinone methide moiety, that rapidly and non-specifically reacts with surrounding nucleophiles. This rapid reaction has been used to label enzymes responsible for the cleavage[83–85]. However, for the delivery of highly cytotoxic drug to cancer cells, this additional toxicity may not be problematic. 1,5-cyclisations, driven by the formation of 2-imidazolidones, enable the release of hydroxyl group coupled via carbamate and has often been combined with a 1,6-elimination for the selective release of amines (Scheme 3.1). The rate of cyclisation is influenced by the Thorpe-Ingold effect, as well as the nucleophilicity of the cyclising amine[82].

3.1 Part I

3.1.1 Aim

The aim of this project is to develop and test an alcohol releasing, aryl-sulfatase cleavable linker scaffold for the development of novel ADCs (Figure 3.2). Drug release is envisaged to happen through a 1,6-elimination, followed by a 1,5-ring closure to release the drug. A convergent synthetic route, allowing for the facile modification of the key intermediates to tune the properties of the final linker, has been envisioned. A stable and efficient sulfatase cleavable linker could provide another weapon in the arsenal against cancer, achieving a second layer of selectivity, by exploiting the intracellular expression levels of sulfatase.

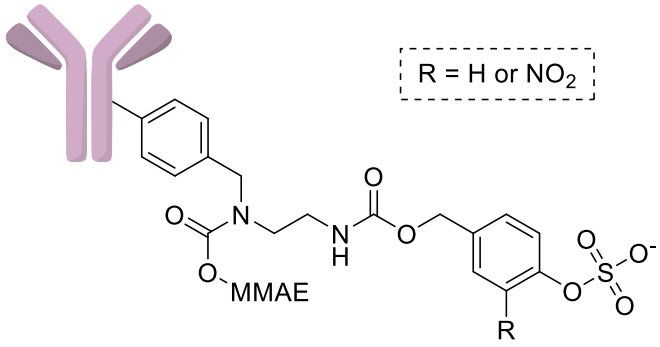

Figure 3.2.Structure of the linker for release of alcohol functionalized drugs.

Release of alcohol functionalities in ADCs

Currently, most linkers take advantage of the PABC self-immolative spacer for the intracellular release of amine functionalities, greatly limiting the scope of attachable cytotoxins[7]. The only ADC on the market that releases a drug through an alcohol functionality, is Trodelvy, which releases the SN-38 drug[27]. The authors of the paper behind Trodelvy, report that the drug release proceeds through an acid mediated cleavage of a carbonate functionality. Limited circulation stability of the linker ($t_{1/2}$~ 20h), however, results in significant premature release, restricting the use of more potent drugs like auristatins and PDB-dimers in combination with this linker type. Furthermore, when comparing the therapeutic response of internalizing ADCs and non-internalizing control ADCs, a difference was not necessarily observed[28]. The unspecific internalization of macromolecules, due to the immature and leaky vessels of cancer cells, is offered as an explanation by the authors. Further research into the release of alcohols has been undertaken with the phosphatase cleavable linkers[49] and the cyanine-based photocleavable linker[86]. However, there is still a need for enzyme cleavable linkers that can release alcohol functionalized drugs in a selective and efficient manner, furthering the tuning of ADC properties.

Design of the linker

Sulfates esters are stable in serum and the enzyme recognition motif offers a highly hydrophilic functionality to counteract hydrophobicity of the cytotoxin, which limits the DARs of current ADCs [2], making sulfatases are an attractive target for the development of cleavable linkers for ADCs in cancer treatment.

For the release of alcohols, a stepwise release mechanism was envisaged taking advantage of the spontaneous 1,6-elimination of the spacer triggered by enzyme-mediated sulfate ester hydrolysis, followed by a 1,5 ring closure, driven by the formation of a stable cyclic urea to release the alcohol-functionalized cargo[80,82] (Scheme 3.2).

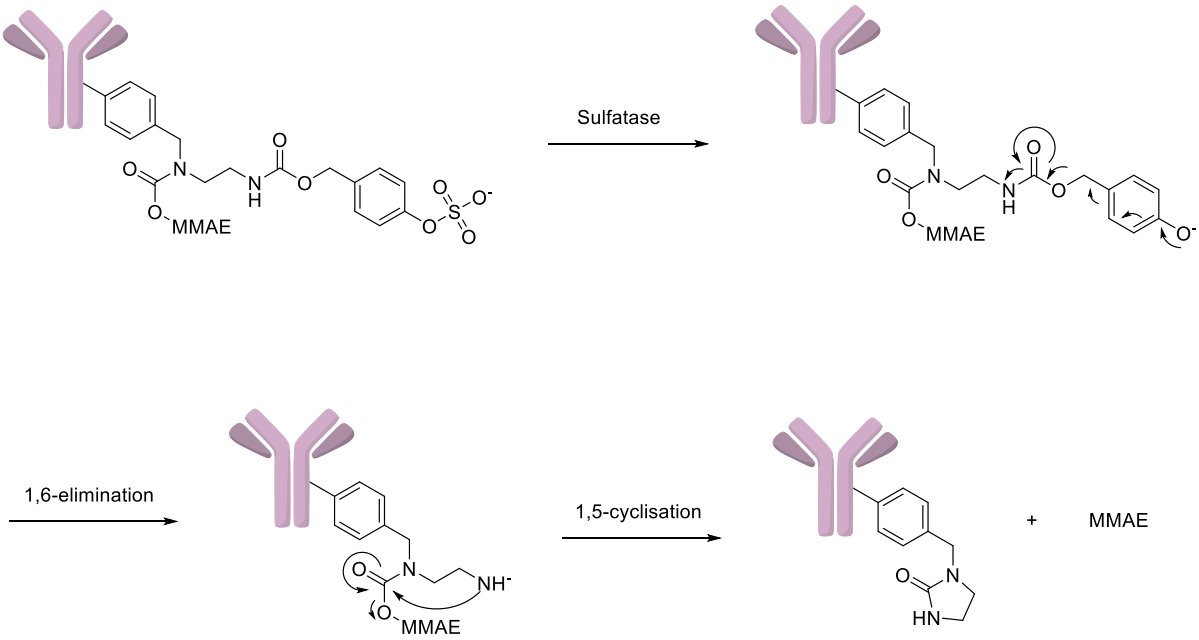

Scheme 3.2. The envisioned release mechanism of the sulfatase cleavable linker, as a 1,6-elimination followed by a 1,5-cyclisation to release the native alcohol functionalized drug.

The payload was functionalized with the well described maleimide conjugation handle. The maleimide group was installed through a PEG-4 chain, increasing both the hydrophilicity of the payload, as well as the distance from the bulky antibody to the enzymatic recognition site (Scheme 3.3). The synthetic route was designed in a convergent manner, synthesizing two key intermediates to be coupled via a carbamate. The synthetic route was designed for late stage incorporation of the expensive and toxic drug, as well as taking into consideration the sequence of sulfate and amine deprotection, as well as maleimide attachment.

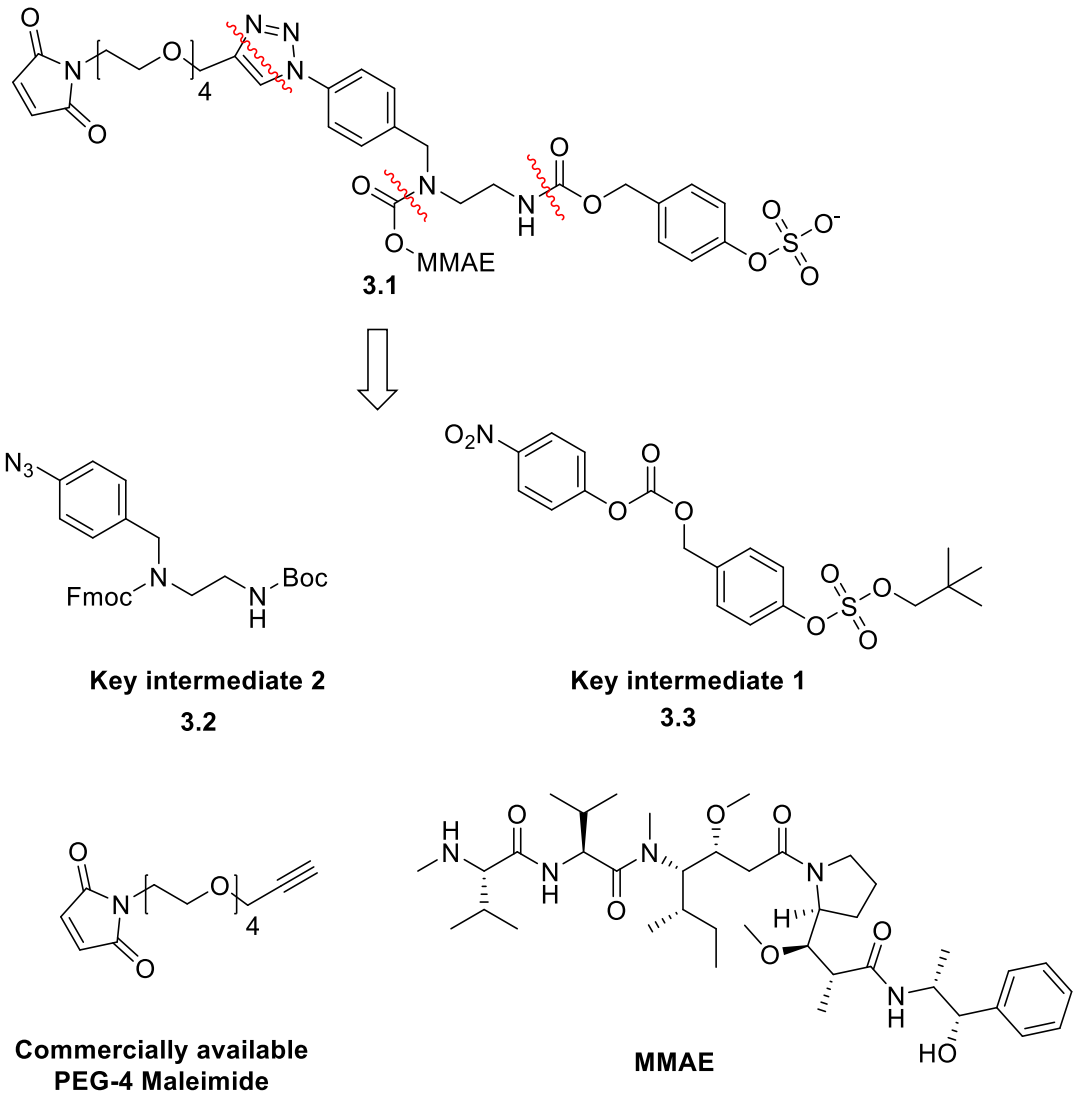

Scheme 3.3. Structure of the linker and the key intermediates.

While optimization and the development of the synthetic strategies was carried out by me, the synthesis of payload 1(**3.1**), as well as cellular testing, was carried out by research assistant Christina Haxvig.

3.1.2 Synthesis of Key intermediate 1

The synthetic conditions of the preparation of Key intermediate 1 **3.3**, is shown below in Scheme 3.4.

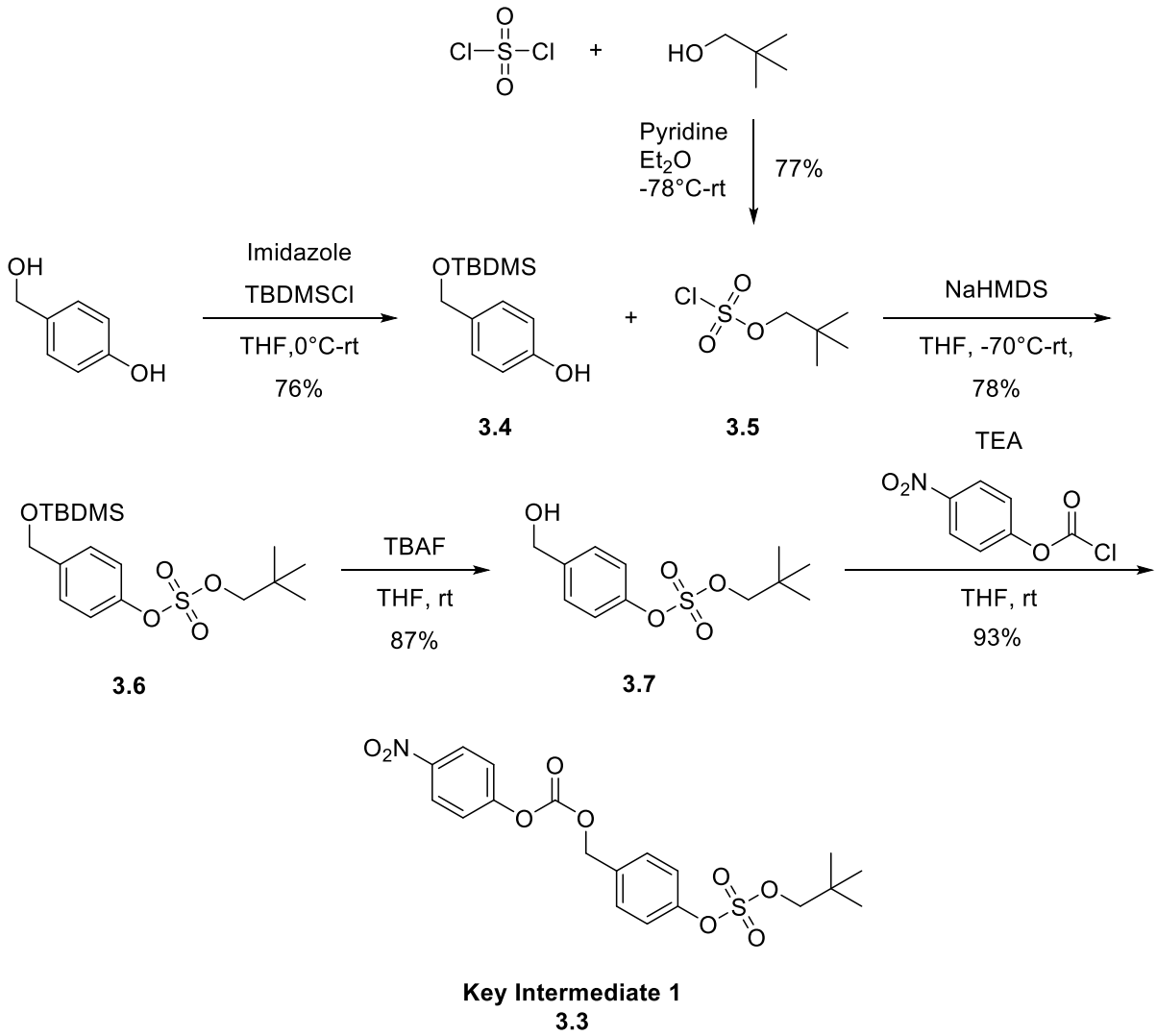

*Scheme 3.4. Conditions and yields of the synthesis of Key Intermediate 1, compound **3.3**.*

The benzylic hydroxyl group of 4-(hydroxyl)phenol was chemoselectively protected using TBDMSCl, yielding 76% of compound **3.4**. Np sulfurochloridate **3.5** was prepared in satisfactory yields and was reacted with the phenol **3.6** affording **3.37** (78%). The TBDMS group was removed by TBAF and the free alcohol **3.7** was reacted with Pnp-chloroformate, affording 48% of key intermediate **3.3** over 4 steps.

3.1.3 Synthesis of Key intermediate 2

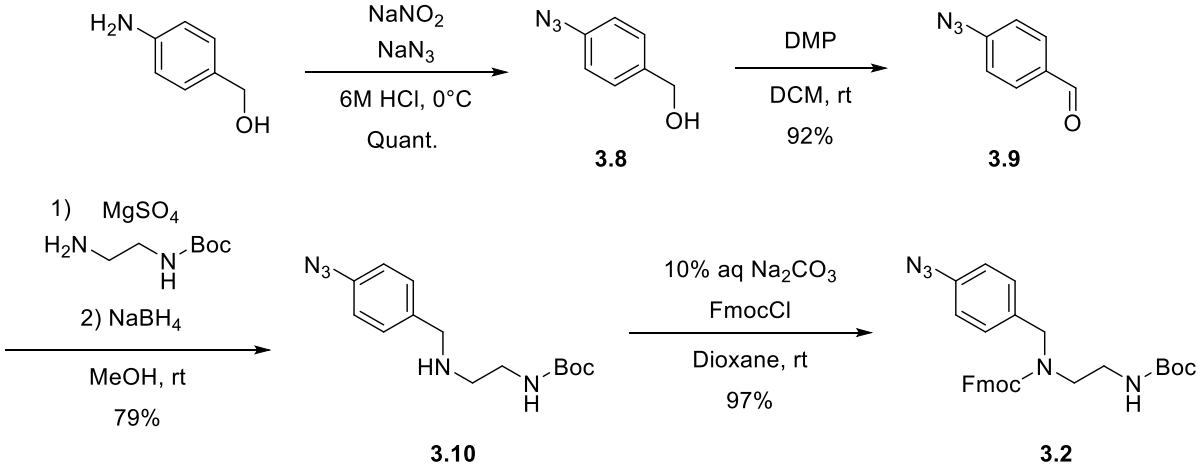

Scheme 3.5. Conditions and yields of the synthetic route of Key Intermediate 2, Compound 3.2

As seen in Scheme 3.5, the azido group was installed by a diazotisation reaction to yield the diazonium salt, followed by a nucleophilic aromatic substitution on the benzene ring, yielding compound **3.8** quantitatively. The benzylic alcohol was oxidized to the corresponding aldehyde **3.9** by Dess Martin periodinane with a yield of 92% and **3.9** was condensed with N-boc ethylenediamine, followed by the reduction of the imine yielding 79% of compound **3.10** in. Lastly, the secondary amine was Fmoc protected yielding 70% of Key Intermediate 2 (**3.2**) over 4 steps.

3.1.4 Synthesis of Payload 1

With key intermediate 1 and 2 in hand, Boc-deprotection of **3.2** was performed to reveal the primary amine, which was followed by a carbamate coupling with Pnp-carbonate **3.3** to yield **3.11** (66%), as seen in Scheme 3.6. Simultaneous removal of the np and Fmoc protection groups was performed using 0.5M aqueous NH_4OAc, affording the deprotected linker as observed by UPLC-MS. Without purification and further analysis, the azido group was reacted with an alkyne functionalized PEG-4 maleimide in a copper(I) catalyzed azido-alkyne cycloaddition, followed by purification by preparative HPLC yielding 31% of compound **3.12** over 2 steps (Scheme 3.6).

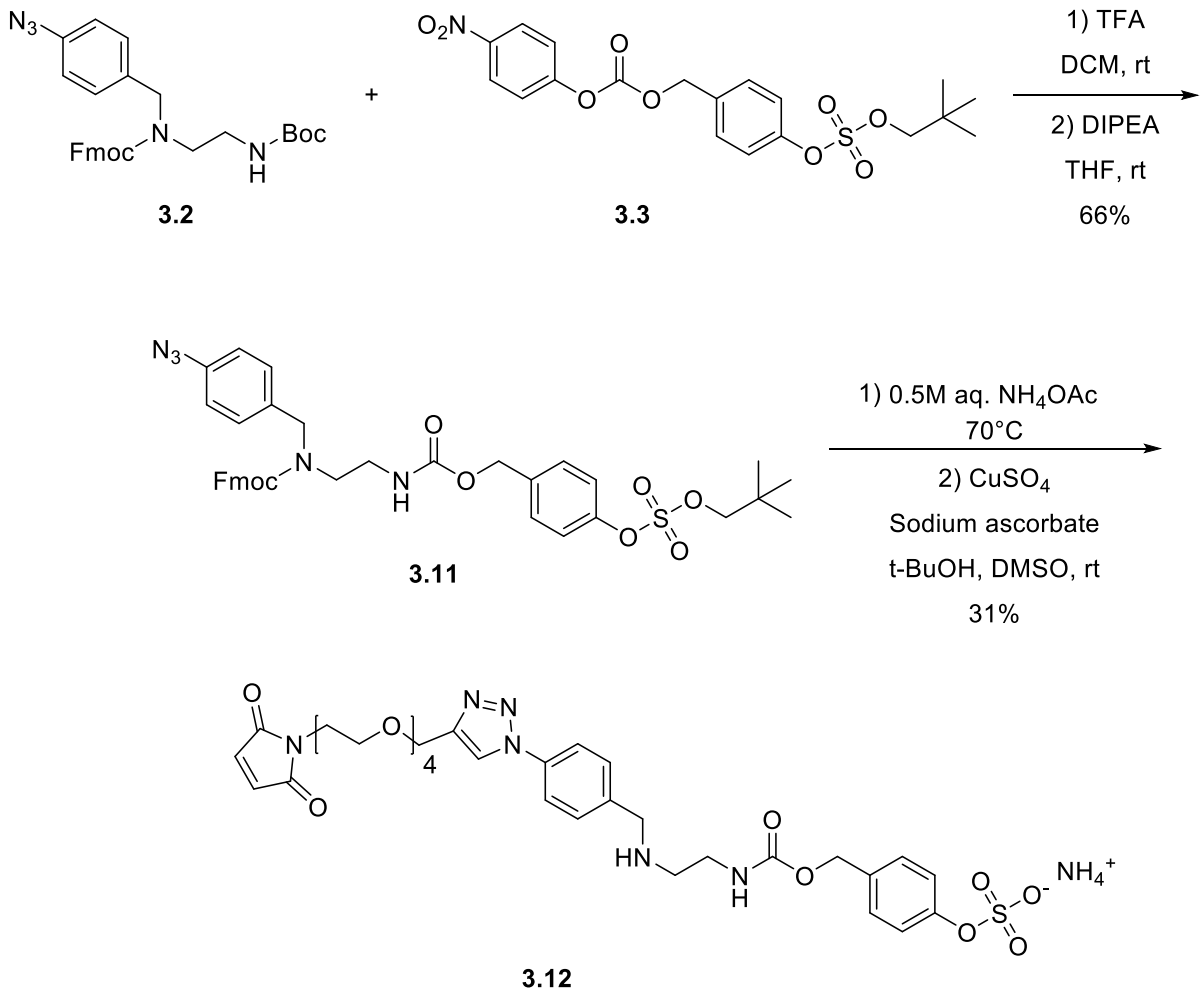

Scheme 3.6. Conditions and yields of the synthesis of compound 3.12.

To attach MMAE via the alcohol, the reactivity of the amine functionality in MMAE was blocked by Boc protection, followed by the formation of a Pnp-carbonate of the alcohol **3.13** (Scheme 3.7).

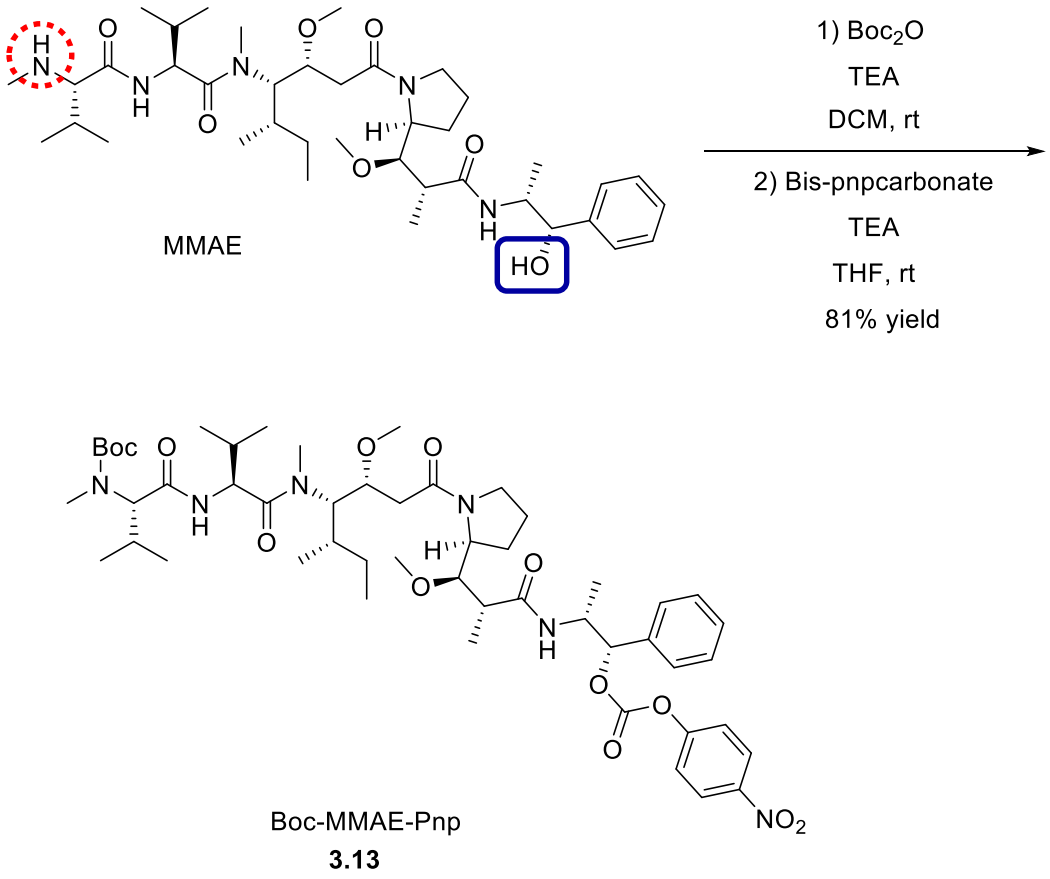

Scheme 3.7. Synthetic conditions and yields for the synthesis of compound 3.13.

Boc-MMAE-Pnp **3.13** was coupled with **3.12** to yield 10% of **3.14** after purification by preparative HPLC. Finally, removal of the Boc group by addition of TFA was carried out to reveal the payload **3.1** in a quantitative yield (Scheme 3.8).

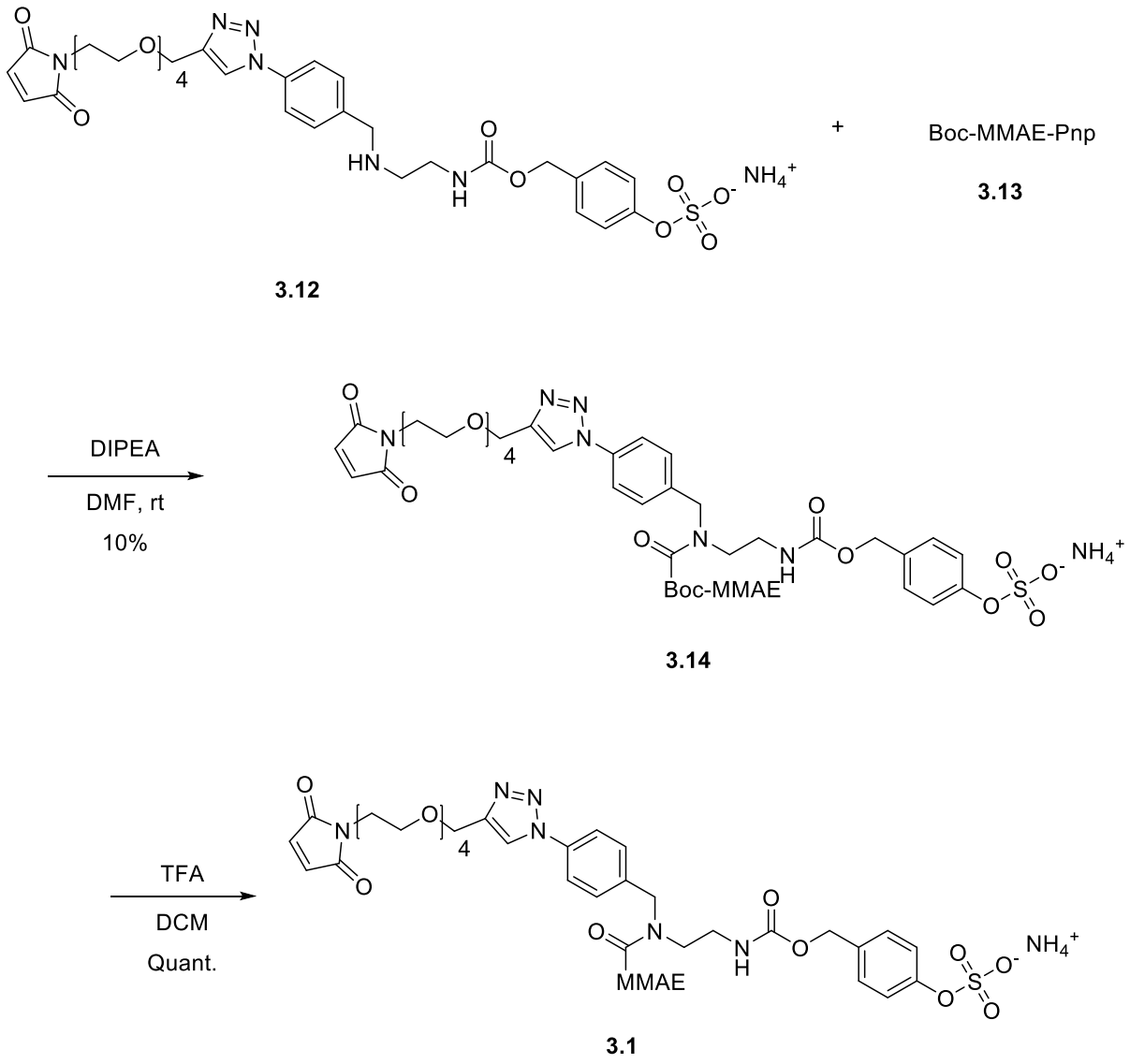

Scheme 3.8. Conditions and yields of the synthesis of compound 3.1

3.1.5 Cell studies

For the initial *in vitro* studies, it was decided to take advantage of the commercially available Trastuzumab for the evaluation of the linker against HER2 positive ($HER2^+$) breast cancer cells. This antigen has been targeted extensively in ADC development and is often used as an initial proof of concept for novel payloads. Furthermore, to validate assay setup and for benchmark performance, the commercially available Maleimide-val-cit-MMAE and Maleimide-mc-MMAE payloads were purchased and used.

ADC preparation proved more difficult than initially expected. In total around 100 attempts were needed to reproducibly synthesize the conjugated ADCs. The difficulty arose from insufficient reduction of the antibody and when changing the reduction reagent from dithiothreitol to the HCl salt of (tris(2-carboxyethyl)phosphine)(TCEP), sufficient reduction of the interchain disulfide bonds was achieved, without complete reduction of the antibody. Trastuzumab was conjugated to the three payloads yielding the ADCs, seen in Table 3.3 below. The B12 antibody is a non-internalizing antibody used in this study as a negative control.

Antibody	Payload	Name	DAR
Tras	**3.1**	Tras-s-MMAE	1
Tras	Maleimide-val-cit-MMAE	Tras-vc-MMAE	3
Tras	Maleimide-mc-MMAE	Tras-mc-MMAE	3
B12	**3.1**	B12-s-MMAE	2
B12	Maleimide-val-cit-MMAE	B12-vc-MMAE	5
B12	Maleimide-mc-MMAE	B12-mc-MMAE	4

Table 3.3. Overview of the ADCs prepared for cell testing. DARs were estimated by gel chromatography of the reduced antibody. Visualized by Coomassie blue.

Cell viability was determined by the MTS assays, wherein readouts are based on the reduction of the central tetrazole by mitochondrial reductase (Figure 3.3) to form the corresponding formazan (λmax 490) by the addition of MTS directly to the cell culture[87–89].

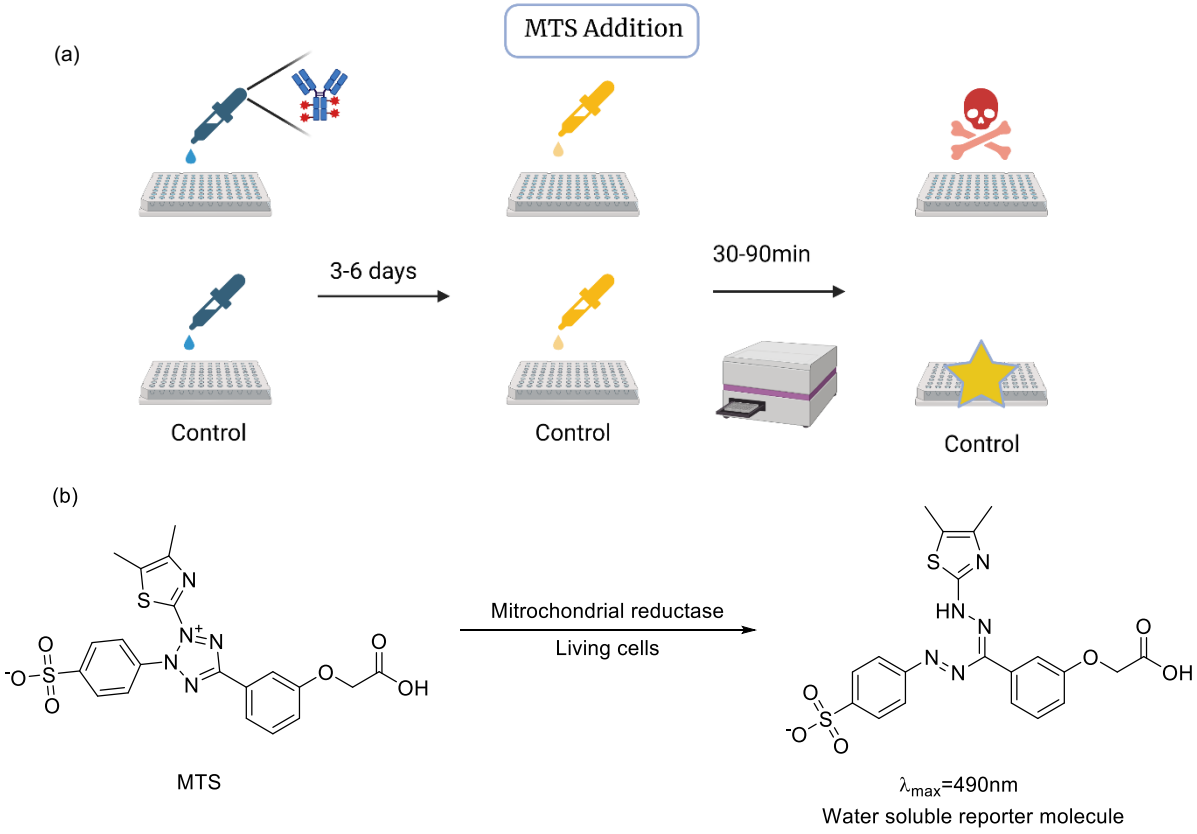

Figure 3.3. (a)The schematic overview of the cell assays. (b) The structure of MTS and the formazan formed during cellular processing, generating the reporter molecule.

The assay was considered to be sufficiently reliable for the initial studies, despite the possible inaccuracies of the method, due to analysis of MTS metabolism directly in the cellular matrix[90,91].

The HER2$^+$ breast cancer cell lines BT474 and SKBR3, as well as the HER2 negative breast cancer cell line MCF7, were purchased and were maintained at Finsen Laboratory. Gratifyingly, Tras-s-MMAE induced a dose-response curve in the two HER2$^+$ cell lines, as seen in Figure 3.4. Furthermore, the assay was validated by the induction of a dose-response curve of Tras-vc-MMAE and Tras-mc-MMAE. The negative control experiments using the HER2 negative MCF7 breast cancer cell line, showed that the toxicity was antigen dependent. Furthermore, the non-

internalizing B12 control ADCs displayed a significant reduction in toxicity supporting antigen dependent toxicity (data not shown). However, the Tras-s-MMAE ADC displayed less potency than the commercially available linkers. One caveat, when regarding the potencies of the different ADCs, is that they all have different DARs making direct comparisons imprecise.

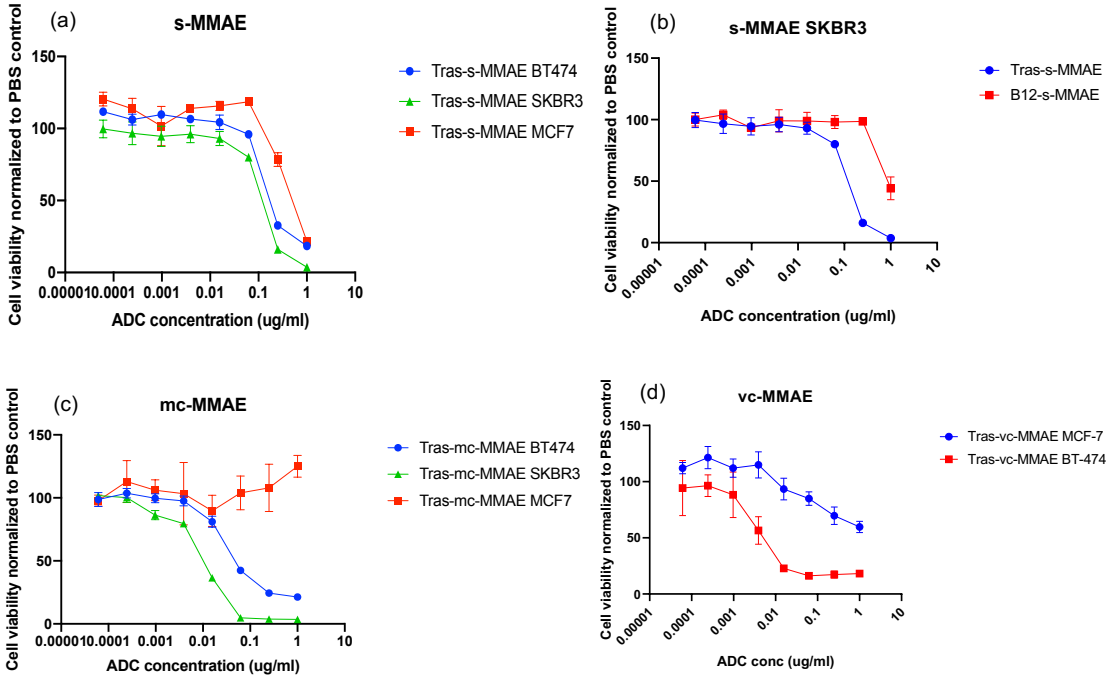

Figure 3.4. Showing the results of the cell studies in dose response curves. (a) Displaying the results of Tras-s-MMAE on the different breast cancer cell lines. (b) The comparison of Tras-s-MMAE and the control ADC. (c) Showing the result of the Tras-mc-MMAE ADC. (d) Results from cell studies with the Tras-vc-MMAE ADC.

Unfortunately, the Tras-s-MMAE did not display a sufficiently good dose response curve compared to the already established linkers. An interesting observation from the lack of potency, is that by tethering MMAE through the alcohol, little toxicity due to antibody metabolism was observed. This novel attachment could provide insight into MMAE induced toxicity in ADCs. Postdoc Anders Højgaard Hansen performed a data mining campaign of the RNA expression levels of lysosomal arylsulfatases, in an effort to understand the potency observed. Interestingly, an inverse relationship between the expression of HER2 and lysosomal sulfatase levels was discovered, suggesting that sulfatase cleavable linkers may not be appropriate for treatment of $HER2^{+}$ cancers (data not shown). Thus, other cancer types were investigated and it was found that osteosarcomas display high sulfatase expression at the RNA level.

The osteosarcoma cell line SaOS-2 was provided by Finsen Laboratory and the payloads were conjugated to a novel uParap-targeting antibody, discovered and validated in-house at Finsen Laboratory[92]. uParap is barely expressed in normal tissue, however this rapidly internalizing antigen is overexpressed in several non-epithelial cancers. The following ADCs were produced (Table 3.4).

Antibody	Payload	Name	DAR
5f4	**3.1**	5f4-s-MMAE	3
5f4	Maleimide-val-cit-MMAE	5f4-vc-MMAE	2
5f4	Maleimide-MC-MMAE	5f4-mc-MMAE	2

Table 3.4. The prepared ADCs for testing on the SaOS-2 cell line. DARs were estimated by gel chromatography of the reduced antibody. Visualized by Coomassie blue.

The results of the *in vitro* assays performed on the osteosarcoma cells when using 5f4-s-MMAE are reported in Figure 3.5.

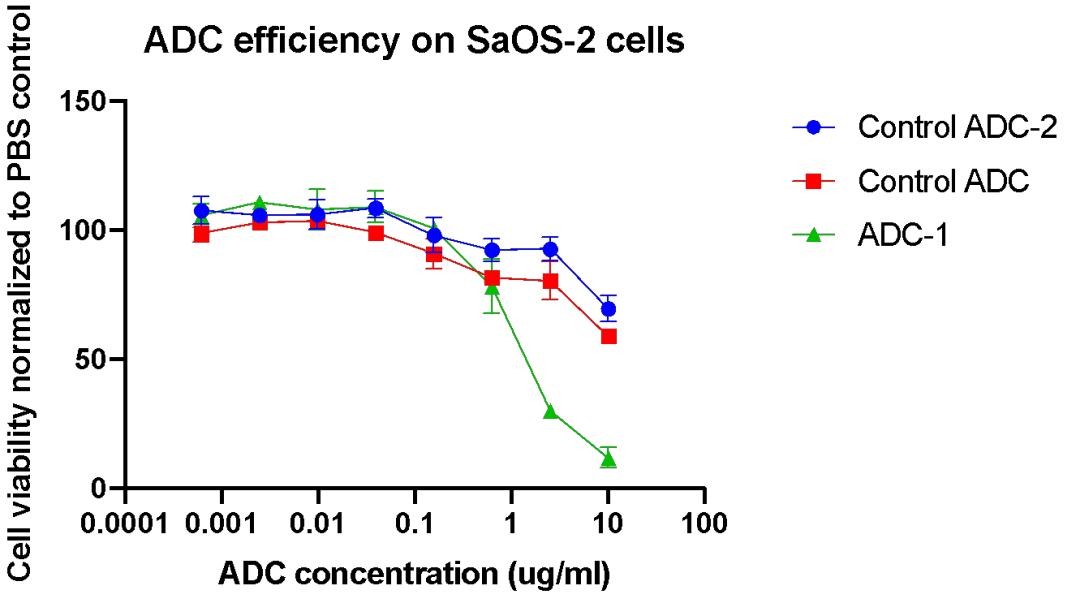

Figure 3.5. Data from the cell viability assay, showing the dose-response curves of the three ADCs; 5f4-s-MMAE, 5f4-vc-MMAE and 5f4-mc-MMAE as analyzed with the MTS assay. The results reported here are after 3days incubation with the ADC. Control ADC is Tras-vc-MMAE control ADC-2 is Tras-mc-MMAE and ADC-1 is Tras-s-MMAE.

An interesting observation was that the ADCs incorporating the commercially available payload displayed low potencies towards the osteosarcoma cells suggesting that osteosarcomas may require different linkers than breast cancer cells.

3.1.6 Synthesis of Payload 2

It was envisioned that introduction of a nitro group in the *ortho* position to the aryl sulfate moiety could increase the potency of the final ADC, as previously shown by data from Bargh et al[50]. To investigate this phenomenon, the synthetic strategy of payload 1 was adapted to using 4-(hydroxymethyl)-2-nitrophenol as starting material, to access payload 2 (Figure 3.6).

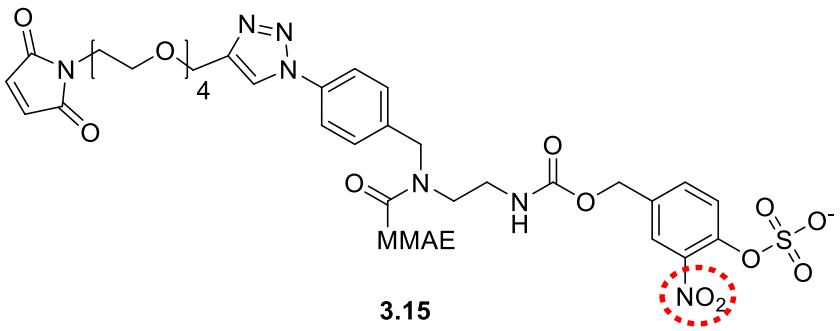

3.15

Figure 3.6. Structure of the o-nitro linker 3.15.

Synthesis of Key intermediate 3

Synthesis of payload 2 was carried out by me as seen in Scheme 3.9 - Scheme 3.12. Any chemical reaction including any MMAE or auristatin moiety was carried out by postdoc Anders H. Hansen.

When chemoselective TBDMS protection was attempted on 4-hydroxy-3-nitrobenzyl alcohol, both the alcohol and the phenol reacted to afford protected *para*-hydroxy benzyl alcohol (Scheme 3.9). The crude was carried forward in a chemoselective removal of phenolic TBDMS using a catalytic amount of DBU[93] yielding 87% of compound **3.16** over two steps. To install the np sulfate group, the conditions published by Bargh et al. were applied affording compound **3.17** (65%). During subsequent TBAF deprotection, partial decomposition of the product was observed and after purification and isolation of the remaining product, decomposition was observed after storage overnight under reduced pressure. It was hypothesized, that the residual fluoride ions could react with the np sulfate group as well as the TBDMS.

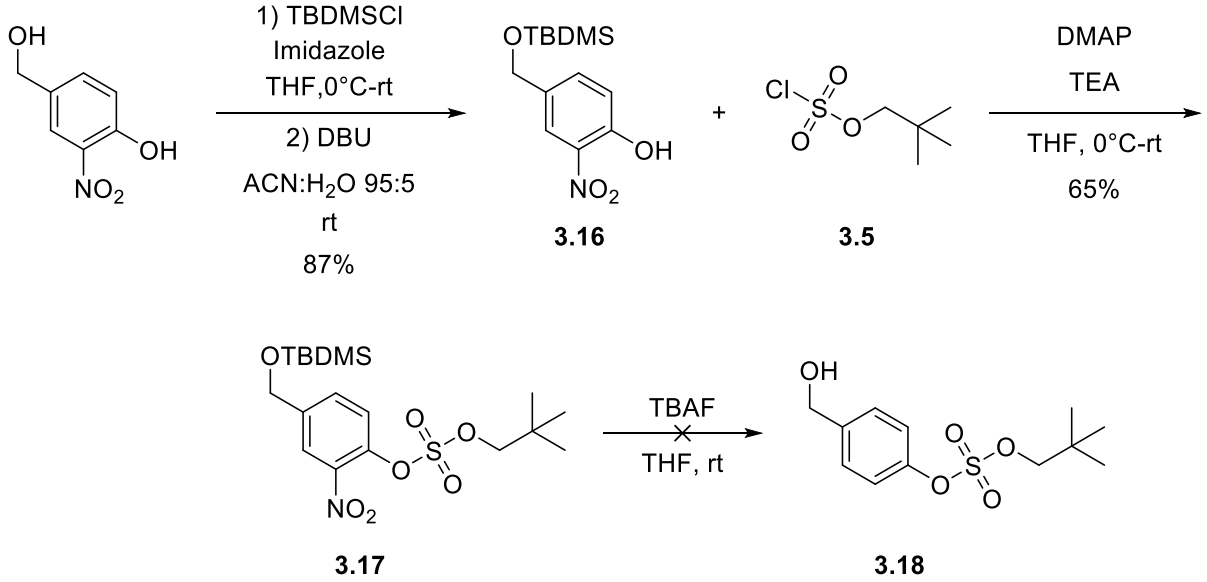

Scheme 3.9. First synthetic strategy applied for the synthesis of Key intermediate 3 3.18.

A new strategy (Scheme 3.10) was envisaged using the commercially available benzaldehyde, eliminating the need for protection groups and decreasing the number of synthetic steps by 1.

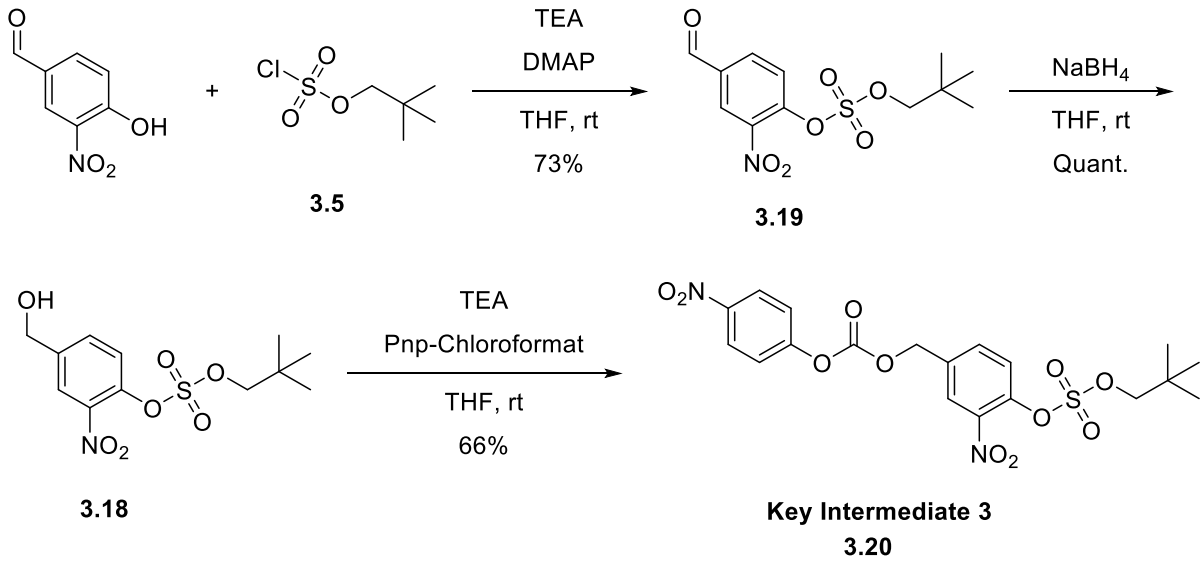

Scheme 3.10. Conditions and yields of the synthesis of Key Intermediate 3, compound 3.20.

Installation of the np sulfate group on 4-hydroxy-3-nitrobenzaldehyde proceeded with a satisfying yield (**3.19**, 73%) and the subsequent reduction using $NaBH_4$, afforded compound **3.18** quantitatively. The alcohol was stored in the freezer after work-up to avoid any degradation of the product. The hydroxyl group was activated with Pnp-chloroformate, yielding 66% of key intermediate 3 (**3.20**). Key intermediate 2 and 3 were reacted affording **3.21** in 78% yield (Scheme 3.11).

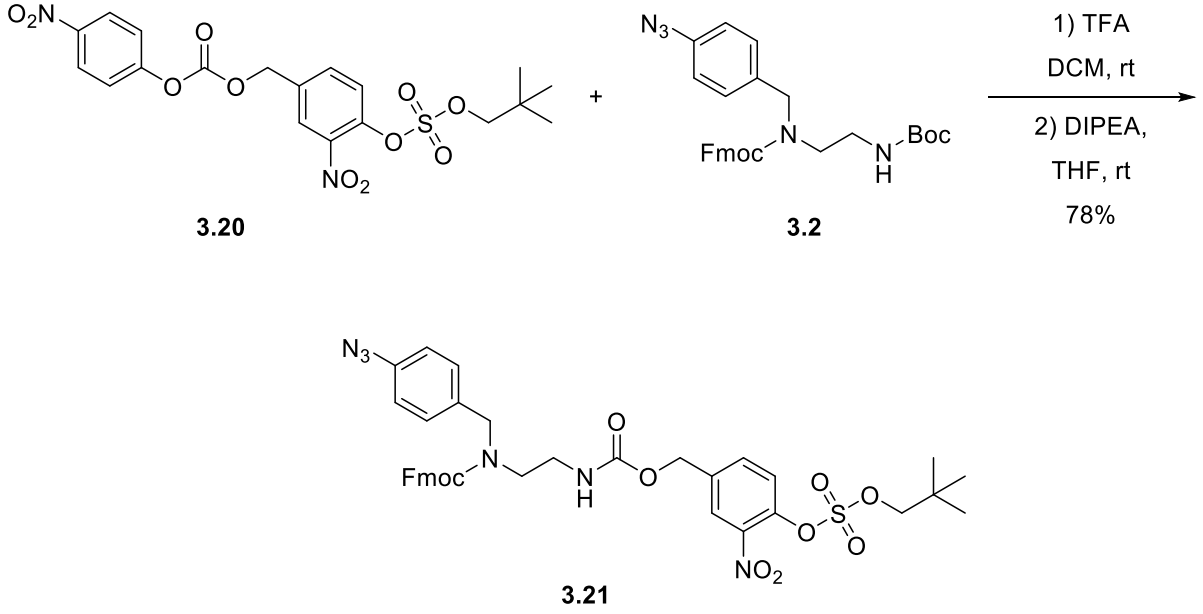

Scheme 3.11. Conditions and yield of the synthesis of compound 3.21.

During neopentyl deprotection of the substituted analogue **3.11**, the reaction was heated to 70°C and the reaction proceeded slowly (4 days). However, when these conditions were applied to nitro-analogue **3.21**, complete decomposition of the starting material was observed after 12h, suggesting significant difference of reactivity of the *o*-nitro neopentyl sulfate. When applying milder conditions (0.5M aqueous NH_4OAc at rt), the Fmoc group was not removed, introducing the need

for an additional step. Addition of the diethylamine for Fmoc-removal to the free sulfate, resulted in the complete degradation of the starting material. Thus, compound **3.21** was initially treated with 10 equivalents of diethylamine, followed by removal of solvent and addition of 0.5M aqueous NH_4OAc. Upon completion, the crude was reacted with PEG-4-maleimide to afford compound **3.22** in a satisfying yield, after purification by preparative HPLC (Scheme 3.12).

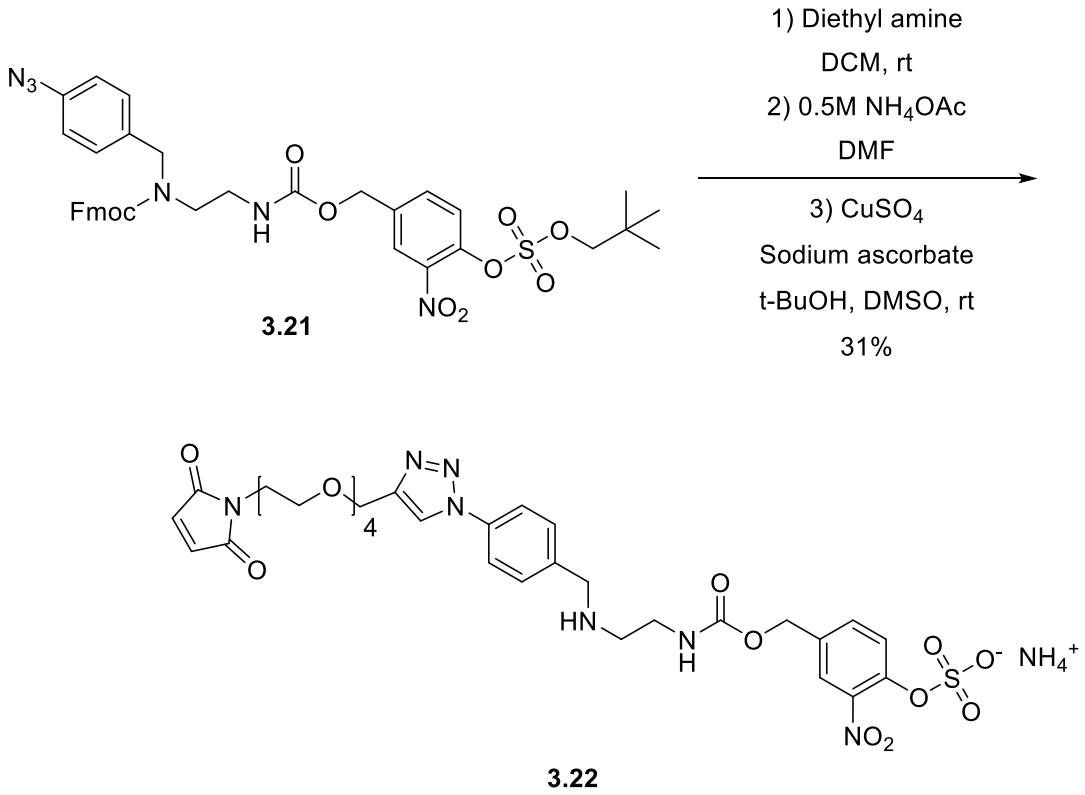

Scheme 3.12. Conditions and yield of the synthesis of compound 3.22.

Compound **3.22** was coupled with pnp-carbonate-Boc-MMAE (Figure 3.7), however, when attempting to remove the Boc-protection group, degradation of the payload was observed and it was not possible to isolate the product.

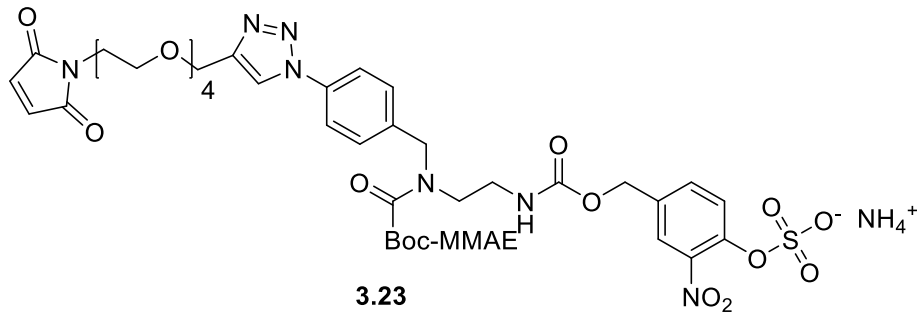

Figure 3.7. Structure of compound 3.23.

This observation was surprising, as no degradation was observed during the synthesis of payload 1, indicating that the nitro-functionalized payload was unstable under acidic conditions. To eliminate the acid-mediated removal of the amine-protection group, the more toxic auristatin E was attached instead. Auristatin E, has until now, not been incorporated into ADCs, due to the

need for attachment through an amine functionality of most conventional linkers. Therefore, the release of auristatin E would highlight the potential of the novel linker strategy. However, this would not allow for direct comparison with the commercially available payloads. Auristatin E activation and attachment studies were performed by Postdoc Anders Hansen. Currently, the payload 2 is awaiting ADC production and subsequent *in vitro* testing.

3.1.7 Discussion of linker design

Investigating the kinetics of the release of the drug, could prove to be important in optimizing and fully understanding the linker's contribution to ADC toxicity. 1,5-Cyclisations have been used extensively for drug release and several studies have optimized ring closure kinetics. This should be relevant, as the 1,5-ring closure generally happens slower than the 1,6-elimination, making it the rate limiting step, after enzymatic triggering[82]. Primarily, the cyclisation kinetics are ruled by the Thorpe-Ingold effect, but the electrophilic and nucleophilic properties also influence cyclisation rate. Furthermore, for lysosomal release using a pH sensitive nucleophile like an amine, cyclisation can be hampered. Recently, Corso et al. published a fast self-immolative spacer based on proline for the lysosomal release of the aliphatic alcohol of camptothecins, as well as correlating the toxicity of the entire ADC to the release rate of the drug[81]. Altering Key intermediate 2 for faster cyclisation rates, could prove beneficial to the toxicity of the final ADC.

3.1.8 Perspectives

During this project, a sulfatase cleavable, alcohol releasing linker was designed and synthesized. The synthetic route allowed for variation of the aryl sulfate moiety and two novel payloads, containing a novel sulfatase cleavable linker scaffold and MMAE and auristatin E were prepared. The synthesis proceeded through a convergent pathway, to afford the key intermediates with high yields. Furthermore, the synthetic route allowed for the introduction of an *o*-nitro group to investigate the electronic effects on sulfatase cleavage.

The payloads were conjugated to trastuzumab, an antibody recognizing the HER2 antigen. Comparing toxicity with the non-internalizing ADC, a small but significant change in the IC_{50} values was observed. However, it was not possible to achieve comparable toxicity to the established linkers mc and vc, leading to an investigation of the lysosomal sulfatase levels, compared to antigenic expression levels. *In vitro* assays on osteosarcoma cells uncovered a potential gap in linker technologies for the treatment of osteosarcoma.

Future work should include experiments to provide a better understanding of the linker release profile under acidic conditions. Furthermore, a better understanding of the sulfatase-mediated cleavage could help tune the properties of the linkers. There are several modifications that can be made to key intermediate 2 in order to promote faster ring-closure, including functionalization of the alkane chain.

3.2 Part II

3.2.1 Aim

The aim of this study, was to synthesize sulfatase cleavable probes, to explore the effect of decorating the aryl sulfate moiety on sulfatase mediated hydrolysis rates and the stability of these probes at lysomal pH. It was envisioned, that enzyme mediated sulfate ester hydrolysis would trigger a 1,6-elimination, resulting in the release of a fluorescent reporter molecule, providing a measurable signal for the detection of cleavage efficiency. To accommodate different aromatic substitution patterns, a simple and modifiable synthetic route was envisioned. The results of this work could facilitate the development of more efficient and selective sulfatase cleavable linkers, by providing valuable insight into aryl-sulfatase activity towards different aromatic substitution patterns.

3.2.2 Aryl sulfate ester hydrolysis

Two publications currently report an effect of substitution of the aromatic ring on arylsulfatase activity. Rush et al.[94] developed a bioluminescent assay to probe the substrate preference of 2,6- and 3,5-difluoro aryl-sulfate esters, as well as the unsubstituted analogue (Figure 3.8). The authors hypothesized, that more efficient cleavage depended on the acidity of the corresponding phenol, however, it was observed that sulfatases derived from different organisms, displayed significantly different substrate preference independent of phenol acidity.

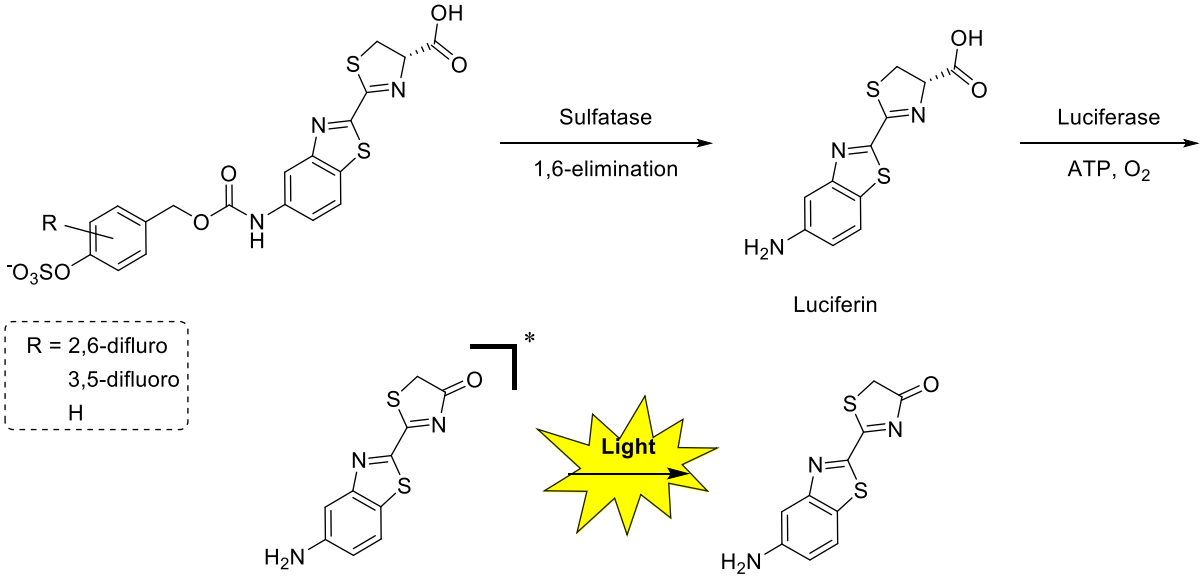

Figure 3.8. Sulfatase activity bioluminescence assay.

Bargh et al.[50] reported the first sulfatase cleavable linker scaffold for the incorporation into ADCs. When comparing IC_{50} values of the of an *o*-nitro sulfate analogue with an unsubstituted linker analogue, the ADC containing the *o*-nitro sulfate linker displayed a lower IC_{50} value. These interesting findings suggest that sulfatase mediated hydrolysis efficiency can be tuned by the introduction of EWG on the aryl sulfate moiety. Thus, it is highly relevant to uncover the relationship between substitution patterns and enzyme specificity.

Retrosynthetic analysis

To investigate the effect of aryl substitution of sulfatase mediated cleavage, a simple synthetic route to access sulfatase probes, containing a fluorescent reporter molecule, was designed (Scheme 3.13).

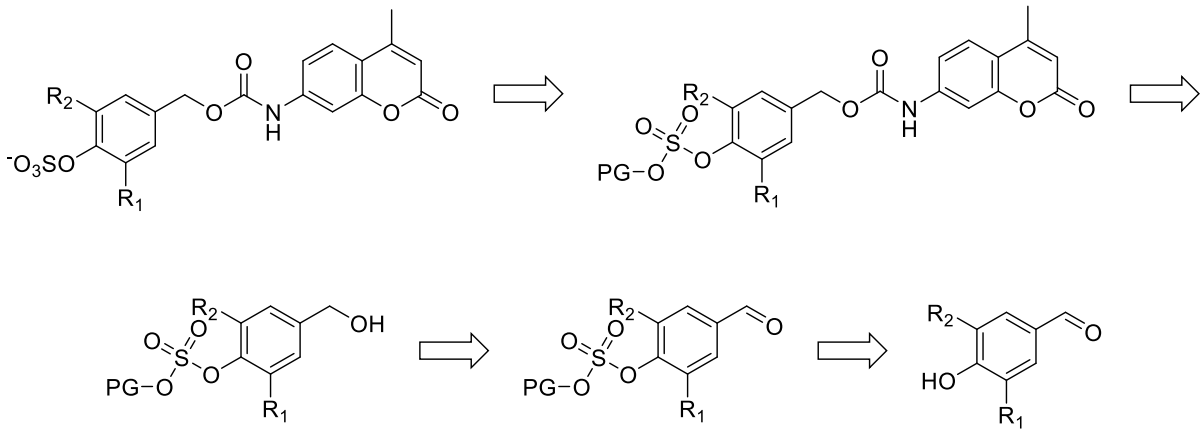

Scheme 3.13. Retrosynthetic analysis of the simple sulfatase probe.

The final step, was envisaged to be sulfate deprotection to avoid the manipulation of highly hydrophilic sulfate ester compounds, as well as avoiding potential acid catalyzed de-sulfation[95]. 7-Amino-4-methylcoumarin (AMC) was chosen as the reporter molecule, as fluorescence is quenched by aniline is acetylation[96–98]. Using a hydroxyl benzaldehyde as starting material would ensure selective sulfate installation on the phenol and the required benzylic alcohol could be accessed from a simple reduction. The envisaged route would provide a sulfatase probe in five synthetic steps.

3.2.3 Sulfate installation and protecting groups

While the synthetic strategy was designed by me, probes **3.41**, **3.42** and TCE sulfate reagent **3.26** were synthesized by MSc student Freja Grauslund under my supervision.

Due to the difficulties experienced when working with the np sulfate reagent, the trichloroethyl (TCE) sulfate protecting group was explored(Scheme 3.14)[99–106].

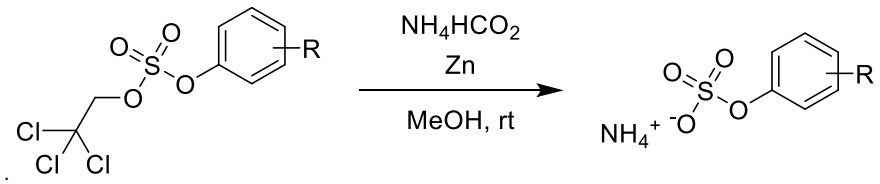

Scheme 3.14. Conditions for the removal of the TCE protection group.

Advantages to this protection group include, the high stability of the synthesized sulfate reagent and mild and efficient deprotection conditions (Zn powder, NH_4HCO_2, 1h)[100]. It should be noted, that the conditions required for removal of the TCE protection were not expected to be compatible with reducible functionalities, such as nitro groups. Scheme 3.15 reports the preparation of TCE sulfation reagent **3.26**.

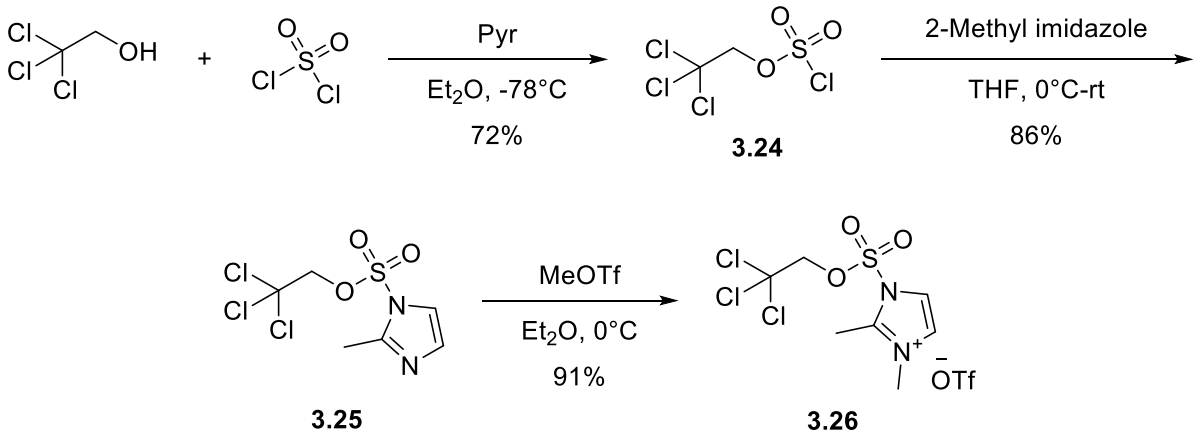

*Scheme 3.15. Synthesis of the TCE protected sulfation reagent **3.26**.*

Sulfate reagent **3.5** was prepared in one step, as previously described (77% yield). The TCE sulfate reagent was prepared by mixing trichloroethanol with sulfuryl chloride yielding **3.24**, which was reacted with 2-methyl imidazole. The imidazole sulfate **3.25** was methylated using methyl triflate and the resulting triflate salt was collected by filtration of the white precipitate, yielding 56% of compound **3.26** over 3 steps.

3.2.4 Synthesis of the sulfatase probes

The effect of EWGs in the *ortho* position to the sulfate was explored and the following four starting materials were purchased, as seen in Figure 3.9.

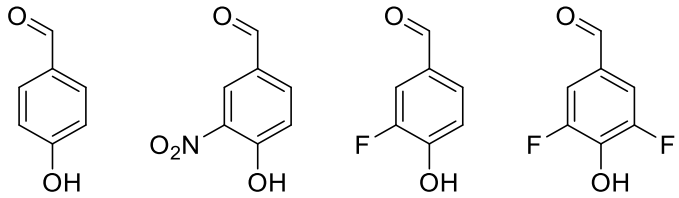

Figure 3.9. Starting aldehydes for the synthesis of sulfatase probes.

TCE sulfate installation afforded high yields, compared to the np sulfate installation as seen in Table 3.5.

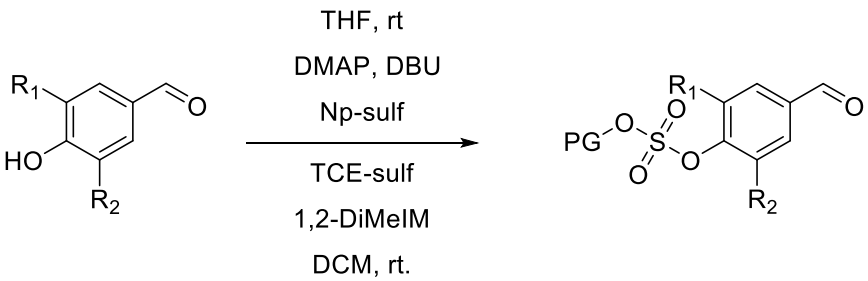

COMPOUND	R-GROUPS	PG	YIELD
3.27	R_1=R_2=H	np	61%
3.19	R_1=**NO_2**, R_2=H	np	0%
3.28	R_1=R_2=**F**,	np	4%
3.29	R_1=R_2=H	TCE	84%

3.30	R_1=**F**, R_2=H	TCE	88%

*Table 3.5. Synthetic conditions and yields of the synthesis of compound **3.27-3.30**.*

The low yield of difluoro **3.28** was unsatisfactory, however, sufficient material was isolated to proceed with the synthesis. The nitro analogue **3.19** was unstable and was not purified from the reaction mixture. Instead, it was envisaged that it would be possible to achieve a chemoselective sulfate installation on the corresponding benzylic alcohol (Scheme 3.16), due to the higher acidity of the *o*-nitro phenol. Indeed, the sulfation proceeded smoothly yielding 89% of **3.18**. For this analogue, TCE protection of the nitro analogue resulted in a lower yield (53%).

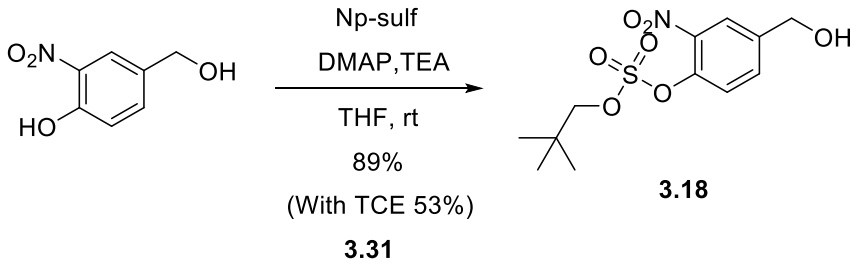

*Scheme 3.16. Synthetic conditions and yield of the synthesis of compound **3.18 and 3.31**.*

The aldehydes of the various analogues were reduced using $NaBH_4$, which generally proceeded in a clean and high yielding manner as seen in Table 3.6.

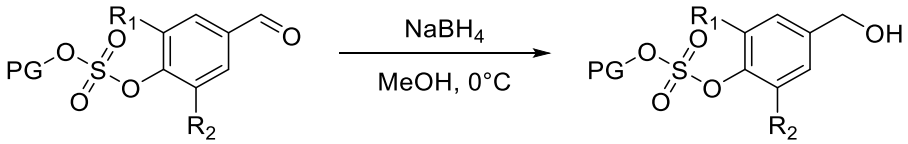

COMPOUND	R-GROUPS	PG	YIELD
3.32	R_1=R_2=H	np	68%
3.33	R_1=R_2=**F**,	np	81%
3.34	R_1=R_2=H	TCE	91%
3.35	R_1=**F**, R_2=H	TCE	88%

*Table 3.6. Synthetic conditions and yields of compounds **3.32-3.35.***

Next, AMC was reacted with triphosgene to form the corresponding isocyanate, then the alcohol, TEA and dibutyltin dilaurate (DBTDL) were added to form the carbamate (Table 3.7).

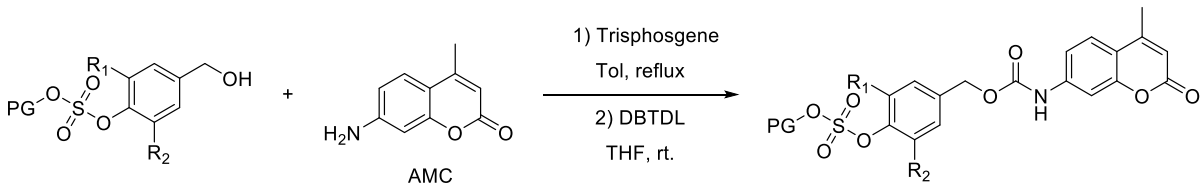

ENTRY	R-GROUPS	PG	YIELD
3.36	R_1=R_2=**F**,	np	10%*
3.37	R_1=**NO**$_2$, R_2=H	np	81%**
3.38	R_1=R_2=H	TCE	70%**
3.39	R_1=**F**, R_2=H	TCE	79%**

3.40	R_1=**NO_2**, R_2=H	TCE	57%**

*Table 3.7. Synthetic conditions and yields of the syntheses of compounds **3.36-3.40**. *Yield after purification by preparative HPLC. **Crude yield after washing the precipitate.*

Despite addition of DBTDL[107], reaction times were long and full conversion was only observed after 3-5 days. After attachment of the dye, the products were difficult to dissolve. The difluoro analogue **3.36** was purified by preparative HPLC, resulting in significant loss of product. It was thought that the deprotection of the np sulfate would proceed cleanly, foregoing the need for purification after deprotection. However, during deprotection, significant amounts of AMC were released and a second purification was required, resulting in the low yields reported. Thus, purification of the compound (**3.36**-**3.40**) was optimized to include repeated washing with H_2O, MeOH and ACN, to isolate products in satisfactory yields.

The TCE-group was removed by zinc catalyzed hydrogenolysis using ammonium formate as the hydrogen source, that also acts to buffer the solution, preventing acid catalyzed sulfate elimination[108] (Table 3.8).

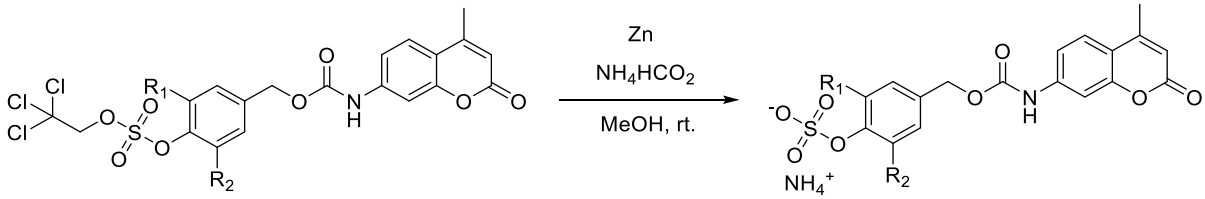

COMPOUND	R-GROUPS	YIELD
3.41	R_1=R_2=H	13%
3.42	R_1=**F**, R_2=H	19%
3.43	R_1=**NO_2**, R_2=H	0%

*Table 3.8. Synthetic conditions and yields of the syntheses of compounds **3.41** and **3.42**.*

Due to the low solubility and the highly hydrophilic nature of sulfates esters (**3.41**-**3.43**), purification was performed by preparative HPLC, resulting in low yields. However, for the enzyme studies, only a miniscule amount of compound is needed and the purification was not optimized further. As expected, the nitro-analogue **3.43** was completely reduced during removal of the TCE protection group, resulting in the corresponding *o*-amino-sulfate.

Lastly, np deprotection was carried out by the addition of 5M aqueous NH_4OAc[109]. The insolubility of the product and purification by preparative HPLC resulted in modest yields (Table 3.9).

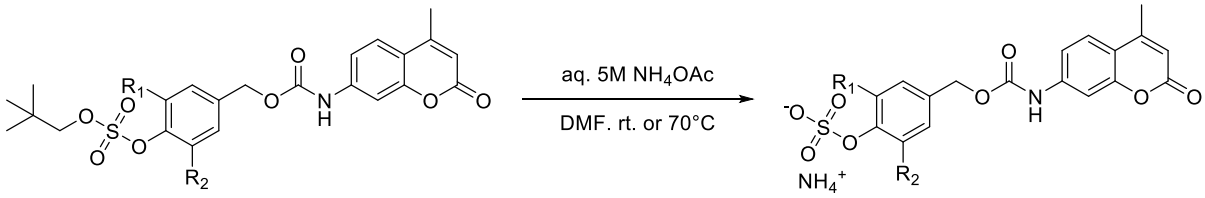

COMPOUND	R-GROUPS	YIELD
3.44	R_1=R_2=**F**,	1%
3.43	R_1=**NO_2**, R_2=H	5%

*Table 3.9. Synthetic conditions and yields of the syntheses of compounds **3.43** and **3.44***

3.2.5 Enzyme assay

While the final enzyme assays and analysis were carried out by me, the calibration curve determination and assay validation were carried out by MSc student Freja Grauslund under my supervision.

With these four analogues in hand, the sulfatase assay was designed. All assays were carried out in triplicate. Firstly, the concentration interval at which a linear correlation between the fluorescence and concentration of AMC could be observed was established (see experimental section). In a black microtiter plate with 96 wells, a dilution series was done, emulating the assay conditions by addition of the appropriate amount of buffer at assay pH (5.0) (λ_{ext} at 387nm and λ_{em} at 470nm). Fortunately, it was found that the linear interval was within the working parameters of the sulfatase assay (3.1nM-2μM). Next, the activity of the sulfatase from *helix pomatia* (EC3.1.6.1) was confirmed by using 4-nitrophenyl sulfate as substrate, measuring the absorbance of the liberated Pnp[110] (see experimental section).

The stability of the probes was investigated in 0.1M NaOAc buffer at pH 5.5-4.5. As can be seen in Figure 3.10, the nitro analogue **3.43** was unstable under the acidic conditions. This result is consistent with the instability observed during acidic Boc-deprotection of payload 2. This result suggests that *o*-nitro aryl sulfate esters may not be an attractive functionality to achieve specific sulfatase mediated release. Gratifyingly, the other analogues were stable at the pH-range relevant for lysosomal delivery (pH 4.5 shown in Figure 3.10).

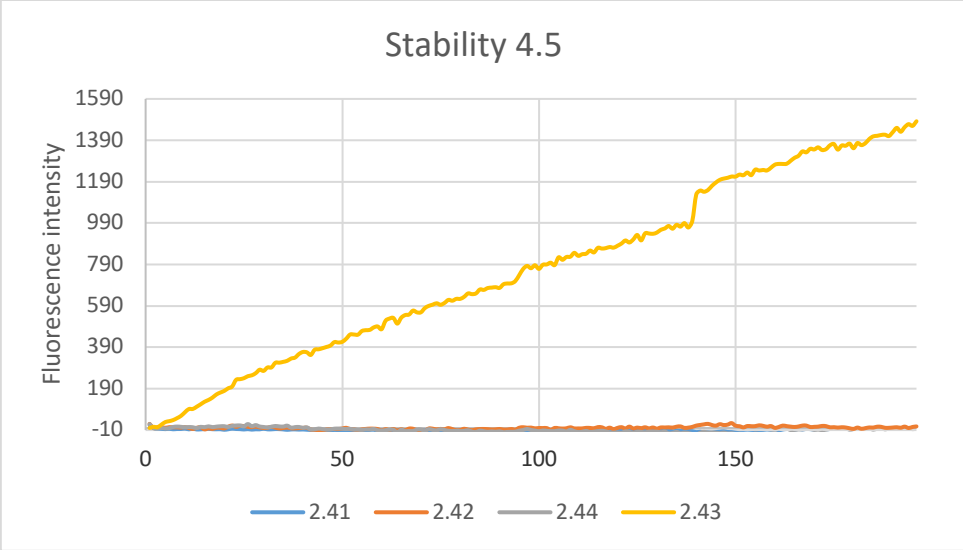

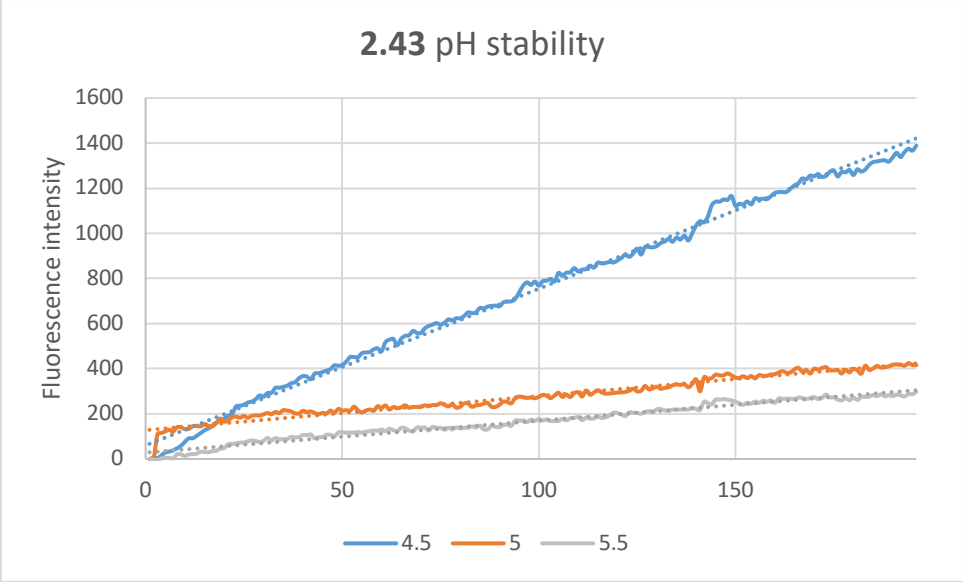

*Figure 3.10. Results of the stability tests determined by the fluorescence intensity of the release AMC. Measurement were done at 1-min intervals, and the plate was shaken at 37°C between measurements. (a) Stability of the **3.41**-**3.44** at pH 4.5 in NaOAc buffer. (b) Showing the stability of nitro analogue **3.43** in pH 4.5-5.5 in NaOAc buffer.*

Finally, the enzyme study was initiated. The study was carried out in a black 96 well chimney plate. Total reaction volume was 200µL, 5% DMSO in 0.1M NaOAc buffer at pH 5.0. Final enzyme concentration was 0.15 U/mL with a substrate concentration of 1.8µM. The plate was shaken at 37°C and measurements were taken at 1-minute intervals. The results are reported in Figure 3.11 below.

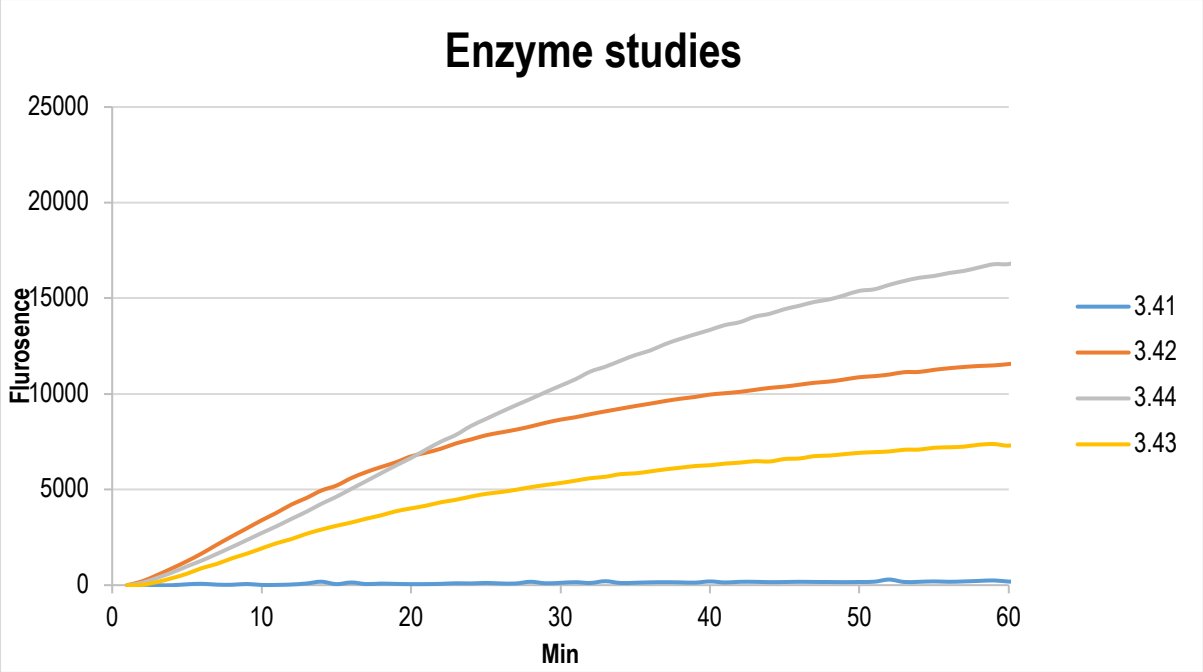

Figure 3.11. Results of the enzyme study determined by the fluorescence intensity of the release of AMC. Measurements were taken at 1 min intervals and the plate was shaken at 37°C between measurements.

For the nitro analogue **3.43**, the sulfatase-induced release of AMC was significantly faster than the auto hydrolysis under acidic pH. The results clearly indicate that the presence of an electron withdrawing group greatly increases the rate of sulfatase mediated hydrolysis, corresponding to the literature. However, more data is needed to quantitatively understand the cleavage profiles of the different analogues, as mediated by sulfatase from *Helix Pomatia*.

3.2.6 Perspectives

During this project, four different sulfatase cleavable probes were prepared by a simple five-step synthetic route, yielding sufficient material for enzyme studies. Two different sulfate ester protection groups were explored. In general, TCE sulfate installation was high yielding, however, the incompatibility of certain functional groups with the deprotection conditions, limits the utility of this protection group.

Enzyme studies were carried out and a significant difference between the analogues was observed, though most notably, a large difference in cleavage of the undecorated probe in comparison to the aryl sulfate esters substituted with EWGs was seen.

Furthermore, it was discovered that the *o*-nitro analogue **3.43** displayed unspecific release at lysosomal pH. This result suggests that *o*-nitro aryl sulfate esters do not present a desirable scaffold for specific sulfatase mediated lysosomal release. The insights provided by this work could contribute to the understanding of sulfatase activity, enabling the development of more potent and specific sulfatase cleavable linkers.

Future work should include further enzymes studies for determination of the specific enzyme kinetics in a quantitative manner. Furthermore, it could prove insightful to investigate the substrate

preference of human lysosomal sulfatases. This could enable an unprecedented selectivity towards specific upregulated enzymes in relevant cancers.

3.3 Part III

3.3.1 Aim

The aim of this work was to design, synthesize and study sulfatase cleavable linkers for the incorporation into ADCs, to understand of the effect of functionalization with various EWGs on cellular toxicity. It was envisaged, that the linker would be attached to the antibody in a site-selective and DAR specific manner, by using the GlyCLICK® conjugation method. Sulfate ester hydrolysis would trigger a 1,6-elimination to release MMAE, which is commonly used in ADCs as a cytotoxin. The results of this work could contribute to the understanding of intracellular sulfatase activity, as well as gaining insight into the effect of decoration of the aryl sulfate on ADC toxicity.

3.3.2 GlyCLICK® antibody modification

In light of the difficulty of accessing consistent DARs during ADC preparation with the maleimide functionalized payloads, a different conjugation method for antibody modification was explored. Achieving the same DARs would enable the direct comparison of cellular toxicity of the prepared ADCs. The GlyCLICK®method enzymatically introduces an azido functionalization on the two sugar moieties located in the hinge region of the ADC[111–113](Figure 3.12).

Figure 3.12. Concept of the GlyCLICK®method for site-selective and DAR specific bioconjugation.

An engineered Fc specific endoglycosidase hydrolyses the inner most GlcNAc of the antibody, followed by the attachment of azido-functionalized galactosamine catalyzed by β-1,4-galactosyltransferase. With two azido functionalities attached to the antibody, it is possible to attach the payload via a 1,3 dipolar strain promoted azido-alkyne cycloaddition. Strain promoted azido-alkyne cycloadditions happen in the absence of Cu and is, therefore, compatible with sensitive biomolecules[114,115]. This enables the homogeneous production of ADC with a DAR of 2.

3.3.3 Design of sulfatase cleavable payloads

Following the interesting results of part II, a novel sulfatase cleavable payload was designed to investigate how the substitution pattern the aryl sulfate influences the *in vitro* potency of the final ADC. To achieve this goal, the following payload structure was designed to incorporate a hydrophilic PEG-2 chain, where the strained alkyne handle 4-dibenzocyclooctynol (DIBO) could be attached (see Figure 3.13). Release would be triggered by sulfatase mediated sulfate ester hydrolysis, followed by a 1,6-elimination releasing MMAE[7].

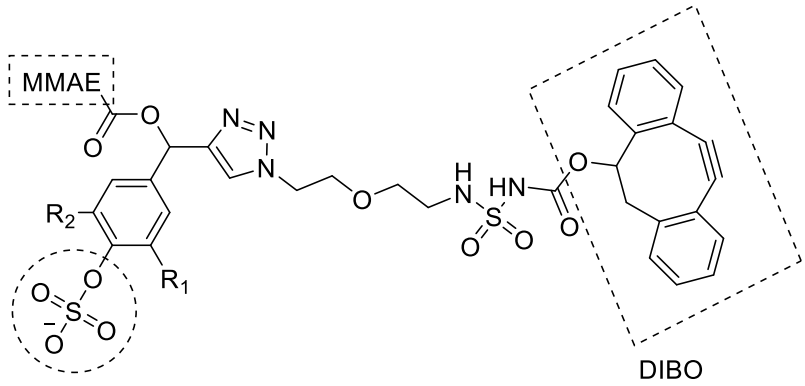

Figure 3.13. The general structure of the sulfatase cleavable linker. The conjugation handle DIBO, the sulfatase trigger and the releasable MMAE are highlighted.

Synthetic route of the linker

By using the commercially available 4-hydroxy benzaldehyde analogues, the first step would be installation of the TMS protected alkyne, while yielding the benzylic alcohol for MMAE attachment, as seen in Scheme 3.17.

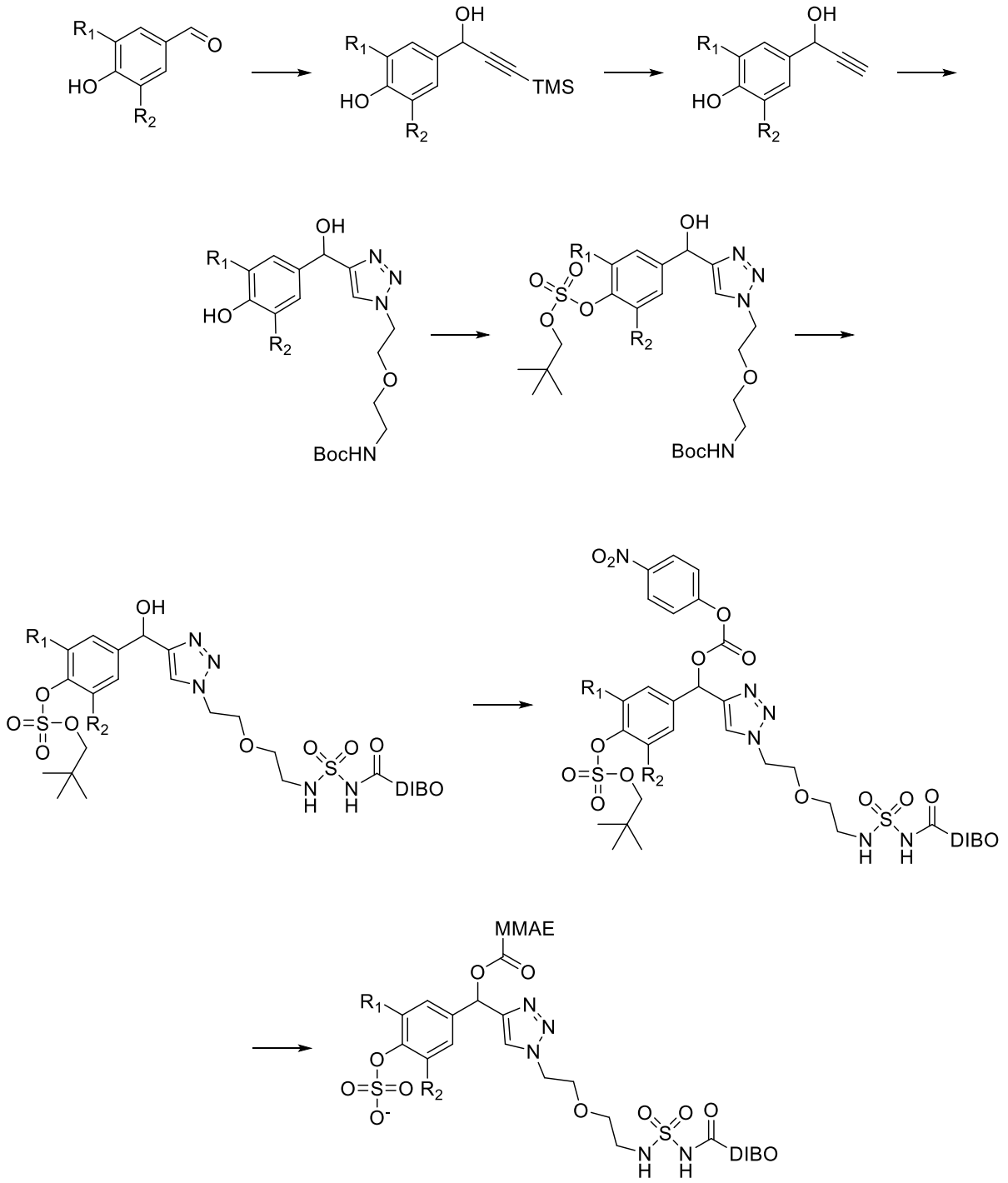

Scheme 3.17. Synthetic strategy of the synthesis of the novel sulfatase payload.

The first reaction introduces a stereocenter, however, stereo chemistry will not be drawn. The following steps would be alkyne deprotection and coupling an N-Boc PEG-2 azido chain. Next, the np sulfate group would be installed, followed by amine liberation. Attachment of the strained alkyne DIBO via a stable N-alkoxy sulfamide was envisioned. First reported by Masui et al.[116], this useful and high yielding reaction has been used extensively[117–121]. The final steps include Pnp-carbonate activation, followed by MMAE attachment. The last step was envisaged to be liberation of the sulfate ester affording the final payload, ready for attachment to an antibody. An additional advantage of the incorporation of the DIBO functionality, is the higher resistance to aqueous

hydrolysis, simplifying the synthetic route, in comparison to the incorporation of the maleimide conjugation handle, which is prone to hydrolysis.

MMAE is commonly incorporated into novel ADCs for the validation of new linkers, targets or conjugation methods. Therefore, the drug was chosen as cargo for this linker study[122–126]. To increase the distance between the conjugation site and the enzymatic recognition site, a hydrophilic PEG-2 spacer was introduced.

3.3.4 Synthesis of payloads

While the design of the linker and optimization of the synthetic conditions were carried out by me, the difluoro-payload **3.65** was synthesized by postdoc Charlotte Uldahl Jansen.

Table 3.10 displays the different methods attempted for the introduction of the TMS protected alkyne.

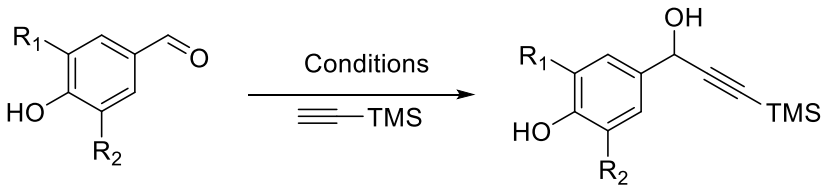

COMPOUND	R-GROUPS	CONDITIONS	YIELD
3.45	R_1=**NO_2**, R_2=H	MeLi · LiBr	47%
3.46	R_1=**F**, R_2=H	MeLi · LiBr	-
3.47	R_1=R_2=**F**	MeLi · LiBr	0%
3.47	R_1=R_2=**F**	BuLi	Quant.

*Table 3.10. Synthetics conditions and yields for the synthesis of compounds **3.45-3.47**.*

The use of MeLi · LiBr was inspired by a procedure from literature[127]. The yields of the reaction varied and during flash column chromatography (FCC) purification of the product, partial TMS deprotection was observed, which complicated purification and resulted in some product loss (Table 3.11). Direct TBAF deprotection of the crude of **3.46** was attempted before FCC purification, resulting in low yields of **3.49** (Table 3.11). The reaction using BuLi afforded a high yield of **3.47** with no side reaction observed during purification, suggesting that these conditions are better for the installation of the TMS-alkyne.

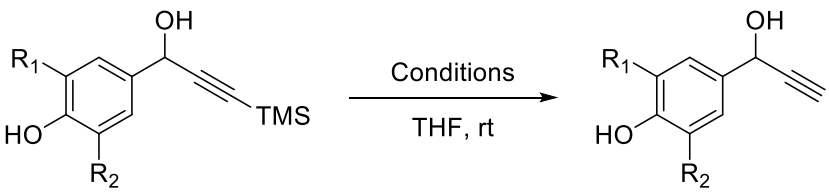

COMPOUND	R-GROUPS	CONDITIONS	YIELD

3.48	R_1=**NO_2**, R_2=H	Silica gel	30%
3.49	R_1=**F**, R_2=H	TBAF	41%
3.50	R_1=R_2=**F**	TBAF·H_2O	Quant.

*Table 3.11. Synthetic conditions and yields for the synthesis of compounds **3.48-3.50**.*

Compound 2.47 was deprotected with TBAF hydrate affording quantitative yields of **3.50.**

N-Boc-azido-Peg-2 **3.51** was prepared from the corresponding alcohol, inspired by a procedure from literature [128]. N-Boc-PEG-2-alcohol was reacted with MsCl, before the addition of tetrabutyl ammonium iodide and NaN_3, yielding **3.51** quantitatively, in a 2 step, 1 pot reaction. With the spacer made, a Cu(I) assisted 1,3-cycloaddition, was performed, as seen in Table 3.12.

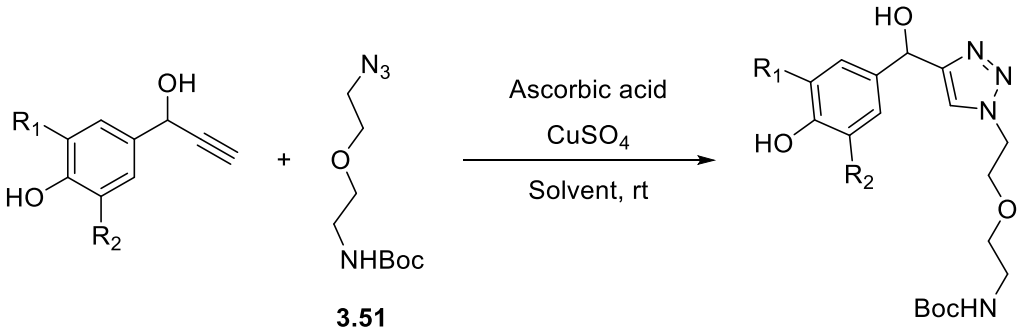

3.51

COMPOUND	R-GROUPS	SOLVENT	YIELD
3.52	R_1=**NO_2**, R_2=H	t-BuOH: H_2O	58%
3.53	R_1=**F**, R_2=H	t-BuOH: H_2O	78%
3.54	R_1=R_2=**F**	THF:t-BuOH:H_2O	77%

*Table 3.12. Synthetic conditions and yields of the synthesis of compounds **3.52-3.54**.*

The reactions proceeded affording satisfying yields, with the exception of nitro analogue **3.52**, likely caused by poor solubility of the starting material in t-BuOH.

The following step was np sulfate installation, as seen in Table 3.13. As previously experienced, it was difficult to achieve satisfactory yields during the installation of np sulfate, likely due to the instability of the sulfation reagent.

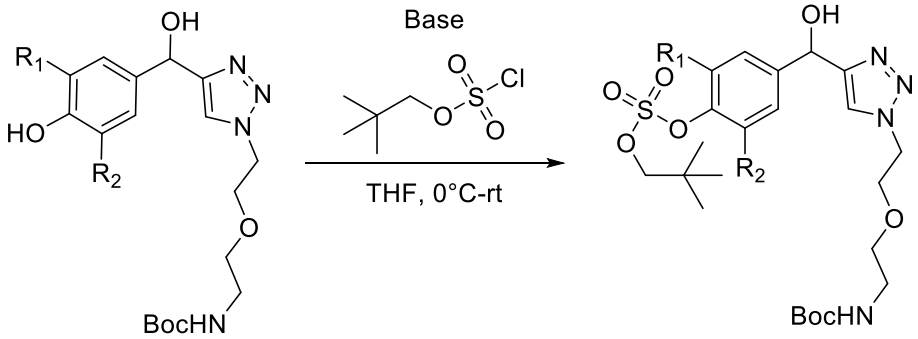

COMPOUND	R-GROUPS	BASE	YIELD
3.55	R_1=**NO_2**, R_2=H	TEA	62%
3.56	R_1=**F**, R_2=H	DBU	50%
3.57	R_1=R_2=**F**	DBU	54%

*Table 3.13. Synthetic conditions and yields of the synthesis of compounds **3.55-3.57**.*

The stronger base, DBU, was used for the monofluoro and difluoro analogues (**3.56** and **3.57**) in an attempt to increase reaction yields. For the nitro analogue (**3.55**), TEA is sufficient for fast reaction. For the reaction of the nitro analogue **3.55,** purification was performed directly after completion of the reaction to avoid product degradation, as has been previously observed.

Before the attachment of the DIBO conjugation handle, the Boc protection group was removed by the addition of 4M HCl in dioxane. The crude was carried forward without purification. For the attachment of the conjugation handle, DIBO was reacted with chlorosulfonyl isocyanate, yielding the corresponding chlorosulfonyl carbamate. This was followed by addition of the amine and TEA, as seen in Table 3.14.

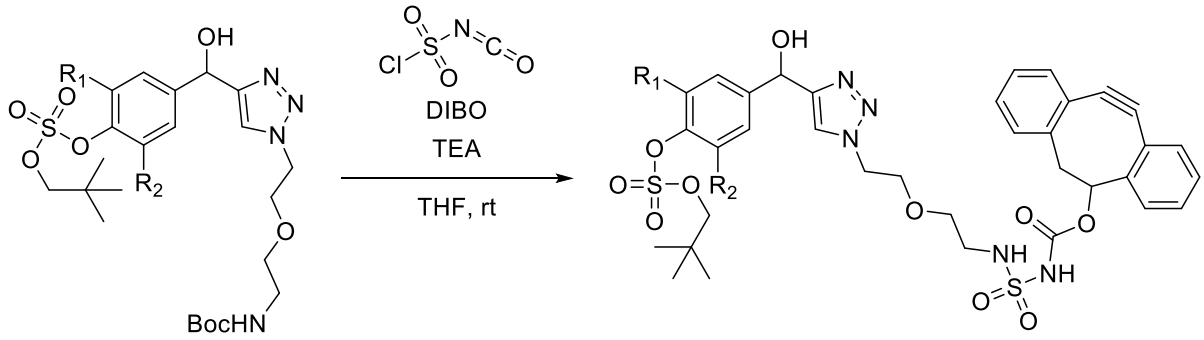

COMPOUND	R-GROUPS	YIELD
3.58	R_1=**NO_2**, R_2=H	48%
3.59	R_1=**F**, R_2=H	31%
3.60	R_1=R_2=**F**	Quant.

*Table 3.14. Synthetic conditions and yields of the synthesis of compounds **3.58-3.60**.*

With the installation of the conjugation handle, Pnp-carbonate activation was carried out, as seen in Table 3.15.

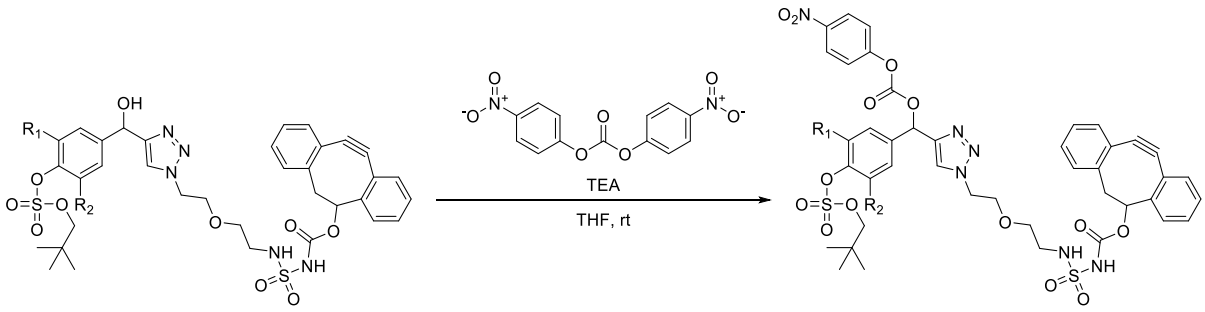

COMPOUND	R-GROUPS	YIELD
3.61	R_1=**NO_2**, R_2=H	38%
3.62	R_1=**F**, R_2=H	75%
3.63	R_1=R_2=**F**	58%

*Table 3.15. Synthetic conditions and yields of the synthesis of compounds **3.61-3.63**.*

Though compound **3.61** was only isolated in a modest yield, there was sufficient material to continue for the final steps.

Finally, the MMAE was attached to linkers, as seen in Table 3.16.

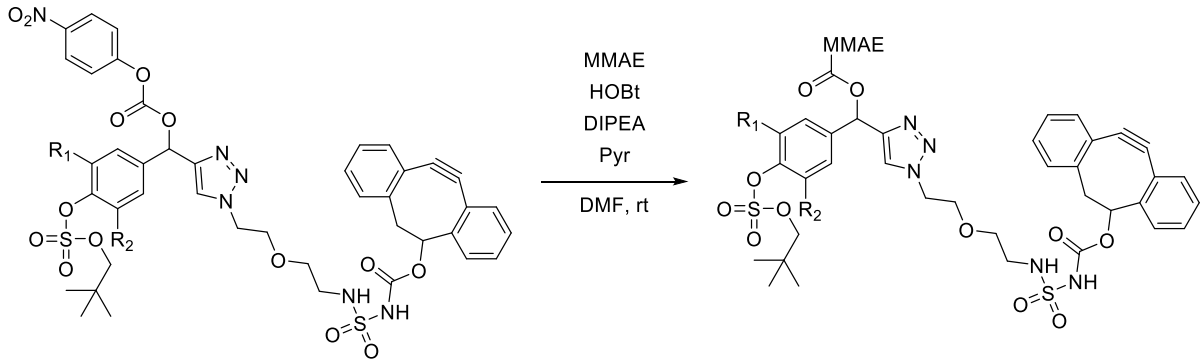

COMPOUND	R-GROUPS	YIELD
3.64	R_1=**NO_2**, R_2=H	5% (3%)*
3.65	R_1=**F**, R_2=H	1% (4%)*
3.66	R_1=R_2=**F**	11%

*Table 3.16. Synthetic conditions and yields for the synthesis of compounds **3.64-3.66**. *Yields of the deprotected sulfate esters (final payloads)*

The reactions were monitored by UPLC-MS and upon completion, were loaded directly on a preparative HPLC, resulting in some product loss, which was done to avoid unnecessary manipulation of the very toxic MMAE. Furthermore, during purification of **3.64** and **3.65**, deprotection of the np group was observed, resulting in loss of product. However, it was possible to purify sufficient amounts of the deprotected compound for analysis by HRMS and for the bioconjugation onto the antibody (**3.64** 0.42mg and **3.65** 0.6 mg).

For the difluoro analogue **3.66**, the np sulfate was removed after preparative HPLC purification and the crude was carried forward for the attachment to the antibody in the preparation of ADCs.

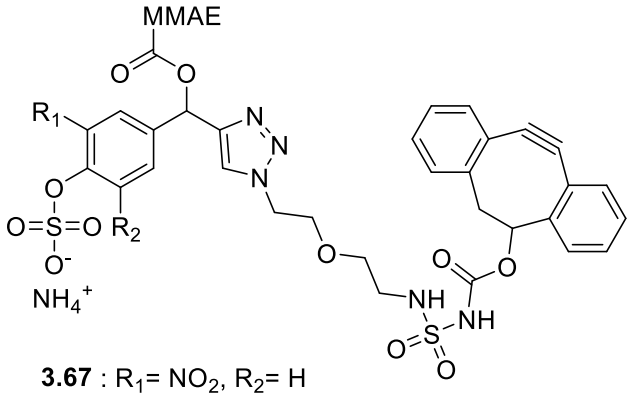

3.67 : R_1= NO_2, R_2= H

3.68 : R_1= F, R_2= H

3.69 : R_1=R_2=F

*Figure 3.14. Structure of the payloads **3.67-3.69**.*

3.3.5 Cell studies

ADC preparation and *in vitro* assays were carried out by MSc student Nicolai Lindegaard at Finsen Laboratory, where the breast cancer cell lines were also maintained.

Payloads **3.67-3.69** were conjugated to trastuzumab functionalized with two azido groups as prepared by the GlyCLICK® method. Below is shown the gel of native antibody, the azido functionalized antibody (Tras-Azide) and conjugation products ADCs Traz-**3.67**, Tras-**3.68** and Tras-**3.69**.

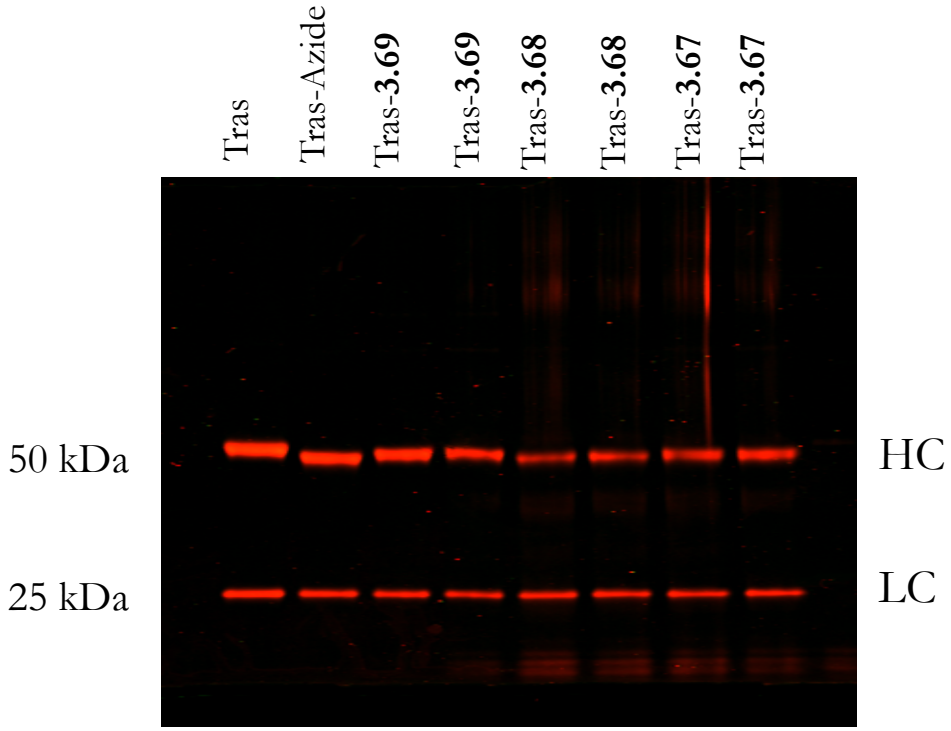

Figure 3.15. Results of antibody functionalization with azido groups and subsequent conjugation reactions.

As seen in Figure 3.15 upon azido-functionalization the antibody as expected loses mass due to the removal of sugar moieties and concurrent installation of the azido groups. Complete deglycosylation was observed. Subsequent attachment of the payloads then results in an increase of mass. Unfortunately, conjugation of **3.68** was ineffective while attachment of **3.67** and **3.69** resulted in complete conversion.

The conjugates Tras-**3.67** and Tras-**3.69** were then tested in two breast cancer cell lines: BT-474(HER2^{+}) and MCF-7(HER2 negative, as a negative control). The cells were incubated with different concentrations of the ADC to determine a dose-response curve. Results are shown in Figure 3.16 below.

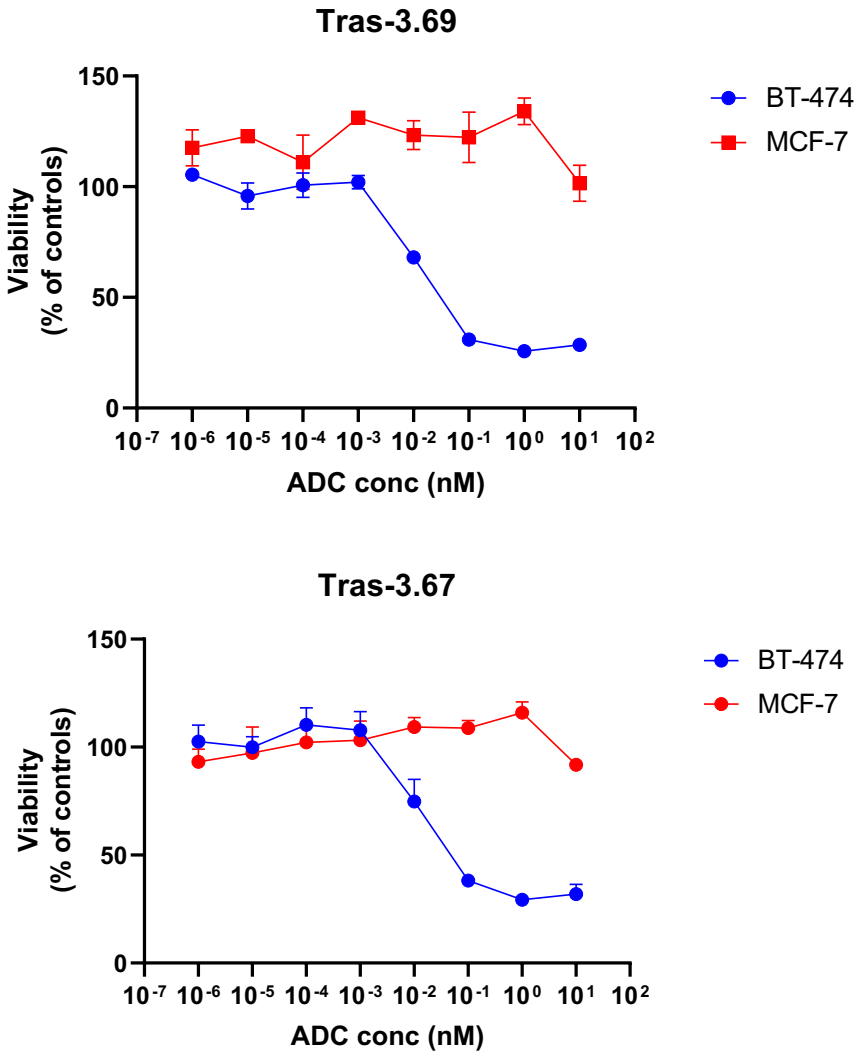

*Figure 3.16. Showing the results of the in vitro assay of Tras-**3.67** and Tras-**3.69** ADCs on breast cancer cell lines BT-474 and MCF-7.*

The result clearly show an antigen dependent dose response curve for the HER2$^+$ BT-474 cell lines. The HER2 negative MCF-7 control cells displayed little response to incubation with the ADC even at high concentrations suggesting that little extracellular release happens. The IC_{50} values were calculated to be 185µmol for Tras-**3.69** and 8.67mM for Tras-**3.67**. Lower IC_{50} values are expected to be observed when incubating the cells with ADC for a longer time, which are closer to the potencies of other published and FDA approved ADCs usually in the nanomolar range[129,130]. Interestingly, Tras-**3.67** displayed lower potency despite of the potential secondary acid promoted cleavage mechanism, suggesting that the sulfatase cleavage of Tras-**3.69** was significantly more efficient. The results somewhat mirror the initial results observed in Chap 3 part II where the difluoro analogue may look to be cleaved more efficiently than the corresponding nitro analogue. This observation makes the results from preparing an ADC with **3.68** even more interesting as correlating the enzyme cleavage rates with *in vitro* toxicity could provide a powerful tool for developing highly efficient sulfatase cleavable linkers.

3.3.6 Perspectives

During this project, three novel arylsulfatase cleavable linkers were designed and synthesized by a simple seven step synthetic route, each step generally affording high yields. The linkers incorporate the strain alkyne DIBO as a conjugation handle, enabling the preparation of highly homogeneous ADCs. Trastuzumab was azido functionalized and it was possible to prepare two ADC of the payloads **3.67** and **3.69**. The ADCs were incubated with two breast cancer cell lines and it was possible to observe an antigen dependent dose-response curve and different potencies of the different ADCs.

Future work will include the full characterization of the ADCs to confirm that a DAR 2 has been achieved as well as conjugating **3.68** to trastuzumab and testing the resulting ADC on BT-474 and MCF-7 cell lines to gain more insight into IC_{50} in relation to aryl sulfate functionalization. It could prove fruitful to prolong the incubation time to achieve complete cell kill. It could be interesting to compare the future results of the sulfatase probes of Part II tested on human lysosomal sulfatases with the IC_{50} values observed in the *in vitro* assays to determine a possible correlation between sulfatase cleavage rates and ADC potency. Synthesizing more payloads with functionalized with other EWG like nitriles or CF_3 while also varying the aromatic substitution pattern would also be of interest.

3.4 Literature

1. Su, D. & Zhang, D. Linker Design Impacts Antibody-Drug Conjugate Pharmacokinetics and Efficacy via Modulating the Stability and Payload Release Efficiency. *Front. Pharmacol.* **12**, (2021).

2. Su, Z. *et al.* Antibody–drug conjugates: Recent advances in linker chemistry. *Acta Pharm. Sin. B* **11**, 3889–3907 (2021).

3. Bargh, J. D., Isidro-Llobet, A., Parker, J. S. & Spring, D. R. Cleavable linkers in antibody-drug conjugates. *Chem. Soc. Rev.* **48**, 4361–4374 (2019).

4. Kostova, V., Désos, P., Starck, J. B. & Kotschy, A. *The chemistry behind adcs. Pharmaceuticals* **14**, (2021).

5. Dal Corso, A., Pignataro, L., Belvisi, L. & Gennari, C. Innovative Linker Strategies for Tumor-Targeted Drug Conjugates. *Chemistry - A European Journal* **25**, 14740–14757 (2019).

6. Sheyi, R., de la Torre, B. G. & Albericio, F. Linkers: An Assurance for Controlled Delivery of Antibody-Drug Conjugate. *Pharmaceutics* **14**, (2022).

7. Edupuganti, V. V. S. R., Tyndall, J. D. A. & Gamble, A. B. Self-immolative Linkers in Prodrugs and Antibody Drug Conjugates in Cancer Treatment. *Recent Pat. Anticancer. Drug Discov.* **16**, 479–497 (2021).

8. Conilh, L. *et al.* Exatecan antibody drug conjugates based on a hydrophilic polysarcosine drug-linker platform. *Pharmaceuticals* **14**, 1–17 (2021).

9. Tedeschini, T. *et al.* Polyethylene glycol-based linkers as hydrophilicity reservoir for antibody-drug conjugates. *J. Control. Release* **337**, 431–447 (2021).

10. Giese, M. *et al.* Linker Architectures as Steric Auxiliaries for Altering Enzyme-Mediated Payload Release from Bioconjugates. *Bioconjug. Chem.* **32**, 2257–2267 (2021).

11. Collins, D. M., Bossenmaier, B., Kollmorgen, G. & Niederfellner, G. Acquired resistance to antibody-drug conjugates. *Cancers (Basel).* **11**, 1–17 (2019).

12. Yaghoubi, S. *et al.* Development and biological assessment of MMAE-trastuzumab antibody–drug conjugates (ADCs). *Breast Cancer* **28**, 216–225 (2021).

13. Tzogani, K. *et al.* EMA Review of Belantamab Mafodotin (Blenrep) for the Treatment of Adult Patients with Relapsed/Refractory Multiple Myeloma. *Oncologist* **26**, 70–76 (2021).

14. Tai, Y. T. *et al.* Novel anti-B-cell maturation antigen antibody-drug conjugate (GSK2857916) selectively induces killing of multiple myeloma. *Blood* **123**, 3128–3138 (2014).

15. Chen, L. *et al.* In-depth structural characterization of Kadcyla® (ado-trastuzumab emtansine) and its biosimilar candidate. *MAbs* **8**, 1210–1223 (2016).

16. Barok, M., Joensuu, H. & Isola, J. Trastuzumab emtansine: Mechanisms of action and drug resistance. *Breast Cancer Res.* **16**, (2014).

17. Wakankar, A. A. *et al.* Physicochemical stability of the antibody - Drug conjugate trastuzumab-DM1: Changes due to modification and conjugation processes. *Bioconjug. Chem.* **21**, 1588–1595 (2010).

18. Godwin, C. D., Gale, R. P. & Walter, R. B. Gemtuzumab ozogamicin in acute myeloid leukemia. *Leukemia* **31**, 1855–1868 (2017).

19. Lambert, J. *et al.* Gemtuzumab ozogamicin for de novo acute myeloid leukemia: Final efficacy and safety updates from the open-label, phase III ALFA-0701 trial. *Haematologica* **104**, 113–119 (2019).

20. Hamann, P. R. *et al.* Gemtuzumab ozogamicin, a potent and selective anti-CD33 antibody - Calicheamicin conjugate for treatment of acute myeloid leukemia. *Bioconjug. Chem.* **13**, 47–58 (2002).

21. Walter, R. B., Raden, B. W., Kamikura, D. M., Cooper, J. A. & Bernstein, I. D. Influence of CD33 expression levels and ITIM-dependent internalization on gemtuzumab ozogamicin-induced cytotoxicity. *Blood* **105**, 1295–1302 (2005).

22. Aujla, A., Aujla, R. & Liu, D. Inotuzumab ozogamicin in clinical development for acute lymphoblastic leukemia and non-Hodgkin lymphoma. *Biomark. Res.* **7**, 1–9 (2019).

23. Dahl, J., Marx, K. & Jabbour, E. Inotuzumab ozogamicin in the treatment of acute lymphoblastic leukemia. *Expert Rev. Hematol.* **9**, 329–334 (2016).

24. Ricart, A. D. Antibody-drug conjugates of calicheamicin derivative: Gemtuzumab ozogamicin and inotuzumab ozogamicin. *Clin. Cancer Res.* **17**, 6417–6427 (2011).

25. Moon, S. J. *et al.* Antibody conjugates of 7-ethyl-10-hydroxycamptothecin (SN-38) for targeted cancer chemotherapy. *J. Med. Chem.* **51**, 6916–6926 (2008).

26. Goldenberg, D. M., Cardillo, T. M., Govindan, S. V., Rossi, E. A. & Sharkey, R. M. Trop-2 is a novel target for solid cancer therapy with sacituzumab govitecan (IMMU-132), an antibody-drug conjugate (ADC) (Oncotarget (2015) 6 (22496-22512) DOI: 10.18632/oncotarget.4318). *Oncotarget* **6**, 22496–22512 (2015).

27. Goldenberg, D. M. & Sharkey, R. M. Antibody-drug conjugates targeting TROP-2 and incorporating SN-38: A case study of anti-TROP-2 sacituzumab govitecan. *MAbs* **11**, 987–995 (2019).

28. Cardillo, T. M., Govindan, S. V., Sharkey, R. M., Trisal, P. & Goldenberg, D. M. Humanized anti-trop-2 IgG-SN-38 conjugate for effective treatment of diverse epithelial cancers: Preclinical studies in human cancer xenograft models and monkeys. *Clin. Cancer Res.* **17**, 3157–3169 (2011).

29. Kreitman, R. J. *et al.* Moxetumomab pasudotox in relapsed/refractory hairy cell leukemia. *Leukemia* **32**, 1768–1777 (2018).

30. Sullivan-Chang, L., O'Donnell, R. T. & Tuscano, J. M. Targeting CD22 in B-cell malignancies: Current status and clinical outlook. *BioDrugs* **27**, 293–304 (2013).

31. Dhillon, S. Moxetumomab Pasudotox: First Global Approval. *Drugs* **78**, 1763–1767 (2018).

32. Dorywalska, M. *et al.* Molecular basis of valine-citrulline-PABC linker instability in site-specific ADCs and its mitigation by linker design. *Mol. Cancer Ther.* **15**, 958–970 (2016).

33. Van De Donk, N. W. C. J. & Dhimolea, E. Brentuximab vedotin. *MAbs* **4**, 458–465 (2012).

34. Liu-Kreyche, P. *et al.* Lysosomal P-gp-MDR1 Confers Drug Resistance of Brentuximab Vedotin and Its Cytotoxic Payload Monomethyl Auristatin E in Tumor Cells. *Front. Pharmacol.* **10**, 1–9 (2019).

35. Narayan, R. *et al.* A phase 1 study of the antibody-drug conjugate brentuximab vedotin with re-induction chemotherapy in patients with CD30-expressing relapsed/refractory acute myeloid leukemia. *Cancer* **126**, 1264–1273 (2020).

36. Kang, L. *et al.* Noninvasive Trafficking of Brentuximab Vedotin and PET Imaging of CD30 in Lung Cancer Murine Models. *Mol. Pharm.* **15**, 1627–1634 (2018).

37. Sehn, L. H. *et al.* Polatuzumab vedotin in relapsed or refractory diffuse large B-cell lymphoma. *J. Clin. Oncol.* **38**, 155–165 (2020).

38. Tilly, H. *et al.* Polatuzumab Vedotin in Previously Untreated Diffuse Large B-Cell Lymphoma. *N. Engl. J. Med.* **386**, 351–363 (2022).

39. Tong, J. T. W., Harris, P. W. R., Brimble, M. A. & Kavianinia, I. An insight into fda approved antibody-drug conjugates for cancer therapy. *Molecules* **26**, (2021).

40. Mohamed Amar, I. A. *et al.* Dual intra- and extracellular release of monomethyl auristatin E from a neutrophil elastase-sensitive antibody-drug conjugate. *Eur. J. Med. Chem.* **229**, (2022).

41. Liu, L. *et al.* Synthesis and evaluation of highly releasable and structurally stable antibody-SN-38-conjugates. *Drug Deliv.* **28**, 2603–2617 (2021).

42. Miller, J. T., Vitro, C. N., Fang, S., Benjamin, S. R. & Tumey, L. N. Enzyme-Agnostic Lysosomal Screen Identifies New Legumain-Cleavable ADC Linkers. *Bioconjug. Chem.* **32**, 842–858 (2021).

43. López Rivas, P. *et al.* β-Glucuronidase triggers extracellular MMAE release from an integrin-targeted conjugate. *Org. Biomol. Chem.* **17**, 4705–4710 (2019).

44. Jeffrey, S. C. *et al.* Development and properties of β-glucuronide linkers for monoclonal antibody-drug conjugates. *Bioconjug. Chem.* **17**, 831–840 (2006).

45. Burke, P. J. *et al.* Optimization of a PEGylated glucuronide-monomethylauristatin E linker for antibody-drug conjugates. *Mol. Cancer Ther.* **16**, 116–123 (2017).

46. Jeffrey, S. C., De Brabander, J., Miyamoto, J. & Senter, P. D. Expanded utility of the β-glucuronide linker: ADCs that deliver phenolic cytotoxic agents. *ACS Med. Chem. Lett.* **1**, 277–280 (2010).

47. Shin, S. H. *et al.* An Elaborate New Linker System Significantly Enhances the Efficacy of an HER2-Antibody-Drug Conjugate against Refractory HER2-Positive Cancers. *Adv. Sci.* **8**, 1–15 (2021).

48. Kolodych, S. *et al.* Development and evaluation of β-galactosidase-sensitive antibody-drug conjugates. *Eur. J. Med. Chem.* **142**, 376–382 (2017).

49. Kern, J. C. *et al.* Discovery of Pyrophosphate Diesters as Tunable, Soluble, and Bioorthogonal Linkers for Site-Specific Antibody-Drug Conjugates. *J. Am. Chem. Soc.* **138**, 1430–1445 (2016).

50. Bargh, J. D. *et al.* Sulfatase-cleavable linkers for antibody-drug conjugates. *Chem. Sci.* **11**, 2375–2380 (2020).

51. Bargh, J. D. *et al.* A dual-enzyme cleavable linker for antibody-drug conjugates. *Chem. Commun.* **57**, 3457–3460 (2021).

52. Williams, S. J., Denehy, E. & Krenske, E. H. Experimental and theoretical insights into the mechanisms of sulfate and sulfamate ester hydrolysis and the end products of type i sulfatase inactivation by aryl sulfamates. *J. Org. Chem.* **79**, 1995–2005 (2014).

53. Van Loo, B. *et al.* Transition-State Interactions in a Promiscuous Enzyme: Sulfate and

Phosphate Monoester Hydrolysis by Pseudomonas aeruginosa Arylsulfatase. *Biochemistry* **58**, 1363–1378 (2019).

54. Zhu, C., He, L., Zhou, X., Nie, X. & Gu, Y. Sulfatase 2 promotes breast cancer progression through regulating some tumor-related factors. *Oncol. Rep.* **35**, 1318–1328 (2016).

55. Hammond, E., Khurana, A., Shridhar, V. & Dredge, K. The role of heparanase and sulfatases in the modification of heparan sulfate proteoglycans within the tumour microenvironment and opportunities for novel cancer therapeutics. *Front. Oncol.* **4 JUL**, 1–15 (2014).

56. McNamara, K. M. *et al.* In breast cancer subtypes steroid sulfatase (STS) is associated with less aggressive tumour characteristics. *Br. J. Cancer* **118**, 1208–1216 (2018).

57. Utsumi, T. *et al.* Elevated steroid sulfatase expression in breast cancers. *J. Steroid Biochem. Mol. Biol.* **73**, 141–145 (2000).

58. Guzman, G., Kajdacsy-balla, A. & Tobacman, J. K. Role as a Biomarker in Prostate Cancer. *Prostate Cancer Prostatic Dis.* **16**, 277–284 (2013).

59. Shaimardanova, A. A. *et al.* Metachromatic Leukodystrophy: Diagnosis, Modeling, and Treatment Approaches. *Frontiers in Medicine* **7**, (2020).

60. Lübke, T. & Damme, M. Lysosomal sulfatases: A growing family. *Biochem. J.* **477**, 3963–3983 (2020).

61. Prabhu, S. V. *et al.* Extra-lysosomal localization of arylsulfatase b in human colonic epithelium. *J. Histochem. Cytochem.* **59**, 328–335 (2011).

62. Bhattacharyya, S., Kotlo, K., Shukla, S., Danziger, R. S. & Tobacman, J. K. Distinct effects of N-acetylgalactosamine-4-sulfatase and galactose-6-sulfatase expression on chondroitin sulfates. *J. Biol. Chem.* **283**, 9523–9530 (2008).

63. Reed, M. J., Purohit, A., Woo, L. W. L., Newman, S. P. & Potter, B. V. L. Steroid sulfatase: Molecular biology, regulation, and inhibition. *Endocr. Rev.* **26**, 171–202 (2005).

64. Lin, Y. *et al.* ARSD, a novel ERα downstream target gene, inhibits proliferation and migration of breast cancer cells via activating Hippo/YAP pathway. *Cell Death Dis.* **12**, (2021).

65. Bahramian, S. *et al.* Evaluation of Arylsulfatase D (ARSD) and long noncoding RNA ARSD-AS1 gene expression in breast cancer patients and their association with oncogenic transcription factors. *J. B.U.ON.* **25**, 1805–1813 (2020).

66. Frese, M. A., Schulz, S. & Dierks, T. Arylsulfatase G, a novel lysosomal sulfatase. *J. Biol. Chem.* **283**, 11388–11395 (2008).

67. Schlotawa, L., Adang, L. A., Radhakrishnan, K. & Ahrens-Nicklas, R. C. Multiple sulfatase deficiency: A disease comprising mucopolysaccharidosis, sphingolipidosis, and more caused by a defect in posttranslational modification. *International Journal of Molecular Sciences* **21**, 1–15 (2020).

68. Dhamale, O. P. *et al.* Arylsulfatase K is the Lysosomal 2-Sulfoglucuronate Sulfatase. *ACS Chem. Biol.* **12**, 367–373 (2017).

69. Wiegmann, E. M. *et al.* Arylsulfatase K, a novel lysosomal sulfatase. *J. Biol. Chem.* **288**, 30019–30028 (2013).

70. Miya, K., Keino-Masu, K., Okada, T., Kobayashi, K. & Masu, M. Expression of Heparan Sulfate Endosulfatases in the Adult Mouse Brain: Co-expression of Sulf1 and Dopamine D1/D2 Receptors. *Front. Neuroanat.* **15**, (2021).

71. Rush, J. S., Beatty, K. E. & Bertozzi, C. R. Bioluminescent Probes of Sulfatase Activity. *Chembiochem.* **11**, 2069–2099 (2010).

72. Li, W. *et al.* Achieving the ratiometric imaging of steroid sulfatase in living cells and tissues with a two-photon fluorescent probe. *Chem. Commun.* **56**, 1349–1352 (2020).

73. Park, H. J., Rhee, H. W. & Hong, J. I. Activity-based fluorescent probes for monitoring sulfatase activity. *Bioorganic Med. Chem. Lett.* **22**, 4939–4941 (2012).

74. Smith, E. L., Bertozzi, C. R. & Beatty, K. E. An Expanded Set of Fluorogenic Sulfatase Activity Probes. *Chembiochem.* **15**, 1101–1105 (2014).

75. Jung, Y. J. *et al.* Prednisolone 21-sulfate sodium: a colon-specific pro-drug of prednisolone. *J. Pharm. Pharmacol.* **55**, 1075–1082 (2010).

76. Yoon, H. Y. & Hong, J. I. Sulfatase activity assay using an activity-based probe by generation of N-methyl isoindole under reducing conditions. *Anal. Biochem.* **526**, 33–38 (2017).

77. Gisbert-Garzarán, M., Manzano, M. & Vallet-Regí, M. Self-immolative chemistry in nanomedicine. *Chem. Eng. J.* **340**, 24–31 (2018).

78. Shelef, O., Gnaim, S. & Shabat, D. Self-Immolative Polymers: An Emerging Class of Degradable Materials with Distinct Disassembly Profiles. *J. Am. Chem. Soc.* **143**, 21177–21188 (2021).

79. Ximenis, M. *et al.* Introducing a squaramide-based self-immolative spacer for controlled drug release. *Chem. Commun.* **57**, 2736–2739 (2021).

80. Gonzaga, R. V. *et al.* Perspectives About Self-Immolative Drug Delivery Systems. *J. Pharm. Sci.* **109**, 3262–3281 (2020).

81. Dal Corso, A. *et al.* Fast Cyclization of a Proline-Derived Self-Immolative Spacer Improves the Efficacy of Carbamate Prodrugs. *Angew. Chemie - Int. Ed.* **59**, 4176–4181 (2020).

82. Alouane, A., Labruère, R., Le Saux, T., Schmidt, F. & Jullien, L. Self-immolative spacers: Kinetic aspects, structure-property relationships, and applications. *Angew. Chemie - Int. Ed.* **54**, 7492–7509 (2015).

83. Tai, C. H., Lu, C. P., Wu, S. H. & Lo, L. C. Synthesis and evaluation of turn-on fluorescent probes for imaging steroid sulfatase activities in cells. *Chem. Commun.* **50**, 6116–6119 (2014).

84. Lenger, J. *et al.* Evaluation of sulfatase-directed quinone methide traps for proteomics. *Bioorganic Med. Chem.* **20**, 622–627 (2012).

85. Lu, C. P., Ren, C. T., Wu, S. H., Chu, C. Y. & Lo, L. C. Development of an activity-based probe for steroid sulfatases. *ChemBioChem* **8**, 2187–2190 (2007).

86. Nani, R. R., Gorka, A. P., Nagaya, T., Kobayashi, H. & Schnermann, M. J. Near-IR Light-Mediated Cleavage of Antibody-Drug Conjugates Using Cyanine Photocages. *Angew. Chemie - Int. Ed.* **54**, 13635–13638 (2015).

87. Malich, G., Markovic, B. & Winder, C. The sensitivity and specificity of the MTS tetrazolium assay for detecting the in vitro cytotoxicity of 20 chemicals using human cell

lines. *Toxicology* **124**, 179–192 (1997).

88. Barltrop, J. A., Owen, T. C., Cory, A. H. & Cory, J. G. 5-(3-carboxymethoxyphenyl)-2-(4,5-dimethylthiazolyl)-3-(4-sulfophenyl)te trazolium, inner salt (MTS) and related analogs of 3-(4,5-dimethylthiazolyl)-2,5-diphenyltetrazolium bromide (MTT) reducing to purple water-soluble formazans As cell-viability indica. *Bioorganic Med. Chem. Lett.* **1**, 611–614 (1991).

89. McGowan, E. M. *et al.* Evaluation of cell cycle arrest in estrogen responsive MCF-7 breast cancer cells: Pitfalls of the MTS assay. *PLoS One* **6**, 1–8 (2011).

90. Huang, K. T., Chen, Y. H. & Walker, A. M. Inaccuracies in MTS assays: Major distorting effects of medium, serum albumin, and fatty acids. *Biotechniques* **37**, 406–412 (2004).

91. O'Toole, S. A. *et al.* The MTS assay as an indicator of chemosensitivity/resistance in malignant gynaecological tumours. *Cancer Detect. Prev.* **27**, 47–54 (2003).

92. Nielsen, C. F. *et al.* The collagen receptor uPARAP/Endo180 as a novel target for antibody-drug conjugate mediated treatment of mesenchymal and leukemic cancers. *Oncotarget* **8**, 44605–44624 (2017).

93. Yeom, C. E., Kim, H. W., Lee, S. Y. & Kim, B. M. DBU-mediated mild and chemoselective deprotection of aryl silyl ethers and tandem biaryl ether formation. *Synlett* 146–150 (2007). doi:10.1055/s-2006-958425

94. Rush, J. S., Beatty, K. E. & Bertozzi, C. R. Bioluminescent probes of sulfatase activity. *ChemBioChem* **11**, 2096–2099 (2010).

95. Al-Horani, R. A. & Desai, U. R. Chemical sulfation of small molecules-advances and challenges. *Tetrahedron* **66**, 2907–2918 (2010).

96. Carneiro, A., Matos, M. J., Uriarte, E. & Santana, L. Trending topics on coumarin and its derivatives in 2020. *Molecules* **26**, 1–15 (2021).

97. Jia, H. *et al.* Characterization of a leucine aminopeptidase from Toxoplasma gondii. *Mol. Biochem. Parasitol.* **170**, 1–6 (2010).

98. Chen, Y. *et al.* Identification and characterization of novel inhibitors of mammalian aspartyl aminopeptidase. *Mol. Pharmacol.* **86**, 231–242 (2014).

99. Gunnarsson, G. T., Riaz, M., Adams, J. & Desai, U. R. Synthesis of per-sulfated flavonoids using 2,2,2-trichloro ethyl protecting group and their factor Xa inhibition potential. *Bioorganic Med. Chem.* **13**, 1783–1789 (2005).

100. Ingram, L. J., Desoky, A., Ali, A. M. & Taylor, S. D. O- and N-sulfations of carbohydrates using sulfuryl imidazolium salts. *J. Org. Chem.* **74**, 6479–6485 (2009).

101. Fürstner, A., Domostoj, M. M. & Scheiper, B. Total syntheses of the telomerase inhibitors dictyodendrin B, C, and E. *J. Am. Chem. Soc.* **128**, 8087–8094 (2006).

102. Reuillon, T. *et al.* Design and synthesis of biphenyl and biphenyl ether inhibitors of sulfatases. *Chem. Sci.* **7**, 2821–2826 (2016).

103. Mikula, H. *et al.* Sulfation of β-resorcylic acid esters - First synthesis of zearalenone-14-sulfate. *Tetrahedron Lett.* **54**, 3290–3293 (2013).

104. Fruhmann, P. *et al.* Sulfation of deoxynivalenol, its acetylated derivatives, and T2-toxin. *Tetrahedron* **70**, 5260–5266 (2014).

105. Fürstner, A., Domostoj, M. M. & Scheiper, B. Total synthesis of dictyodendrin B. *J. Am.*

Chem. Soc. **127**, 11620–11621 (2005).

106. Bunschoten, A. *et al.* A general sequence independent solid phase method for the site specific synthesis of multiple sulfated-tyrosine containing peptides. *Chem. Commun.* 2999–3001 (2009). doi:10.1039/b823425f

107. Davies, A. G. Organotin compounds in technology and industry. *J. Chem. Res.* **34**, 181–190 (2010).

108. Liu, Y., Lien, I. F. F., Ruttgaizer, S., Dove, P. & Taylor, S. D. Synthesis and Protection of Aryl Sulfates Using the 2,2,2-Trichloroethyl Moiety. *Org. Lett.* **6**, 209–212 (2004).

109. Simpson, L. S. & Widlanski, T. S. A comprehensive approach to the synthesis of sulfate esters. *J. Am. Chem. Soc.* **128**, 1605–1610 (2006).

110. Steimle, A., Grant, E. T. & Desai, M. S. Quantitative assay to detect bacterial glycan-degrading enzyme activities in mouse and human fecal samples. *STAR Protoc.* **2**, 100326 (2021).

111. Sadiki, A. *et al.* Site-specific conjugation of native antibody. *Antib. Ther.* **3**, 271–284 (2020).

112. Duivelshof, B. L. *et al.* Glycan-Mediated Technology for Obtaining Homogeneous Site-Specific Conjugated Antibody-Drug Conjugates: Synthesis and Analytical Characterization by Using Complementary Middle-up LC/HRMS Analysis. *Anal. Chem.* **92**, 8170–8177 (2020).

113. Van Geel, R. *et al.* Chemoenzymatic Conjugation of Toxic Payloads to the Globally Conserved N-Glycan of Native mAbs Provides Homogeneous and Highly Efficacious Antibody-Drug Conjugates. *Bioconjug. Chem.* **26**, 2233–2242 (2015).

114. Li, K., Fong, D., Meichsner, E. & Adronov, A. A Survey of Strain-Promoted Azide–Alkyne Cycloaddition in Polymer Chemistry. *Chemistry - A European Journal* **27**, 5057–5073 (2021).

115. Dommerholt, J., Rutjes, F. P. J. T. & van Delft, F. L. Strain-Promoted 1,3-Dipolar Cycloaddition of Cycloalkynes and Organic Azides. *Top. Curr. Chem.* **374**, 1–20 (2016).

116. Masui, Y., Watanabe, H. & Masui, T. One-pot synthesis of N-acyl-substituted sulfamides from chlorosulfonyl isocyanate via the Burgess-type intermediates. *Tetrahedron Lett.* **45**, 1853–1856 (2004).

117. Van Hoof, S. *et al.* Synthesis of analogues of (E)-1-hydroxy-2-methylbut-2-enyl 4-diphosphate, an isoprenoid precursor and human γδ T cell activator. *J. Org. Chem.* **73**, 1365–1370 (2008).

118. Rikimaru, K. *et al.* Structure-activity relationships and key structural feature of pyridyloxybenzene-acylsulfonamides as new, potent, and selective peroxisome proliferator-activated receptor (PPAR) γ Agonists. *Bioorganic Med. Chem.* **20**, 3332–3358 (2012).

119. Crampton, R. H., Fox, M. & Woodward, S. N-(Alkylsulfamoyl)aldimines: Easily deprotected precursors for diarylmethylamine synthesis. *Tetrahedron Asymmetry* **24**, 599–605 (2013).

120. Barnych, B. *et al.* Development of Tetramethylenedisulfotetramine (TETS) Hapten Library: Synthesis, Electrophysiological Studies, and Immune Response in Rabbits. *Chem. - A Eur. J.* **23**, 8466–8472 (2017).

121. Wang, H. M., Xiong, C. D., Chen, X. Q., Hu, C. & Wang, D. Y. Preparation of Sulfamates and Sulfamides Using a Selective Sulfamoylation Agent. *Org. Lett.* **23**, 2595–2599 (2021).

122. Lofgren, K. A., Sreekumar, S., Jenkins, E. C., Ernzen, K. J. & Kenny, P. A. Anti-tumor efficacy of an MMAE-conjugated antibody targeting cell surface TACE/ADAM17-cleaved Amphiregulin in breast cancer. *Antib. Ther.* **4**, 252–261 (2021).

123. LI, L. *et al.* Conjugating MMAE to a novel anti-HER2 antibody for selective targeted delivery. *Eur. Rev. Med. Pharmacol. Sci.* **25**, 12929–12937 (2021).

124. Akaiwa, M., Dugal-Tessier, J. & Mendelsohn, B. A. Antibody – Drug Conjugate Payloads ; Study of Auristatin Derivatives. *Chem. Pharm. Bull. (Tokyo).* **68**, 201–211 (2020).

125. Li, C. *et al.* Clinical pharmacology of vc-MMAE antibody–drug conjugates in cancer patients: learning from eight first-in-human Phase 1 studies. *mAbs* **12**, (2020).

126. Sokka, I. K., Ekholm, F. S. & Johansson, M. P. Increasing the Potential of the Auristatin Cancer-Drug Family by Shifting the Conformational Equilibrium. *Mol. Pharm.* **16**, 3600–3608 (2019).

127. Luu Nguyen, Q., Baire, B. & Hoye, T. R. Competition between classical and hexadehydro-Diels-Alder (HDDA) reactions of HDDA triynes with furan We dedicate this Letter to the memory of Harry H. Wasserman, whose amalgamation of scholarship, artistry, and humanity stand as an admirable model for al. *Tetrahedron Lett.* **56**, 3265–3267 (2015).

128. Azagarsamy, M. A., Yesilyurt, V. & Thayumanavan, S. Disassembly of dendritic micellar containers due to protein binding. *J. Am. Chem. Soc.* **132**, 4550–4551 (2010).

129. Dahlgren, D. & Lennernäs, H. Antibody-Drug Conjugates and Targeted Treatment Strategies for Hepatocellular Carcinoma: A Drug-Delivery Perspective. *Molecules* **25**, (2020).

130. Chiang, Z. C. *et al.* Preparation and characterization of antibody-drug conjugates acting on HER2-positive cancer cells. *PLoS One* **15**, 1–15 (2020).

3.5 Experimentals

General procedures: see section 2.4

4-(((T*ert*-butyldimethylsilyl)oxy)methyl)phenol 3.4

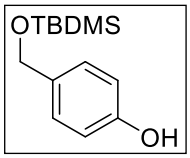

4-(hydroxymethyl)phenol (5.00g, 40.28mmol, 1 equiv.) was dissolved in 42mL dry THF under inert atmosphere and cooled to 0°C, followed by addition of imidazole (5.28g, 80.55mmol, 2 equiv.). The reaction was stirred for 10min before the addition of *tert*-butylchlorodimethylsilane (7.28g, 48.33mmol, 1.2 equiv.). The reaction was stirred for 1 h at 0°C, before being allowed to reach rt and was stirred for an additional 18 h. The reaction was quenched by the addition of sat. aq. NH_4Cl, followed by extraction with 3x EtOAc. The combined organic phase was dried over $MgSO_4$ and concentrated *in vacuo*. The crude was purified by FCC, affording the title compound **3.4** in a yield of 76%.

^{1}H NMR (400 MHz, $CDCl_3$) δ 7.22 – 7.16 (m, 2H), 6.82 – 6.74 (m, 2H), 5.21 (s, 1H), 4.66 (s, 2H), 0.93 (s, 9H), 0.09 (s, 6H).
^{13}C NMR (101 MHz, $CDCl_3$) δ 154.80, 133.62, 127.95, 115.22, 64.94, 26.12, 18.59, -5.03.

Neopentyl sulfurochloridate 3.5

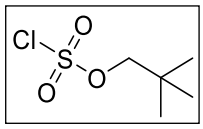

In a dry 3-necked RBF, sulfuryl chloride (5.00 mL, 61.69mmol, 1 equiv.) was dissolved in 5mL dry Et_2O at -78°C under inert atmosphere. A solution of neophenyl alcohol (5.44g, 61.69mmol, 1 equiv.) and pyridine (4.97mL, 61.69mmol, 1 equiv.) in 12.5mL dry Et_2O was prepared and was added dropwise to the cooled solution over 45 min under vigorous stirring. The reaction was stirred for 2 h before being allowed reach rt over 2 h. The reaction was filtered twice to remove precipitate, before concentrating *in vacuo*. The crude was purified by distillation under reduced pressure, affording the title compound **3.5** in a yield of 77%.

^{1}H NMR (400 MHz, $CDCl_3$) δ 4.17 (s, 2H), 1.05 (d, J = 0.8 Hz, 9H).
^{13}C NMR (101 MHz, $CDCl_3$) δ 85.61, 32.05, 26.01.

4-(((*Tert*-butyldimethylsilyl)oxy)methyl)phenyl neopentyl sulfate 3.6

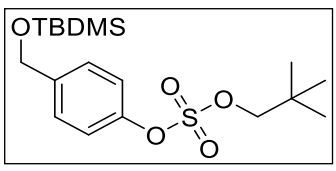

Compound **2.4** (5.00g, 20.97mmol, 1 equiv.) was dissolved in 45mL dry THF under inert atmosphere and cooled to -70°C, before dropwise addition of NAHMDS (1.0M in THF, 23.7mL, 23.07mmol, 1.1 equiv.). The reaction was stirred for 20min, before the quick addition of compound **3.2** (4.31g, 23.07mmol, 1.1 equiv.). The reaction was allowed to reach rt and stirred overnight. The reaction was quenched by the slow addition of sat. aq. $NaHCO_3$, followed by extraction with 4x EtOAc. The combined organic phase was washed with 2x H_2O

and brine, before being dried over $MgSO_4$ and the solvent removed *in vacuo*. The crude was purified by FCC, affording the title compound **3.6** in a yield of 78%.

^{1}H NMR (400 MHz, $CDCl_3$) δ 7.37 (d, *J* = 8.4 Hz, 2H), 7.30 – 7.25 (m, 2H), 4.74 (s, 2H), 4.08 (s, 2H), 1.01 (s, 9H), 0.95 (s, 9H), 0.11 (s, 6H).
^{13}C NMR (101 MHz, $CDCl_3$) δ 149.21, 140.87, 127.45, 120.94, 83.51, 64.27, 32.08, 26.11, 26.05, 18.52, -5.15.

4-(Hydroxymethyl)phenyl neopentyl sulfate 3.7

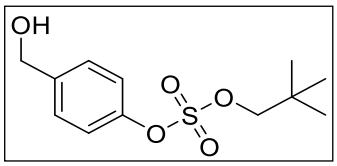

Compound **3.6** (5.00g, 12.87mmol, 1.0 eq.) was dissolved in 28mL dry THF under inert atmosphere and cooled to 0 °C. TBAF (1.0 M in THF, 32.2mL, 32.17mmol, 2.5 eq.) was added over 15min. The reaction was stirred for 1.5h, before being quenched by the addition of PBS buffer (pH 7.4, 5.0M) and the reaction was extracted with 4x EtOAc. The combined organic phase was washed with 3x H_2O and brine , before being dried over $MgSO_4$ and the solvent removed *in vacuo*, affording the title compound **3.7** in a yield of 87%.

^{1}H NMR (400 MHz, $CDCl_3$) δ 7.42, 7.41, 7.40, 7.40, 7.31, 7.30, 7.29, 7.28, 7.28, 7.27, 4.70, 4.09, 1.83, 1.00, 1.00, 0.99, 0.98, 0.98, 0.98.
^{13}C NMR (101 MHz, $CDCl_3$) δ 149.66, 140.22, 128.44, 121.27, 83.61, 64.49, 32.08, 26.09.
HRMS (ESI) calculated for $[C_{12}H_{18}O_5S]$ $[M-H]^-$ 273.0802, found 273.0802

Neopentyl (4-((((4-nitrophenoxy)carbonyl)oxy)methyl)phenyl) sulfate 3.3

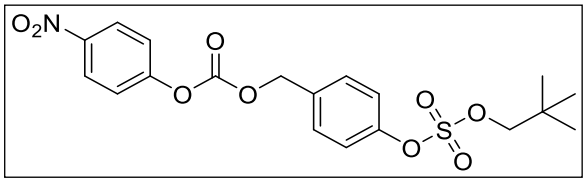

Compound **3.6** (729mg, 2.66mmol, 1 equiv.) was dissolved in 8mL dry DCM under inert atmosphere and cooled to 0°C. Pyridine (278.2µL, 3.45mmol, 1.3 equiv.) was added, followed by the addition of 4-nitrophenyl chloroformate (696.1mg, 3.45mmol, 1.3 equiv.). The reaction was allowed to reach rt and was stirred for 18h. The reaction was diluted with DCM and washed with 1 M HCl, sat. aq. $NaHCO_3$, 10x H_2O and brine. The organic phase was dried over $MgSO_4$ and the solvent removed *in vacuo*. The crude was purified by FCC, affording the title compound **3.3** in a yield of 93%.

^{1}H NMR (400 MHz, Chloroform-*d*) δ 8.30 – 8.26 (m, 2H), 7.54 – 7.48 (m, 2H), 7.41 – 7.33 (m, 4H), 5.30 (s, 2H), 4.11 (s, 2H), 1.01 (s, 9H).
^{13}C NMR (101 MHz, Chloroform-*d*) δ 155.52, 152.50, 150.70, 145.62, 133.57, 130.46, 125.48, 121.89, 121.61, 83.81, 69.93, 32.11, 26.09.

(4-Azidophenyl)methanol 3.8

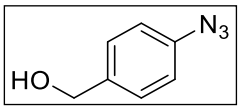

4-aminobenzylalcohol (1.00g, 8.12mmol, 1 equiv.) was dissolved in 8.1mL 6M HCl and cooled to 0°C. A solution of $NaNO_2$ (0.84g, 12.2mmol, 1.5 equiv.) in 21mL H_2O was cooled to 0°C and added dropwise to the solution of 4-aminobenzylalcohol. The reaction was stirred for 30 min at 0 °C before the dropwise addition of NaN_3 (2.10g, 32.5mmol, 4 equiv.) in 41mL H_2O, while keeping the temperature below 0°C. After 30min at 0°C, the reaction was neutralized by the addition of NaOAc until the reaction reached a basic pH and the reaction was allowed to reach rt and stirred for an additional 2h. The reaction was extracted with 3x Et_2O, dried over $MgSO_4$ and the solvent was removed *in vacuo*. The crude product was purified FCC, affording the title compound **3.8** in a yield of 99%.

^{1}H-NMR (400 MHz, CDCl3) δ 7.28 (d, J = 8.5 Hz, 2H), 6.97 (d, J = 8.5 Hz, 2H), 4.56 (s, 2H), 2.88 (s, 1H).
^{13}C-NMR (101 MHz, CDCl3) δ 139.27, 137.58, 128.52, 119.07, 64.44.

4-Azidobenzaldehyde 3.9

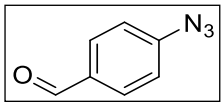

Compound **3.8** (2.16g, 14.48mmol, 1 equiv.) was dissolved in 75mL dry DCM, followed by the addition of Dess-Martin Periodinane (9.21g, 21.72mmol, 1.5 equiv.) and the reaction stirred for 18 h. The reaction was partitioned between EtOAc and H_2O. The precipitate was filtered to ease the extraction and washed with EtOAc. The resulting mixture was separated and the aqueous phase extracted with DCM. The combined organic phase was washed with sat. aq. $Na_2S_2O_3$, sat. aq. $NaHCO_3$ and brine. The organic phase was dried over Na_2SO_4 and the solvent removed *in vacuo*. The crude was FCC, affording the title compound **23.9** in a yield of 92%.

^{1}H-NMR (400 MHz, Chloroform-d) δ 9.96 (s, 1H), 7.90 (d, J = 8.5 Hz, 2H), 7.17 (d, J = 8.6 Hz, 2H).
^{13}C-NMR (101 MHz, Chloroform-d) δ 190.69, 146.38, 133.35, 131.66, 119.59.

***Tert*-butyl (2-((4-azidobenzyl)amino)ethyl)carbamate 3.10**

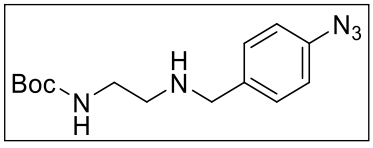

Compound **3.9** (2.00g, 13.57mmol, 1 equiv.) was dissolved in 24mL dry MeOH under inert atmosphere and $MgSO_4$ (6.53g, 54.29mmol, 4equiv.) was added. *N*-Boc-ethylenediamine (2.15 mL, 13.57mmol, 1 equiv.) was added and the reaction stirred overnight at rt. The reaction was cooled to 0°C and $NaBH_4$ (514mg, 13.57mmol, 1 equiv.) was added in portions. The reaction was stirred at 0°C for 3.5 h, before the addition of H_2O. The reaction was extracted with 3x EtOAc and DCM. The combined organic phase was washed with brine before being dried over $MgSO_4$ and the solvent was removed *in vacuo*. The crude was purified by FCC, affording the title compound **3.10** in a yield of 79%.

^{1}H NMR (400 MHz, $CDCl_3$) δ 7.33 – 7.29 (m, 2H), 7.00 – 6.96 (m, 2H), 4.99 (s, 1H), 3.77 (s, 2H), 3.24 (q, *J* = 5.8 Hz, 2H), 2.75 (t, *J* = 5.8 Hz, 2H), 2.55 (s, 2H), 1.99 (s, 0H), 1.44 (s, 9H).
^{13}C NMR (101 MHz, $CDCl_3$) δ 156.28, 139.06, 138.36, 136.46, 135.33, 130.37, 129.80, 119.19, 117.91, 80.60, 53.57, 52.83, 48.54, 40.18, 28.55.

(9*H*-Fluoren-9-yl)methyl (4-azidobenzyl)(2-((*tert*-butoxycarbonyl)amino)ethyl)carbamate 3.2

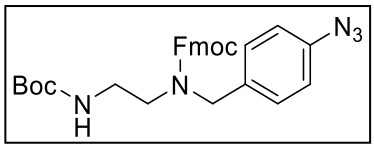

Compound **3.10** (2.96g, 10.15mmol, 1 equiv.) was dissolved in 7.5mL 1,4-dioxane and 15mL Na_2CO_3 (10 % w/w) and cooled to 0°C before the dropwise addition of 9-fluorenylmethyl chloroformate (3.94g, 15.23mmol, 1.5 equiv.) in 7.5mL 1,4-dioxane. The reaction was stirred for 1 h at 0°C and upon completion, the reaction was extracted 3x with DCM. The combined organic phase was washed with brine before, being dried over $MgsO_4$ and the solvent was removed *in vacuo*. The crude was purified by FCC, affording the title compound **3.2** in a yield of 97%.

^{1}H NMR (400 MHz, DMSO-d_6) δ 7.87 (dd, *J* = 17.1, 7.5 Hz, 2H), 7.66 (dd, *J* = 7.8, 3.3 Hz, 1H), 7.52 (d, *J* = 7.5 Hz, 1H), 7.48 – 7.23 (m, 4H), 7.19 (d, *J* = 8.1 Hz, 1H), 7.07 (d, *J* = 8.0 Hz, 1H), 6.95 (q, *J* = 8.3 Hz, 2H), 6.80 (t, *J* = 5.8 Hz, 1H), 4.50 (d, *J* = 5.5 Hz, 1H), 4.40 (d, *J* = 7.9 Hz, 2H), 4.27 (dt, *J* = 20.3, 5.9 Hz, 1H), 4.15 (s, 1H), 3.12 (d, *J* = 7.0 Hz, 2H), 2.96 (q, *J* = 6.5 Hz, 2H), 1.35 (s, 9H).
^{13}C NMR (101 MHz, DMSO-d_6) δ 156.21, 156.05, 144.33, 141.28, 138.71, 135.38, 129.54, 129.33, 128.10, 127.63, 125.20, 120.56, 119.57, 78.16, 66.83, 49.78, 47.21, 28.66.

4-(7-(4-Azidobenzyl)-10-(9*H*-fluoren-9-yl)-3,8-dioxo-2,9-dioxa-4,7-diazadecyl)phenyl neopentyl sulfate 3.11

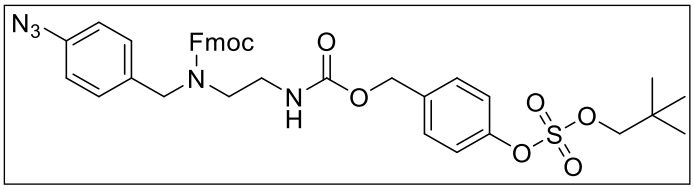

Compound **3.2** (1.16g, 2.25mmol, 1.0 equiv.) was dissolved in 25mL dry DCM under inert atmosphere and 5mL TFA added. The reaction was stirred for 30min and on completion, the reaction was co-evaporated with toluene *in vacuo*, until the collected solvent was no longer acidic and was stored on under vacuum overnight. The resulting crude was dissolved in 19mL dry THF under inert atmosphere and compound **3.3** (1.03g, 2.32mmol, 1 equiv.) dissolved in 4.6 mL dry THF, was added. Dry DIPEA was added until the pH was basic (2mL added). The reaction was stirred at rt for 66h. Upon completion, the reaction was diluted with EtOAc and the organic phase washed 14x with H_2O and 1x brine. The organic phase was dried over $MgSO_4$ and the solvent removed *in vacuo*. The crude was purified by FCC, affording the title compound **3.11** in a yield of 66%.

^{1}H NMR (400 MHz, Chloroform-*d*) δ 7.79 – 7.67 (m, 2H), 7.61 – 7.52 (m, 1H), 7.52 – 7.44 (m, 1H), 7.43 – 7.21 (m, 8H), 7.11 – 7.04 (m, 1H), 6.96 – 6.83 (m, 3H), 5.05 – 5.00 (m, 2H), 4.70 – 4.66 (m, 1H), 4.60 – 4.55 (m, 1H), 4.36 – 4.17 (m, 3H), 4.09 (s, 3H), 3.39 – 3.18 (m, 2H), 2.94 – 2.73 (m, 2H), 1.00 (bs, 12H) (broadening of peaks and rotamers observed).

^{13}C NMR (101 MHz, Chloroform-*d*) δ 156.24, 149.90, 149.52, 141.41, 140.15, 139.26, 129.54, 128.79, 128.29, 127.75, 127.08, 124.68, 121.13, 120.02, 119.90, 119.22, 83.53, 83.47, 65.59, 50.26, 47.31, 46.46, 39.70, 30.61, 25.97.
HRMS (ESI) calculated for $[C_{37}H_{39}N_5O_8S]$ $[M+Na]^+$ 736.2412, found 736.2418.

4-((((2-((4-(4-(13-(2,5-Dioxo-2,5-dihydro-1*H*-pyrrol-1-yl)-2,5,8,11-tetraoxatridecyl)-1*H*-1,2,3-triazol-1-yl)benzyl)amino)ethyl)carbamoyl)oxy)methyl)phenyl hydrogen sulfate 3.12

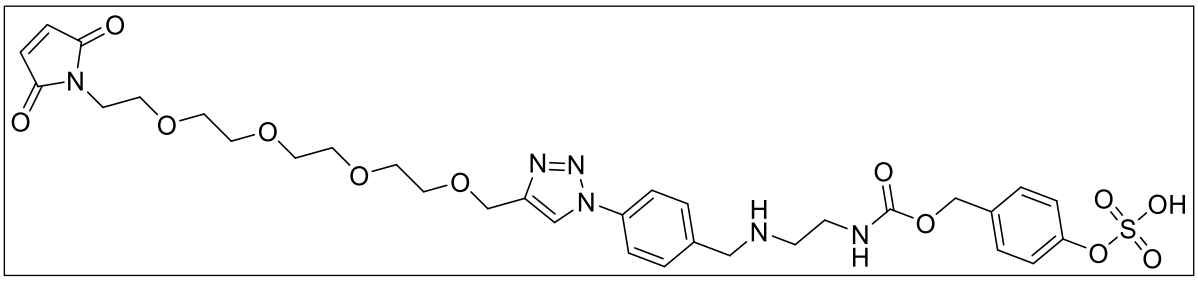

Compound **3.11** (188mg, 263.4μmol, 1 equiv.) was dissolved in 6.4mL dry DMF under inert atmosphere. 4.6mL of freshly prepared 0.5M NH_4OAc (aq.) was added, the reaction fitted with a condenser and heated to 70°C for 66h. Upon completion, the reaction mixture was concentrated under a stream of nitrogen. The crude (100mg, 229.3μmol, 1.3 eq.) was dissolved in 464μL degassed H_2O and 850μL degassed *t*BuOH. A 0.05M solution of $CuSO_4 \cdot 5H_2O$ (176μL, 8.82μmol, 0.05 equiv.) in degassed H_2O, was added to the crude, solution followed by the addition of a 2M solution of Alkyne-PEG4-maleimide (88μL, 176.37μmol, 1 equiv.) in DMSO. The reaction was degassed for 30min before the addition of a 0.1M solution of sodium ascorbate (212μL, 21.16μmol, 0.12 equiv.). The reaction was stirred at rt overnight. The reaction mixture was purified by preparative HPLC, affording the title compound **3.12** in a yield of 31%.

^{1}H NMR (800 MHz, DMSO-d_6) δ 8.81 (s, 1H), 8.02 – 7.89 (m, 2H), 7.69 (d, *J* = 8.1 Hz, 2H), 7.34 (d, *J* = 6.0 Hz, 1H), 7.28 – 7.25 (m, 2H), 7.20 – 7.13 (m, 2H), 6.99 (s, 2H), 4.99 (s, 2H), 4.64 (s, 2H), 4.23 (s, 2H), 3.65 – 3.61 (m, 2H), 3.59 – 3.53 (m, 4H), 3.53 – 3.49 (m, 4H), 3.49 – 3.46 (m, 4H), 3.45 (ddd, *J* = 6.1, 3.3, 1.3 Hz, 2H), 3.34 (q, *J* = 6.2 Hz, 2H), 3.07 – 2.94 (m, 2H).
^{13}C NMR (201 MHz, DMSO-d_6) δ 170.72, 156.31, 153.36, 145.22, 136.79, 134.40, 131.34, 131.05, 128.74, 122.03, 120.22, 119.98, 69.69, 69.67, 69.59, 69.53, 69.31, 69.09, 66.81, 65.42, 63.33, 49.52, 46.48, 36.90, 36.73.
HRMS (ESI) calculated for $[C_{32}H_{40}N_6O_{12}S]$ $[M+NH_4]^+$ 750.2763, found 750.2775.

tert-butyl ((S)-1-(((S)-1-(((3R,4S,5S)-3-methoxy-1-((S)-2-((1R,2R)-1-methoxy-2-methyl-3-(((1S,2R)-1-(((4-nitrophenoxy)carbonyl)oxy)-1-phenylpropan-2-yl)amino)-3-oxopropyl)pyrrolidin-1-yl)-5-methyl-1-oxoheptan-4-yl)(methyl)amino)-3-methyl-1-oxobutan-2-yl)amino)-3-methyl-1-oxobutan-2-yl)(methyl)carbamate 3.13

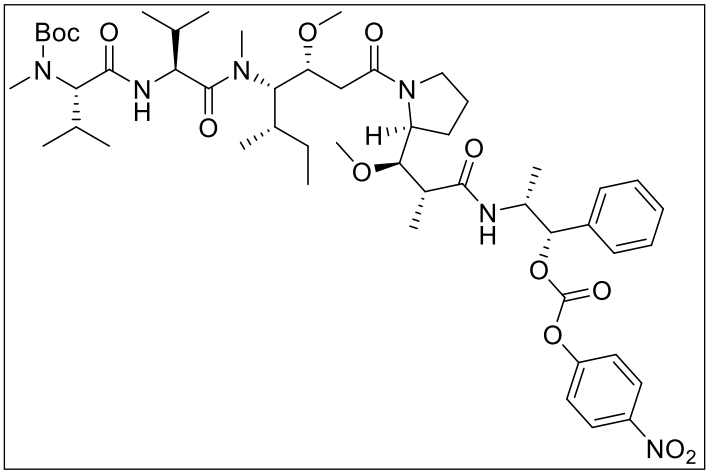

MMAE (42mg, 58.5μmol, 1 equiv.) was weighed in a pre-dried MW-vial followed by the addition of TEA (8.2μL, 58.5μmol, 1 equiv.). The MW-vial was capped and stored under argon. A solution of Boc_2O (565mM, 114μL, 1.1 equiv.) in 500 μL dry DCM was added dropwise to the sides of the MW-vial. The reaction was stirred for 24h. Additional Boc_2O solution (21μL, 0.2 equiv.) was added and stirred for and additional 24h. Upon completion, the reaction was diluted with 1mL DCM before washing with sat. aq. $NaHCO_3$, H_2O and brine. The organic phase was dried over $MgSO_4$, filtered and the solvent removed *in vacuo*. The crude was dissolved in 2mL dry DMF under inert atmosphere in a MW-vial. To the solution TEA (41μL, 345μL, 4 equiv.) and bis-Pnp-carbonate (79mg, 259μL, 3 equiv.) was added and the MW-vial was capped and stirred at rt overnight. The solvent was removed under a stream of nitrogen and the crude purified by FCC, affording the title compound **3.13** in a yield of 81%

^{1}H NMR (400 MHz, Chloroform-*d*) δ 8.31 – 8.23 (m, 2H), 7.52 – 7.34 (m, 7H), 6.76 – 6.44 (m, 2H), 5.81 (d, *J* = 5.0 Hz, 1H), 4.90 – 4.49 (m, 3H), 4.14 – 3.98 (m, 3H), 3.94 – 3.83 (m, 1H), 3.56 – 3.29 (m, 8H), 3.18 (s, 1H), 3.01 (s, 3H), 2.95 – 2.73 (m, 4H), 2.51 – 2.33 (m, 2H), 2.28 – 2.13 (m, 1H), 2.03 (pd, *J* = 10.9, 9.4, 6.5 Hz, 3H), 1.90 (s, 1H), 1.86 – 1.73 (m, *J* = 5.2, 4.5 Hz, 2H), 1.59 – 1.44 (m, 11H), 1.28 – 1.14 (m, 6H), 1.13 – 0.74 (m, 18H).
UPLC-MS (ESI) calculated for $[C_{51}H_{78}N_6O_{13}]$ $[M+H]^+$m/z 983.6, found m/z 983.5

4-((10S,11R,14R,15R)-15-((S)-1-((6S,9S,12S,13R)-12-((R)-sec-butyl)-6,9-diisopropyl-13-methoxy-2,2,5,11-tetramethyl-4,7,10-trioxo-3-oxa-5,8,11-triazapentadecan-15-oyl)pyrrolidin-2-yl)-7-(4-(4-(13-(2,5-dioxo-2,5-dihydro-1H-pyrrol-1-yl)-2,5,8,11-tetraoxatridecyl)-1H-1,2,3-triazol-1-yl)benzyl)-11,14-dimethyl-3,8,13-trioxo-10-phenyl-2,9,16-trioxa-4,7,12-triazaheptadecyl)phenyl hydrogen sulfate 3.14

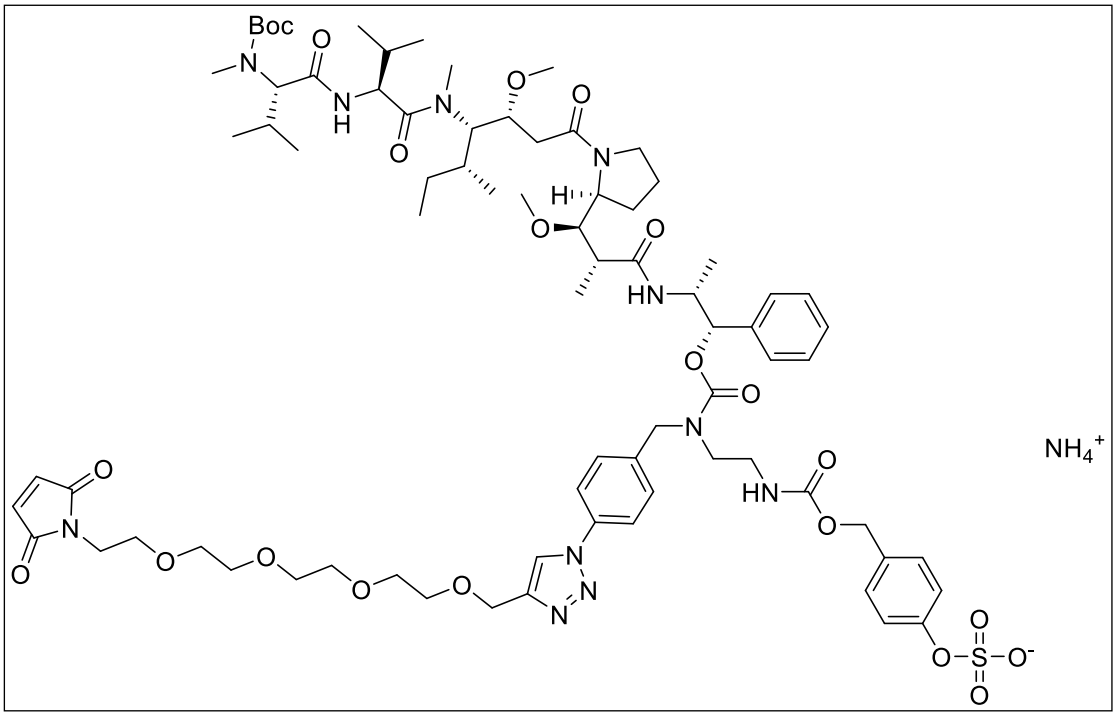

4-((((2-((4-(4-(13-(2,5-Dioxo-2,5-dihydro-1*H*-pyrrol-1-yl)-2,5,8,11-tetraoxatridecyl)-1*H*-1,2,3-triazol-1-yl)benzyl)amino)ethyl)carbamoyl)oxy)methyl)phenyl hydrogen sulfate **3.12** (13mg, 17μmol, 1 equiv.) was dissolved in 270μL dry DMF under inert atmosphere in a MW-vial and cooled to 0°C. Dry DIPEA (30μL, 173μmol, 10 equiv.) was added, followed by the addition of Boc-MMAE-pnp (17mg, 17μmol, 1 equiv.) and the reaction was capped. The reaction was stirred overnight at rt, followed by purification by preparative HPLC, affording compound **3.14** in a yield of 10%.

UPLC MS (ESI) calculated for $[C_{77}H_{113}N_{11}O_{22}S]$ $[M-H]^-$ m/z 1574.8, found m/z 1574.6
UPLC MS (ESI) calculated for $[C_{77}H_{113}N_{12}O_{22}S]$ $[M+NH_4]^+$ m/z 1593.8, found m/z 1593.8

4-((10S,11R,14R,15R)-15-((S)-1-((3R,4S,5R)-4-((S)-N,3-Dimethyl-2-((S)-3-methyl-2-(methylamino)butanamido)butanamido)-3-methoxy-5-methylheptanoyl)pyrrolidin-2-yl)-7-(4-(4-(13-(2,5-dioxo-2,5-dihydro-1H-pyrrol-1-yl)-2,5,8,11-tetraoxatridecyl)-1H-1,2,3-triazol-1-yl)benzyl)-11,14-dimethyl-3,8,13-trioxo-10-phenyl-2,9,16-trioxa-4,7,12-triazaheptadecyl)phenyl hydrogen sulfate 3.15

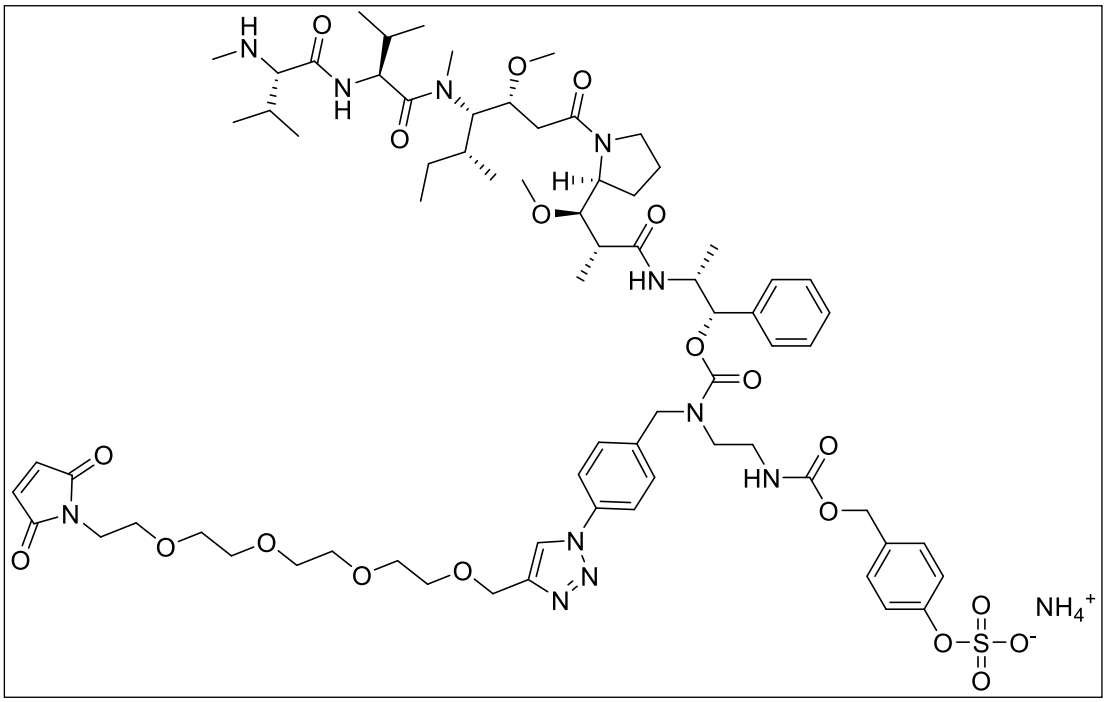

Compound **3.14** (2mg, 1.27μmol, 1 equiv.) was transferred with 1.00mL dry DCM to a pre-dried MW-vial. The MW-vial was capped and cooled to 0°C. 200μL TFA was added and the reaction stirred for 5min at 0°C. The reaction was allowed to warm up to rt and stirred for 30min. Upon completion, the TFA and DCM was removed under a stream of nitrogen, affording the title compound **3.15** in a quantitative yield.

UPLC MS (ESI) calculated for $[C_{72}H_{105}N_{11}O_{20}S]$ $[M-H]^-$ m/z 1474.7, found m/z 1474.8

4-(((*Tert*-butyldimethylsilyl)oxy)methyl)-2-nitrophenol 3.16

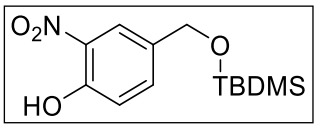

4-(hydroxymethyl)-2-nitrophenol (2.00g, 11.8mmol, 1 equiv.) was dissolved in 15mL dry THF under inert atmosphere. The solution was cooled to 0°C and imidazole(1.16g, 23.7mmol, 2 equiv.) was added. Reaction was stirred for 10min before the addition of tert-butyldimethylsilyl chloride (2.14g, 14.9mmol, 1.2 equiv.). The reaction was stirred at 0°C for 1h, after which the reaction was allowed to reach rt and stirred for an additional 18h. The reaction was quenched with sat. NH_4Cl and was extracted 3x with EtOAc. The combined organic phase was dried over $MgSO_4$ and solvent was removed *in vacuo*. The crude was dissolved in 24mL ACN:H_2O (95:5) and DBU (176μL, 1.18mmol, 0.1 equiv.) was added. The reaction was allowed to stir overnight at rt. Solvent was removed *in vacuo*, the crude was taken up in EtOAc and the organic phase washed 3x with water and 3x with

brine. The organic phase was dried over $MgSO_4$ and the solvent removed *in vacuo*. The crude was purified by FFC, affording the title compound **3.16** as a yellow solid in a yield of 86%.

^{1}H NMR (400 MHz, Chloroform-*d*) δ 10.56 (s, 1H), 8.08 (d, *J* = 2.2, 1H), 7.56 (dd, *J* = 8.8, 2.1 Hz, 1H), 7.15 (d, *J* = 8.6 Hz, 1H), 4.71 (s, 2H), 0.97 (d, *J* = 0.8 Hz, 10H), 0.14 (d, *J* = 0.8 Hz, 6H).
^{13}C NMR (101 MHz, Chloroform-*d*) δ 154.12, 135.54, 134.00, 133.30, 122.08, 119.85, 63.53, 25.88, 18.36, -5.27.

4-(((*Tert*-butyldimethylsilyl)oxy)methyl)-2-nitrophenyl neopentyl sulfate 3.17

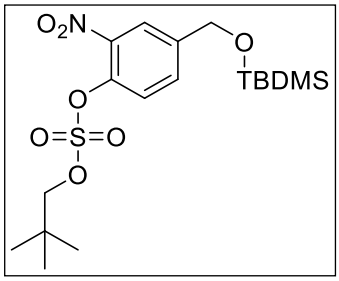

4-(((tert-butyldimethylsilyl)oxy)methyl)-2- nitrophenol **3.16** (1.00g, 3.53mmol, 1 equiv.) was dissolved in 36mL dry THF under inert atmosphere. DMAP (0.43g, 3.53mmol, 1 equiv.) and TEA (962µL, 7.06mmol, 2 equiv.) were added and the reaction was cooled to 0°C followed by the dropwise addition of neopentyl sulfurochloridate. After 1h reaction time, the reaction was allowed to warm to rt and stirred for an additional 2h. The reaction was concentrated *in vacuo* and diluted with EtOAc. The organic phase was washed with aqueous 1M HCl, the organic phase dried over $MgSO_4$ and the solvent removed *in vacuo*. The crude was purified by FCC, affording the title compound **3.17** in a quantitative yield.

^{1}H NMR (400 MHz, Chloroform-*d*) δ 8.01 – 7.95 (m, 1H), 7.64 – 7.53 (m, 2H), 4.79 (s, 2H), 4.21 (s, 2H), 1.02 (d, *J* = 0.8 Hz, 9H), 0.95 (d, *J* = 0.8 Hz, 9H), 0.13 (d, *J* = 0.9 Hz, 6H).
^{13}C NMR (101 MHz, Chloroform-*d*) δ 142.21, 141.87, 140.61, 131.38, 123.72, 123.16, 84.89, 63.20, 31.92, 25.85, 18.34, -5.36.

4-Formyl-2-nitrophenyl neopentyl sulfate 3.19

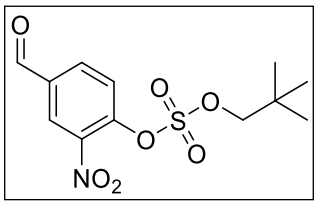

4-hydroxy-3-nitrobenzaldehyde (1.00g, 5.98mmol, 1 equiv.), DMAP (0.73g, 5.98mmol, 1 equiv.) and TEA (1.67mL, 11.97mmol, 2 equiv.) was dissolved in 30mL of dry THF under inert atmosphere. Neopentyl sulfurochloridate (1.12g, 5.98mmol, 1 equiv.) was added dropwise to the stirred solution over 10min. The reaction was quenched after 2 h reaction time by the addition of brine and EtOAc. The phases were partitioned and the organic phase dried over $MgSO_4$. The solvent was removed *in vacuo* and the crude purified by FCC, affording the title compound **3.19** (45%)

^{1}H NMR (400 MHz, Chloroform-*d*) δ 10.09 (s, 1H), 8.53 (d, *J* = 2.0 Hz, 1H), 8.22 (dd, *J* = 8.5, 2.0 Hz, 1H), 7.87 (d, *J* = 8.5 Hz, 1H), 4.28 (s, 2H), 1.06 (s, 9H).
^{13}C NMR (101 MHz, Chloroform-*d*) δ 188.19, 145.93, 134.82, 134.60, 126.97, 124.43, 85.70, 31.99, 25.80.

4-(Hydroxymethyl)-2-nitrophenyl neopentyl sulfate 3.18

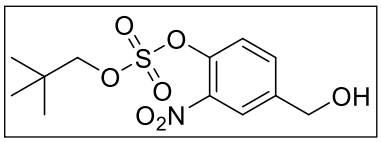

4-formyl-2-nitrophenyl neopentyl sulfate **3.19** (0.70g, 2.21mmol, 1 equiv.) was dissolved in 20mL dry MeOH under an inert atmosphere and the solution cooled to 0°C. $NaBH_4$ (167mg, 4.41mmol, 2 equiv.) was added portion wise over 20min after which the reaction was heated to rt and stirred for an additional 2h. Upon complete reaction, as observed by TLC, the reaction was carefully quenched by the addition of water. The reaction was extracted with EtOAc and the organic phase dried over $MgSO_4$. The solvent was removed *in vacuo* and the crude purified by a short silica plug, affording the title compound **3.18** in 97% yield.

^{1}H NMR (400 MHz, Chloroform-*d*) δ 8.05 – 8.00 (m, 1H), 7.66 (dd, *J* = 8.7, 2.1 Hz, 1H), 7.59 (d, *J* = 8.5 Hz, 1H), 4.79 (s, 2H), 4.21 (s, 2H), 1.02 (s, 8H).
^{13}C NMR (101 MHz, Chloroform-*d*) δ 141.97, 141.43, 140.98, 132.19, 123.96, 123.87, 85.02, 63.17, 31.93, 25.84.

Neopentyl (2-nitro-4-((((4-nitrophenoxy)carbonyl)oxy)methyl)phenyl) sulfate 3.20

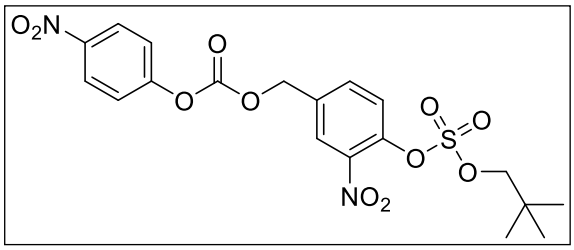

4-(hydroxymethyl)-2-nitrophenyl neo-pentyl sulfate **3.18** (679mg, 2.12mmol, 1 equiv.) was dissolved in 40mL of dry DCM and para-nitrochlorofomate (977mg, 4.85mmol, 2.2 equiv.) and pyridine (444µL, 5.51mmol, 2.5 equiv.) were added. The reaction was stirred overnight under inert atmosphere. The reaction was partitioned between water and DCM and the organic phase washed with 2x water, dried over $MgSO_4$ and solvent was removed *in vacuo*. The crude was purified by FCC, affording the title compound **3.20** in 66% yield.

^{1}H NMR (400 MHz, Chloroform-*d*) δ 8.34 – 8.27 (m, 2H), 8.12 (d, *J* = 2.1 Hz, 1H), 7.76 (dd, *J* = 8.5, 2.2 Hz, 1H), 7.69 (d, *J* = 8.5 Hz, 1H), 7.40 (d, *J* = 9.1 Hz, 2H), 5.35 (s, 2H), 4.25 (s, 2H), 1.04 (s, 9H).
^{13}C NMR (101 MHz, Chloroform-*d*) δ 155.31, 142.41, 134.76, 134.28, 126.39, 126.04, 125.56, 124.60, 121.86, 115.78, 85.47, 68.48, 32.11, 25.98.

4-(7-(4-Azidobenzyl)-10-(9H-fluoren-9-yl)-3,8-dioxo-2,9-dioxa-4,7-diazadecyl)-2-nitrophenyl neopentyl sulfate 3.21

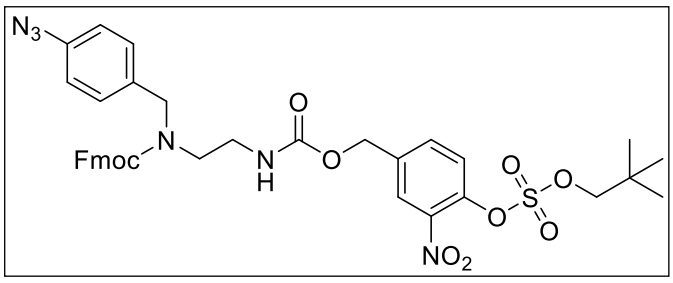

(9H-fluoren-9-yl) methyl(4-azido-benzyl) (2-((tert butoxycarbonyl) amino) ethyl)carbamate **3.2** was dissolved in 10mL DCM and 1 mL TFA added. The reaction was stirred for 1h whereupon THF was added to the reaction and the solvent removed *in vacuo*. The crude was dissolved in THF together with neopentyl (2-nitro-4-((((4-nitrophenoxy) carbonyl)oxy) methyl) phenyl) sulfate **3.20** (543mg, 1.12mmol, 1 equiv.), before the addition of DIPEA. The reaction was stirred

at rt overnight and TLC confirmed full conversion. The reaction was partitioned between EtOAc and water and the organic phase was washed with 2x brine, dried over $MgSO_4$ and the solvent removed *in vacuo*. The crude was purified by FCC, affording the title **3.21** in a yield of 78%.

^{1}H NMR (400 MHz, Chloroform-*d*) δ 7.96 (s, 1H), 7.74 (dd, *J* = 13.9, 7.5 Hz, 2H), 7.58 (d, *J* = 6.3 Hz, 3H), 7.48 (d, *J* = 7.5 Hz, 1H), 7.45 – 7.24 (m, 3H), 7.07 (d, *J* = 8.0 Hz, 1H), 6.90 (t, *J* = 6.3 Hz, 3H), 5.33 (s, 1H), 5.07 (d, *J* = 5.5 Hz, 2H), 4.75 – 4.49 (m, 2H), 4.38 – 4.19 (m, 5H), 3.31 (dd, *J* = 26.6, 6.1 Hz, 2H), 2.96 – 2.65 (m, 2H), 1.03 (s, 9H) (broadening of peaks and rotamers observed.
^{13}C NMR (101 MHz, Chloroform-*d*) δ 143.69, 141.42, 139.33, 137.19, 133.75, 133.41, 129.30, 128.82, 127.78, 127.32, 127.10, 126.18, 125.06, 124.68, 124.08, 123.99, 120.05, 119.93, 119.25, 115.58, 85.11, 67.37, 64.37, 50.29, 47.26, 46.33, 39.89, 31.94, 25.85.
HRMS (ESI) calculated for $[C_{37}H_{38}N_6O_{10}S]$ $[M+H]^+$ 759.2443, found 759.2441

Ammonium 4-((((2-((4-(4-(13-(2,5-dioxo-2,5-dihydro-1H-pyrrol-1-yl)-2,5,8,11-tetraoxatridecyl)-1H-1,2,3-triazol-1-yl)benzyl)amino)ethyl)carbamoyl)oxy)methyl)-2-nitrophenyl sulfate 3.22

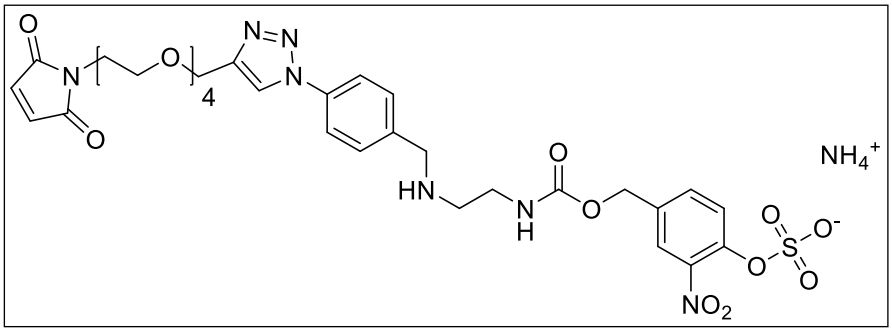

Compound **3.21** was dissolved in t-BuOH and H_2O with $CuSO_4$ and Alkyne-PEG4-maleimide. The solution was degassed with N_2 gas for 10min, after which ascorbic acid was added. The reaction was stirred overnight and upon completion, the solvent removed under a stream of nitrogen. The crude was purified by preparative HPLC affording the title compound **3.22** in a yield of 31%.

HRMS (ESI) calculated for **[**$C_{32}H_{39}N_7O_{14}S$] $[M+Na]^+$ 800.2168, found 800.217

Ammonium 4-((10S,11R,14R,15R)-15-((S)-1-((6S,9S,12S,13R)-12-((S)-sec-butyl)-6,9-diisopropyl-13-methoxy-2,2,5,11-tetramethyl-4,7,10-trioxo-3-oxa-5,8,11-triazapentadecan-15-oyl)pyrrolidin-2-yl)-7-(4-(4-(13-(2,5-dioxo-2,5-dihydro-1H-pyrrol-1-yl)-2,5,8,11-tetraoxatridecyl)-1H-1,2,3-triazol-1-yl)benzyl)-11,14-dimethyl-3,8,13-trioxo-10-phenyl-2,9,16-trioxa-4,7,12-triazaheptadecyl)-2-nitrophenyl sulfate 3.23

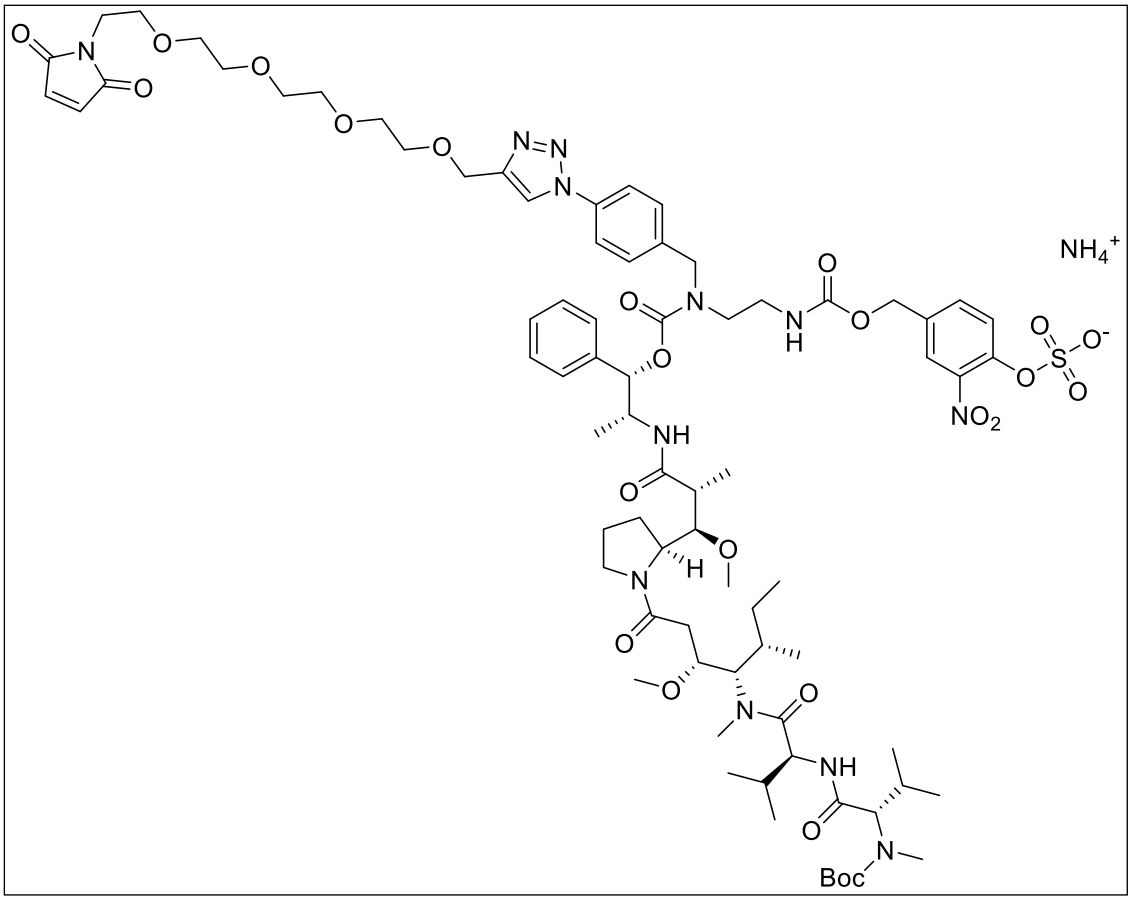

Ammonium 4-((((2-((4-(4-(13-(2,5-dioxo-2,5-dihydro-1H-pyrrol-1-yl)-2,5,8,11-tetra oxatridecyl)-1H-1,2,3-triazol-1-yl)benzyl)amino)ethyl)carbamoyl)oxy)methyl)-2-nitrophenyl sulfate **3.22** (16mg, 21μmol, 1 equiv.) was dissolved in 200μL dry DMF under inert atmosphere in a MW-vial and was cooled to 0°C. DIPEA (36μL, 205μmol, 10 equiv.) and Boc-MMAE-Pnp **3.13** (20mg, 21μmol, 1 equiv.) was added. The vial was capped and the reaction stirred overnight at rt. The crude was purified by preparative HPLC, affording the title compound **3.23** in a yield of 12%.

UPLC MS (ESI) calculated for $[C_{77}H_{112}N_{12}O_{24}S]$ $[M-H]^-$ m/z 1619.8, found m/z 1619.8

Part II

2,2,2-Trichloroethyl sulfurochloridate 3.24

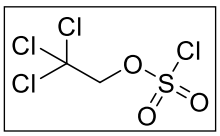

To a solution of dry pyridine (6.0mL, 74.19mmol, 1 equiv.) and 2,2,2-trichloroethanol (7.1mL, 74.10mmol, 1 equiv.) in 40mL Et_2O at -78°C, sulfuryl chloride (6.0mL, 74.19mmol, 1 equiv.) was added dropwise for 1h. The reaction was stirred at -78°C, after which the reaction was allowed to reach rt and stirred for an additional 3h. The reaction was filtered and the solvent of the filtrate removed *in vacuo*. The crude was purified by vacuum distillation, affording the title compound **3.24** as a colorless oil (72%).

^{1}H NMR (400 MHz, Chloroform-*d*) δ 4.92 (s, 2H).
^{13}C NMR (101 MHz, Chloroform-*d*) δ 91.45, 81.34.

2,2,2-Trichloroethyl 2-methyl-1H-imidazole-1-sulfonate 3.25

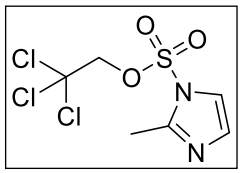

2-methylimidazole (10.68g, 130mmol, 3.6 equiv.) was dissolved in 55mL dry THF and cooled to 0°C. A solution of 2,2,2-Trichloroethyl sulfurochloridate **3.24** (8.98g, 36.23mmol, 1 equiv.) in 60mL dry THF was added dropwise over 15min and the reaction stirred at 0°C, before allowing the reaction to reach rt, then stirring for an additional 2h. The reaction was filtered and the solvent of the filtrate removed. The crude was partitioned between EtOAc and water and the organic phase washed with 0.1M HCL and brine. The organic phase was dried over $MgSO_4$ and the solvent removed *in vacuo*, affording the title compound **3.25** in a yield of 86%.

^{1}H NMR (400 MHz, Chloroform-*d*) δ 7.36 (d, J=1.7Hz, 1H), 7.01 (d, J=1.8Hz, 1H), 4.69 (s, 2H), 2.73 (s, 3H).
^{13}C NMR (101 MHz, Chloroform-*d*) δ 146.59, 127.79, 120.15, 91.70, 80.11, 14.82.

2,3-Dimethyl-1-((2,2,2-trichloroethoxy)sulfonyl)-1H-imidazol-3-ium trifluoromethanesulfonate 3.26

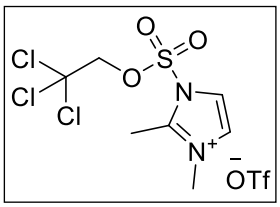

Methyl triflate (3.4mL, 30.66mmol, 1 equiv.) was added dropwise to a solution of 2,2,2-trichloroethyl 2-methyl-1H-imidazole-1-sulfonate **3.25** (5.03g, 30.55mmol, 1 equiv.) in 150mL dry Et_2O stirred at 0°C. The reaction was stirred at 0°C overnight, followed by filtration, affording the title compound **3.26** as a white solid in a yield of 91%.

^{1}H NMR (400 MHz, DMSO-d_6) δ 8.21 (d, J=2.3Hz, 1H), 7.95 (d, J=2.4Hz, 1H), 5.53 (s, 2H), 3.86 (s, 3H), 2.83 (s, 3H).
^{13}C NMR (101 MHz, DMSO-d_6) δ 148.62, 123.73, 120.85, 91.84, 81.47, 35.92, 11.72.

4-Formylphenyl neopentyl sulfate 3.27

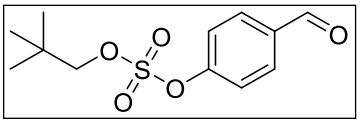

4-hydroxybenzaldehyde (1.04g, 8.19mmol, 1equiv.), DMAP (1.01g, 8.18mmol, 1 equiv.) and TEA (2.3mL, 16.4mmol, 2 equiv.) was dissolved in 16mL dry THF under inert atmosphere and neopentyl sulfufochloridate **2.5** (1.6mL, 9.80mmol, 1.2 equiv.) was added dropwise at rt. The reaction was stirred for 1h at rt, before removal of the solvent *in vacuo*. The crude was partitioned between EtOAc and water. The organic phase was washed with 1M HCl before drying over $MgSO_4$. The crude was purified by FCC, affording the title compound **3.27** in a yield of 61%.

^{1}H NMR (400 MHz, Chloroform-*d*) δ 10.02, (s, 1H), 7.96 (d, J=8.6Hz, 2H), 7.48 (d, J=8.6Hz, 2H), 4.12 (s, 2H), 1.00 (s, 9H).
^{13}C NMR (101 MHz, Chloroform-*d*) δ 190.60, 154.45, 135.05, 131.73, 121.63, 84.18, 32.11, 26.04.

2,6-Difluoro-4-formylphenyl neopentyl sulfate 3.28

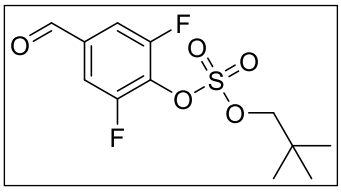

3,5-difluoro-4-hydroxybenzaldehyde (2.00g, 12.65mmol, 1 equiv.) and DBU (3.85mL, 25.30mmol, 2 equiv.) was dissolved in 20 mL dry DCM under inert atmosphere and neopentyl sulfurochloridate **3.5** (2.83g, 15.18mmol, 1.2 equiv.) was added dropwise. The reaction was stirred overnight at rt and the reaction quenched by the addition of water. The organic phase was dried over $MgSO_4$ and the solvent removed *in vacuo*. The crude was purified by FCC, affording the title compound **3.28** in a yield of 4%.

^{1}H NMR (400 MHz, Chloroform-*d*) δ 9.96 (t, J = 1.8 Hz, 1H), 7.67 – 7.54 (m, 2H), 4.29 (s, 2H), 1.07 (s, 10H).
^{13}C NMR (101 MHz, Chloroform-*d*) δ. 188.14 (t, J = 2.0 Hz), 156.08 (dd, J = 258.3, 2.6 Hz), 135.43 (t, J = 6.3 Hz), 131.40, 113.37 (d, J = 23.2 Hz), 84.93, 31.98, 25.84.

4-Formylphenyl (2,2,2-trichloroethyl) sulfate 3.29

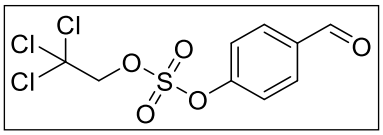

4-hydroxybenzaldehyde (222mg, 1.81mmol, 1 equiv.) and 2,3-dimethyl-1-((2,2,2-trichloroethoxy) sulfonyl) -1H-imidazol-3-ium trifluoromethanesulfonate **3.26** (845mg, 1.85mmol, 1 equiv.) were dissolved in dry DCM under inert atmosphere and the reaction cooled to 0°C. 1,2-dimethyl-1H-imidazole (330µL, 3.86mmol, 2 equiv.) was added dropwise and the reaction allowed to reach rt. The reaction was stirred overnight and the solvent removed *in vacuo*. The crude was purified by FCC, affording the title compound **3.29** in a yield of 84%.

^{1}H NMR (400 MHz, Chloroform-*d*) δ 10.04 (s, 1H), 7.98 (d, J=8.7Hz, 2H), 5.54 (d, J=8.7Hz, 2H), 4.87, (s, 2H).
^{13}C NMR (101 MHz, Chloroform-*d*) δ 190.41, 154.06, 135.56, 131.85, 121.84, 92.27, 80.74.

2-Fluoro-4-formylphenyl (2,2,2-trichloroethyl) sulfate 3.30

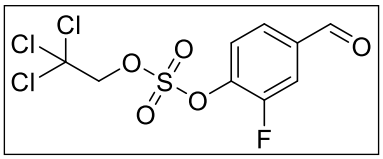

3-Fluoro-4-hydroxybenzaldehyde (400mg, 2.85mmol, 1 equiv.) and 2,3-dimethyl-1-((2,2,2-trichloroethoxy)s ulfonyl)-1H-imidazol-3-ium trifluoromethanesulfonate **3.26** (1.30g, 2.85mmol, 1 equiv.) were dissolved in 18mL dry DCM under inert atmosphere and the reaction was cooled to 0°C, before the dropwise addition of 1,2-dimethyl-1H-imidazole (0.51mL, 5.73mmol, 2 equiv.). Upon completion, the solvent was removed *in vacuo* and the crude purified by FCC, affording the title compound **3.30** in a yield of 88%.

^{1}H NMR (400 MHz, Chloroform-*d*) 10.00 (d, J=1.9, 1H), 7.78 (d, J=8.7, 2H), 7.73-7.66 (m, 1H) 4.94 (s, 2H).
^{13}C NMR (101 MHz, Chloroform-*d*) δ 189.31, 154.40 (d, J=256.1Hz), 141.57 (d, J=13.1Hz), 136.87 (d, J=5.2Hz), 127.09 (d, J=3.8), 124.76, 117.50 (d, J=19.1Hz), 92.15, 80.98 (d, J=2.3Hz)

4-(Hydroxymethyl)-2-nitrophenyl neopentyl sulfate 3.18

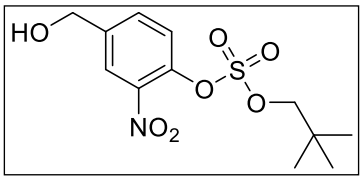

4-(hydroxymethyl)2-nitrophenol (200mg, 1.18mmol, 1 equiv.), DMAP (60mg, 0.59mmol, 0.5 equiv.) and TEA (198μL, 1.18mmol, 1 equiv.) was dissolved in 10mL dry THF under inert atmosphere and neopentyl sulfurochloridate **3.5** (220mg, 1.18mmo, 1 equiv.) was added dropwise. The reaction was stirred at rt for 2h before the solvent was removed *in vacuo* and the crude purified by FCC, affording the title compound **3.18** in a yield of 89%.

^{1}H NMR (400 MHz, Chloroform-*d*) δ 8.05 – 8.00 (m, 1H), 7.66 (dd, *J* = 8.7, 2.1 Hz, 1H), 7.59 (d, *J* = 8.5 Hz, 1H), 4.79 (s, 2H), 4.21 (s, 2H), 1.02 (s, 8H).
^{13}C NMR (101 MHz, Chloroform-*d*) δ 141.97, 141.43, 140.98, 132.19, 123.96, 123.87, 85.02, 63.17, 31.93, 25.84.

4-(Hydroxymethyl)-2-nitrophenyl (2,2,2-trichloroethyl) sulfate 3.31

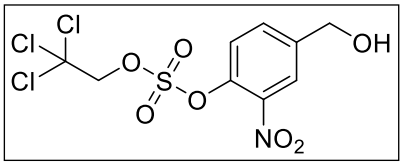

4-(hydroxymethyl)2-nitrophenol (681mg, 1.49mmol, 1 equiv.) and 2,3-dimethyl-1-((2,2,2-trichloroethoxy) sulfonyl)-1H-imidazol-3-ium trifluoro methane sulfonate **3.26** (251mg, 1.48mmol, 1 equiv.) were dissolved in 9mL dry DCM under inert atmosphere. 1,2-dimethyl-1H-imidazole (260μL, 2.97mmol, 0.3 equiv.) was added and the reaction stirred overnight at rt. The solvent was removed *in vacuo* and the crude purified be FCC, affording the title compound **3.31** in a yield of 53%.

^{1}H NMR (400 MHz, Chloroform-*d*) δ 8.12 (d, J=1.4Hz, 1H), 7.71 (dd, J=8.7, 2.0Hz, 1H), 7.74 (d, J=8.5Hz, 1H), 4.97 (s, 2H), 4.83 (s, 2H).
^{13}C NMR (101 MHz, Chloroform-*d*) δ 142.37, 141.73, 140.87, 132.64, 124.27, 92.24, 81.18, 63.23.

4-(Hydroxymethyl)phenyl neopentyl sulfate 3.32

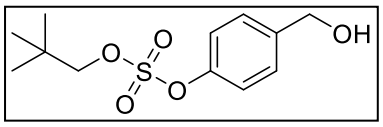

4-formylphenyl neopentyl sulfate **3.27** (1.06g, 3.89mmol, 1 equiv.) was dissolved in 12mL dry MeOH under inert atmosphere and the solution cooled to 0°C. $NaBH_4$ (293mg, 7.79mmol, 2 equiv.) was added in portions and the reaction stirred at 0°C for 1.5h. Upon completion the reaction was quenched by careful addition of water and the solvent was removed *in vacuo*. The crude was portioned between EtOAC and brine. The organic phase was dried over $MgSO_4$ and the solvent removed *in vacuo*, affording the title compound **3.32** in a yield of 68%.

^{1}H NMR (400 MHz, Chloroform-*d*) δ 7.41 (d, J=8.4Hz, 2H), 7.29 (d, J=8.6Hz, 2H), 4.70, (s, 2H), 4.09 (s, 2H), 1.00 (s, 9H).
^{13}C NMR (101 MHz, Chloroform-*d*) δ 149.66, 140.20, 128.44, 121.27, 83.61, 64.50, 32.08, 26.09.

2,6-Difluoro-4-(hydroxymethyl)phenyl neopentyl sulfate 3.33

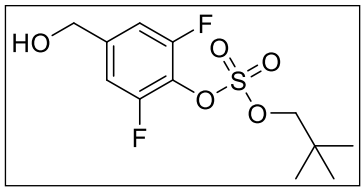

2,6-difluoro-4-formylphenyl neopentyl sulfate **3.28** (150mg, 486μmol, 1 equiv.) was dissolved in 5mL dry MeOH under inert atmosphere, the solution cooled to 0°C and $NaBH_4$ (22mg, 584μmol, 1.2 equiv.) was added in 2 portions. The reaction was stirred for 2h before being quenched by the addition of water and the reaction was extracted with EtOAc. The organic phase was dried over $MgSO_4$ and the solvent removed *in vacuo*. The crude was purified by FCC, affording the title compound **3.33** in a yield of 81%.

^{1}H NMR (400 MHz, Chloroform-*d*) δ 7.12 – 7.04 (m, 2H), 4.72 (d, *J* = 0.8 Hz, 3H), 4.25 (s, 3H), 1.06 (s, 11H).
^{13}C NMR (101 MHz, Chloroform-*d*) δ 155.42 (dd, *J* = 254.4, 3.4 Hz), 142.16 (t, *J* = 7.8 Hz), 125.69 (d, *J* = 15.8 Hz), 110.26 (d, *J* = 22.9 Hz), 84.38, 77.34, 63.51 (t, *J* = 1.7 Hz), 31.92, 25.86.

4-(Hydroxymethyl)phenyl (2,2,2-trichloroethyl) sulfate 3.34

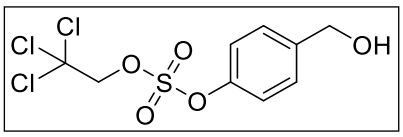

4-formylphenyl (2,2,2-trichloroethyl) sulfate **3.29** (506mg, 1.51mmol, 1 equiv.) was dissolved in 7.5mL dry MeOH under inert atmosphere and the solution cooled to 0°C. $NaBH_4$ (114mg, 3.02mmol, 2 equiv.) was added in portions, after which the reaction was allowed to reach rt and stirred for an additional 2.5h. The reaction was quenched by the addition of water and EtOAc. The aqueous phase was extracted with 3x EtOAc and the combined organic phase washed with brine, dried over $MgSO_4$ and the solvent removed *in vacuo*, affording the title compound **3.34** in a yield of 91%.

^{1}H NMR (400 MHz, Chloroform-*d*) δ 7.44 (d, J=8.6Hz, 2H), 7.35 d, J=8.6Hz, 2H), 4.83 (s, 2H), 4.73 (s, 2H).

^{13}C NMR (101 MHz, Chloroform-*d*) δ 149.45, 140.89, 128.58, 121.32, 92.49, 80.53, 64.40.

2-Fluoro-4-(hydroxymethyl)phenyl (2,2,2-trichloroethyl) sulfate 3.35

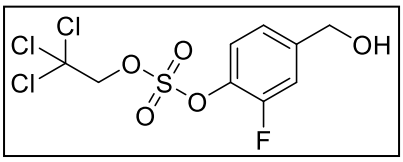

2-fluoro-4-formylphenyl (2,2,2-trichloroethyl) sulfate **3.30** (848mg, 2.41mmol, 1 equiv.) was dissolved in 12mL dry MeOH under inert atmosphere and the solution cooled to 0°C. $NaBH_4$ (183mg, 4.82mmol, 2 equiv.) was added in portions, after which the reaction was allowed to reach rt. Upon completion, the reaction was quenched by the addition of water and the reaction extracted with EtOAc and the organic phase washed with brine. The organic phase was dried over $MgSO_4$ and the solvent removed in *vacuo*, affording the title compound **3.35** in a yield of 88%.

^{1}H NMR (400 MHz, Chloroform-*d*) δ 7.45 (t, J=8.0Hz, 1H), 7.32-7.27 (m, 1H), 7.21-7.16 (m, 1H), 491 (s, 2H) 4.72 (s, 2H)
^{13}C NMR (101 MHz, Chloroform-*d*) δ 153.95 (d, J=252.5Hz), 143.09 (d, J=6.3Hz), 123.98, 122.86 (d, J=3.6Hz), 115.61 (d, J=18.9Hz), 92.38, 80.73 (d, J=2.8Hz), 68.12, 63.85.

2,6-Difluoro-4-((((4-methyl-2-oxo-2H-chromen-7-yl)carbamoyl)oxy)methyl)phenyl neopentyl sulfate 3.36

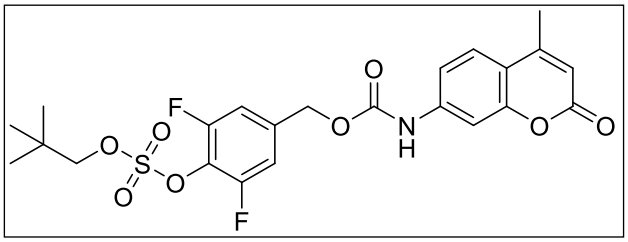

7-amino-4-methylcoumarin (81mg, 0.50mmol, 1.04 equiv.) and triphosgene (72mg, 0.24mmol, 0.5 equiv.) were refluxed in 18mL dry toluene under inert atmosphere for 2h. The solvent was removed *in vacuo* and the crude was dispersed in 18mL dry THF. 2,6-Difluoro-4-(hydroxymethyl)phenyl neopentyl sulfate (**3.33**) (150mg, 0.48mmol, 1 equiv.) and DBTDL (31mg, 48μmol, 0.1 equiv.) were added and the reaction waas stirred at rt for 72h. Upon completion, the solvent was removed and the crude purified by preparative HPLC, affording the title compound **3.36** in a yield of 10%.

^{1}H NMR (400 MHz, DMSO-d_6) δ 10.37 (s, 1H), 7.71 (d, J = 8.7 Hz, 1H), 7.56 (d, J = 2.1 Hz, 1H), 7.55 – 7.47 (m, 2H), 7.42 (dd, J = 8.6, 2.1 Hz, 1H), 6.25 (s, 1H), 5.23 (s, 2H), 4.31 (s, 2H), 2.39 (s, 3H), 0.98 (s, 9H).
^{13}C NMR (101 MHz, DMSO-d_6) δ 159.98, 155.65, 153.81, 153.15, 152.88, 152.73, 142.43, 138.81, 126.09, 114.43 (d, J = 24.4 Hz), 112.32 (d, J = 22.0 Hz), 112.21, 112.04, 104.55, 84.70, 64.40, 31.62, 25.34, 17.99.
HRMS (ESI) calculated for $[C_{22}H_{21}F_2NO_8S]$ $[M+H]^+$ 512.1185, found 512.1187.

4-((((4-Methyl-2-oxo-2H-chromen-7-yl)carbamoyl)oxy)methyl)phenyl (2,2,2-trichloroethyl) sulfate 3.38

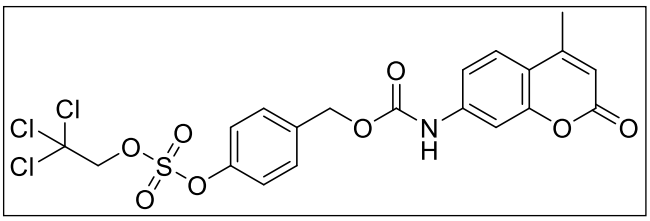

7-amino-4-methylcoumarin (209mg, 1.19mmol, 0.9 equiv.) and triphosgene (182mg, 0.61mmol, 0.47 equiv.) were suspended in 39mL dry toluene under inert atmosphere and the reaction heated to reflux for 2h. The solvent was removed under a stream of nitrogen and the crude dissolved in 39mL dry THF. 4-(hydroxymethyl)phenyl (2,2,2-trichloroethyl) sulfate (**3.34**) (37mg, 1.3mmol, 1 equiv.) and DBTDL (15µL, 0.13mmol, 0.1 equiv.) were added and the reaction was stirred at rt. Upon completion (72h), the reaction was quenched by the addition of water and the solvent removed *in vacuo*. The insoluble crude was washed with 4x water and 3x MeOH, to afford the title compound **3.38** in a yield of 70%.

^{1}H NMR (400 MHz, DMSO-d_6) δ 10.32 (s, 1H), 7.69 (d, J=8.7Hz, 1H), 7.62 (d, J=8.5Hz, 2H) 7.58-7.54 (m, 3H), 7.40 (dd, J=8.5, 2.1, 1H), 6.23 (s, 1H), 5.39 (s, 2H), 5.23 (s, 2H), 2.38 (s, 3H).
^{13}C NMR (101 MHz, DMSO-d_6) δ 160.00, 153.81, 153.15, 153.02, 149.17, 142.57, 136.49, 130.14, 126.05, 121.69, 114.45, 114.25, 111.97, 104.47, 92.91, 80.07, 65.28, 17.99.

2-Fluoro-4-((((4-methyl-2-oxo-2H-chromen-7-yl)carbamoyl)oxy)methyl)phenyl (2,2,2-trichloroethyl) sulfate 3.39

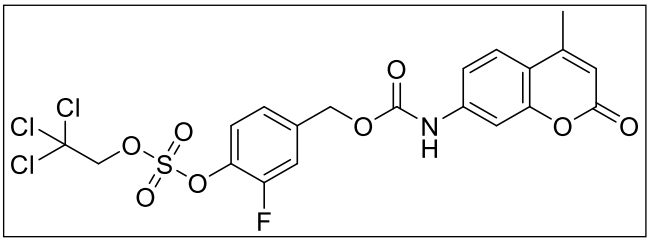

7-amino-4-methylcoumarin (199mg, 1.13mmol, 1.04 equiv.) and triphosgene (172mg, 0.58mmol, 0.53 equiv.) were refluxed in 40mL dry toluene under inert atmosphere for 2h. The solvent was removed under a stream of nitrogen and the crude dissolved in 40mL dry THF. 2-fluoro-4-(hydroxymethyl)phenyl (2,2,2-trichloroethyl) sulfate **3.35** (385mg, 1.09mmol, 1 equiv.) and DBTDL (69µL, 0.12mmol, 0.1 equiv.) were added and the reaction was stirred at rt. Upon completion (72h), the reaction was quenched by the addition of water and the solvent removed *in vacuo*. The insoluble crude was washed with 10x DCM and 8x ACN, affording the title compound **3.39** in a yield of 79%.

^{1}H NMR (400 MHz, DMSO-d_6) δ 10.36 (s, 1H), 7.79-7.68 (m, 2H), 7.67-7.60 (m, 1H), 7.43 (m, 2H), 6.25 (s, 1H), 5.43 (s, 2H) 5.24, (s, 2H), 2.39 (s, 3H).
^{13}C NMR (101 MHz, DMSO-d_6) δ 160.21, 154.03, 153.23 (D, J=27.9Hz), 142.71, 139.16, 126.29, 125.20, 124.25, 117.26 (d, J=18.8Hz), 114.61 (d, J=21.7Hz) 112.23, 104.73, 92.96, 80.60, 64.95, 18.20.

4-((((4-Methyl-2-oxo-2H-chromen-7-yl)carbamoyl)oxy)methyl)-2-nitrophenyl (2,2,2-trichloroethyl) sulfate 3.40

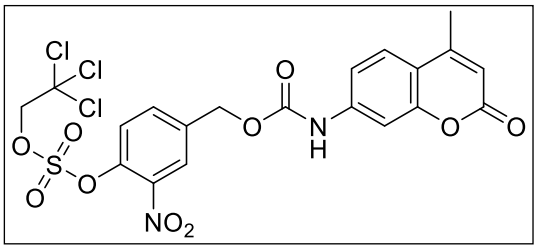

7-amino-4-methylcoumarin (82mg, 467µmol, 1 equiv.) and triphosgene (66mg, 223µmol, 0.47 equiv.) was refluxed in 15mL dry toluene under inert atmosphere for 1.5h, whereupon the solvent was removed *in vauo*. The crude was dissolved in 15mL dry THF followed by the addition of 4-(hydroxymethyl)-2-nitrophenyl (2,2,2-trichloroethyl) sulfate **3.31** (179mg, 0.47mmol, 1 equiv.) and DBTDL (5µL, 47µmol, 0.1 equiv.) and the reaction was stirred a rt for 120h. Upon completion, the solvent was removed and the insoluble crude washed with water, 6x MeOH and ACN, affording the title compound **3.40** in a yield of 57%.

^{1}H NMR (400 MHz, DMSO-d_6) δ 10.39 (s, 1H), 8.35 (d, J=2.0Hz, 1H), 8.00 (dd, J=8.6, 2.1 Hz, 1H), 7.92 (d, J=8.5Hz, 1H), 7.70 (d, J=8.7Hz, 1H), 7.55 (d, J=2.0Hz, 1H), 7.41 (dd, J=8.9, 2.2Hz, 1H), 6.24 (s, 1H), 5.48 (s, 2H), 5.34 (s, 2H), 2.39 (s, 3H).
^{13}C NMR (101 MHz, DMSO-d_6) δ 159.98, 153.80, 153.15, 152.80, 142.43, 141.54, 140.23, 138.45, 134.92, 126.09, 125.75, 124.49, 114.55, 114.31, 112.04, 104.56, 92.65, 80.65, 64.28, 17.99.

Ammonium 4-((((4-methyl-2-oxo-2H-chromen-7-yl)carbamoyl)oxy)methyl)phenyl sulfate 3.41

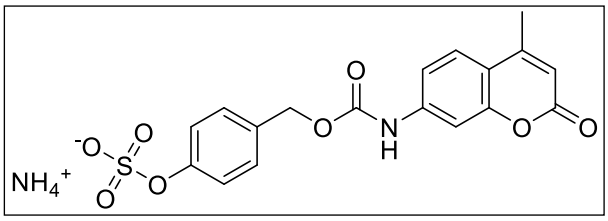

Zinc (174mg, 2.66mmol, 6.66 equiv.), 4-((((4-methyl-2-oxo-2H-chromen-7yl)carbamoyl)oxy)methyl)phenyl (2,2,2-trichloroethyl) sulfate (**3.38**) (214mg, 0.40mmol, 1 equiv.) and NH_4HCO_2 (150mg, 2.36mmol, 5.95 equiv.) were suspended in dry MeOH under inert atmosphere. The suspension was stirred at rt and upon completion (40h), as determined by UPLC-MS, the reaction was filtered over celite and washed 8x with MeOH. The filtrate was concentrated *in vacuo* and the crude purified by preparative HPLC, affording the title compound **3.41** in a yield of 13%.

^{1}H NMR (400 MHz, DMSO-d_6) δ δ 10.26 (s,1H), 7.69 (d, J=8.7Hz, 1H), 7.55 (d, J=1.9Hz, 1H), 7.41 (dd, J=8.7, 2.1Hz, 1H), 7.36 (d, J=8.4Hz, 2H), 7.21-7-16 (m, 2H) 6.23 (s, 1H), 5.12 (s,2H), 2.38 (s, 3H).
^{13}C NMR (101 MHz, DMSO-d_6) δ 160.04, 153.83, 153.64, 153.18, 142.77, 130.48, 129.64, 129.35, 126.04, 120.38, 114.34, 114.23, 111.86, 104.38, 66.15, 18.00.
HRMS (ESI) calculated for $[C_{18}H_{15}NO_8S]$ $[M-H]^-$ 404.0446, found 404.0440

Ammonium 2-fluoro-4-((((4-methyl-2-oxo-2H-chromen-7-yl)carbamoyl) oxy) methyl) phenyl sulfate 3.42

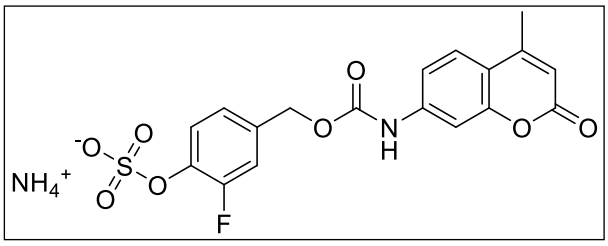

Zinc (115mg, 1.76mmol, 4.6 equiv.), 2-fluoro-4-((((4-methyl-2-oxo-2H-chromen -7-yl)carbamoyl)o xy)methyl) phenyl (2,2,2-trichloroethyl) sulfate (**3.39**) (207mg, 0.37mmol, 1 equiv.) and NH_4HCO_2 (165mg, 2.61mmol, 7 equiv.) were suspended in 6mL dry MeOH under inert atmosphere. The reaction was stirred at rt and on completion (96h), the crude was filtered and washed 10x with ACN. The crude was purified by preparative HPLC, affording the title compound (**3.42**) in a yield of 19%.

^{1}H NMR (400 MHz, DMSO-d_6) δ 10.29 (s, 1H), 7.69 (d, J=8.7Hz, 1H), 5.55 (d, J=2.0Hz, 1H), 7.51 (t, J=8.4Hz, 1H), 7.40 (dd, J= 8.4, 2.1Hz, 1H), 7.30 (dd, J=11.3, 2.0 Hz, 1H), 7.18 (dd, J=8.7, 2.1 Hz, 1H), 6.23 (d, J=1.4Hz, 1H) 5.12 (s, 2H), 2.38 (s, 3H).
^{13}C NMR (101 MHz, DMSO-d_6) δ 160.06, 153.83, 153.13 (d, J= 15.0Hz), 142.68, 132.08 (d, J=11.3Hz), 126.06, 124.17 (d, J=3.5Hz) 123.04, 116.13 (d, J=19.5Hz) 114.33 (d, =13.6Hz), 111.92, 104.44, 65.49, 18.00.
HRMS (ESI) calculated for [C18H14FNO8S] $[M+H]^+$ 424.0497, found 424.0496

Ammonium 2,6-difluoro-4-((((4-methyl-2-oxo-2H-chromen-7-yl)carbamoyl)oxy) methyl) phenyl sulfate 3.44

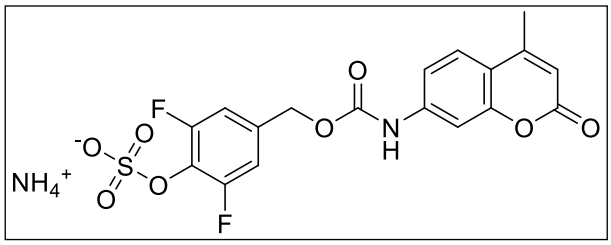

2,6-difluoro-4-((((4-methyl-2-oxo-2H ch-romen-7-yl)carbamoyl) oxy)methyl)phenyl neo-pentyl sulfate **3.36** (10mg, 20μmol, 1 equiv.) was dissolved in 6mL DMF and 2mL 5M aq. NH_4OAc under inert atmosphere. The reaction was heated to 70°C for 72h. The solvent was removed under a stream of nitrogen and the crude purified by preparative HPLC, affording compound **3.44** in a yield of 5%.

UPLC MS (ESI) calculated for $[C_{18}H_{12}F_2NO_8S]$ $[M-H]^-$ m/z 440.0, found m/z 440.2
UPLC MS (ESI) calculated for $[C_{18}H_{13}F_2NO_8S]$ $[M+H]^+$ m/z 442.0, found m/z 442.0

Ammonium 4-((((4-methyl-2-oxo-2H-chromen-7-yl)carbamoyl)oxy)methyl)-2-nitrophenyl sulfate 3.43

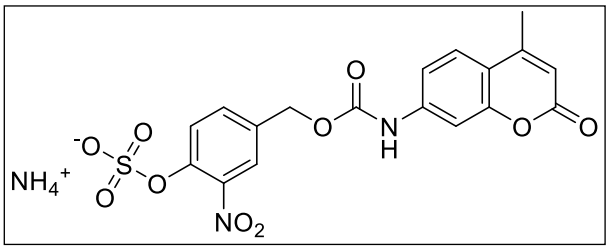

7-amino-4-methylcoumarin (66mg, 0.38mmol, 1.2 equiv.) and triphosgene (46mg, 0.16mmolm, 0.5 equiv.) were dissolved in 15mL dry toluene under inert atmosphere and the reaction was refluxed for 2h. The solvent was removed *in vacuo* and the crude dissolved in dry THF. 4-(Hydroxymethyl)-2-nitrophenyl neopentyl sulfate **3.37** (100mg, 0.31mmol, 1 equiv.) and DBTDL (20mg, 31μmol, 0.1 equiv.) was added and the reaction stirred at rt for 72h. Upon completion, the solvent was removed under a stream of nitrogen and the crude dissolved in 2mL DMF and 2mL 5M NH_4OAc under inert atmosphere. The reaction was stirred at rt for 24h and the crude purified by preparative HPLC, affording the title compound **3.43** in a yield of 1% over 2 steps.

HRMS (ESI) calculated for $[C_{18}H_{14}N_2O_{10}S]$ $[M-H]^-$ 449.0296, found 449.0305.

Determination of concentration-fluorescence range of AMC

AMC samples were prepared in a concentration range of 3.125nM-2.00µM in a series of 13. The samples were added to a black microtiter plate with 96 wells. The samples were added the relevant amount of sulfatase from *Helix pomatia* (0.3U/mL) in NaOAc buffer (0.1M, pH 5.0), to mimic conditions during sulfatase assay. Total volume was 200µL with 5%DMSO in sodium acetate buffer (0.1M, pH 5.0). All samples were prepared in triplicate and fluorescence was measured with λ_{ex} 387nm and at λ_{em} 470nm on an Infinite M200 PRO Tecan instrument plate reader. Linear curve can be seen below in.

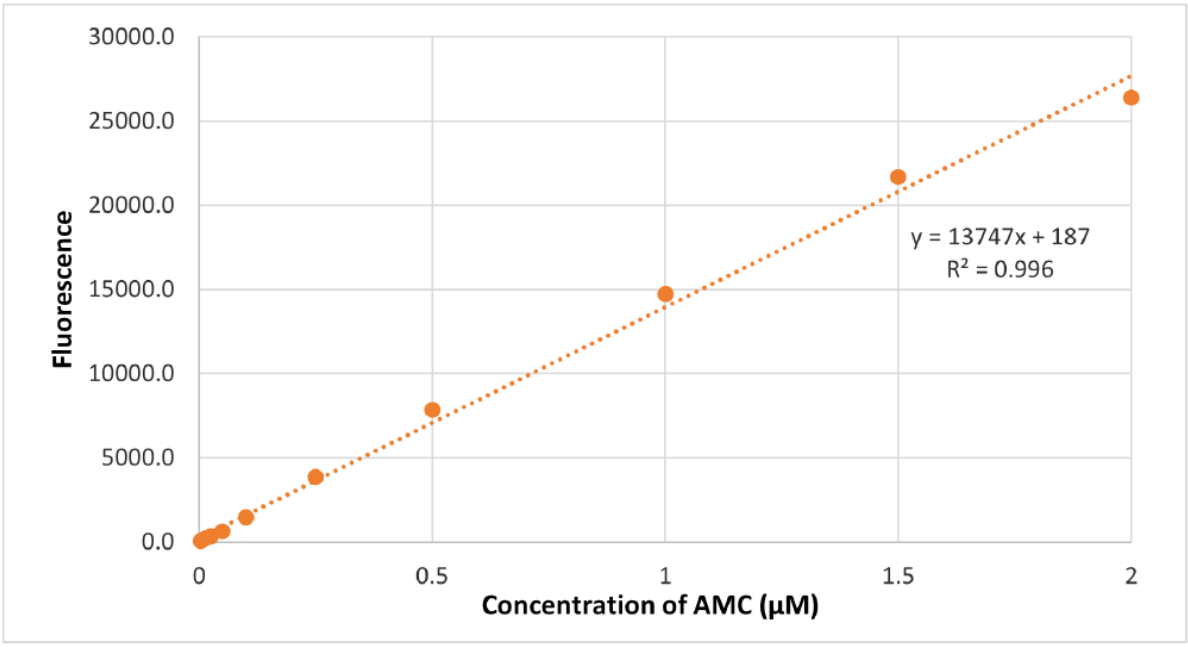

Figure 3.17. Concentration-fluorescence intensity curve of AMC in the concentration range of 3.125nM-2.00µM. AMC was excited by irradiation with λex 387nm and fluorescence was recorded at λem 470nm.

Determination of concentration-absorbance range of Pnp-sulfate

The enzyme activity was validated using potassium Pnp-sulfate. Absorbance of Pnp and Pnp-sulfate was measured and a concentration-absorbance curve was recorded at λ_{abs} 320nm in NaOAc buffer (0.1M, pH 5.0), with 5% DMSO at a concentration range of 0.98µM - 625µM. The results were recorded in triplicate in a transparent microtiter plate with 96 wells. Final volume was 200µL and samples were measured on an Infinite M200 PRO Tecan instrument plate reader. Results are reported in Figure 3.18.

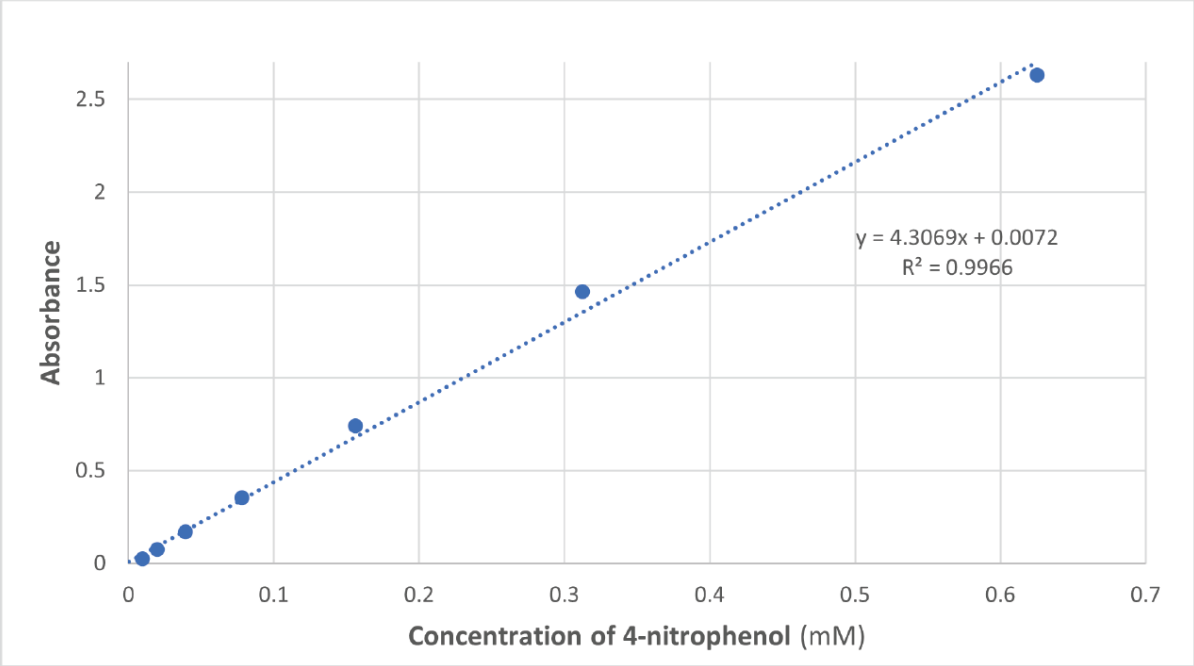

Figure 3.18. Concentration-absorbance curve for Pnp at a concentration range of 0.98μM - 625μM (λ_{abs} 320nm).

Enzyme activity validation

Lyophilized Sulfatase (*Helix pomatia*, EC 3.1.6.1, purchased from Sigma Aldrich) was prepared as a 0.3 U/mL stock in NaOAc buffer (0.1M, pH 5.0). Pnp-sulfate was prepared in 11.89mM in DMSO. 13μL of the sulfatase stock was added to a well containing 182μL NaOAc buffer and 5μL Pnp-sulfate stock. For the control experiments, 13μL NaOAc buffer was added instead. Total volume was 200μL and the experiments were carried out in a transparent microtiter plate with 96 wells. The absorbance was measured at λ 320nm over 3h at 37°C under shaking on an Infinite M200 PRO Tecan instrument plate reader. Measurements were recorded at 2min intervals. The results are reported in Figure 3.19.

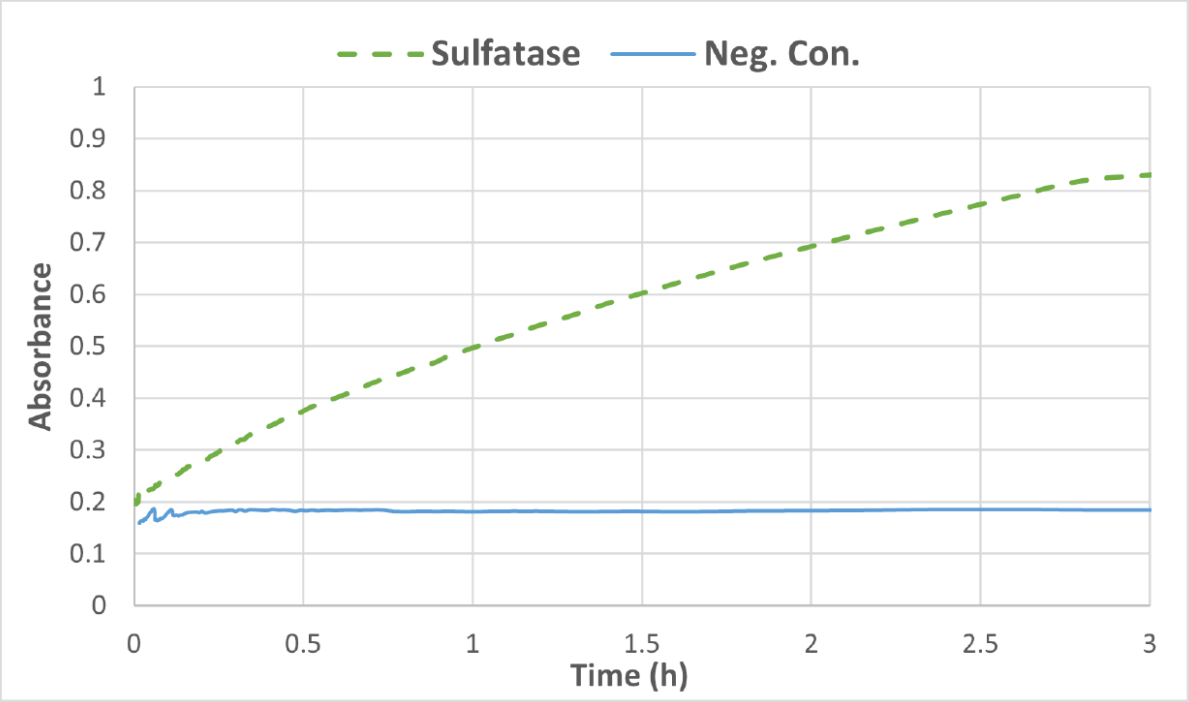

Figure 3.19. Sulfatase validation assay recorded over 3h.

Probe pH stability assay

The probes (**3.40-3.43**) were dissolved in DMSO to make a stock of 36μM. The solution was added to black microtiter plate with 96 wells to which 190μL NaOAc buffer had previously been added at pH 4.5, 5.0 and 5.5. The stability was recorded by heating to 37°C and shaking between measurements over 3h. All assays were carried out in triplicate on an Infinite M200 PRO Tecan instrument plate reader.

Sulfatase assay

For the enzyme assay, the substrates (**3.40**-**3.43**) were prepared in a 36μM solutions in DMSO. Lyophilized sulfatase (*Helix pomatia*, EC 3.1.6.1, purchased from Sigma Aldrich) was prepared in a 3U/mL NaOAc buffer (0.1M, pH 5.0). 10μL substrate stock, 180μL NaOAc buffer (0.1M, pH 5.0) and 10μL enzyme stock was added to black microtiter plate with 96 wells. The results were recorded at 37°C in 1min intervals over 3h. All assays were carried out in triplicate on an Infinite M200 PRO Tecan instrument plate reader.

Part III

4-(1-Hydroxy-3-(trimethylsilyl)prop-2-yn-1-yl)-2-nitrophenol 3.45

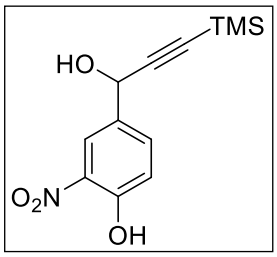

TMS-acetylene (0.94mL, 6.58mmol, 2.20 equiv.) was dissolved in dry THF under inert atmosphere and the solution cooled to 0°C. 1.5M MeLi ·LiBr in Et_2O (4.4mL, 6.58mmol, 2.20 equiv.) was added and the solution was stirred at rt for 4h. The reaction was again cooled to 0°C and 4-hydroxy-3-nitrobenzaldehyde (500mg, 2.99mmol, 1 equiv.) was added portion-wise. Upon completion (1h), the reaction was quenched by the addition of sat. aq. NH_4Cl and the reaction was extracted with EtOAc. The organic phase was washed with brine, dried over $MgSO_4$ and the solvent removed *in vacuo*. The crude was purified by FCC, affording compound **3.44** in a yield of 47%.

^{1}H NMR (400 MHz, Chloroform-*d*) δ 10.63 (s, 1H), 8.40 – 8.26 (m, 1H), 7.79 (ddt, *J* = 8.7, 2.2, 0.5 Hz, 1H), 7.20 (d, *J* = 8.7 Hz, 1H), 5.46 (d, *J* = 0.7 Hz, 1H), 0.24 (s, 9H).
^{13}C NMR (101 MHz, Chloroform-*d*) δ 154.97, 136.06, 133.17, 132.91, 123.19, 120.32, 103.71, 92.97, 63.47, -0.28.

2,6-Difluoro-4-(1-hydroxy-3-(trimethylsilyl)prop-2-yn-1-yl)phenol 3.47

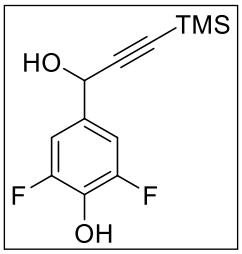

TMS-acetylene (4.10g, 41.73mmol, 2.2 equiv.) was dissolved in 100mL dry THF under inert atmosphere and the solution cooled to -78°C, followed by the slow addition of 2.2M n-BuLi in hexane (18mL, 39.84mmol, 2.1 equiv.). The reaction was allowed to reach -40°C for 1h, before being cooled to -78°C and a solution of 3,5-difluoro-4-hydroxybenzaldehyde (3.00g, 18.97mmol, 1 equiv.) in 100mL dry THF was added dropwise. The reaction was stirred at -78°C for 4h before being quenched by the addition of sat. aq. NH_4Cl. The reaction was extracted with Et_2O, the organic phase dried over Na_2SO_4 and the solvent removed *in vacuo*. The crude was purified by dry column chromatography, to afford the title compound **3.47** in a quantitative yield.

^{1}H NMR (400 MHz, DMSO) δ 10.21 (s, 1H), 7.13 – 7.00 (m, 2H), 6.14 (d, *J* = 6.2 Hz, 1H), 5.30 (d, *J* = 6.2 Hz, 1H), 0.16 (s, 9H).
^{13}C NMR (101 MHz, DMSO) δ 152.38 (dd, *J* = 242.0, 7.0 Hz), 151.17 (d, *J* = 7.1 Hz), 133.40, 133.24, 110.29 (d, *J* = 7.3 Hz), 110.14 (d, *J* = 7.3 Hz), 107.48, 89.52, 62.20, 0.27.

4-(1-Hydroxyprop-2-yn-1-yl)-2-nitrophenol 3.48

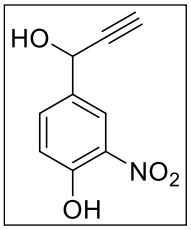

Compound **2.48** was collected during purification of compound **3.45** in a yield of 30%.

^{1}H NMR (400 MHz, Chloroform-*d*) δ 10.64 (s, 1H), 8.33 (dd, *J* = 2.3, 0.7 Hz, 1H), 7.81 (dd, *J* = 8.7, 2.3 Hz, 1H), 7.22 (d, *J* = 8.7 Hz, 1H), 5.49 (dt, *J* = 2.2, 0.7 Hz, 1H).
^{13}C NMR (101 MHz, Chloroform-*d*) δ 155.08, 135.95, 132.50, 123.11, 120.45, 82.38, 75.87, 62.94.

2-Fluoro-4-(1-hydroxyprop-2-yn-1-yl)phenol 3.49

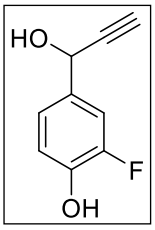

TMS-acetylene (1.54g, 15.70mmol, 2.2 equiv.) was dissolved in 14mL dry THF under inert atmosphere and the solution cooled to 0°C. 1.5M MeLi · LiBr in Et_2O (10.5mL, 15.70mmol, 2.2 equiv.) was added dropwise and the reaction stirred at rt for 4h before being cooled to 0°C. 3-Fluoro-4-hydroxybenzaldehyde (1.00g, 7.14mmol, 1 equiv.) was added in portions. The reaction was stirred for 1h, before being quenched by the addition of sat. aq. NH_4Cl and the reaction was extracted with EtOAc. The organic phase was washed with brine, dried over $MgSO_4$ and the solvent removed *in vacuo*. The crude was dissolved in dry 14mL THF and 1M TBAF in THF (8.57mL, 8.57mmol, 1.2 equiv.) was added dropwise. Upon completion, the solvent was removed *in vacuo* and the crude purified by FCC, affording the title compound **3.49** in a yield of 41%.

^{1}H NMR (400 MHz, DMSO-d_6) δ 9.83 (s, 1H), 7.22 – 7.14 (m, 1H), 7.07 (dd, *J* = 8.3, 2.1 Hz, 1H), 6.98 – 6.86 (m, 1H), 5.96 (d, *J* = 6.0 Hz, 1H), 5.24 (dd, *J* = 6.0, 2.2 Hz, 1H), 3.48 (d, *J* = 2.2 Hz, 1H).
^{13}C NMR (101 MHz, DMSO-d_6) δ 150.59 (d, *J* = 240.6 Hz), 144.24 (d, *J* = 12.1 Hz), 133.46 (d, *J* = 5.3 Hz), 122.59, 117.33 (d, *J* = 3.1 Hz), 114.14 (d, *J* = 19.0 Hz), 85.39, 75.72, 61.53.

2,6-Difluoro-4-(1-hydroxyprop-2-yn-1-yl)phenol 3.50

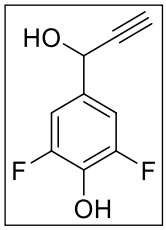

2,6-difluoro-4-(1-hydroxy-3-(trimethylsilyl)prop-2-yn-1-yl) **3.47** phenol (4.86g, 18.97mmol, 1 equiv.) was dissolved in 7mL THF and a solution of TBAF hydrate (5.83g, 20.87mmol, 1.1 equiv.) in 21mL THF added. Upon completion (1h), the reaction was quenched by the addition of water and the reaction extracted with 3x EtOAc. The combined organic phase was dried over Na_2SO_4 and the solvent removed *in vacuo*, affording the title compound **3.50** in a quantitative yield.

^{1}H NMR (400 MHz, DMSO) δ 7.03 (ddd, *J* = 7.9, 1.8, 0.6 Hz, 2H), 5.26 – 5.25 (m, 1H), 3.51 (d, *J* = 2.2 Hz, 1H). (crude)
^{13}C NMR (101 MHz, DMSO) δ 152.70 (dd, *J* = 241.5, 7.5 Hz), 134.42 (d, *J* = 16.3 Hz), 132.23, 110.17 (t, *J* = 6.1 Hz), 109.99 (d, *J* = 7.4 Hz), 85.37, 76.42, 61.73 (d, *J* = 2.1 Hz).

***Tert*-butyl (2-(2-azidoethoxy)ethyl)carbamate 3.51**

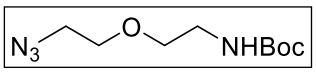

Tert-butyl (2-(2-hydroxyethoxy)ethyl)carbamate (7.00g, 34.1mmol, 1 equiv.) and TEA (4.75mL, 34.10mmol, 1 equiv.) were dissolved in 21mL dry toluene. The reaction was cooled to 0°C and MsCl (3.91g, 34.1mmol 1 equiv.) was added in portions. The reaction was allowed to reach rt and after 10 min, TBAI (12.60g, 34.10mmol, 1 equiv.) was added, followed by the addition of NaN_3 (2.22g, 34.10mmol, 1 equiv.) in 11mL water. The reaction was heated to 70°C and stirred for 4h. The reaction was extracted with EtOAc, the organic phase dried over Na_2SO_4 and the solvent removed *in vacuo*. The crude was purified by dry column chromatography, to afford the title compound **3.51** in a quantitative yield.

^{1}H NMR (400 MHz, $CDCl_3$) δ 4.91 (s, 1H), 3.64 (m, 2H), 3.54 (t, *J* = 5.2 Hz, 2H), 3.37 (m, 2H), 3.32 (q, *J* = 5.2 Hz, 2H), 1.44 (s, 9H).
^{13}C NMR (101 MHz, $CDCl_3$) δ 155.97, 79.34, 70.34, 69.92, 50.67, 40.36, 28.39.

Tert-butyl (2-(2-(4-(hydroxy(4-hydroxy-3-nitrophenyl)methyl)-1H-1,2,3-triazol-1-yl)ethoxy)ethyl)carbamate 3.52

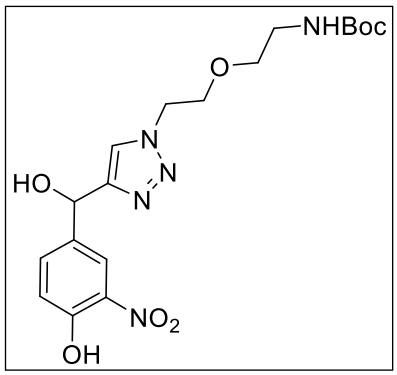

4-(1-Hydroxyprop-2-yn-1-yl)-2-nitrophenol **3.48** (350mg, 1.81mmol, 1 equiv.), *tert*-butyl (2-(2-azidoethoxy)ethyl)carbamate (459mg, 1.99mmol, 1.1 equiv.) and $CuSO_4 \cdot 5H_2O$ (144mg, 0.91mmol, 0.5equiv.) were dissolved in 6mL H_2O:*t*-BuOH 1:1 and the solution degassed with N_2 for 10min, after which sodium ascorbate (160mg, 0.91mmol, 0.5 equiv.) was added. The reaction was stirred at rt under inert atmosphere overnight and the solvent removed *in vacuo*. The crude was purified by FCC, affording the title compound **3.52** in a yield of 58%.

^{1}H NMR (400 MHz, Methanol-d_4) δ 8.19 (dd, *J* = 2.2, 0.7 Hz, 1H), 7.93 (d, *J* = 0.6 Hz, 1H), 7.69 (ddd, *J* = 8.7, 2.3, 0.5 Hz, 1H), 7.16 (d, *J* = 8.7 Hz, 1H), 5.95 (d, *J* = 0.6 Hz, 1H), 4.58 (dd, *J* = 5.6, 4.6 Hz, 2H), 3.85 (dd, *J* = 5.5, 4.7 Hz, 2H), 3.47 (t, *J* = 5.7 Hz, 2H), 3.18 (t, *J* = 5.7 Hz, 2H), 1.44 (s, 9H).
^{13}C NMR (101 MHz, Methanol-d_4) δ 153.52, 150.50, 135.35, 135.02, 134.03, 122.97, 122.43, 119.61, 78.74, 69.64, 68.74, 67.17, 50.10, 39.71, 27.33.

***Tert*-butyl (2-(2-(4-((3-fluoro-4-hydroxyphenyl)(hydroxy)methyl)-1H-1,2,3-triazol-1-yl) ethoxy)ethyl)carbamate 3.53**

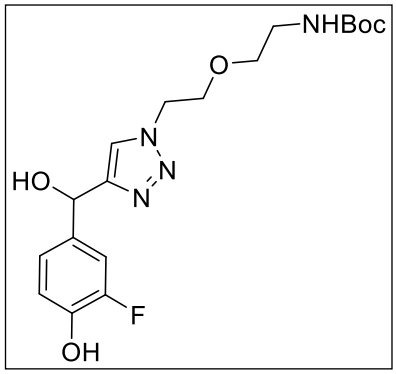

2-Fluoro-4-(1-hydroxyprop-2-yn-1-yl)phenol **3.49** (483mg, 2.91mmol, 1 equiv.), *tert*-butyl (2-(2-azidoethoxy) ethyl) carbamate (736mg, 3.20mmol, 1.1 equiv.) and $CuSO_4 \cdot 5H_2O$ (232mg, 1.45mmol, 0.5 equiv.) were dissolved in 8mL H_2O:*t*-BuOH 1:1 and the solution was degassed with N_2 for 10min, after which sodium ascorbate (256mg, 1.45mmol, 0.5 equiv.) was added. The reaction was stirred at rt under inert atmosphere overnight and the solvent removed *in vacuo*. The crude was purified by FCC, affording the title compound **3.53** in a yield of 78%.

^{1}H NMR (400 MHz, DMSO-d_6) δ 9.71 (d, J = 1.0 Hz, 1H), 7.85 (s, 1H), 7.13 (dd, J = 12.4, 2.0 Hz, 1H), 7.00 – 6.94 (m, 1H), 6.88 (t, J = 8.6 Hz, 1H), 6.77 (t, J = 5.7 Hz, 1H), 5.90 (d, J = 4.6 Hz, 1H), 5.71 (d, J = 4.5 Hz, 1H), 4.53 – 4.37 (m, 2H), 3.76 (t, J = 5.3 Hz, 2H), 3.37 (t, J = 6.1 Hz, 2H), 3.03 (q, J = 6.0 Hz, 2H), 1.38 (s, 9H).
^{13}C NMR (101 MHz, DMSO-d_6) δ 156.05, 151.13 (d, J = 240.0 Hz, 144.10, 136.21, 122.96, 122.80, 117.67, 114.50 (d, J = 18.7 Hz), 78.12, 69.43, 68.87, 67.60, 55.37, 49.70, 28.68.

***Tert*-butyl (2-(2-(4-((3,5-difluoro-4-hydroxyphenyl)(hydroxy)methyl)-1H-1,2,3-triazol-1-yl)ethoxy)ethyl)carbamate 3.54**

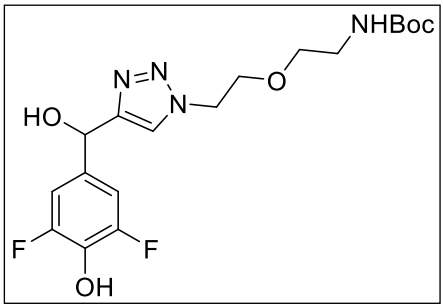

2,6-Difluoro-4-(1-hydroxyprop-2-yn-1-yl)phenol **3.50** (3.49g, 18.95mmol, 1 equiv.) and *tert*-butyl (2-(2-azidoethoxy)ethyl)carbamate (50.02g, 21.97mmol, 1.15 eq.) were dissolved in 45mL water, 90mL THF and 90mL *t*BuOH and the reaction degassed with N_2 for 70min. A solution of $CuSO_4 \cdot 5H_2O$ (237mg, 0.95mmol. 0.05 equiv.) and sodium ascorbate (751mg, 3.79mmol, 0.2 equiv.) in 45mL water was degassed with N_2 for 70min. The solutions were mixed and upon completion (2h), EtOAc was added. The organic phase was washed with sat. aq. $NaHCO_3$ and water, before being dried over $MgSO_4$ and the solvent removed *in vacuo*. The crude was purified by dry column chromatography, affording the title compound **3.54** in a yield of 77%.

^{1}H NMR (400 MHz, MeOD) δ 7.87 (s, 1H), 7.06 – 6.94 (m, 2H), 5.84 (s, 1H), 4.56 (t, J = 5.1 Hz, 2H), 3.85 (t, J = 5.1 Hz, 2H), 3.47 (t, J = 5.6 Hz, 2H), 3.23 – 3.15 (m, 2H), 1.45 (s, 9H).
^{13}C NMR (101 MHz, MeOD) δ 157.08, 152.36 (dd, J = 242.3, 6.8 Hz), 150.77, 134.03 (t, J = 7.1 Hz), 133.13, 122.78, 109.39 (d, J = 7.4 Hz), 109.31 – 109.12 (m), 78.76, 69.65, 68.77, 67.48, 50.02, 39.72, 27.34.

4-((1-(2-(2-((*Tert*-butoxycarbonyl)amino)ethoxy)ethyl)-1H-1,2,3-triazol-4-yl)(hydroxy)methyl)-2-nitrophenyl neopentyl sulfate 3.55

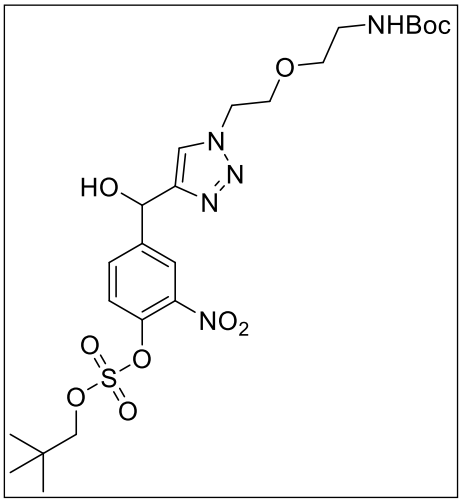

Tert-butyl (2-(2-(4-(hydroxy(4-hydroxy-3-nitrophenyl) methyl)-1H-1,2,3-triazol-1-yl)ethoxy)ethyl) carbamate **3.52** (140mg, 330μmol, 1 equiv.), DMAP (40mg, 330μmol, 1 equiv.) and TEA (96μL, 661μmol, 2 equiv.) were dissolved in 10mL dry THF under inert atmosphere. To the reaction neopentyl sulfurochloridate (123mg, 661μmol, 2 equiv.) was added dropwise and the reaction was stirred at rt for 2h. The reaction was then quenched by the addition of sat. aq. $NaHCO_3$. The reaction was extracted with EtOAc and the organic phase washed with brine. The organic phase was dried over $MgSO_4$ and the solvent removed *in vacuo*. The crude was purified by FCC, affording the title compound **3.55** in a yield of 62%.

^{1}H NMR (400 MHz, Methanol-d_4) δ 8.20 (dd, J = 2.2, 0.7 Hz, 1H), 7.98 – 7.93 (m, 1H), 7.87 (ddd, J = 8.6, 2.2, 0.7 Hz, 1H), 7.65 (d, J = 8.5 Hz, 1H), 6.07 (d, J = 0.7 Hz, 1H), 5.51 (s, 2H), 4.57 (dd, J = 5.7, 4.5 Hz, 2H), 4.24 (s, 2H), 3.94 – 3.71 (m, 2H), 3.47 (t, J = 5.6 Hz, 2H), 3.18 (t, J = 5.7 Hz, 2H), 1.44 (s, 9H), 1.03 (s, 9H).
^{13}C NMR (101 MHz, Methanol-d_4) δ 157.05, 149.95, 144.33, 142.26, 140.71, 132.26, 123.73, 123.56, 123.09, 84.43, 78.75, 69.64, 68.72, 66.89, 53.40, 50.08, 39.72, 31.38, 27.36, 24.71.

4-((1-(2-(2-((*Tert*-butoxycarbonyl)amino)ethoxy)ethyl)-1H-1,2,3-triazol-4-yl)(hydroxy)methyl)-2-fluorophenyl neopentyl sulfate 3.56

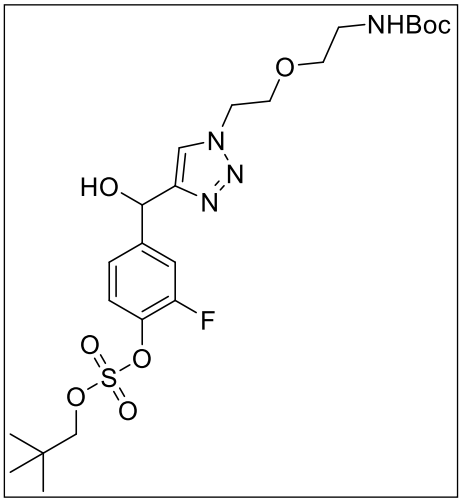

Tert-butyl (2-(2-(4-((3,5-difluoro-4-hydroxyphenyl) (hydroxy) methyl)-1H-1,2,3-triazol-1-yl)ethoxy)ethyl) carbamate **3.53** (200mg, 0.50mmol, 1 equiv.), DMAP (62mg, 0.50mmol, 1 equiv.) and DBU (153μL, 1.01mmol, 2 equiv.) were dissolved in 10mL dry THF under inert atmosphere and to the solution neopentyl sulfurochloridate (188mg, 1.01mmol, 2 equiv.) was added dropwise. The reaction was stirred overnight at rt. The reaction was then quenched by the addition of sat. aq. $NaHCO_3$. The reaction was extracted with EtOAc and the organic phase washed with brine, dried over $MgSO_4$ and the solvent removed *in vacuo*. The crude was purified by FCC, affording the title compound **3.56** in a yield of 50%.

^{1}H NMR (400 MHz, Methanol-d_4) δ 7.91 (s, 1H), 7.52 – 7.41 (m, 2H), 7.34 (ddt, J = 8.5, 1.9, 0.8 Hz, 1H), 5.98 (s, 1H), 4.56 (dd, J = 5.7, 4.5 Hz, 2H), 4.21 (s, 2H), 3.84 (t, J = 5.1 Hz, 2H), 3.46 (t, J = 5.6 Hz, 2H), 3.18 (t, J = 5.6 Hz, 2H), 1.45 (s, 9H), 1.02 (s, 9H).

^{13}C NMR (101 MHz, Methanol-d_4) δ 157.04, 153.76 (d, J = 250.8 Hz), 150.39, 144.93 (d, J = 6.0 Hz), 136.44 (d, J = 12.8 Hz), 123.42, 122.92, 122.64 (d, J = 3.5 Hz), 114.91 (d, J = 19.6 Hz), 83.71, 78.75, 69.63, 68.74, 67.36, 50.05, 39.72, 31.36, 27.38, 24.77.

4-((1-(2-(2-((*Tert*-butoxycarbonyl)amino)ethoxy)ethyl)-1H-1,2,3-triazol-4-yl)(hydroxy)methyl)-2,6-difluorophenyl neopentyl sulfate 3.57

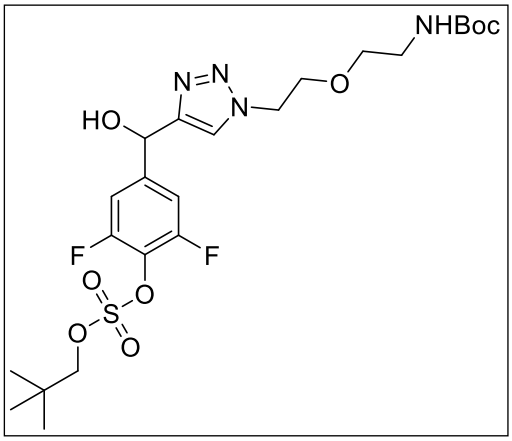

Tert-butyl (2-(2-(4-((3,5-difluoro-4-hydroxyphenyl) (hydroxy)methyl) -1H-1,2,3-triazol-1-yl)ethoxy)ethyl)carbamate **3.54** (0.99g, 2.39mmol, 1 equiv.) and DMAP (292mg, 2.39mmol, 1 equiv.) were dissolved in 24mL dry THF under inert atmosphere, followed by the dropwise addition of neopentyl sulfurochloridate (892mg, 4.78mmol, 2 equiv.) and DBU (364µL, 2.39mmol, 1 equiv.). The reaction was stirred for 75min at rt and quenched by the addition of sat. aq. $NaHCO_3$. The reaction was extracted with EtOAc and the organic phase washed with sat. aq. $NaHCO_3$, dried over $MgSO_4$ and the solvent removed *in vacuo*. The crude was purified dry column chromatography, affording the title compound **3.57** in a yield of 54%.

^{1}H NMR (400 MHz, DMSO) δ 7.97 (s, 1H), 7.43 – 7.34 (m, 2H), 6.77 (d, J = 6.0 Hz, 1H), 5.89 (s, 1H), 4.48 (d, J = 5.3 Hz, 2H), 4.30 (s, 2H), 3.77 (t, J = 5.3 Hz, 2H), 3.38 (d, J = 6.0 Hz, 2H), 3.03 (d, J = 6.0 Hz, 2H), 1.37 (s, 9H), 0.98 (s, 9H).
^{13}C NMR (101 MHz, DMSO) δ 156.06, 153.40 (dd, J = 252.6, 3.3 Hz), 150.13, 146.99, 124.80, 123.32, 111.31, 111.12, 85.05, 78.11, 69.45, 68.81, 66.99, 49.83, 32.08, 28.67, 25.81.

Compound 3.58

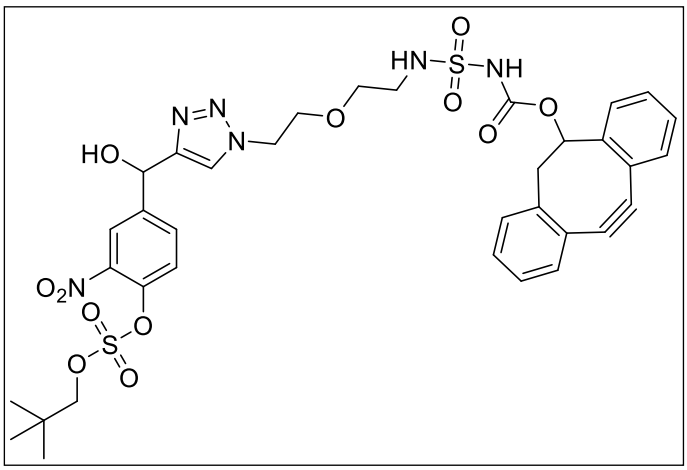

4-((1-(2-(2-((*Tert*-butoxycarbonyl) amino)ethoxy)ethyl)-1H-1,2,3-triazol-4-yl)(hydroxy)methyl)-2,6-difluorophenyl neopentyl sulfate **3.55** (110mg, 192µmol, 1 equiv.) was dissolved in 4M HCl in dioxane and stirred at rt for 45min, before the removal of the solvent *in vacuo*. In a separate flask dibenzo[*a*,*e*]cycloocten-5-ol (DIBO) (42mg, 190µmol, 1 equiv.) and chlorosulfonyl isocyanide (27mg, 190µmol, 1 equiv.) were dissolved in 0.6mL dry DCM under inert atmosphere and the solution stirred at rt for 20min, whereupon the solvent was removed under a stream of N_2. The crude was dissolved in 1.2mL dry THF, followed by the addition of the Boc deprotected crude and TEA

(55µL, 381µmol, 2 equiv.). The reaction was stirred at rt for 1h and upon completion, the solvent was removed *in vacuo*. The crude was purified by FCC, affording the title compound **3.58** in a yield of 48%.

^{1}H NMR (400 MHz, Methanol-d_4) δ 8.17 (ddd, J = 3.0, 2.2, 0.7 Hz, 1H), 7.86 (bs, 1H), 7.79 (ddd, J = 8.6, 2.2, 0.7 Hz, 1H), 7.62 – 7.54 (m, 2H), 7.48 – 7.21 (m, 7H), 5.99 (s, 1H), 5.54 – 5.50 (m, 1H), 5.49 (s, 1H), 4.42 (dd, J = 6.8, 3.3 Hz, 2H), 4.21 (s, 2H), 3.75 – 3.69 (m, 2H), 3.66 (s, 1H), 3.55 – 3.47 (m, 3H), 3.32 (p, J = 1.7 Hz, 2H), 3.28 (ddd, J = 15.3, 2.4, 1.2 Hz, 1H), 3.21 (ddd, J = 6.9, 5.2, 2.0 Hz, 2H), 2.92 – 2.83 (m, 1H), 1.00 (s, 9H).
^{13}C NMR (101 MHz, Methanol-d_4) δ 151.46, 150.84, 150.55, 149.69, 144.11, 142.18, 140.69, 135.92, 132.37, 129.72, 128.08, 127.31, 127.09, 125.96, 123.74, 123.59, 123.49, 123.43, 123.31, 120.98, 112.63, 109.38, 84.42, 77.96, 68.89, 68.69, 66.72, 49.90, 45.33, 42.80, 31.38, 24.73.

Compound 3.59

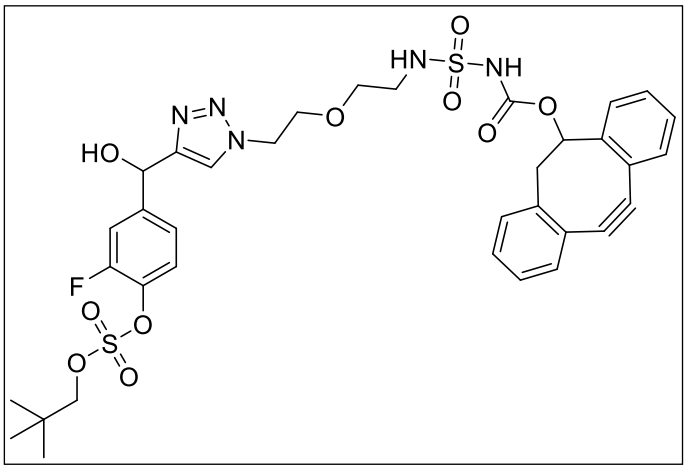

4-((1-(2-(2-((*Tert*-butoxycarbonyl)amino)ethoxy)ethyl)-1H-1,2,3-triazol-4-yl)(hydroxy)methyl)-2,6-difluorophenyl neopentyl sulfate **3.56** (130mg, 238µmol, 1 equiv.) was dissolved in 4M HCl in dioxane and was stirred at rt for 45min, before the removal of the solvent *in vacuo*. In a separate flask, dibenzo[*a*,*e*]cycloocten-5-ol (DIBO) (62mg, 236µmol, 1 equiv.) and chlorosulfonyl isocyanide (33mg, 236µmol, 1 equiv.) were dissolved in 1.0mL dry DCM under inert atmosphere and the solution stirred at rt for 20min, whereupon the solvent was removed under a stream of N_2. The crude was dissolved in 1.6mL dry THF, followed by the addition of the Boc deprotected crude and TEA (68µL, 472µmol, 2 equiv.). The reaction was stirred at rt for 1h and upon completion, the solvent was removed *in vacuo*. The crude was purified by FCC, affording the title compound **2.59** in a yield of 31%

^{1}H NMR (400 MHz, Methanol-d_4) δ 7.83 – 7.77 (m, 1H), 7.58 (dq, J = 7.7, 1.0 Hz, 1H), 7.44 – 7.25 (m, 10H), 5.90 (s, 1H), 5.53 – 5.50 (m, 1H), 5.48 (s, 1H), 4.44 – 4.35 (m, 2H), 4.17 (s, 2H), 3.71 (t, J = 5.1 Hz, 2H), 3.50 (t, J = 5.4 Hz, 2H), 3.34 – 3.28 (m, 1H), 3.26 (dd, J = 2.3, 1.1 Hz, 1H), 3.20 (td, J = 5.3, 1.6 Hz, 2H), 2.86 (dd, J = 15.2, 3.9 Hz, 1H), 0.98 (s, 9H).
^{13}C NMR (101 MHz, Methanol-d_4) δ 153.73 (d, J = 250.7 Hz), 152.49, 151.61, 150.90, 150.57, 150.22, 144.78 (d, J = 6.0 Hz), 136.40 (d, J = 12.8 Hz), 129.71, 128.07, 127.30, 127.08, 125.94, 125.64, 123.51, 123.41, 123.03, 122.66 (d, J= 3.9), 120.99, 115.02, 114.92 (d, J = 19.8 Hz), 112.62, 109.40, 83.71, 77.93, 68.95, 68.73, 67.26, 53.42, 45.34, 42.78, 31.35, 24.76.

Compound 3.60

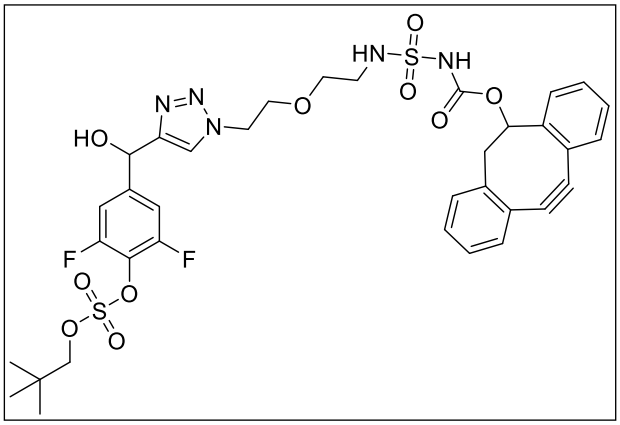

4-((1-(2-(2-((*Tert*-butoxycarbonyl) amino)ethoxy)ethyl)-1H-1,2,3-triazol-4-yl) (hydroxyl) methyl) -2,6-difluorophenyl neopentyl sulfate **3.57** (500mg, 886μmol, 1 equiv.) was dissolved in cooled 4M HCl in dioxane and the reaction was stirred at rt for 30min, before removing the solvent *in vacuo*. In a separate flask, dibenzo[*a*,*e*]cycloocten-5-ol DIBO (205mg, 930μmol, 1.05 equiv.) and chlorosulfonyl isocyanide (132mg, 930μmol, 1 equiv.) were dissolved in 2.7mL dry DCM under inert atmosphere and the reaction stirred for 20min. at rt, before the dropwise addition of TEA (370μL, 2.66mmol, 3 equiv.). The reaction was stirred for 5min. before the addition of the Boc-deprotected linker in 1.7mL dry THF. Upon completion (1h), the solvent was removed *in vacuo* and the crude purified by FCC, affording the title compound **3.60** in a quantitative yield.

^{1}H NMR (400 MHz, MeOD) δ 7.86 (d, *J* = 2.2 Hz, 1H), 7.60 (dq, *J* = 7.7, 1.0 Hz, 1H), 7.47 – 7.27 (m, 6H), 7.29 – 7.21 (m, 2H), 5.90 (s, 1H), 5.53 (t, *J* = 3.9, 2.1 Hz, 1H), 4.46 – 4.42 (m, 2H), 4.25 (s, 2H), 3.74 (t, *J* = 5.1 Hz, 2H), 3.54 (t, *J* = 5.3 Hz, 2H), 3.32 – 3.27 (m, 1H), 3.23 (td, *J* = 5.3, 1.7 Hz, 2H), 2.89 (dd, *J* = 15.2, 3.9 Hz, 1H), 1.03 (s, 9H).
^{13}C NMR (101 MHz, MeOD) δ 155.08 (dd, *J* = 252.9, 3.3 Hz), 151.46, 150.87, 150.56, 149.67, 129.71, 128.04, 127.30, 127.08, 125.94, 125.63, 123.50, 123.46, 123.19 (d, *J* = 1.9 Hz), 121.00, 112.61, 110.36, 110.14 (d, *J* = 3.0 Hz), 109.37, 84.12, 77.95, 68.94, 68.70, 66.92, 49.87, 45.35, 42.76, 31.34, 24.73.

Compound 3.61

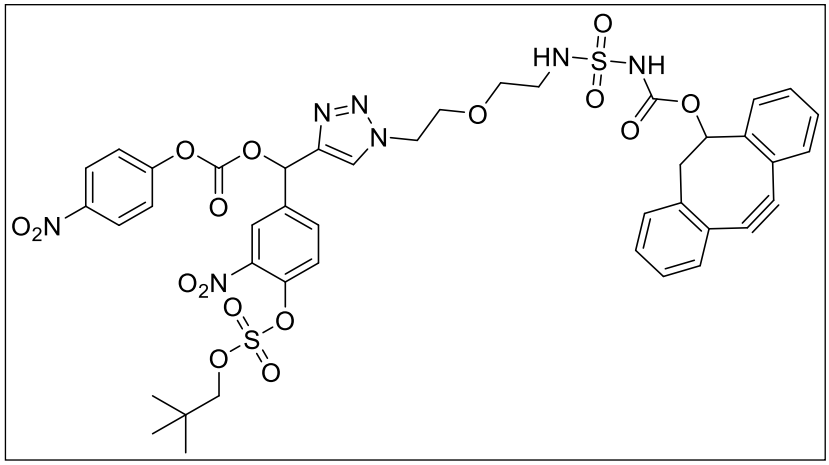

Compound **3.58** (60mg, 75μmol, 1 equiv.) was dissolved in 1mL dry DMF under inert atmosphere and TEA (42μL, 300μmol, 4 equiv.) and bis(4-nitrophenyl) carbonate (69mg, 225μmol, 3 equiv.) were added. The reaction was stirred overnight at rt and upon completion, was acidified by the addition of 1% aq. HCl. The reaction was extracted with EtOAc and the organic phase then washed with sat. aq. $NaHCO_3$ and brine, dried over $MgSO_4$ and the solvent removed *in vacuo*. The crude was purified by FCC, affording the title compound **3.61** in a yield of 38%.

^{1}H NMR (400 MHz, Methanol-d_4) δ 8.26 (dt, J = 9.0, 1.8 Hz, 3H), 8.00 (s, 1H), 7.92 – 7.86 (m, 1H), 7.68 (s, 0H), 7.60 – 7.51 (m, 1H), 7.50 – 7.20 (m, 6H), 6.98 (d, J = 7.9 Hz, 1H), 5.58 – 5.48 (m, 1H), 4.46 (dq, J = 9.4, 4.6 Hz, 2H), 4.25 (d, J = 1.7 Hz, 2H), 3.81 – 3.63 (m, 2H), 3.54 (dq, J = 6.8, 5.2, 4.6 Hz, 2H), 3.28 (ddd, J = 15.3, 4.7, 2.2 Hz, 1H), 3.23 (td, J = 5.2, 1.7 Hz, 2H), 2.93 – 2.76 (m, 1H), 1.02 (dd, J = 3.9, 1.3 Hz, 9H).
^{13}C NMR (101 MHz, Methanol-d_4) δ 156.76, 153.21, 152.86, 152.33, 151.96, 146.99, 145.43, 143.03, 139.36, 134.65, 131.04, 129.43, 128.66, 128.47, 127.35, 127.06, 126.67, 126.24, 126.07, 125.54, 124.89, 123.28, 122.37, 116.50, 110.81, 86.02, 79.28, 79.22, 74.10, 70.12, 69.93, 51.45, 46.73, 44.31, 32.80, 26.11.

Compound 3.62

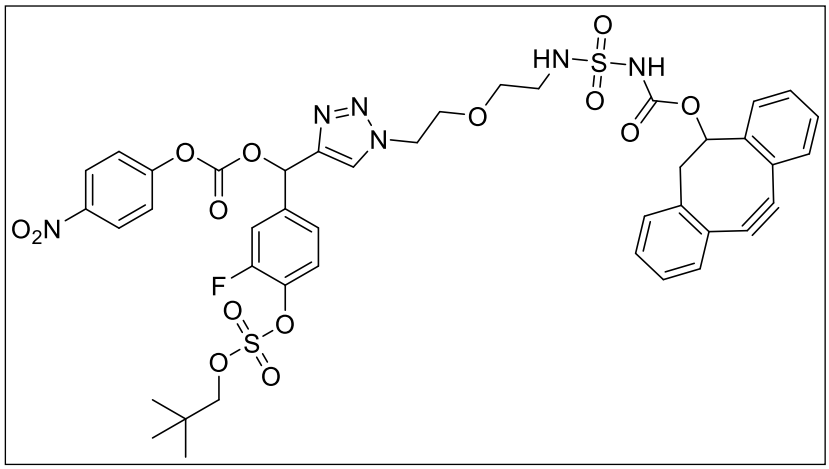

Compound **3.50** (50mg, 65μmol, 1 equiv.) was dissolved in 1mL dry DMF under inert atmosphere and TEA (37μL, 259μmol, 2 equiv.) and bis(4-nitrophenyl) carbonate (59mg, 194μmol, 2.5 equiv.) were added. The reaction was stirred overnight at rt and upon completion, was acidified by the addition of 1% aq. HCl. The reaction was extracted with EtOAc and the organic phase then washed with sat. aq. $NaHCO_3$ and brine, dried over $MgSO_4$ and the solvent removed *in vacuo*. The crude was purified by FCC, affording the title compound **3.62** in a yield of 75%.

^{1}H NMR (400 MHz, Methanol-d_4) δ 8.26 – 8.19 (m, 2H), 7.96 (d, J = 2.7 Hz, 1H), 7.62 – 7.20 (m, 9H), 5.55 – 5.51 (m, 1H), 5.49 (s, 0H), 4.50 – 4.42 (m, 2H), 4.20 (d, J = 1.3 Hz, 2H), 3.79 – 3.70 (m, 2H), 3.57 – 3.49 (m, 2H), 3.32 (p, J = 1.7 Hz, 2H), 3.26 – 3.20 (m, 2H), 1.01 – 0.98 (m, 9H).
^{13}C NMR (101 MHz, Methanol-d_4) δ 156.77, 153.88, 152.91, 152.22, 151.91, 146.90, 145.95, 140.04, 138.84, 131.04, 129.41, 128.66, 128.45, 127.33, 127.03, 125.29, 125.03, 124.83, 123.23, 122.34, 117.51, 117.31, 114.02, 110.78, 85.31, 79.27, 74.67, 70.20, 69.96, 51.37, 46.70, 44.26, 32.74, 26.13.

Compound 3.63

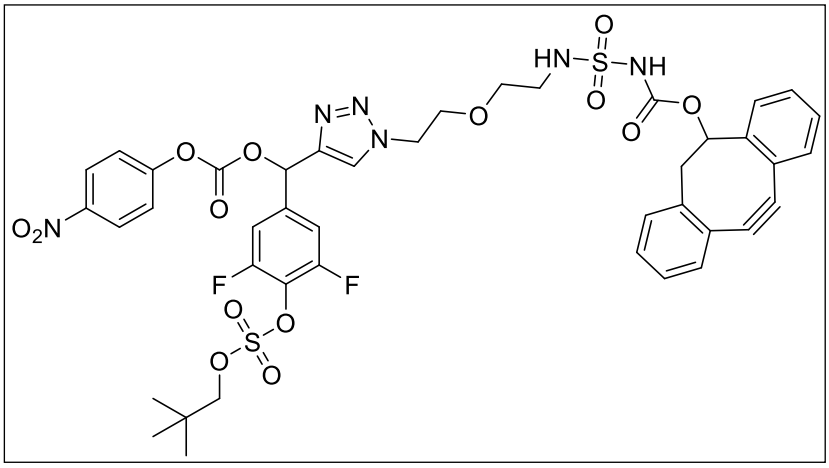

Compound **3.60** (405mg, 513μmol, 1 equiv.) was dissolved in 17mL dry DMF under inert atmosphere and TEA (143μL, 1.03mmol, 2 equiv.) and bis(4-nitrophenyl) carbonate (468mg, 1.54mmol, 3 equiv.) were added. The reaction was stirred overnight at rt and upon completion, was acidified by the addition of 1% aq. HCl. The reaction was extracted with EtOAc and the organic phase then washed with sat. aq. $NaHCO_3$ and brine, dried over $MgSO_4$ and the solvent removed *in vacuo*. The crude was purified by FCC, affording the title compound **3.63** in a yield of 58%.

^{1}H NMR (400 MHz, MeOD) δ 8.31 – 8.22 (m, 2H), 8.00 (d, *J* = 4.3 Hz, 1H), 7.57 (t, *J* = 7.9 Hz, 1H), 7.51 – 7.24 (m, 11H), 6.90 (d, *J* = 6.3 Hz, 1H), 5.54 (dtd, *J* = 4.7, 3.0, 1.7 Hz, 1H), 4.47 (dt, *J* = 7.9, 4.8 Hz, 2H), 4.28 (d, *J* = 1.7 Hz, 2H), 3.81 – 3.70 (m, 2H), 3.60 – 3.51 (m, 2H), 3.34 – 3.27 (m, 1H), 3.29 – 3.19 (m, 2H), 2.92 – 2.82 (m, 1H), 2.05 (s, 2H), 1.04 (d, *J* = 1.0 Hz, 9H).
^{13}C NMR (101 MHz, MeOD) δ 155.38 (d, *J* = 1.5 Hz), 155.27 (dd, *J* = 253.7, 3.3 Hz), 151.59, 151.46, 150.89, 150.56, 145.61, 144.03, 129.66, 128.03, 127.28, 127.07, 125.95, 125.63 (d, *J* = 3.5 Hz), 125.12, 124.84, 123.47 (d, *J* = 2.7 Hz), 121.89, 121.00, 120.98, 112.63 (d, *J* = 1.6 Hz), 111.54, 111.33, 109.40, 84.34, 77.91, 77.88, 72.78, 68.80, 68.77, 68.56, 50.03, 45.34, 45.28, 42.89, 31.37, 24.72.

Compound 3.64

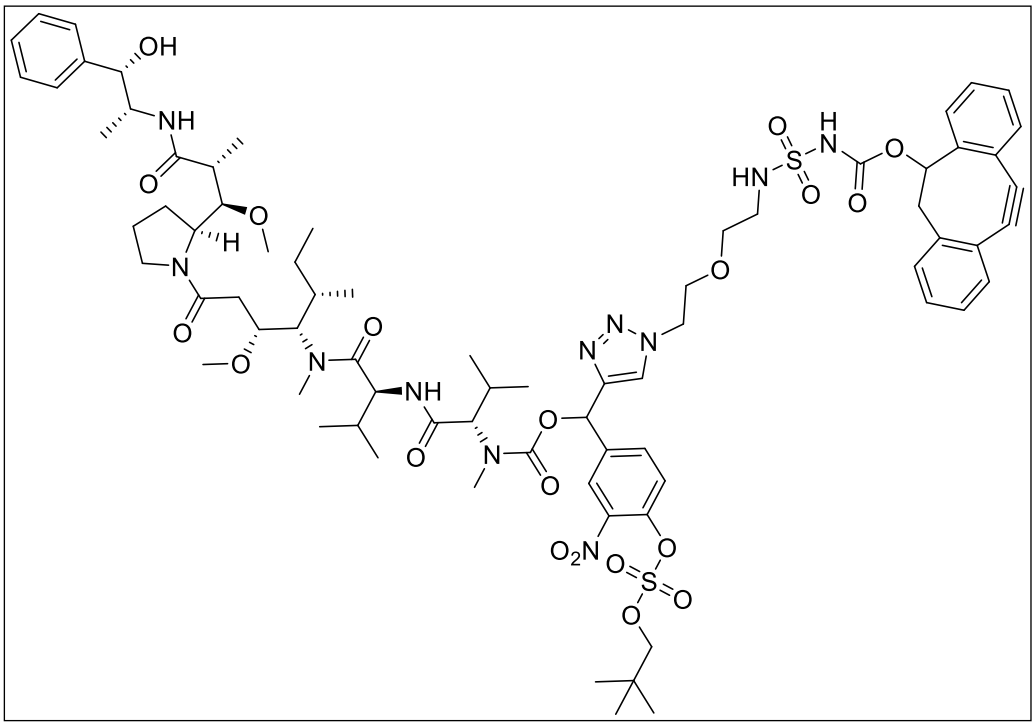

Compound **3.61** (10mg, 10μmol, 1 equiv.), MMAE (7mg, 10μmol, 1 equiv.) and pyridine (29μL, 363μmol, 35 equiv.) were dissolved in 300μL dry DMF under inert atmosphere. To the reaction, were added DIPEA (2μL, 10μmol, 1 equiv.) and HOBt hydrate (2mg, 13μmol, 1.25 equiv.) and the reaction was stirred for 72h at rt. The reaction was purified by preparative HPLC, affording the title compound **3.64** in a yield of 1%.

HRMS (ESI) calculated for $[C_{75}H_{103}N_{11}O_{20}S_2]$ $[M+H]^+$ 1542.6895, found 1541.6891

Compound 3.65

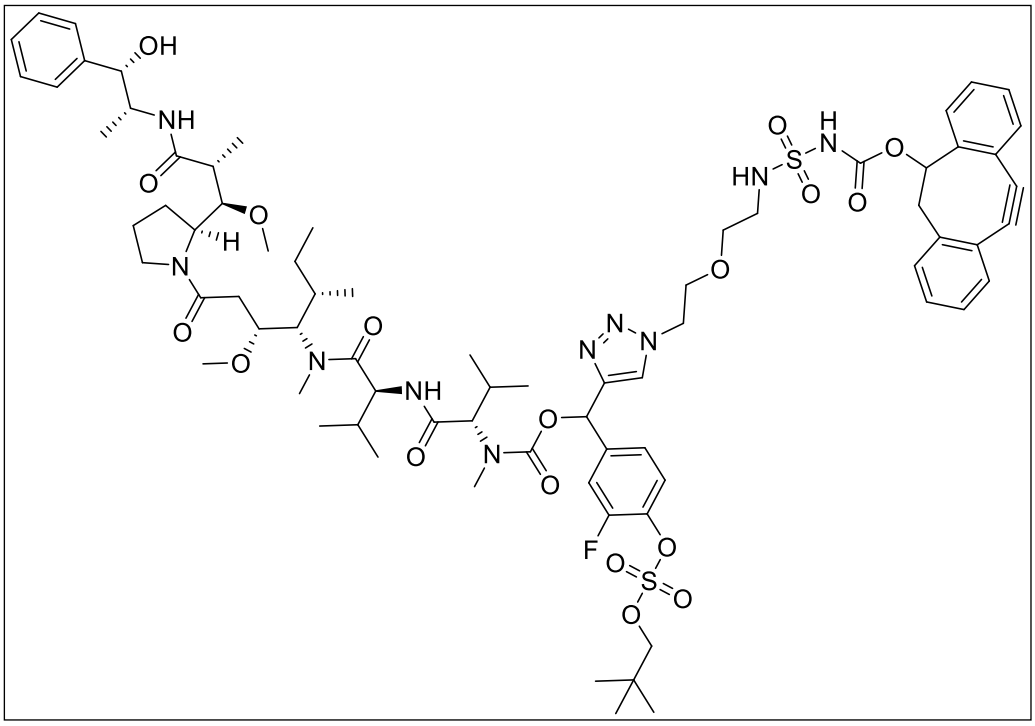

Compound **3.62** (10mg, 11μmol, 1 equiv.), MMAE (8mg, 11μmol, 1 equiv.) and pyridine (30μL, 374μmol, 35 equiv.) were dissolved in 300μL dry DMF under inert atmosphere. To the reaction, were added DIPEA (2μL, 11μmol, 1 equiv.) and HOBt hydrate (2mg, 13μmol, 1.05 equiv.) and the reaction was stirred for 44h at rt. The reaction was purified by preparative HPLC, affording the title compound **3.65** in a yield of 1%.

HRMS (ESI) calculated for $[C_{75}H_{103}FN_{10}O_{18}S_2]$ $[M+Na]^+$ 1537.6769, found 1537.6832

Compound 3.66

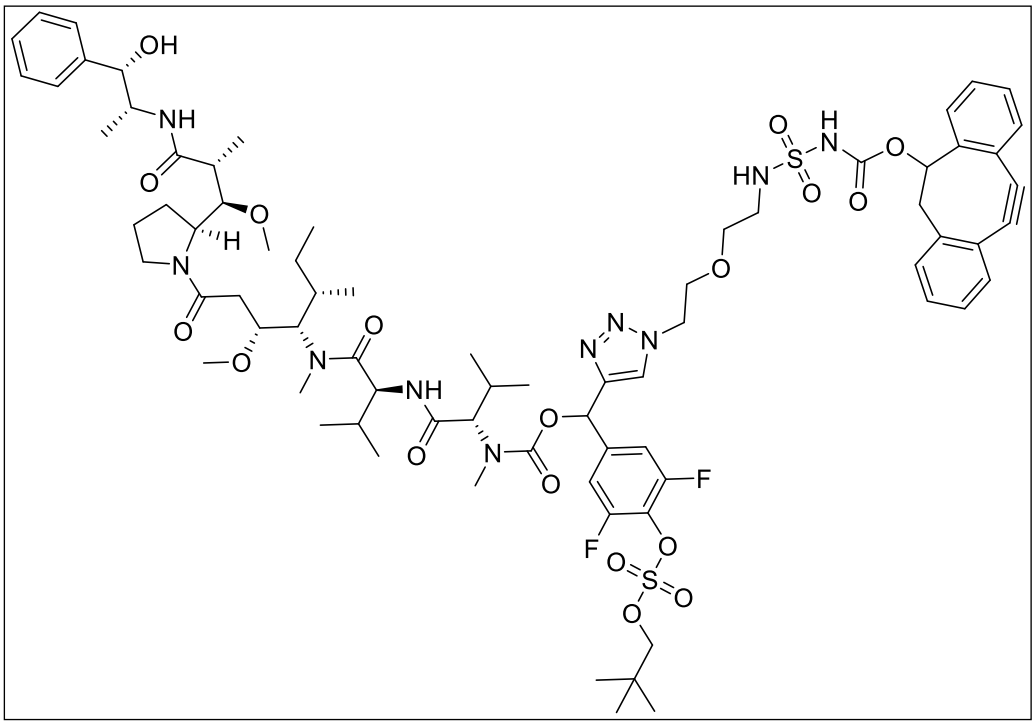

Compound **3.63** (50mg, 52μmol, 1 equiv.), MMAE (56mg, 79μmol, 1.5 equiv.) and pyridine (148μL, 1.83mmol, 35 equiv.) were dissolved in 520μL dry DMF under inert atmosphere. To the reaction, were added DIPEA (9μL, 52μmol, 1 equiv.) and HOBt hydrate (8mg, 55μmol, 1.05 equiv.) and the reaction was stirred for 47h at rt. Upon completion, the reaction was purified by preparative HPLC, affording the title compound **3.66** in a yield of 11%.

HRMS (ESI) calculated for $[C_{75}H_{102}F_2N_{10}O_{18}S_2]$ $[M+H]^+$ 1533.6856, found 1533.6885.

Compound 3.67

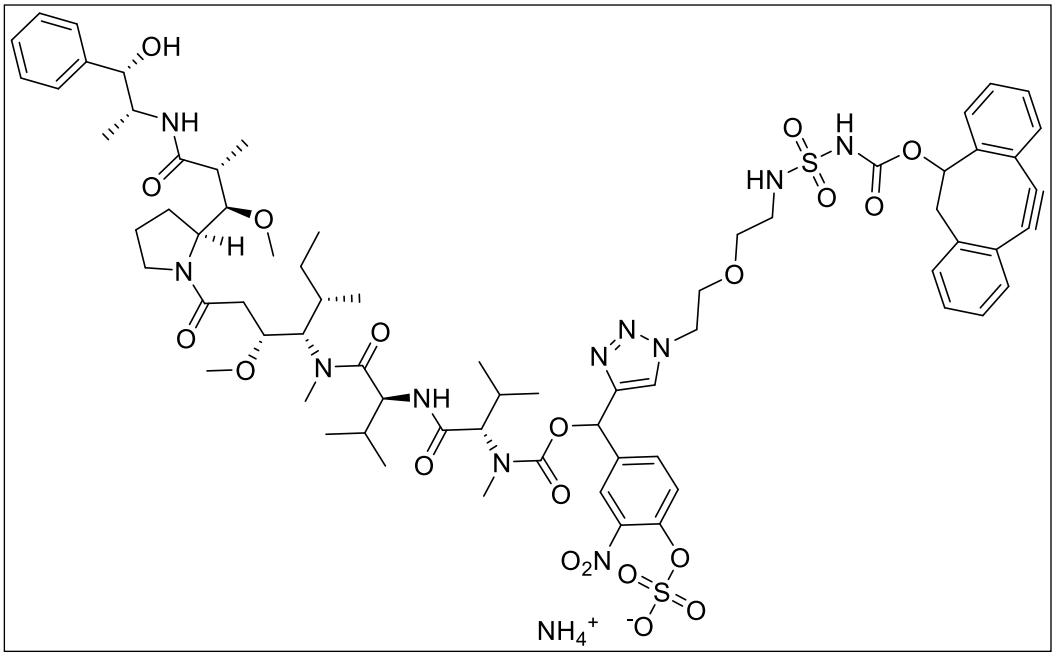

Compound **3.67** was isolated during the purification of compound **3.64** in a 0.6mg yield.

HRMS (ESI) calculated for $[C_{70}H_{93}N_{11}O_{20}S_2]$ $[M-H]^-$ 1470.5967, found 1470.5975.

Compound 3.68

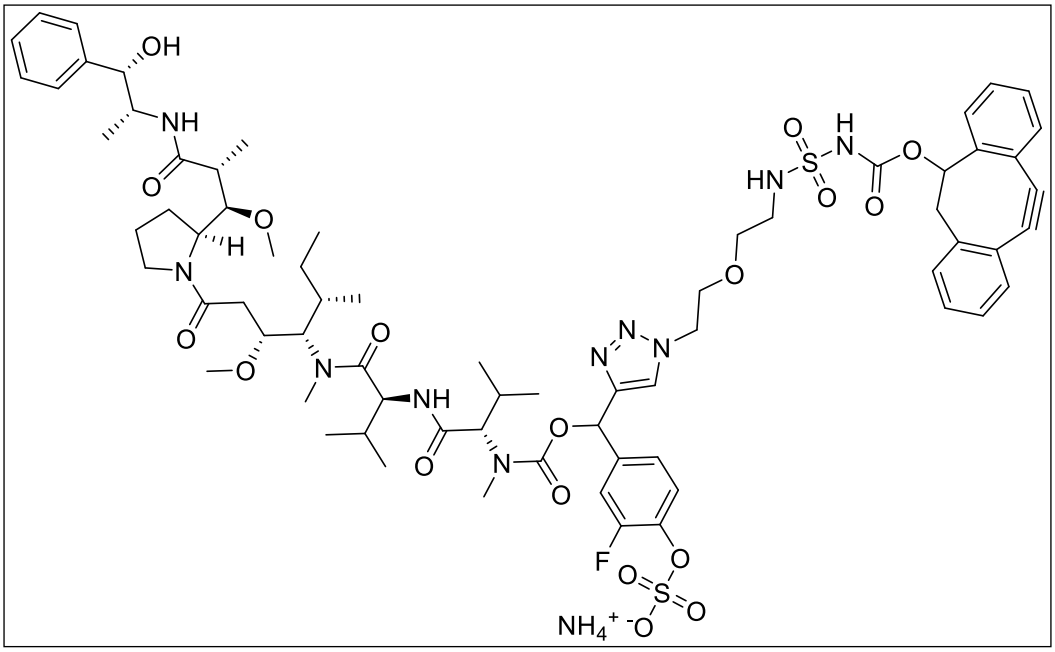

Compound **3.68** was isolated during the purification of compound **3.65** in a 0.4mg yield.

HRMS (ESI) calculated for $[C_{70}H_{93}FN_{10}O_{18}S_2]$ $[M-H]^-$ 1443.6022, found 1443.6028.

Compound 3.69

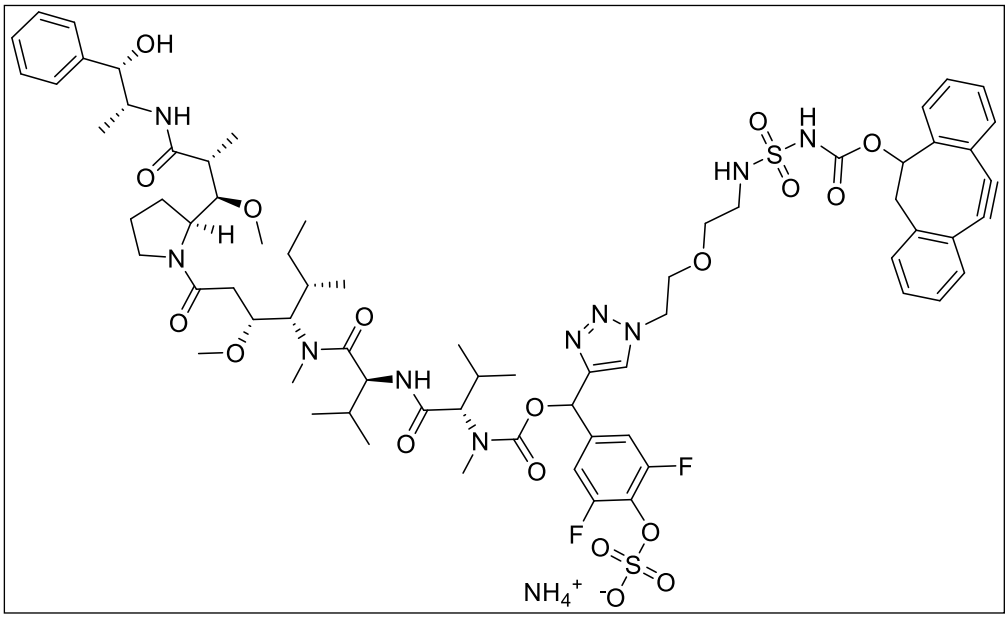

Compound **3.66** (4.5mg, 2.93μmol, 1 equiv.) was dissolved in 108μL DMF and 108μL 2M NH_4OAc and the reaction stirred overnight at rt. Analysis by UPLC-MS the following day, showed little reaction and the reaction was heated to 50°C overnight, after which full conversion was observed. The solvent was removed under a stream of air, affording the title compound **3.69** in a quantitative yield.

HRMS (ESI) calculated for $[C_{70}H_{92}F_2N_{10}O_{18}S_2]$ $[M\text{-}H]^-$ 1461.5928, found 1461.6007.

Conclusion and outlook

This thesis presents novel bioconjugation and linker strategies towards the development of ADCs.

Chapter 2 presents two bioconjugation strategies for the preparation of highly homogeneous conjugates. Part I describes the initial studies towards a novel serine site-selective conjugation strategy, using an NHC organocatalyst. By optimizing the sequence to tune the microenvironment of the serine, it was possible to achieve high conversion and selective conjugation, demonstrating the potential of this strategy. Part II covers the work conducted during my external stay at Cambridge University in the group of prof. David Spring, where they developed a novel approach towards homogeneous cysteine rebridging antibody conjugates. Synthesis of the central scaffold and two cysteine rebridging head groups was performed and the bis-sulfone head group was attached to the tetra anchor, affording a novel conjugation handle.

Chapter 3 describes the design, synthesis and *in vitro* testing of novel sulfatase cleavable linkers and the investigation of sulfatase substrate preference. In part I, the synthesis of a novel sulfatase cleavable linker for the release of alcohol functionalized cargo is described. Two sulfatase cleavable payloads were synthesized, functionalized with MMAE/auristatin E and a maleimide conjugation handle. The linker containing an undecorated aryl sulfate trigger was conjugated to an antibody. The resulting ADC was tested *in vitro* against breast cancer cells and an antigen dependent dose-response curve was observed. Part II describes the synthesis of sulfatase cleavable probes for the testing of substrate preference of sulfatases. Four analogues with differently substituted on the aryl sulfate moiety were prepared and cleavage rates by sulfatase from *Helix Pomatia* were significantly increased by the incorporation of EWG. Finally, part III describes the synthesis of three sulfatase cleavable payloads, for the investigation of the effect of aryl substitution of potency of ADCs. The linkers incorporated MMAE and DIBO for the attachment to azido functionalized antibodies in a DAR specific manner. *In vitro* testing displayed a difference in the IC_{50} values demonstrating the possibility of tuning ADC toxicity by substitution of the aryl sulfate moiety.

There are many interesting things to investigate when moving forward with this work. For the serine site-selective bioconjugation, more studies are needed to explore conditions and different optimized peptide sequences. Finally, to demonstrate the utility of the strategy, the optimized sequence should be recombinantly incorporated into a full length protein for the determination of bioconjugation yields. It could be advantageous to expand the series of sulfatase probes, as well as testing these against human sulfatases and cancer cell lysates, to elucidate the substrate preference of human lysosomal sulfatases.

Multidisciplinary expertise is required in the development of ADCs and it is my hope, that the work presented in this thesis, may help to expand the framework of ADC linker technology and bioconjugation strategies.

Publications in preparation

A Study of Arylsulfatase Activity Towards Differently Decorated Benzene Moieties

Targeting Difficult Drug Targets: Dual-specificity Phosphatases

Novel Oxime Based Photo-cleavable Protection Group for the Release of Carbonyls